Master's thesis

NTNU
Norwegian University of Science and Technology
Faculty of Information Technology and Electrical Engineering
Department of Electric Power Engineering

Olav Henry Sagøy

Dielectric Characterization of Semi Conducting Field Grading Varnish for Hydro Generators

Master's thesis in Electric Power Engineering
Supervisor: Frank Mauseth
Co-supervisor: Jorunn Hølto, Espen Eberg
June 2021

NTNU
Norwegian University of Science and Technology

Olav Henry Sagøy

Dielectric Characterization of Semi Conducting Field Grading Varnish for Hydro Generators

Master's thesis in Electric Power Engineering
Supervisor: Frank Mauseth
Co-supervisor: Jorunn Hølto, Espen Eberg
June 2021

Norwegian University of Science and Technology
Faculty of Information Technology and Electrical Engineering
Department of Electric Power Engineering

NTNU
Kunnskap for en bedre verden

Abstract

The main purpose of this work was to characterize a field grading varnish that was used in hydro generators. The varnish tested is used in the end-windings of generators. It is made to even out field concentrations in the transition between slot and air in the end-windings.

This work mainly focuses on the characterization and the behavior of the varnish. It is also introducing the use, purpose and design around field controlling materials. This project includes several measuring methods, calculations and approximations to end up with acceptable results.

The first characterization method used was the insulation diagnostic analyzer, IDA 200. This is a measuring device that can apply a high voltage and a wide range of frequencies. The inconvenience with this apparatus is that it can only deliver a certain amount of current. With great losses from the varnish, this was not the optimal solution.

The IDAX 206 was used to apply a higher frequency. It was equipped with a thermal cabinet, that made it possible to test the temperature dependency at the same time as the field and frequency dependency.

With a Megohmmeter, there was performed polarization and depolarization measurements to obtain values for calculation. The values were used to produce graphs that represented the relationship between the applied electric field and the conductivity of the varnish.

Finally, it was done a potential measurement on the surface of the varnish on several different test samples. These measurements were done to see how the varnish influenced the already existing electrical field present without varnish.

The results of these methods show different graphs and values. The most interesting measured values are the loss factor ($tan\ \delta$), conductivity and the surface potential. The results show different dependencies when it comes to the losses of the varnish. Temperature, frequency and the electric field are parameters considered in this work. The varnish has much higher losses compared to a dielectric material and the conductivity of the material plays a major role here.

Sammendrag

Hovedformålet med dette arbeidet er å karakterisere en feltstyrende lakk som brukes i vannkraftgeneratorer. Lakken som er testet brukes i endeviklingene til generatorer. Den er laget for å utjevne feltkonsentrasjoner i overgangen mellom stator og luft i endeviklingene.

Dette arbeidet konsentrerer seg hovedsakelig om karakteriseringen og oppførselen til lakken. Den introduserer også anvendelse, formål og design rundt feltstyrende materialer. Dette arbeidet inkluderer flere målemetoder, beregninger og tilnærminger for å komme med akseptable resultater.

Den første karakteriseringen som ble gjort var ved hjelp av isolasjonsdiagnoseanalysatoren, IDA 200. Dette er en enhet som kan påtrykke høy spenning og et bredt spekter av frekvenser. Ulempen med denne enheten er at den bare kan levere en viss mengde strøm. Med store tap fra lakken var ikke dette den optimale løsningen.

En annen isolasjonsdiagnoseanalysator, IDAX 206, ble også brukt. For å bruke en høyere frekvens var det nødvendig med en ny analysator. I tillegg var dette måleapparatet utstyrt med et termisk skap. Dette gjorde det mulig å teste temperaturavhengigheten samtidig med felt- og frekvensavhengigheten.

Med en megger ble det utført en polarisering- og depolariserings måling for å få verdier til beregninger. Verdiene ble brukt til å produsere grafer som presenterer forholdet mellom det påførte elektriske feltet og ledningsevnen til lakken.

Til slutt ble det utført potensial målinger på overflaten av lakken. Målingene ble brukt til å se hvordan lakken påvirket det allerede eksisterende elektriske feltet som var tilstede uten lakk.

Resultatene av disse metodene som ble brukt viser forskjellige typer grafer og verdier. De mest brukte verdiene er tapsfaktoren ($tan\ \delta$), den er også en av de mest interessante verdiene sammen med ledningsevnen og det målte overflatepotensialet. Resultatene viser at det er forskjellige avhengigheter når det gjelder lakkens tap. Temperatur, frekvens og elektrisk felt er parametrene som vurderes i dette arbeidet. Lakken har vist at den har mye høyere tap sammenlignet med et dielektrisk materiale. Materialets ledningsevne spiller en stor rolle her.

Preface

This master thesis is written by Olav Henry Sagøy, a student at the Department of Electric Power Engineering at NTNU. The background of the thesis started with a student that wanted to learn more about a subject he had only some knowledge about from before. First, a project report was produced and now, this thesis as a continuation is completed. The work was made possible with the help of Frank Mauseth and SINTEF. With a lot of help and pleasant discussions from the main supervisor Frank Mauseth, I want to show special gratitude to him. He made the work easier and understandable, the whole process was also made easier with his good sense of humor and a funny comment always lurking. He made it possible to learn a lot and to understand the different parts of the work, regarding this thesis. I also want to provide a special thanks to the co-supervisors Jorunn Hølto and Espen Eberg for their guidance, help and making the work possible.

NTNU, Trondheim

December 2020

Olav Henry Sagøy

Contents

1 Introduction

The majority of hydro generators in production today are built to run in the traditional way. This means with a certain speed on the rotor that the resulting frequency the stator delivers is at 50 or 60Hz. The speed resulting in this grid frequency is not always the optimal speed for the generator in terms of efficiency. It is a goal to make hydropower generators operate with a flexibility as high as possible. This is important because the utilization of the storage capability and power will then aim towards a max. As little energy as possible will then go to waste. The desired development is to make the generators run in their most efficient region and thus increase the utilization of the reservoirs. It would demand much more versatility from the machines to run the old generators this way. The flexibility can be obtained by using power electronics. These units will control the generators and more specifically their output. With a new controller system like this, the insulation and other dielectric material in the machines will experience new and different kinds of voltage and current stresses.

The insulation system and the dielectric materials will be subjected to new types of voltage stresses from the new power electronics. These new voltage stresses will mainly consist of voltages with different frequencies, which are results from the switching in the electronics. It is the voltages with the additional frequencies to the fundamental frequency that will influence the generators' insulation and dielectric materials. If the hydro generators continue to be made in the traditional way, there might be too much stress for its dielectric materials. The problem is if the new stresses affect the properties of the insulating materials and thus make the machine degrade and break down in the long run.

One of the most critical areas in a generator is the end-windings. This is where the electrical field gets its highest concentration, due to the transition between the slot and the air. The energized stator bar exits the grounded stator core, which makes a great potential difference. In this end-winding area, it is typical that discharges occur, especially surface and partial discharges. These discharges will damage the insulation or other dielectrics in the area. In a traditional generator, there are usually applied a field grading material in the end-winding area to avoid discharges. These field controlling materials are not tested or examined regarding the new types of stresses from the flexible drives. As mentioned, the power electronic converters will make noise in both the voltage and the current. The noise in the voltage will work as new stress for the insulation and the other dielectric materials. To be able to use the new voltage stresses to examine the tolerance of the field grading and insulating materials, the materials need to be characterized. The characterization needs to show how the material behaves with different stresses. It needs to include the material's dependency on temperature, electric field and frequency. These parameters can change while the generators are operating, therefore are all these dependencies relevant for the machines. This thesis will mainly deal with the characterization of a field controlling varnish. Regarding the tests of the field grading varnish in this work, different characterizations and analyzes are done. First, an insulation diagnostic analysis was performed with high voltage and frequencies from 100 down to 0.1 Hz. An insulation

diagnostic analysis was also done with low voltage and frequencies from 1000 down to 0.1 Hz. Later, a megging of the varnish was conducted, the values were used for calculations. Special test objects were made for these three tests. It was also used different generator bars as test samples later for potential measurements.

2 Background - Theoretical Basis

The theoretical knowledge below is based on several references and the previous project of this work [1]. Most of the figures and the theory are taken from the project work [1], the original references are nevertheless shown and marked in this theoretical section of the work. Some changes and improvements were made.

2.1 Electric Machine

Both motors and generators are electric machines. The electric machines are usually constructed and made to only do one of the two things, convert mechanical energy into electrical energy or vice versa. Each build and construction of a machine is made to fit the customers' needs. Important requirements for the specific application, are usually considering the speed and the efficiency of the machine.

In a generator, the magnetic field in the rotor is used to induce a current in the stator windings to produce energy. In a motor it is the opposite. A current in the stator makes a rotating magnetic field that drives the rotor. As mentioned with a generator, the physical forces utilized will make the rotor rotate. The rotor has a magnetic field that will start rotating with it. The rotating field will induce currents in the stator coils which get further distributed to the grid. It exists several different rotor designs, but all work with the same principle. [3]

2.1.1 Stator

Two of the large components inside a stator housing are the stator core and the windings. The stator core consists of many thin steel plates that are covered with a coat of insulating substance.

If a larger high voltage machine is considered, the windings are typically made out of stiff bars which consist of several rectangular conductors inside. The bars are also rectangular due to the shape of the conductors inside and the shape of the slots it is placed in. Different from the coils in small machines, these are form wounded. The bars are suited for large machines. They can handle both mechanical and electrical stress better than the construction of smaller machines. The high voltage stator bars have several different layers of insulation, both between the conductors themselves and the conductors and ground. Due to the greater cross-section of the conductors in the larger machines, they are able to carry a greater current than the smaller machines. The slots are utilized in a better way. The stiff construction of the bars contributes to a machine that can handle physical stress. Large generators or motors may experience different types of vibrations and will therefore need a certain mechanical strength to avoid degradation and finally breakdown.

When considering machines with high voltages, it is important to consider the electrical fields. Increased voltage leads to a stronger field. With a strong field, there may occur degradation of insulation in the machine. This may lead to breakdown eventually. High voltage machines must be void- and cavity-free, this is because of the field distribution. The purpose of the insulation is always to prevent current from flowing between two different potentials. Typically in machines, it is between core and conductors. With the optimal insulating material, it should be possible to achieve no current flowing between two potentials. In reality, this is not possible, it will always be a small current flowing. This is known as the leakage current or loss. A specific insulation will only be able to withstand a certain amount of voltage stress. If this limit is exceeded, there will not be an insulating layer present. When the electrical stress is high enough, the insulation will be considered conductive due to the current flowing. [3] [8]

In figure 1, a typical cross-section of a stator construction is shown. The stator is designed with slots for the bars and teeth that keep the bars inside the slots. In larger machines, the slots are usually made to fit several bars.

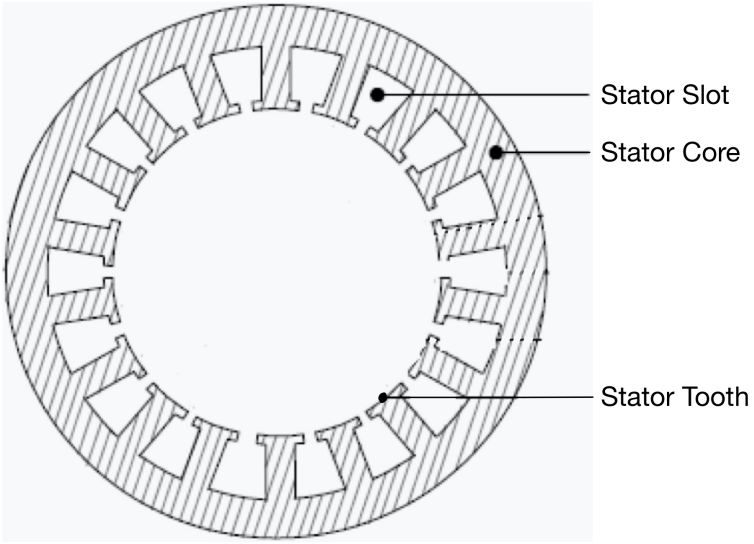

Figure 1: Stator construction with slots and teeth. [2]

It is normal for the bars to be molded in place with epoxy or resin. There is also a layer of insulation or field grading between the stator bars and the core. This could be in the form of a tape, strip or varnish. A typical design is shown in figure 2. The strips on the sides, bottom and top of the bar, are protection strips and fillers. These wave-shaped strips are also used to keep the bars in place inside the slots. To protect the bars and core from corona, the strips are made of a conductive material. From the figure, the configuration of the conductors is shown as a Roebel configuration. This is often used in large high voltage generators to vary the position of the different conductors in the bars. [8]

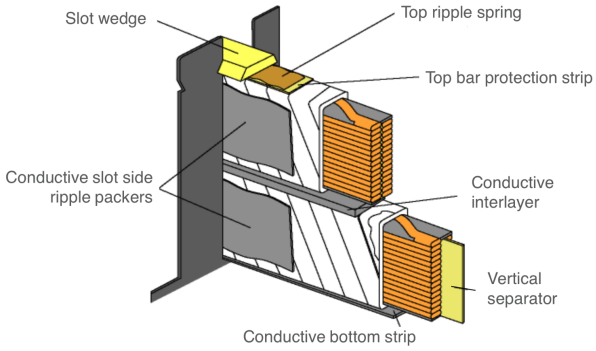

Figure 2: Slot design with two Roebel bars, different attachments are also present. [6]

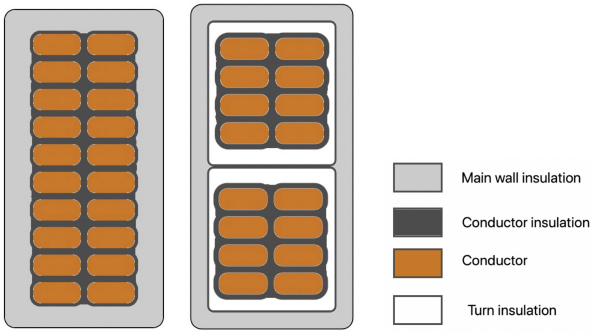

Figure 3: Two different stator bar designs with single and double windings and the corresponding insulation layers.

All bars inside the slots are insulated. In Figure 3 the design of two different stator bars and their structures are shown. The conductors themselves are covered with a thin insulation layer inside the bar. This is preventing them from having a connection. The main wall insulation is shown as the outermost layer of the bars in both figure 2 and 3. It is marked white in figure 2 and light grey in figure 3. The Roebel configured bars have a vertical separator in addition to separate the conductors, see figure 2. The bar to the left in figure 3 shows a cross-section of a single bar with 20 conductors per turn, while the bar to the right is a 2-turn coil with 8 conductors per turn. In bars that contain several turns, there are dedicated layers of insulation surrounding each turn in addition to the conductor- and main insulation. [8]

2.1.2 Field Grading Materials

The stator coils can be divided into two main sections, the part that goes into the slots of the stator core and the part that is outside of it. These areas are usually called the slot section and the end-windings. The location of the two sections are illustrated in figure 4, for a diamond bar. The red area is the end-winding, this is typically where the field grading is applied. It is therefore also known as the field grading or field-controlling area. The black area in the middle of the diamond bar is the section that goes inside the slots of the stator. It is usually covered with another special semi- or fully conductive layer. With a conducting material, there will be no potential differences considering the different layers. Therefore will the majority of the discharges in the area be avoided. [8]

To grade an electric field or distribute the concentration of a strong electric field, a material with certain features or characteristics is needed. With a strong concentration of electric field, there may occur discharges, corona and an increased rate of aging. If a material is going to be able to distribute the concentration of a field, the material needs to have a higher conductivity than the surrounding insulation material. In addition, the field grading materials (FGM) need to have a specific permittivity. [8]

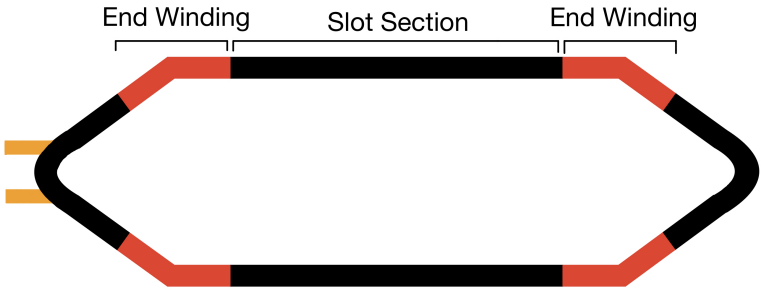

Figure 4: Stator bar sections.

As mentioned, the part of the stator bar that is not located inside the stator slots is known as the end-windings. The end-windings start at the exit of the slot and go outwards. Then it twists and goes back into their next given slot, this is where it stops. The field grading material should be applied from where the bar comes out of the slot and outward to a given length. The length is based on the voltage level of the machine. When comparing the field grading materials with the other material used in the slots, the FGM´s usually have nonlinear properties to obtain their purpose. The purpose of the field grading material is that they prevent the machine from developing discharges. The most common type in the end-windings is surface discharges. They will eventually lead to damaged insulation and breakdown. [8]

The field grading elements are usually meant to prevent an area from developing corona or surface discharges. The breakdown of an electric machine is usually due to erosion or wear of the organic materials in the insulation. The erosion is usually a product of the discharges that have occurred in the machine. These usually take place in the areas with a high concentrated electric field. The consequences of the discharges are, as mentioned, that the materials surrounding will be destroyed. The materials will be weakened and the machine can not perform with the same mechanical or electrical strength as before. If the degradation in the slots continues, the stator bars may loosen and the machine will capitulate. This is mainly when it comes to the molding materials and the other layers of materials in the slots. The problems with the end-windings are often related to breakdown due to insulation degradation and flashovers. When flashovers occur in the end-windings, they usually happen on the surface of the stator bars, between the grounded core and the insulated bar. [7]

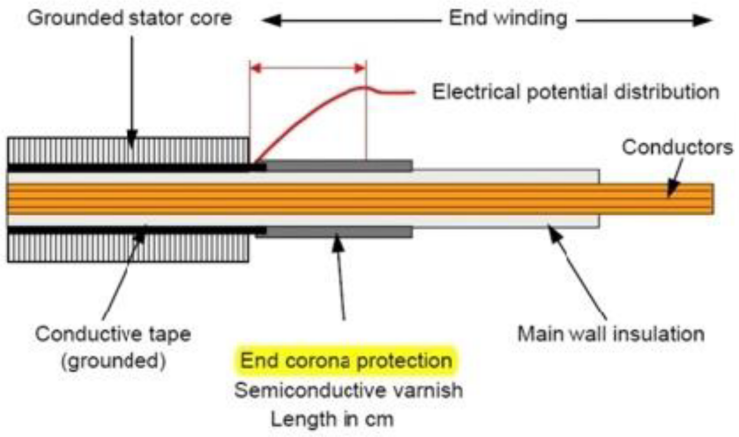

Figure 5: Field grading in the end-windings. [7]

In Figure 5 the location and structure of an FGM are shown with a cross-section illustration. The slot protective layer, shown in black along the conductor, will typically protrude slightly from the slot so that the field-controlling layer can overlap, shown in grey. With this seamless transition, the best distribution of the electric field will be achieved in this area. [7]

2.1.3 Nonlinear Field Grading Material

When it comes to the nonlinear field grading materials, there are no standards in how they behave. To be able to describe a material like this, different methods and levels of accuracy are used. The σ-E graph is often used to show the characterization of the material and its properties. This graph shows how the field influences the conductivity of the specific material. An example can be seen in figure 6. [5]

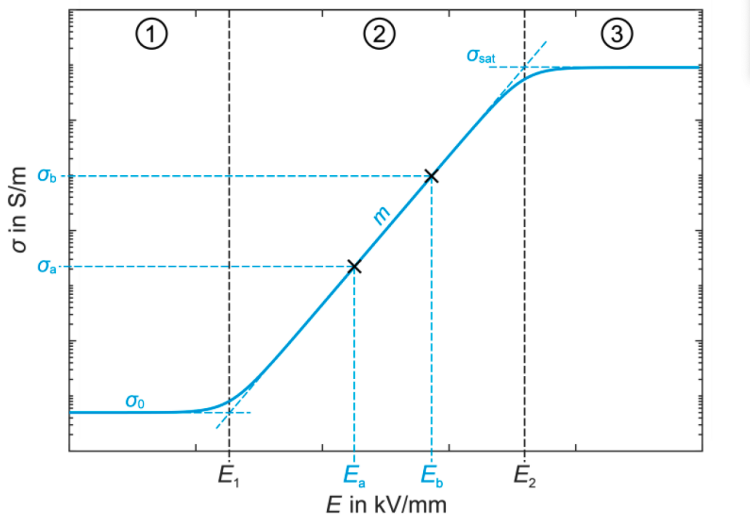

Figure 6: Example of a σ-E -characteristic for a nonlinear field grading material. [9]

The value E_1, on the x-axis in figure 6, is where the dependency of the electric field starts to interact. This value is also known as the switching field strength, where the base conductivity σ_0 starts to change. From this point, the field is influencing the conductivity of the material. E_2 or E_{sat} is where the field dependency is saturated, this value is therefore called the saturation field strength. The conductivity at this specific field strength is called the saturation conductivity, σ_{sat}. The section of the graph between E_1 and E_2 is called the nonlinear region. This part of the graph is often described with an exponent of nonlinearity α. [5]

$$\alpha = (\frac{\lg(J_b/J_a)}{\lg(E_b/E_a)}) \tag{1}$$

In equation 1, J_a and J_b are the current density from the two field strengths E_a and E_b from the nonlinear section in the middle of the graph. The current density values are calculated by dividing the current on the cross-section of the conducting material. [5]

To be able to create a graph similar to the example in figure 6, equation 2, 3 and 4 can be used. As figure 6 shows, σ_0 is the conductivity the material has when it is unaffected by the electric field. [5]

There are given three equations from the technical brochure.[5] The first one, equation 2, represents only the nonlinear part of the characteristic curve of the material. This one does not include the base conductivity or the saturation. [5]

$$\sigma(E) = \sigma_0 \cdot (\frac{E}{E_1})^{\alpha-1} \tag{2}$$

The second equation, 3, represents both the nonlinear part of the characteristic curve and the base conductivity. With this equation, the switching field strength gets included. [5]

$$\sigma(E) = \sigma_0 \cdot (1 + \frac{E}{E_1})^{\alpha-1} \tag{3}$$

The third equation, 4, includes all the three elements of the characteristic curve of the nonlinear material. The base conductivity and the switching field strength are included in the first part of the graph. The nonlinear part of the graph is represented in the middle, the part that gets saturated in the third part is included as well. [5]

$$\sigma(E) = \sigma_0 \cdot \frac{1 + (\frac{E}{E_1})^{\alpha-1}}{1 + (\frac{E}{E_2})^{\alpha-1}} \tag{4}$$

With equation 2, 3 and 4, three different variants of the σ-E-characteristic are shown. Equation 4 fits the graph in figure 6 the best. [5]

2.1.4 Electric Field Stress

The ideal dielectric will be homogeneous and not electrically conductive. In addition, the permittivity is considered independent regarding frequency and temperature. An ideal dielectric material is therefore loss-free. [3]

If two or more ideal dielectric materials are combined, the voltage applied will be distributed according to the permittivity of the chosen materials. The relationship between the voltages across the different parts of the dielectric is called a capacitive voltage distribution. [3]

When designing and dimensioning insulation for equipment in electrical engineering, the magnitude and distribution of the electric field can be crucial. Maxwell´s equations are often used to make calculations in electromagnetic fields. The equations show the relationship between $\overrightarrow{E}$, $\overrightarrow{D}$, $\overrightarrow{H}$ and $\overrightarrow{B}$, which respectively represents the electric field, the electrical flux density, the magnetic field strength and the magnetic field density. [3]

From Maxwell´s equations, these are valid:

$$\overrightarrow{D} = \epsilon_r \epsilon_0 \overrightarrow{E} \tag{5}$$

$$\overrightarrow{E} = -grad\phi \tag{6}$$

$$\int_1^2 \overrightarrow{E}\ d\overrightarrow{s} = -\int_1^2 grad\phi\ d\overrightarrow{s} = \phi_1 - \phi_2 = U_{12} \tag{7}$$

In these equations, ϵ_r is the relative permittivity of the dielectric, ϵ_0 is $8.85\frac{pF}{m}$, which is the permittivity of vacuum. The ϕ_n is the potential at point n in the material. U_{12} is the difference in potential between point 1 and 2. [3]

With equation 5, 6 and 7, this equation can be derived:

$$\begin{aligned} div\ \epsilon_r \epsilon_0 (-grad\phi) &= \rho \\ \nabla^2 \phi &= -\frac{\rho}{\epsilon_r \epsilon_0} \end{aligned} \tag{8}$$

It can be assumed that there will be no space charges in the insulation with a homogeneous material with AC applied. This also makes it possible to apply Laplace´s equation. [3]

$$\nabla^2 \phi = 0 \tag{9}$$

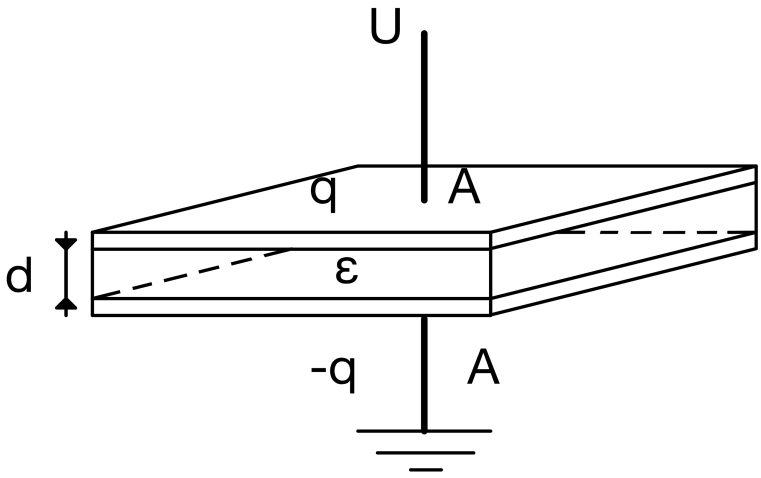

Figure 7: Parallel plate capacitor with one dielectric materiel between the plates.

With this assumption, the electric field can be found in different compositions of materials. The example in figure 7 is a one-layer capacitor with two plane parallel electrodes with an area A and a distance d between each of the plates. From the figure, a voltage U is applied over the plates. With space charges in the insulating material, the number of surface charges on the electrodes may be assumed equal to q $[C/m^2]$. The electric flux density is given by the equation below. [3]

$$D = q \tag{10}$$

By utilizing the surface charges and permittivity, the electric field can be found:

$$E = \frac{q}{\epsilon} = \frac{q}{\epsilon_r \epsilon_0} \tag{11}$$

The voltage over the capacitor is usually given by equation 12. The voltage will be the strength of the field and its length multiplied. With a non-constant or inhomogeneous field, it would be necessary to add the different sections with the different field strengths separately. [3]

$$U = \int_0^d E \, dx \tag{12}$$

If the electric field is constant homogeneous the equation above can be rearranged to:

$$\begin{aligned} U &= \frac{q \cdot d}{\epsilon_r \epsilon_0} = E \cdot d \\ E &= \frac{U}{d} \end{aligned} \tag{13}$$

The capacitance of the capacitor can be expressed from the charges and the voltage, but also the permittivity and the dimensions of the dielectric in the capacitor:

$$C = \frac{Q}{U} = \frac{A \cdot q}{U} = \epsilon_r \epsilon_0 \cdot \frac{A}{d} \tag{14}$$

In an ideal capacitor with two parallel planes, the field between the plates will have even distribution and the same strength everywhere. This makes no minimum or maximum regions between the plates. [3]

2.2 Polarization and Analysis of Materials

2.2.1 Polarization Mechanisms

When applying a voltage to a capacitor, the dielectric material between the electrodes will be polarized. The applied voltage makes different dipoles in the material. The different charges will be canceled out by the opposite polarities of the applied voltage on the electrodes. This phenomenon occurs every time the direction of the applied electric field changes.[3]

Electronic Polarization (Atomic)
The electronic polarization mechanism, also known as atomic polarization, utilizes the charge of the different elements in an atom, the positive proton and the negative electron. When applying an electric field in a capacitor, the negative electrode will attract the proton and the positive electrode will attract the electron. This force from the electrical field will make the electrons stay in one side of the atom more than the other, this makes a temporary dipole out of each atom between the plates. The process happens momentarily. The atom becomes oval with one positive and one negative side, with an electric field present. See figure 8. [3]

Ionic Polarization
Ionic polarization uses ions to form dipoles, which again align with the applied field. With an electric field applied, each ion will be attracted towards the different poles and thereby make temporary dipoles. The dipoles are made due to the force from the field that pushes the ions with opposite polarity in opposite directions and therefore together. See figure 9. [3]

Orientation Polarization
By utilizing the already existing dipoles in a dielectric material, we get the orientation polarization mechanism. This mechanism uses the dipoles and tries to align them when an electric field is applied. The dipoles will align with the applied field relatively fast. If the temperature is higher or if the applied field is stronger, the alignment will happen faster. [3]

Interfacial Polarization
Contamination or a defective part of the dielectric results in an area of lower permittivity or very high conductivity compared to the dielectric itself. This difference in permittivity and conductivity leads to polarization of the area and is known as the interfacial polarization mechanism. An example could be the interface between the layers of dielectrics, the transition between insulation and field grading materials in a stator can be a more specific example. Figure 10 shows an example of a void or contaminant inside a solid material. [3]

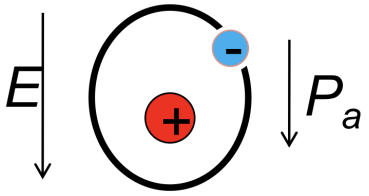

Figure 8: Electronic Polarization (atomic) [3]

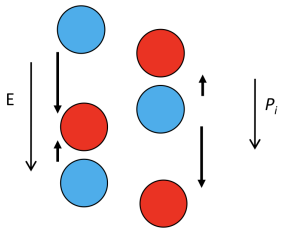

Figure 9: Ionic Polarization. [3]

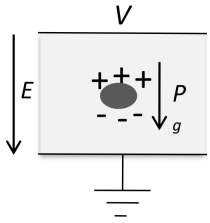

Figure 10: Interfacial Polarization. [3]

Without a voltage applied, the dipoles will be pointing in random directions considering the polarity. When a voltage is applied, an electric field will be present. The dipoles will then align with the direction of the field. This is shown in figure 11. Both the existing and induced dipoles in the dielectric materials align like this. [3]

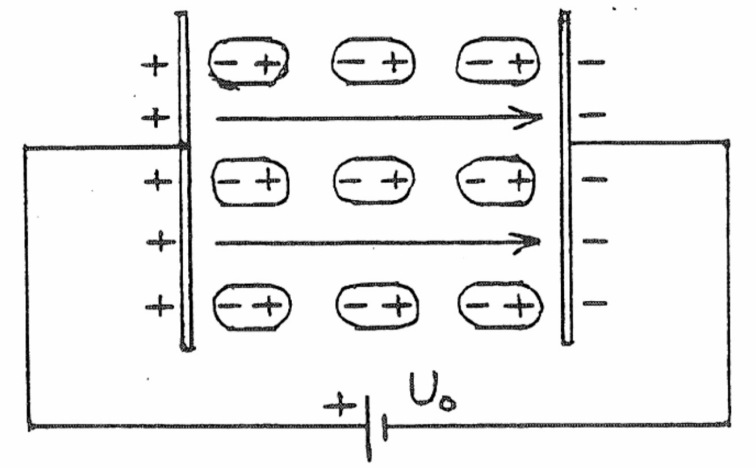

Figure 11: Energized dielectric with dipoles aligned with the applied electric field. [3]

Both electronic polarization and ionic polarization are considered momentary mechanisms. Orientation polarization and interfacial polarization are called relaxation mechanisms, due to the slow reaction to the applied field. The inertia of the relaxation mechanisms makes them lag behind the fluctuation of the electric field. The inertia may lead to both loss dissipation and contribution that makes ϵ_r vary, dependent on the frequency. [3]

2.2.2 Time and Frequency

When dielectric materials are exposed to voltage, an electric field will occur. The polarization mechanisms mentioned in section 2.2.1 will likely happen in all dielectrics when the voltage is applied. The charge of the polarization will still be present when the voltage is removed, assuming that there is no connection to ground. The one measurement that is

interesting during the polarization is the measurement of the current drawn by the mechanisms. It is possible to measure both the current drawn when the dielectric material gets polarized and the current delivered during the materials depolarization. The polarization current is measured from when a voltage is applied and until it reaches a steady state, with DC considered. With AC there is not as easy to measure the polarization. The measurement can be done over a period of time to be able to extract the polarization part of the current. The same applies when the discharge- or depolarization current is measured. The measurement of the depolarization current starts when the poles are connected to ground and stops when it reaches a steady state. [3]

From figure 12 the build-up of charges are shown. The first part, from 0 to t_1, represents a typical polarization. The second part, from t_1 and onwards, represents a depolarization. At zero time, the contribution from both the material itself and the momentary polarization mechanisms are shown. From voltage application, the accumulation of charges due to relaxation mechanisms will increase. This is shown in figure 12. When the amount of charges gets stable, it can be observed that the graph flattens out. As mentioned, the depolarization can be seen in the graph from t_1. The same contribution from the material and the momentary mechanisms are shown. After the momentary part, the relaxation discharge starts. This graph has the same shape as the first part of the graph, only decreasing. [3]

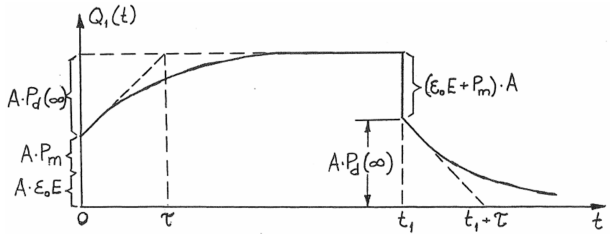

Figure 12: Electrode charge build-up due to polarization, with the contributions from the different mechanisms of the dielectric material shown. [3]

The dielectric is represented as a capacitor. Polarization will occur when a field is applied, which means accumulation of charges. The current that flows during polarization of the dielectric material is related to the accumulated charges.

The current drawn by the polarization will decrease when the accumulation of charges decreases. Figure 12 and figure 13 have a relation. Figure 13 shows a typical shape of a current drawn and supplied during polarization and depolarization of a dielectric. At zero time when voltage is applied, the current needed to charge the capacitor itself is drawn. After this initial current, the polarization current will decrease evenly with an exponential shape. The shape of the current will look like the inverse of the charges accumulated. With different dielectrics, there will be differences between their given relaxation mechanisms, which will determine the shapes of their polarization and depolarization currents. The current will decrease to a stable value which represents the losses due to resistance, shown as the top horizontal dotted line in figure 13. The steady state value will represent the

leakage current that flows through the dielectric material due to its conductivity, this is also known as the conductive losses of the material. This is the only part of the current that will flow after the capacitive current of the polarization is done. When the capacitors poles are connected to ground the depolarization will start, the principle is similar. After the initiation at t_1, the capacitor will deliver a current from the capacitor itself due to the momentary mechanisms. The relaxation mechanisms will start to discharge at the same time, then there will be delivered a current similar to the one drawn for the polarization. The discharge current will go towards zero with an exponential shape as shown below in figure 13. [3]

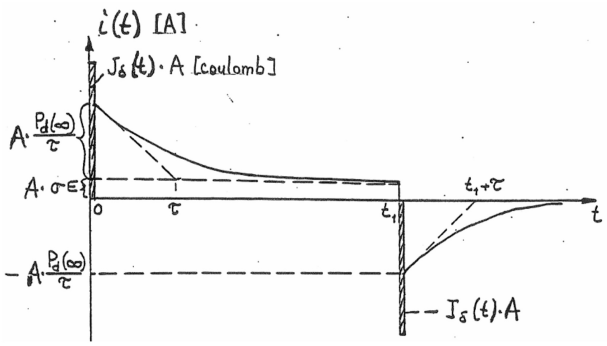

Figure 13: The polarization and depolarization current with the contributions from the relaxation mechanism, the capacitance of the dielectric itself and the conductivity. [3]

Polarization is a phenomenon considered as a loss, especially during AC application. With a capacitor representing the poles and the dielectric material in between, both AC and DC voltages can be applied to obtain polarization. With DC voltage the polarization will happen once every voltage application, assuming a discharge between. With an AC voltage energizing the dielectric, the dipoles move and align with the applied field just like DC. The only difference is that when the direction of the electric field alternates with the sinusoidal voltage, the direction of the dipoles needs to do the same. Typically an AC source changes polarity 50 or 60 times in one second, which means the corresponding field will change direction at the same pace. Polarization and depolarization happen every time the polarity of the source changes. The dipoles in the dielectric material, both induced and existing, will need to align with the field every time the polarity changes. This process will require a current every time the dipoles need to re-align, a current equivalent to the DC polarization current. The currents needed, each time the direction of the field changes for the polarization, will contribute to losses and can also influence other properties of the dielectric material. With small currents flowing during these processes, the temperature of the dielectric will increase. With a nonlinear dielectric, this may lead to increased conductivity, which again can lead to higher currents and increased temperatures. This will result in a vicious circle. [3]

With AC voltage the polarization needs to keep up with the alternating polarity, this is usually not a problem with low frequencies. When the dielectric is exposed to higher frequencies, some of the polarization mechanisms will not be able to keep up with the

rapid changes of the applied field. This makes the polarization of each fluctuation, both positive and negative, not able to complete the phenomenon. With the electric field pointing in either direction, the polarization process will not be able to complete before the polarity and thus the electric field changes direction again. With the incomplete polarization sequences each time the polarity changes, the relative permittivity (ϵ_r) will be lower. This is compared to the relative permittivity with complete polarization. The ϵ_r will be lower with increased frequency, which means that the values are indirectly proportional. [3]

The complex relative permittivity ϵ_r^* is used in this work in addition to ϵ_0, ϵ_r' and ϵ_r''. The parameters are the vacuum permittivity, the real and the imaginary relative permittivity respectively. The complex relative permittivity is shown in equation 15 assuming that the conductivity is zero and resistance is infinite. As mentioned earlier, E represents the electric field. Equations 17 show that the relative permittivity is depending on the frequency. [3]

$$\underline{\epsilon_r^*} = \frac{\underline{D}}{\epsilon_0 \underline{E}} = \frac{D}{\epsilon_0 E} \cdot e^{-j\delta} = \frac{Dcos(\delta)}{\epsilon_0 E} - j\frac{Dsin(\delta)}{\epsilon_0 E} = \epsilon_r' - j\epsilon_r'' \tag{15}$$

$$\frac{\epsilon_r''}{\epsilon_r'} = \frac{sin(\delta)}{cos(\delta)} = tan(\delta) \tag{16}$$

By reorganized equation 15, equation 16 are found. This shows the relationship between the real and imaginary parts of the permittivity. They are both dependent on the frequency, their formulas can be seen in equation 17. The phase-shift δ and the loss factor $tan(\delta)$ can be found by utilizing the relationship between the real and the imaginary part of the permittivity. The parameter ω is the angular frequency. The ϵ' with the different subscriptions are the permittivities of the different relaxation mechanisms. τ is the time constant for the mechanisms. [3]

$$\begin{aligned} \epsilon' &= \epsilon_m' + \frac{\epsilon_s' - \epsilon_m'}{1 + \omega^2 \tau_d^2} \\ \epsilon'' &= \frac{\omega \tau_d (\epsilon_s' - \epsilon_m')}{1 + \omega^2 \tau_d^2} \end{aligned} \tag{17}$$

Taking the formulas in equation 17 into consideration, very low frequencies leads to $\epsilon_r'' \approx 0$. Very high frequencies will do the same, the imaginary part of the relative permittivity will become approximately zero. If the frequency is approximately equal to 1, $\epsilon_r'' > 0$. If the losses of a material are desired to a minimum, it is preferred to keep the ϵ_r' high. A small value will give a bigger loss factor, $tan(\delta) = \frac{\epsilon_r''}{\epsilon_r'}$. [3]

From figure 14 the dependency of the frequency is shown. The permittivity is given

from this curve, with different contributions from the different frequencies. The indirect proportionality mentioned earlier, between the parameters, is evident in this figure. The relationship between the frequency and the permittivity has different drops due to the different mechanisms. The permittivity ϵ' will lose the contributions from the different relaxation mechanisms by increasing the frequency. On the y-axis of figure 14, there are marked three different mechanisms that contribute with one part each to the total permittivity of the dielectric material. The momentary mechanisms ϵ'_m are shown at the bottom and two relaxation mechanisms, ϵ'_h and ϵ'_s, above it. As mentioned, when the frequency is increased the relaxation mechanisms will have trouble keeping up with the alternating field. The contribution from different mechanisms will stop when the frequency is high enough, as seen in figure 14 by examining the descending areas of the graph. When $\omega\tau_i$ and $\omega\tau_d \approx 1$ the dipoles will be able to complete the polarization and follow the alternating field to some extent. Due to this, there will be a phase shift which leads to losses. This means that the flat areas of the graph have no losses due to the phase shift, but the transition areas from one level to another leads to losses. When the frequency exceeds the transitions and reaches the flat area, the contribution from the previous mechanism is gone. The lowest level ϵ'_m which represents the momentary mechanisms, will follow the changing field independent of the frequency of the applied voltage. It will therefore always contribute to the permittivity. [3]

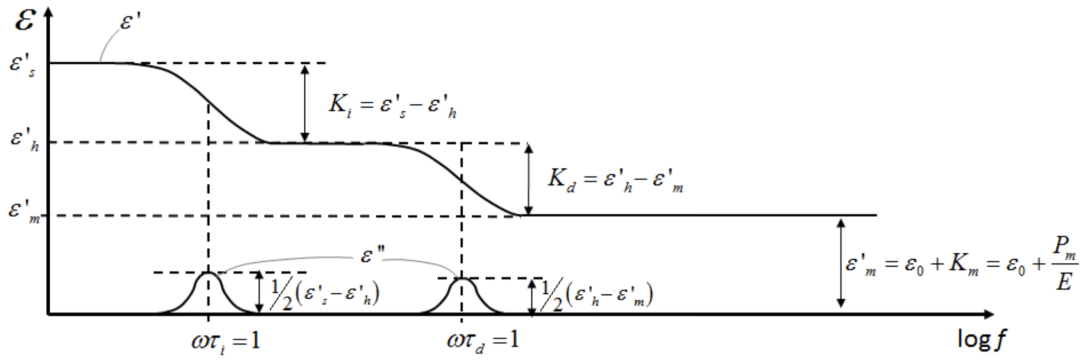

Figure 14: Graph of how the frequency contributes to cancel out the contribution in permittivity from the relaxation mechanisms of a dielectric material. [3]

2.2.3 Losses

With AC voltage applied, the losses are greater than with DC voltage. As mentioned, this is because the polarization and depolarization will happen every time the field changes direction. It is necessary with an associated current that contributes to losses. $tan(\delta)$ is a commonly used parameter for loss, it is also known as the loss factor. This value is often used in conjunction with the characterization of insulation materials. Typically used to determine how good a dielectric is regarding leakage. [3]

$$tan(\delta) = tan(\delta_1) + \frac{\sigma}{\omega\epsilon'_r\epsilon_0} = \frac{\epsilon''_r}{\epsilon'_r} + \frac{\sigma}{\omega\epsilon'_r\epsilon_0} \tag{18}$$

Equation 18 shows an expression for the loss factor, it consists of two parts, which represent different losses. In the equation, σ is the conductivity. The first term gives the actual losses due to the polarization and depolarization of the dielectric. The second term represents losses due to the conductivity of the material. With DC voltage, it is possible to distinguish between the two different loss contributions. However, with an AC voltage applied, it is not easy to separate the two parts.

Figure 13 show that the current is stable where the graph is flat. this is the region where the current drawn due to conductive losses are represented. The initiating part of the graph represents the polarization current and its associated losses. This shows an easy way to extract the two different parts. It is not possible to separate the two different terms of the losses as explained with an AC voltage applied. [3]

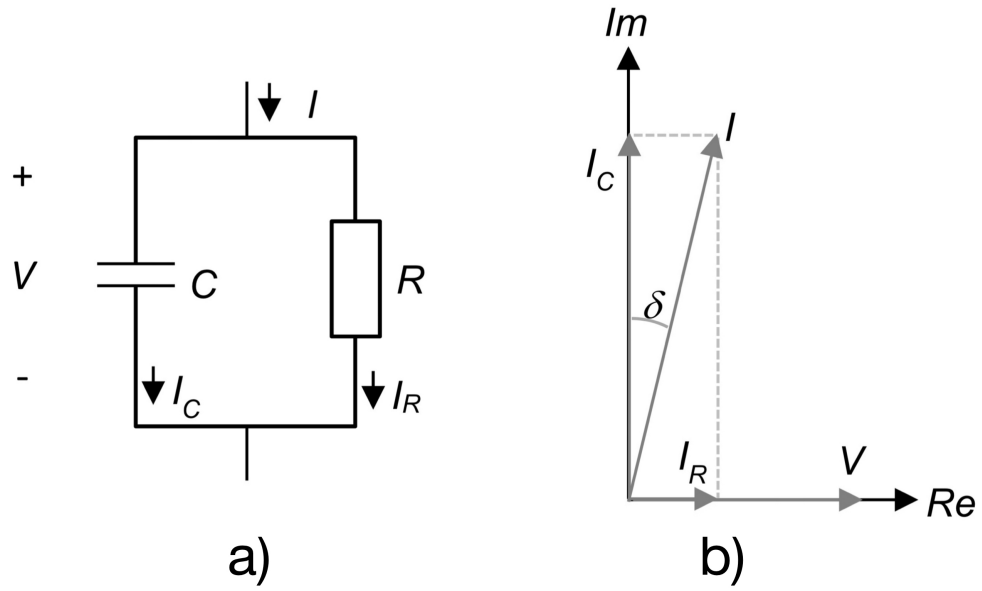

Figure 15: Equivalent circuit for a capacitor with losses and the phasor diagram showing the different parts of the total current. [3]

If a dielectric material is placed between ground and potential, the layout will act as a capacitor. Losses of a material can be presented by using an equivalent circuit, this circuit is shown in figure 15a). The circuit consists mainly of two elements, resistance and capacitance. The resistance in the circuit has a real current flowing. The capacitance is responsible for the imaginary part of the total current in the circuit. The loss angle δ is the angle between the capacitive current I_c and the total current I, shown in figure 15b). The loss angle will increase when I_R increases and I_C decreases. The current flowing through R represents the loss due to the conductivity of the material. While the current flowing through C represents the loss due to the polarization mechanisms. I_R will in addition consist of the loss from the imaginary part of the dielectric material´s permittivity. The conductivity and imaginary permittivity part are the two contributions to the real current in the circuit. Therefore, if any of these two increase, I_R will increase and thus the loss angle and loss factor. [3]

In the equations below, A is the area of the capacitor and d is the distance between the electrodes.

$$\begin{aligned} I_C &= \frac{V}{Z}\ ,\ Z = \frac{1}{j\omega C} \Longrightarrow I_C = j\omega CV \\ C &= \epsilon_0 \epsilon_r^* \cdot \frac{A}{d}\ ,\ \epsilon_r^* = \epsilon_r' - j\epsilon_r'' \\ I_C &= j\omega\epsilon_0\epsilon_r^* \frac{A}{d} V = j\omega\epsilon_0(\epsilon_r' - j\epsilon_r'')\frac{A}{d}V \end{aligned} \tag{19}$$

$$I_C = (\omega\epsilon_0\epsilon_r'' \frac{A}{d} + j\omega\epsilon_0\epsilon_r' \frac{A}{d})V \tag{20}$$

As mentioned, in addition to the current due to the conductivity, the contribution from the real part of I_C will lead to losses in the material. The real part of I_C is represented by the first part of equation 20. The loss due to conductivity can be included by adding the current I_σ, which represents the same current as I_R in figure 15. [3]

$$\begin{aligned} I_\sigma &= \sigma \cdot \frac{V \cdot A}{d} \\ I_{Losses(Real)} &= \omega\epsilon_0\epsilon_r'' \frac{A}{d} + I_\sigma \end{aligned} \tag{21}$$

From equation 21 it can be noticed that the contribution from the real part of the permittivity from equation 20 is removed. In addition, the losses due to the conductivity of the material are added. Equation 21 now shows the two parts of the current that represent the real loss in the circuit. The properties of the material will change and therefore also the two terms in the equation, depending on the temperature, frequency and electric field applied to it. The I_R-vector in figure 15 consists of the two terms in equation 21. The two values are not possible to separate during measurements.[3]

Temperature is usually a big factor when it comes to parameters that affect the losses of a dielectric material. The temperature often affects the conductivity of a material. When it comes to polarization, the temperature typically affects the orientation polarization mechanism. With higher temperatures, the process will accelerate due to the dipoles aligning faster with the field. The relaxation time constant will therefore be smaller and the corresponding frequency will be higher with a higher temperature. This means that the polarization mechanism of the dielectric will be able to keep up with higher frequencies before the mechanism gets too slow. It is conceivable that one of the peaks or the transitions in figure 14 represents the losses of the orientation polarization mechanism. To visualize it with an increase in temperature, the peak and transition are moved further

right on the x-axis, to a higher frequency. Because τ becomes smaller, the frequency or ω needs to be larger to fulfill $\omega\tau = 1$. [3]

3 Method

This work consists of different methods and several series of tests to characterize the field grading varnish. The goal was to get a result that shows the relationship between the properties of the varnish and the temperature, frequency and electric field applied.

This work is focused on a varnish that is field grading, nonlinear and used for end corona protection in large hydro generators. It is used for windings or bars that are typically in the stator of the electric machine. The varnish is both compatible with the Rich Resin method and the Vacuum Pressure Impregnation method (VPI). The varnish is graded as a class F material considering its thermal resistance. This is stated in the data sheet, found in appendix 7.3.[7] This makes the varnish capable of withstanding temperatures of 155°C. It is also given from the data sheet that the length of the varnish, when applied to the stator bars, is given by the maximum test voltage of one coil divided on two. This length of the varnish, the same as the one mentioned in section 2.1.2, is from where the bars exit the slots and the given distance away from the stator core. Figure 16 visualizes the distribution of the applied electric field in relation to the distance from the slot exit, considering three different field grading materials. This work is based on the varnish called "CoronaShield P 8001", shown as the green graph in the figure. Measurements and comparisons with both the black and green graphs are investigated later in this work. [7]

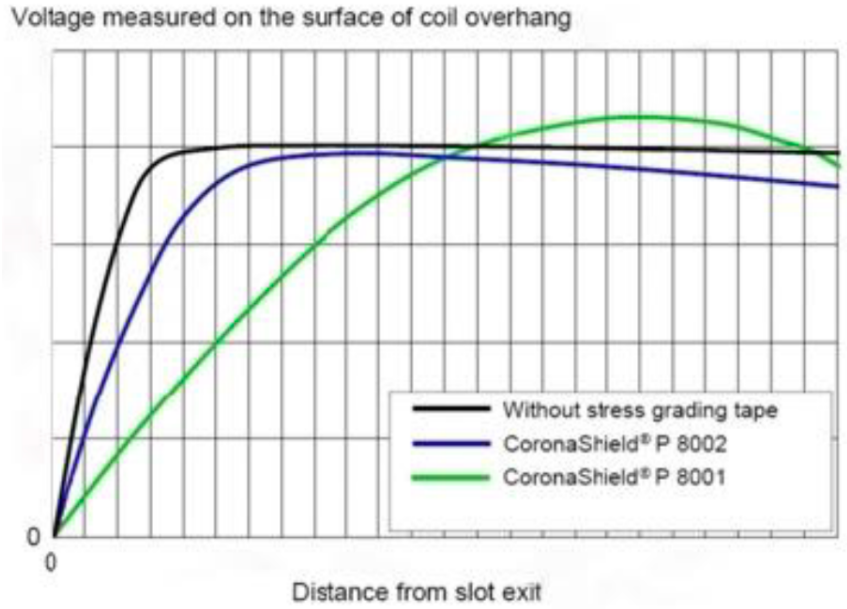

Figure 16: Curve from manufacturer for two of their field grading varnishes. Showing the potential distribution the varnishes can contribute with. An example which shows length from the grounded stator core on the x-axis and surface potential on the y-axis. [7]

3.1 Characterization using IDA 200 with HVU

IDA is a device that is used for characterization and diagnostics of insulating materials. It consists of one main unit and an additional high voltage unit(HVU). Both units were used in this part for characterizing the varnish. The insulation diagnostic analyzer uses different frequencies and voltages to get an overview of the different properties or conditions of the materials examined.

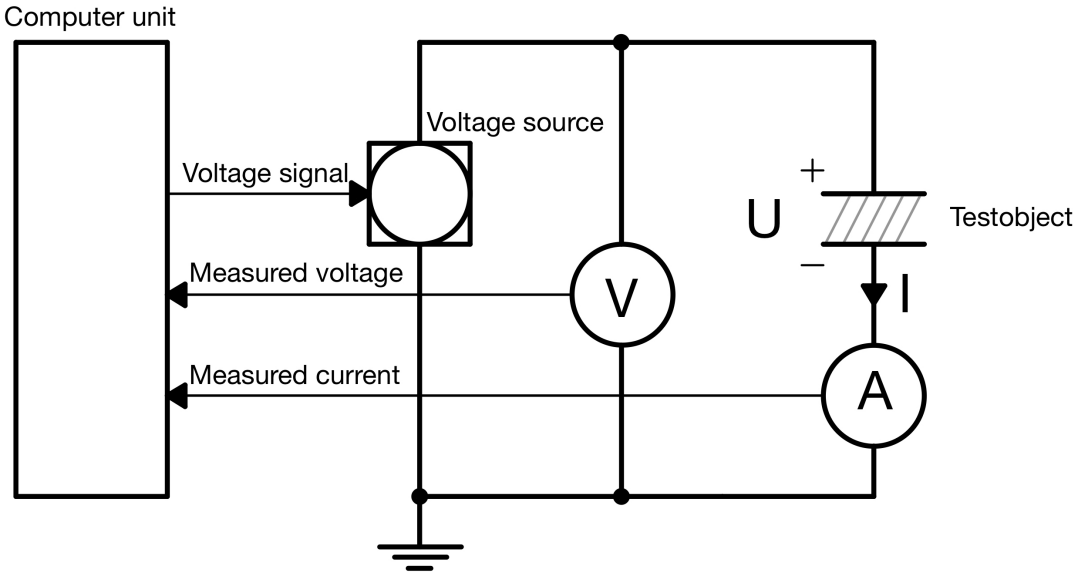

Figure 17: Circuit for the measuring equipment IDA 200. [4]

The IDA unit has its own screen and keyboard to interact with it. The screen shows the readings performed while the measurements are live. Each measuring point will appear eventually when the sequence is started, from highest to lowest frequency. The screen can display the readings performed previously and bring up several graphs from different readings in the same picture. In measurement, a sweep is done with the desired frequencies and voltages. The measurement sweep starts on a chosen voltage level, goes through the frequencies from highest to lowest and then starts on the next chosen voltage level. This continues until the last voltage and frequency are done.

The results given by the IDA 200 are typically the real and imaginary part of the capacitance of the test object. In addition, the value of the losses, $tan\ \delta$ is also commonly extracted from the measuring. It is often an advantage to utilize the readings of the currents and voltages from the insulation diagnostic system. In this work, these are used to show and explain how the varnish behaves with the different electric fields applied. The high voltage unit can apply up to 30 kV and deliver a current of 20 mA, both peak values. The frequency region of the IDA goes from 0.0001 Hz to 1 kHz. With this measuring apparatus, there was used a room temperature around $20°C$ during the measurements. Unfortunately, a wide range of temperatures was not possible. IDA 200 was not used without the high voltage unit during this work. [4]

The drawback of this method was not being able to increase the temperature of the sample examined. The dependency of the temperature was therefore not established. It was not an option to increase the room temperature of the lab. The IDA 200 with the high voltage unit was only able to run to a certain level of frequencies when the voltage level increased. Due to the high loss of the varnish, the current flowing exceeded the limit of 20 mA.

3.1.1 Preparation of Test Object

The test object from the previous project [1] was a good design, the shape and parts were sufficient for the tests planned. There was no problem with applying varnish to the even surface and there were no disturbances in regards to measuring the sample.

After the tests in the previous project [1], new test objects were made. They were made with a newer varnish, considering the production date. The varnish was less viscous, which led to easier application and thin layers. The old varnish used previously was starting to get thick and solid. The test object was made with a method that made it easy to apply varnish and make the layers even eventually. The process of making the test objects is shown in figure 18.

The test objects were made of two cylindrical steel electrodes with a teflon cylinder in the middle. The cylindrical shape gives a homogeneous field distribution, the thickness of the teflon piece decides the concentration of the electric field together with the voltage applied. To be able to apply voltage and characterize the varnish, holes with threads were made on the top and bottom of the cylinders. The start object used with IDA 200 is number 1 in figure 18. With the steel pieces fixed together with the teflon spacer, two 1 mm thick steel rings were placed onto the cylinder. This is number 2 in figure 18. The rings were placed so that the varnish overlapped 5 mm of the electrodes on both top and bottom to get a good connection. The varnish covered the yellow area in number 3 in figure 18. The teflon spacer was chosen to be 20 mm and the length of the varnish then became 30 mm due to the 5mm overlap of the steel. The finished test object is shown as number 4. The dark section in the middle of number 4 is the varnish applied.

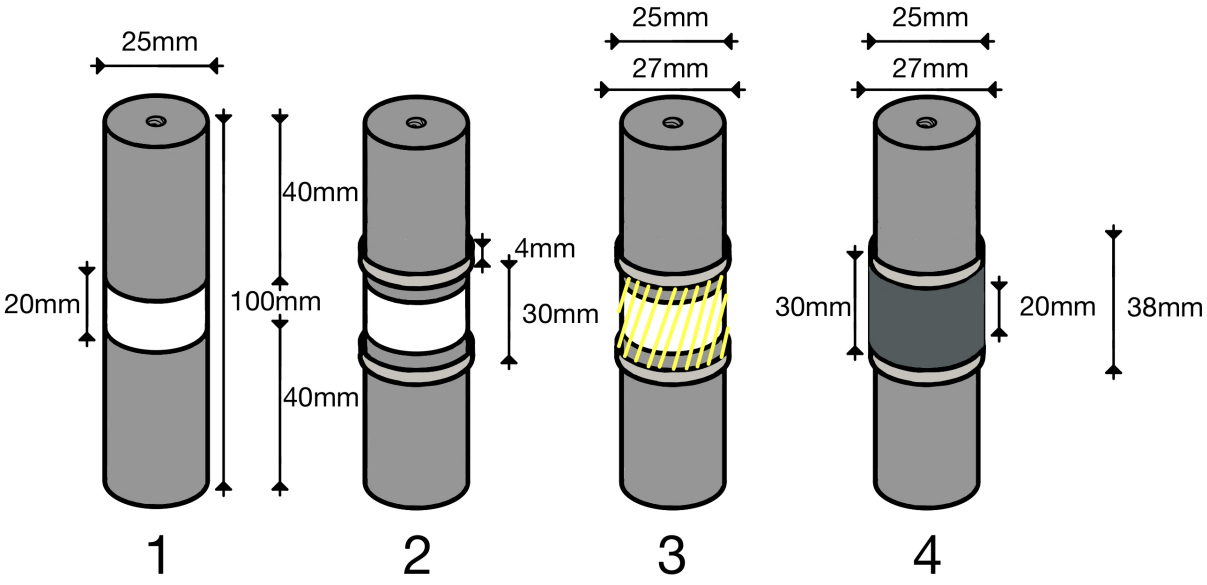

Figure 18: Preparation of test objects step by step with dimensions.

With a brush, the varnish was applied one layer at a time, between the rings. From the data sheet, the normal thickness and time needed for drying were noted. The parameters were important for the finished sample to become as optimal as possible. The thickness of the varnish was chosen to 1 mm, this was a value suited for testing and measuring. The rings were made 1 mm to visualize the thickness wanted during painting. The rings were in addition there to make the surface as smooth and even as possible. Each layer needed to dry for 30 minutes before the next was applied. The last layer was applied when the thickness was just a little thicker than the rings. This was done to make it possible to even out the surface with a sandpaper. 24 hours later, the sandpaper was put against the steel rings. It was fixed to a block of wood and used to sand along the longitudinal direction around the cylinder. This gave a smooth result when gradually finer sandpaper was used.

A homogeneous field distribution was necessary to characterize the varnish properly. As in the specialization project [1], a design with two aluminum toroids was used. In addition, a steel spring was used for the connection point on the top. The spring was used on top of the toroids to avoid any sharp edges around the area where the voltage source was connected. This was used to get rid of inhomogeneities and concentrations in the field around the test object. This would have led to bad measuring results. These same toroids were used during measurements with IDAX 206. The set-up is shown in figure 19.

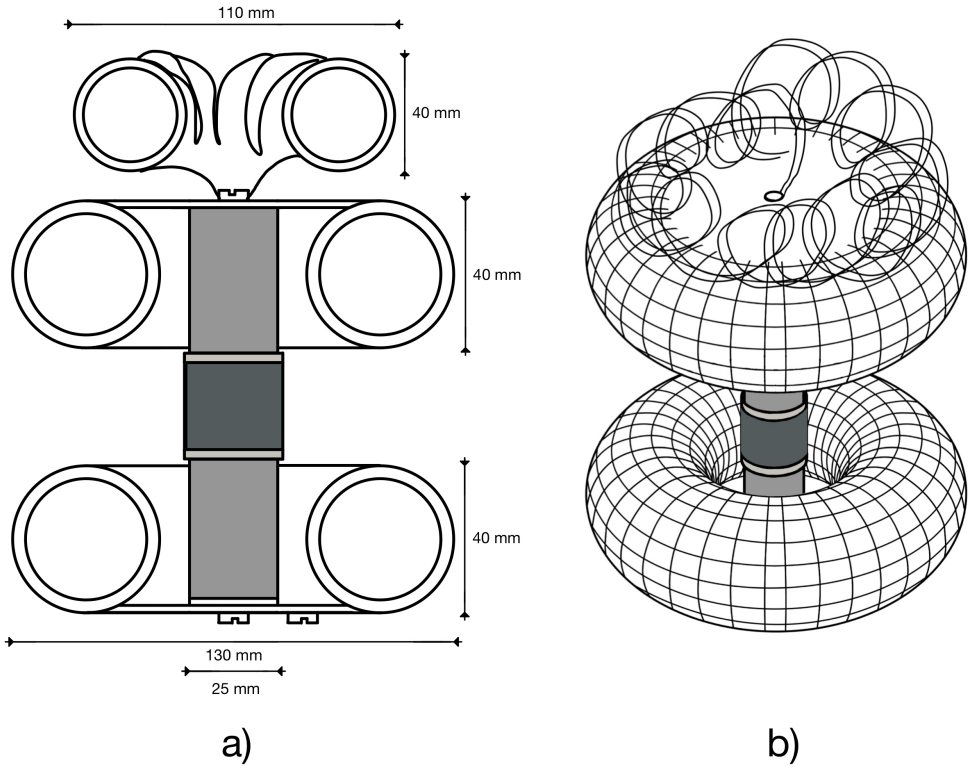

Figure 19: Cross section and 3D illustration of the set-up used, toroides surrounding the test objects with dimensions.

The plates on top of the toroids have holes for fixing the cylinder between them, shown in figure 19a). The figure also shows one screw on the top and two on the bottom, the one on the top is for connecting the voltage. The one in the center underneath is for measuring or ground. The third screw, placed on the lower toroid, is for a guard. When a guard is used, the center screw and the cylinder are insulated from the lower toroid with a thin washer made out of teflon, as shown in the bottom of figure 19a). The whole set-up, as shown in b), was placed on top of an insulating stand to avoid disturbances.

3.1.2 Preparation of Test Set-Up and Characterization

Before the characterization, the IDA 200 needed to be prepared. First, the test object was connected to the voltage application clamp on top and the ground clamp on the bottom. The insulating washer was removed from the bottom of the lower toroid. This toroid had a connection to ground during these measurements with the IDA 200. The one on top had potential applied. The measuring circuit can be seen in figure 17.

Before applying voltage and starting the measurements, the desired parameters needed to be inserted. There was done a couple of measurements to find the limits of the apparatus considering the given test object. This was done to get as much information as possible from the different parameters. It was for example not possible to use frequencies higher

than 100 Hz and lower than 4.6417 Hz at 7.5 kV, for the newest test sample. With high voltage and low frequencies, there were often problems with the values measured. These are neglected from the results. There were no measurements that could pass 10 kV, the majority of the measurements ended at 7.5 kV. 7.5 kV was used as a base and 10 kV was tried until a possible over-current occurred. The voltage levels used was 0.5, 1.0, 2.5, 5.0, 7.5, and 10 kV. The frequencies applied were always from 100 Hz down to 0.1 Hz.

It was possible for the high voltage to destroyed or influenced the test object. The 1 kV measurement was therefore repeated at the end of the measuring sequence. The reason for the repetition is to see if the measurements are any different. The test object could be damaged or affected by the voltage stress. In addition, there was performed two measurements on the sample with the new varnish. This was mainly to confirm the results.

After the sweeps of frequencies and voltages, the data could be extracted from the computer unit and exported to Excel and MATLAB.

3.2 Characterization with IDAX

3.2.1 IDAX 206 with Heating Cabinet

IDAX 206 is a device made for insulation diagnostic analyzes, such as the IDA 200. The biggest difference is that the IDAX can use higher frequencies because of the low voltage. The spectrum of frequencies is an advantage but the lower voltage level is a disadvantage, compared to the IDA 200. In addition to the analyzer itself, a thermal cabinet was used during these measurements. The diagnostic system uses a range of different frequencies and voltages. The circuit of the IDAX 206 is the same as the IDA 200, shown in figure 17.

The analyzer has its own screen and keyboard, as the IDA, to navigate in its software. The measured points will appear on the screen during the sweeps. Unlike the IDA 200, the IDAX 206 was set to only go through one voltage level. The IDAX 206 can apply from 0 to 200 V_{peak} and a current from 0 to 50 mA_{peak}. The frequency range of the unit goes from 0.0001 Hz to 1 kHz. The voltage chosen for the measurements of this characterization device was 200 V. The highest possible voltage was desired to get the electric field as strong as possible. Other voltages were also tested during this measurement and used in the results. At the chosen voltage the analyzer goes through the chosen frequencies, the values are then shown on the screen. The results from the IDAX 206 were chosen to be the same parameters as the IDA 200, the real and imaginary capacitance and the loss factor $tan\ \delta$. [10]

The thermal cabinet was also a huge advantage considering the characterization of the varnish regarding its dependence on the temperature. During the measurements with the IDAX, the thermal cabinet was used consistently. The measurements were done at seven different temperatures with the same frequency sweep. The voltages used during the measurements were 50, 100, 150 and 200 V. The temperatures 20, 50, 75, 100, 125 and 150 °C were used with the voltages. There was performed a 20°C measurement a second time, after the sample had been exposed to the thermal stress to check if the sample took any damage or got influenced by the stress.

3.2.2 Preparation of Test Object

The same test object was used with the IDAX 206 as with the IDA 200 in the beginning. After characterizing the same sample as previous, shown in figure 18, it was observed that the concentration of the electric field did not reach the desired levels. Because the maximum voltage was applied, the other parameter in expression 13 needed to be changed. The thickness of the teflon spacer was therefore changed from 20 mm to 5 mm, the new test object is shown in figure 20. By utilizing and changing the parameters in equation 13, this new sample made it possible to get a more concentrated electric field around the varnish.

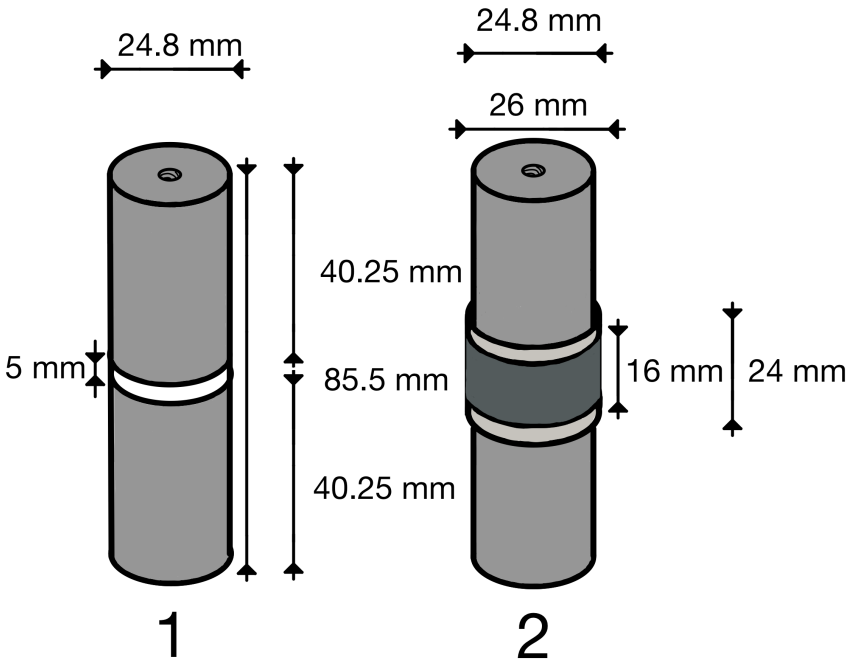

Figure 20: Illustration with dimensions of the test object with 5 mm teflon between the electrodes.

The new test object consisted of the same two steel electrodes and the thinner teflon spacer in between. As with the first test sample, the section of varnish is selected by sliding and placing the thin rings so that the varnish overlaps the electrodes approximately 5 mm on each side. It is important to establish a good connection to the electrodes.

The varnish was painted in the same way as in the preparation of the previous test sample. With a brush, one layer was painted at a time, with 30 minutes drying in between. The thickness of the rings and the varnish were chosen to be thinner this time. The thickness of the varnish after sanding was therefore 0.6 mm for this new sample. The reference thickness of the rings was thus changed from 1.0 to 0.6 mm.

3.2.3 Preparation of Test Set-Up and Characterization

With the IDA 200 measurements, some field controlling toroids and a spring was added. This was also mounted on the new test object for the IDAX 206 measurements. The guard, which in this work is represented by the lower toroid, was used for the measurements with the IDAX. The test object was placed in the heating cabinet, then the voltage, guard and measuring connections were made. After it being placed in the cabinet, the desired temperature was set. The temperature inside the cabinet was kept for approximately 24 hours. This was done to heat up the sample so that the temperature was evenly distributed in the whole varnish geometry. The inertia of the heat in the varnish is then taken into consideration, the innermost layer is the same temperature as the outermost layer. This process was repeated for each temperature setting and the measurements were

done after the 24 hours of heating before the temperature was set and increased to the next step.

As mentioned, the test sweep for the sample was performed with 200, 150, 100 and 50 V. The frequencies used were from 1000 down to 0.1 Hz. In the beginning, it was performed experimental sweeps with frequencies up to 1000 Hz. The results from using 1000 Hz could resemble the results from using 100 Hz. The highest frequency that gave a total measurement with the different voltages was 100 Hz. These are shown in the results. 1000 Hz was still used due to the similarities. The limitation of frequency was most likely caused by the limitation of 50 mA_{peak} for the maximum allowed current. The most interesting part of these tests was to see the dependency of the frequency and temperature. It was difficult to achieve an electric field as strong as desired, with the low voltage from the source of the IDAX 206.

After the sweeps of frequencies with 200 V_{peak} and other voltages, the data could be extracted from the computer unit and exported to Excel.

3.3 Potential Measurements Using an Electrostatic Voltmeter

3.3.1 Electrostatic Voltmeter

An electrostatic voltmeter measures the potential on a surface with a probe. The voltmeter is made for voltages from a couple of hundreds to several thousand. This particular electrostatic voltmeter can measure potentials from approximately 1000 V up to 50 kV, values below 1 kV will be very imprecise. The apparatus has 4 different measuring settings, each for different voltage levels. The first setting is from 0 to 5 kV, the second is from 0 to 10 kV, the third is from 0 to 25 kV and the last one is from 0 and 50 kV. The only preparation needed for the electrostatic voltmeter was to set the indication needle to zero so that the measurement starts at zero potential. In addition, the right interval of voltage level needed to be set.

3.3.2 Preparation of Test Object

There was used five different test objects for these measurements, mainly two cylindrical objects and three generator bars. The two cylinders were made like the previous cylinders used with the IDA 200 and IDAX 206. The cylinders consist of the two cylindrical steel electrodes and the teflon spacer in between. The biggest difference compared with the previous test samples is the length of the teflon spacer. One of the three generator bars was used by a researcher from SINTEF and had been exposed to a thermal cycle, which means the varnish had been affected by heat. The other two bars were made with a sander and new layers of varnish.

The spacers used in the cylinder test objects were 100 mm, in difference to 20 mm and 5 mm used in the earlier measuring methods. The varnish was applied in the same way as previously mentioned. The two reference rings were placed 7.5 mm from the teflon, which means the varnish overlapped the same length of each steel electrode. The overlap was slightly greater than the one on the previous test object from the IDA 200 and IDAX 206 measurements, which had an overlap of 5 mm. This made the varnish obtain a good connection to the electrodes, like the other test samples. The rings were made 1 mm thick and the thickness of the varnish, therefore, became 1 mm after sanding the redundant and uneven surface. The test object is shown in figure 21.

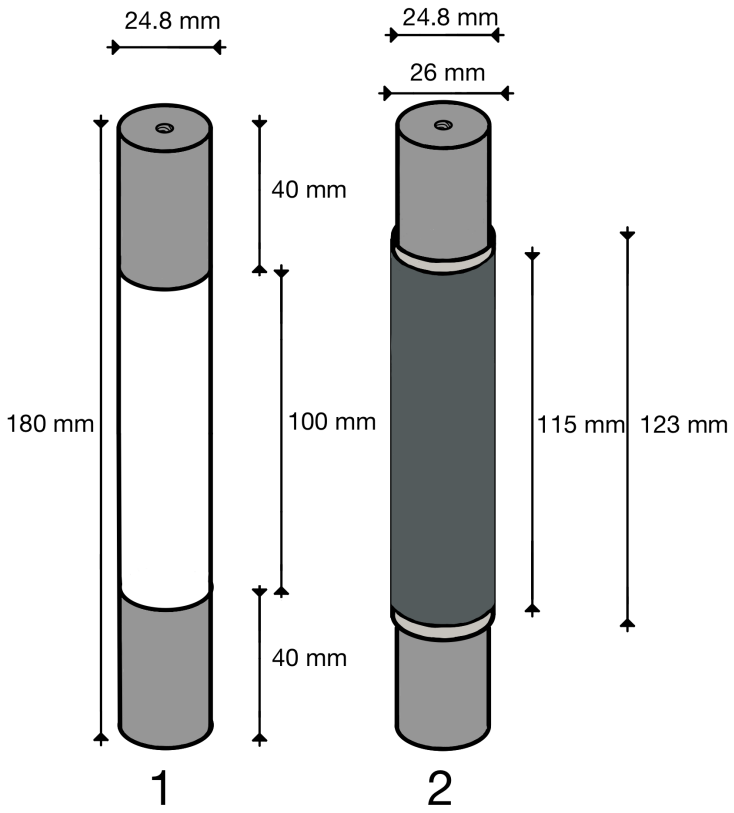

Figure 21: Illustration with dimensions of the test object with 100 mm teflon between the electrodes.

The generator bars were cut into 460 mm pieces as shown in figure 23. At the outer ends of the bars, 20 mm of the insulation was removed to be able to get a good connection when applying voltage. The bars had many thin layers of insulation and a conductive outer layer. This outer layer was removed with a sander in both ends. The sections sanded were going to represent the end windings. These sections with no conductive layer were made 150 mm long, leaving 120 mm of the conductive layer in the center of the bars. This is shown in figure 22. The end winding area was going to be covered with the field grading varnish, a couple of layers at a time. The varnish needed to overlap the conductive area as shown in figure 16. The length of the varnish layers was therefore chosen to 155 mm, illustrated in yellow in figure 22. Measurements were performed before application, on the insulation, and between the layers of the varnish. The varnish was applied with the same tool as the one used on the other test objects, with a painting brush. The length was chosen considering getting an area similar to a real-life scenario. This would result in a more realistic measurement of the surface potential. It was important to get a good and even distribution of the potential measurements. The varnish was applied one layer at a time, with 30 minutes of drying in between. The thickness recommended from the data-sheet was between 0.2 and 0.5 mm.[7] There were performed measurements on 0.2 - 0.3 and 1 mm thick varnish on the bar. When taking the generator bars into account, the layer of finished varnish was not even at all. The varnish was therefore sanded, like the cylinder samples, to get rid of the uneven elevations on the surface of the varnish.

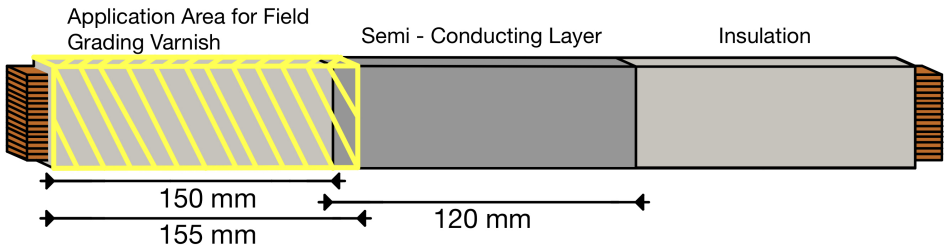

Figure 22: Illustration of the test bars with a transparent layer of varnish marked in yellow and the conductive layer removed on both outer ends.

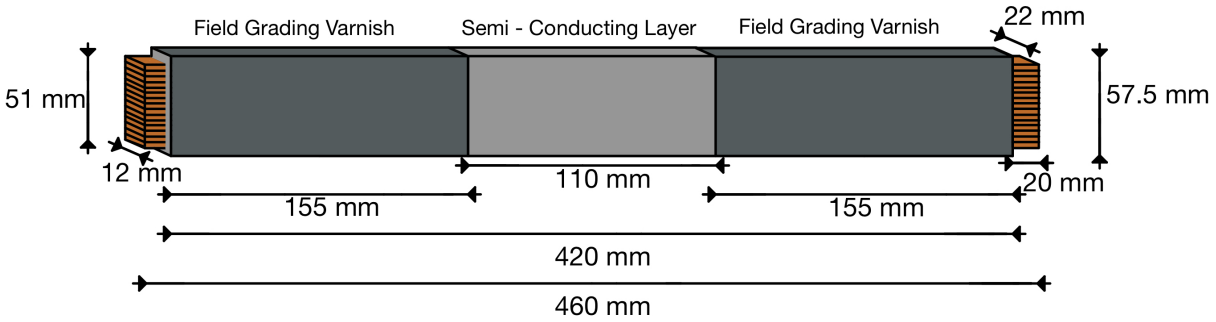

Figure 23: Illustration of the test bars with 155mm of varnish applied and a 110 mm remaining section in the middle with the conductive layer. Dimensions of the generator bar sample.

3.3.3 Preparation of Test Set-Up and Measurements

Both the cylindrical test objects with the 1 mm thick varnish and the generator bars were placed in an insulating stand that kept them away from the ground and other objects that could interfere with the measurements. The different samples were compared to each other. The measurements on both the cylinders and generator bars were done by fixing a steel wire around the section with varnish and securing the ends of the measuring wire to the electrostatic voltmeter. More precisely, the steel wire was attached by wrapping it around the varnish twice and then tightened so it became completely snug to the surface of the varnish. With the test object in the stand and the wire being perpendicular to the surface of the varnish, the application of voltage and measuring could start. The cylinder sample used one screw in each end to apply voltage and ground. For the generator bars, all the conductors had to be connected before voltage could be applied. This was done by using a clamp that touched all the conductors and created a good connection between them. The voltage source was connected to this clamp. To represent the grounded stator core, a steel wire was wrapped snugly around the 110 mm long middle section of the bar and connected to ground. The core was simulated approximately at the end of the varnish. The voltage source consisted of an adjustable 230 V source and a transformer with the ratio of $230\,V : 100\,kV$. The voltages for the cylindrical test object were 15 and 20 kV. For the generator bars with a rated line voltage of 6.4 kV, both 6.4 kV and 11 kV

were applied. The measurements started when the voltage was increased from zero to the given potential.

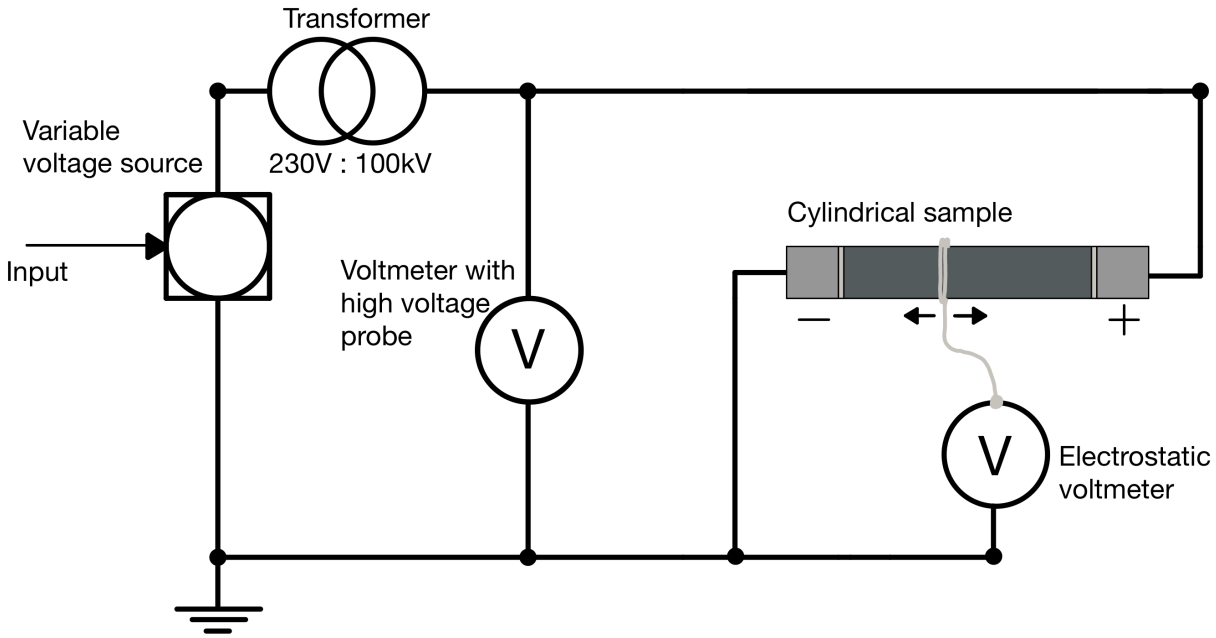

Figure 24: Illustration of Test Set-Up, voltage source, transformer, test object, voltmeter and electrostatic voltmeter.

The measurements were performed by placing the measuring wire at a given position on the varnish on the cylinder. The test set-up for the cylinders is shown in figure 24. The positioning of the measurement wire is shown by the opposing arrows below the cylindrical sample in the figure. On the cylinder sample, the measuring wire was placed in eleven different positions between the steel rings on the varnish. The voltage was applied on one side of the cylinder and the other side was grounded. When the voltage was applied, the needle of the electrostatic voltmeter moved to the measured value. A precise measurement assumes that the needle was set to zero before starting the measurements. The measured value shown on the electrostatic voltmeter was noted before the voltage was turned off. The same goes for the generator bars. On the generator bars, the different measurements were performed by changing the position of the measuring wire that was wrapped around the varnish. It was performed one measurement at every centimeter all the way down the insulation and area covered by varnish, on both test bars. The same method was used on both cylinders and generator bars. With the varnish applied, there were performed denser measurements in a section. In the section from 0 to 4 cm, there were performed measurements every 0.5 cm. This was necessary to get a more detailed curve in this section.

The measuring set-up for the generator bars is shown in figure 25. An additional measurement was performed on the two generator bars prepared from scratch. After the conductive layer was sanded in the outer ends, there was performed potential measurements on the insulation before applying the varnish. The potential was also measured

after four layers of varnish and finally after eight layers. The thickness of the four layers was measured to approximately 0.3 mm at bar number 1 and 0.2 mm at bar number 2 after sanding. The thickness of all the eight layers, sanded, was measured to approximately 1.0 mm on both. For the bars, there were performed measurements on both sides of the grounded middle section. The bars were therefore flipped and measured again on their other end.

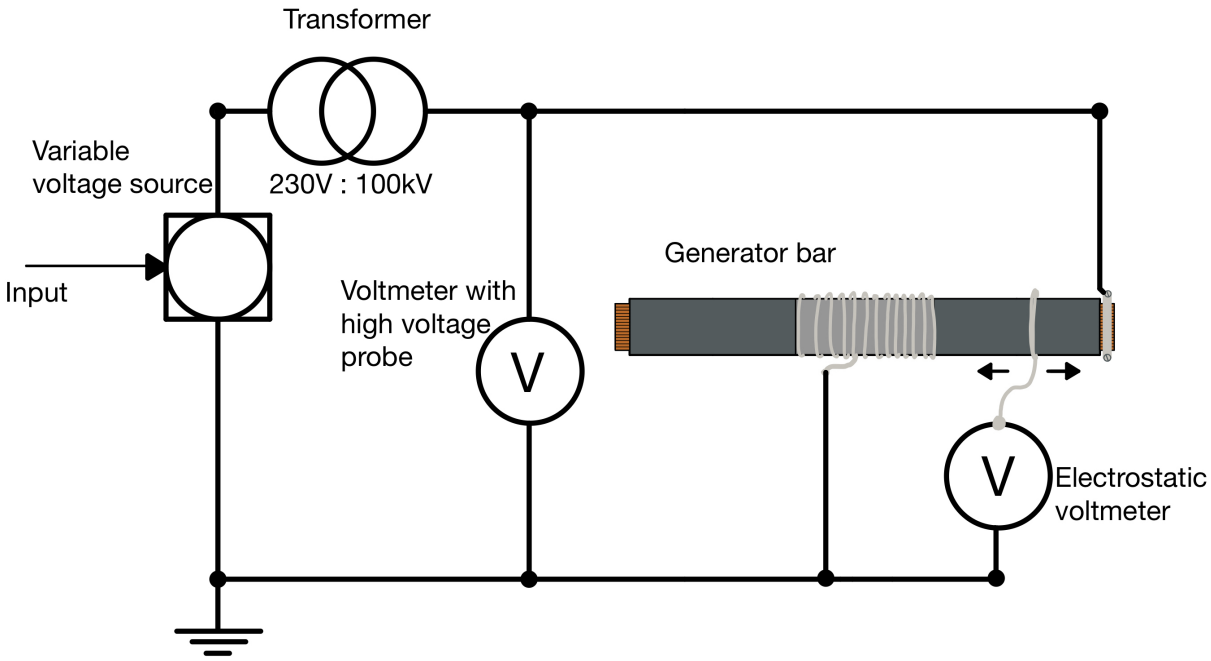

Figure 25: Illustration of Test Set-Up, voltage source, transformer, test object, voltmeter and electrostatic voltmeter.

3.4 Analysis Using a Megger

3.4.1 The Megger

To characterize the varnish considering the conductivity and resistance a megohmmeter, also called a megger, was used. The megger can perform different tests and measurements, mainly on insulation and dielectric materials. It can perform resistance and polarization measurements, both used in this work. During the polarization measurements, the resistance and current were investigated. The megger used, had different presets when voltages were considered, 1.0, 2.5, 5.0, 10 and 15 kV. The voltage applied from the apparatus was DC, it used a positive, negative and guard probe for application and measuring. The megger had a measuring interval of 5 seconds, which means it reads the current and voltage every 5 seconds. Data from the megger was easily transferred to a computer after the measurements.

3.4.2 Resistance, Polarization and Depolarization

The same cylinders from the previous tests with the IDA and IDAX were used with the megger. The cylindrical samples with both 20 and 5 mm teflon spacers. The toroids were used in the set-up as well. In the specialization project [1], polarization and depolarization measurements were performed, the currents measured did not obtain a steady state value as desired. Therefore, a series of new measurements were performed. This time with a longer polarization and depolarization time. The new time for the measuring was set to 100 minutes, 50 minutes for each of them.

The resulting values from these charge and discharge tests were the steady state currents and resistances. The applied voltage and the corresponding electric field applied during the measurements were also used. The conductivity was calculated from the resistance measured and the geometry of the varnish. These values were plotted together with the applied electric field. The currents and conductivities were used in the modeling process.

An old test object from the previous work in the specialization project [1] was used in addition to the ones from IDA and IDAX. In total 5 different test objects were used for the megging. Two samples with 20 mm teflon spacer. One with varnish from the previous work and one with varnish that had been heated in the thermal cabinet from the IDAX measurement sequence earlier. The remaining three test objects were made with new varnish, one of them failed during the polarization with a field of 1 kV/mm. The sample was probably badly produced. The layers of the varnish were unique, not one similar to the other. The varnish was brittle and hard to mount to the toroids without affecting the sample. Two test objects were used to make it possible to compare them afterward. A new one had to be made when one failed. It was intended 2 samples of each type, 5 mm and 20 mm.

The measured values from the megging were used to calculate the conductivity of the varnish. By using the geometry of the varnish, equation 22 can be utilized.

$$\begin{aligned} R &= \rho \cdot \frac{l}{A} \rightarrow \rho = R \cdot \frac{A}{l} \\ \sigma &= \frac{1}{\rho} = \frac{l}{R \cdot A} \end{aligned} \tag{22}$$

The A in equation 22 above is representing the cross-section of the varnish on the cylindrical test sample. The l is representing the length of the space between the electrodes. R is the measured resistance from the megger. The resistivity ρ is found from the measured value R and the dimensions of the varnish. The conductivity is then extracted from these values, the inverse of the resistivity.

In addition to the graphs obtained from these measurements and calculations, it was interesting to find and develop a common graph and expression. The goal was to find an expression and graph that represents the measured values. The theory from section 2.1.3 was therefore needed.

4 Experimental Results & Discussion

It was performed four different tests to characterize the varnish. This section consists of five subsections. The first two are the IDA 200 and the IDAX 206 measurements. The third subsection is a comparison of these two. The last two subsections are the megging and the potential measurements.

4.1 IDA 200 Measurements

With the IDA 200 mainly the $tan\ \delta$ and capacitance were measured. The measurements were done on both a test sample with a new and old varnish. Graphs of the field dependency were made from the same measurements. From the current measure, a clear change was possible to observe in the sinusoidal.

The electric fields present during the measurements performed with the IDA 200 was 0.025, 0.05, 0.125, 0.25, 0.375 and 0.5 kV/mm with the voltages 0.5, 1.0, 2.5, 5.0, 7.5 and 10 kV respectively.

No Varnish

The measurements, without varnish applied to the cylinder, were low compared to the ones with varnish. The goal of these measurements was to check how the teflon influenced the measurements. The values were necessary so that they could be subtracted from the later measurements with varnish. The negative values in figure 26 and 27, could mean that the losses of the teflon are lower than the ones of the inner components of the measuring equipment. A negative loss factor is not possible in real life. The measurements for both the loss and the capacitance can be observed in figure 26 and 27.

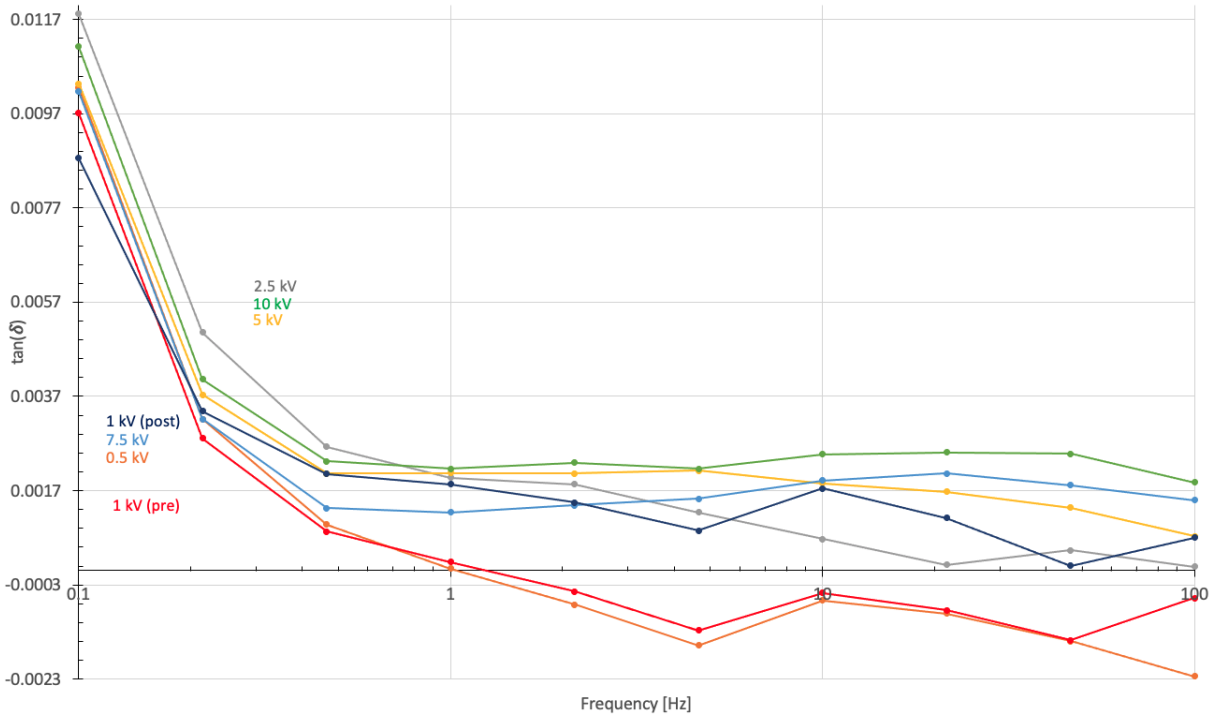

Figure 26: Dielectric loss as a function of frequency measured with no varnish applied to the test object.

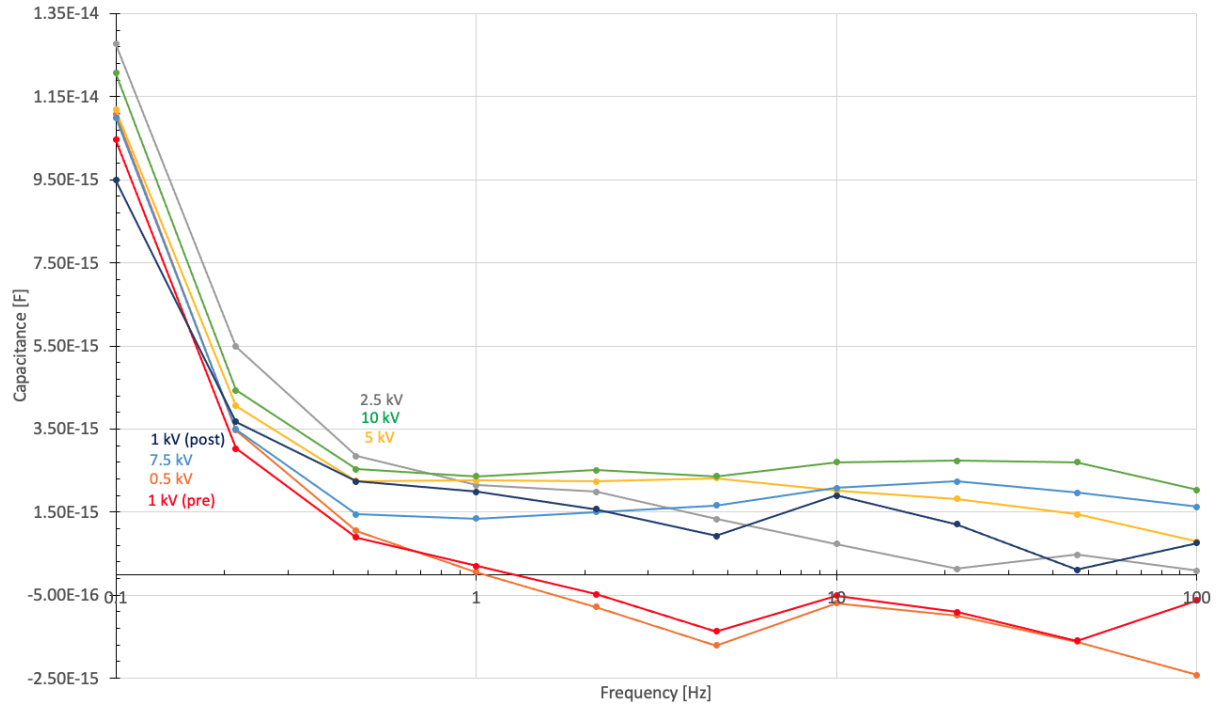

Figure 27: Imaginary part of the capacitance, C'', as a function of frequency measured with no varnish applied to the test object.

4.1.1 Loss Factor

The measurements from the IDA 200 were performed with two different samples, one with old and one with new varnish. The old sample was from the previous work [1]. It was performed two measurements on the new sample to see if there were any differences. In addition, it was performed two measurements with 1 kV, one before and one after the voltage stresses. They were given the names "pre" and "post" respectively. These two graphs are shown on top of each other, which means that the stresses did not influence the properties of the varnish. This applies to both loss and capacitance.

Old Varnish

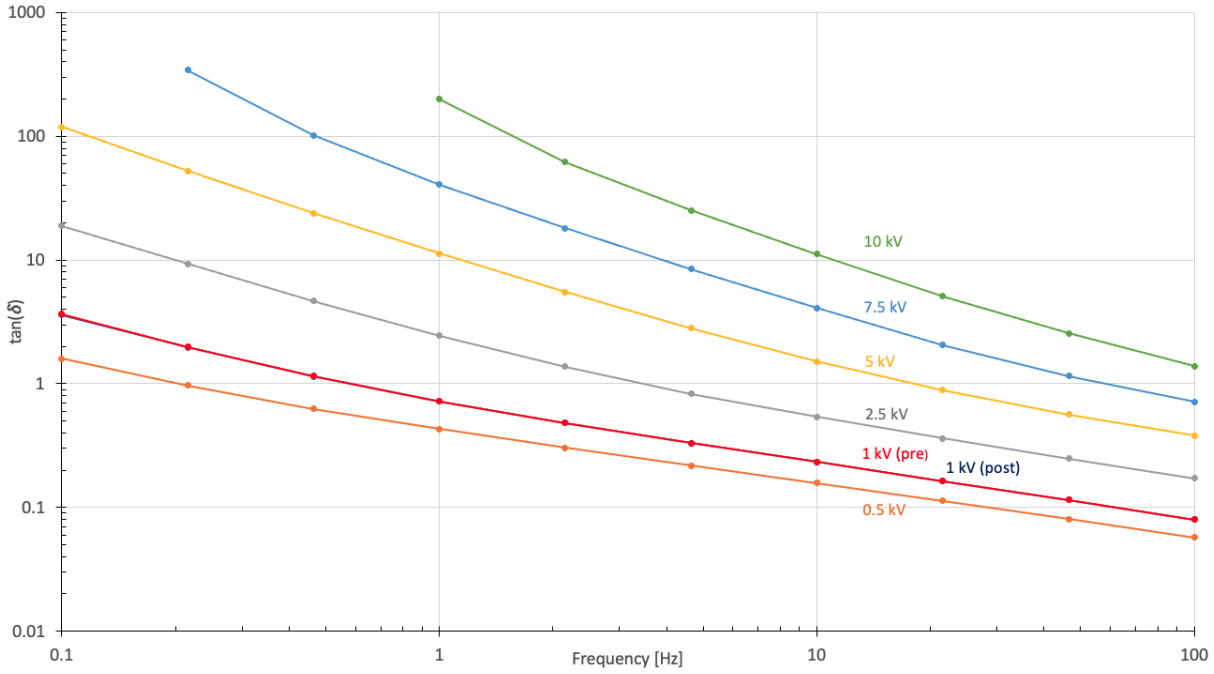

Figure 28: Dielectric loss as a function of frequency measured with the old varnish applied to the test object. This test object is from the earlier specialization project.

The old varnish had a higher viscosity than the new one. It is therefore a possibility that there will be a difference in the dielectric properties of the two varnishes. Measurements were therefore performed for both the old and the new sample. The graph from the old one is shown in figure 28 and the new one is shown in figure 29. The IDA was able to apply 10 kV on the old varnish and not the new one.

New Varnish

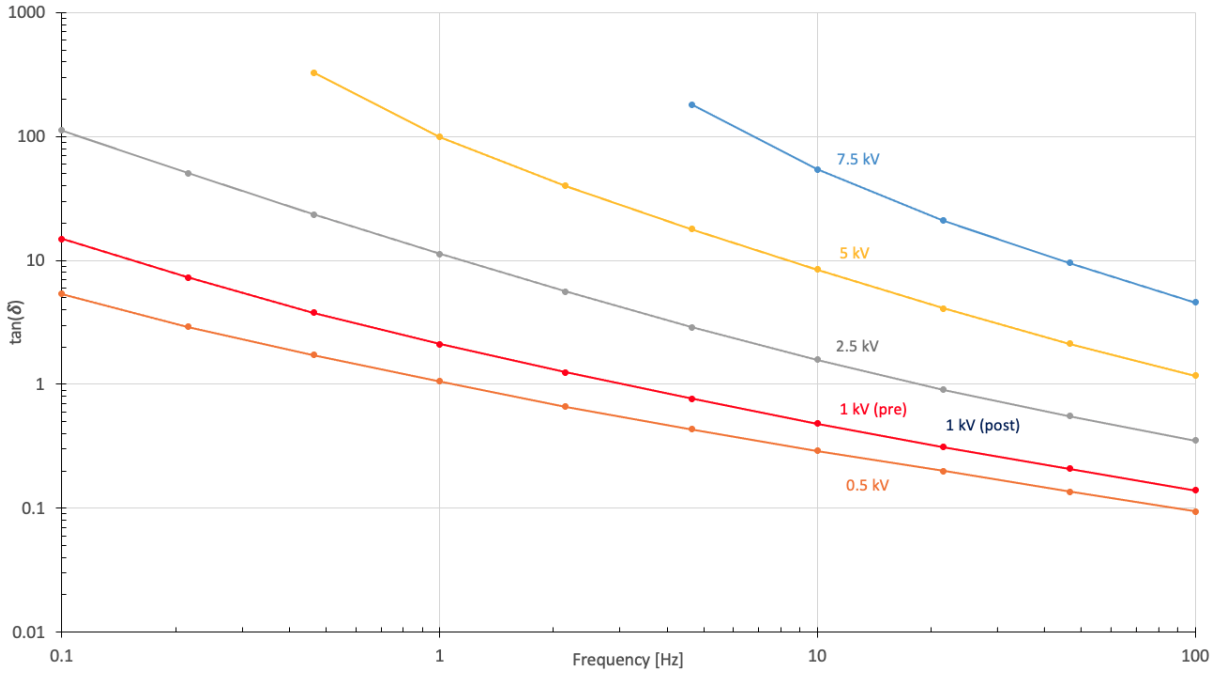

Figure 29: Dielectric loss as a function of the frequency measured in measurement number 1 with the new varnish applied to the test object.

The graphs are pretty stable and linear, this tells us that the losses are most dependent on the conductivity of the material. When the frequency increases the losses decrease. This means that the conductivity is decreasing as well. This was also discovered in the previous work [1].

The IDA 200 was not able to apply the high voltages with the low frequencies, as the figures in this section show. Some measuring points are not present due to this. With a 100% successful test, it would have been measuring points from 0.1 up to 100 Hz at all voltage levels.

The difference due to the electric field is greater with the low frequencies than the high frequencies. This difference in losses is best represented by the graphs from the new varnish. The test object had a 20 mm teflon spacer, which means the fields were 0.025, 0.05, 0.125, 0.25, 0.375 and 0.5 kV/mm.

The biggest difference between the old and the new varnish sample is that the values of the new one are higher. For example, the 5 kV graph shown in yellow, crosses approximately 10 with the old varnish and 100 with the new varnish at 1 Hz. This could be caused by a bad sample or that the old varnish was compromised. The difference is approximately one order at the high voltages, below 2.5 kV the losses are similar.

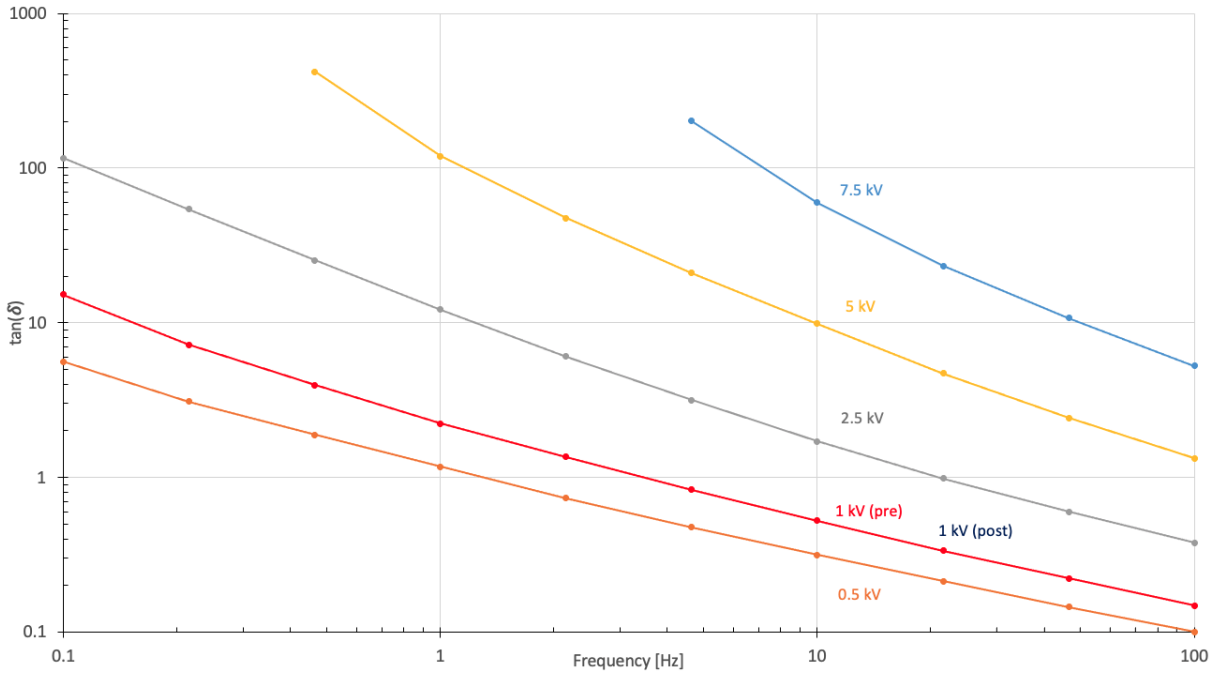

Figure 30: Dielectric loss as a function of the frequency measured in measurement number 2 with the new varnish applied to the test object.

Figure 28, 29 and 30 are, as mentioned, different from each other. The figures from the tests of the new varnish are almost identical. Figure 28 has lower values, if the results from the old and new varnish are compared. Human factors are a typical reason for the differences in the results of the new samples. The difference between the old and the new varnish could be caused by the old thick varnish or that the old sample was exposed to voltage stress earlier. It is also possible that human factors may have influenced the old sample. The varnish was mixed before application by hand and there is no guarantee that the mixture becomes identical every time a layer was painted on. The varnish may cure over time, which means that the old one had cured longer than the new. During the painting it was noticed that the varnish became thicker and more viscous with time. As the bucket became more empty the varnish became worse. With small amounts of the old varnish left, the remaining substance was much thicker and more cured compared to when it was new. This was confirmed when a new bucket of varnish was opened. The varnish with high viscosity made the application harder and the heavy particles were probably denser in the remaining part of the varnish in the bucket.

4.1.2 Capacitance

The IDA 200 measured both the real and the imaginary parts of the capacitance. It was only the imaginary part that changed during the measurements, according to the insulation diagnostic analyzer. From figure 31, it is easy to see that the readings are linear and pretty stable. The curve of the graphs is similar to the losses from the previous section.

Old Varnish

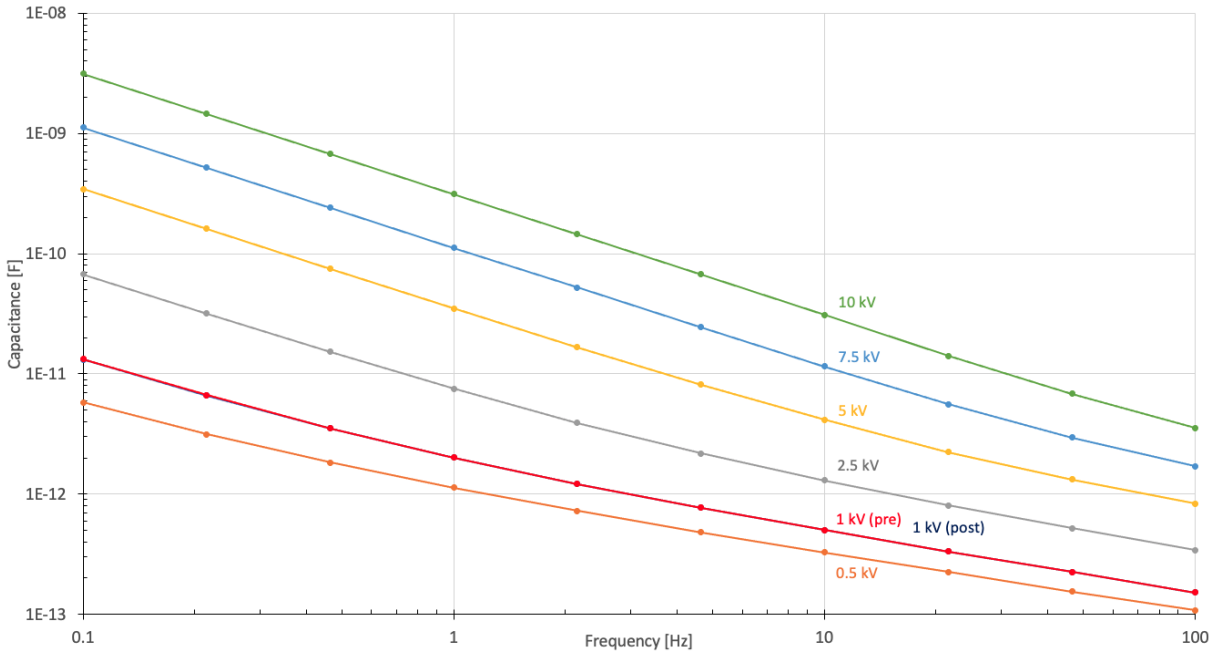

Figure 31: Imaginary part of the capacitance as a function of the frequency measured with the old varnish applied to the test object.

The graphs that show the measured values of the new and the old varnish can be compared. These are found in figure 31 and 32. These graphs are more similar than the graphs of the losses. But still some difference considering the capacitance. For example at 5 kV, shown in the yellow graph, the old varnish crosses 1 Hz at approximately $3.7 \cdot 10^{-11}$ F. For the new varnish, it crosses at approximately $2.4 \cdot 10^{-10}$ F.

New Varnish

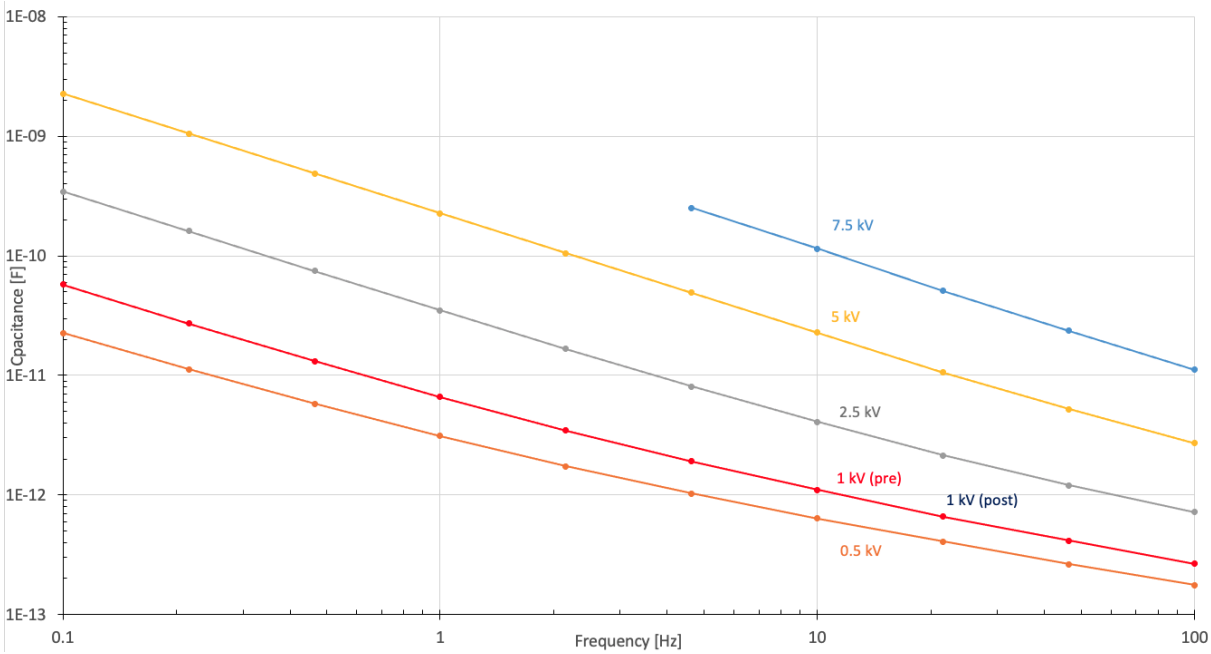

Figure 32: Imaginary part of the capacitance as a function of the frequency measured in measurement number 1 with the new varnish applied to the test object.

The two measurements on the new varnish are almost identical, this is of course desired. They cross 1 Hz at approximately $2.4 \cdot 10^{-10}$ F and $2.9 \cdot 10^{-10}$ F at 5 kV, which is quite similar. The difference is expected because each measurement will have some variations.

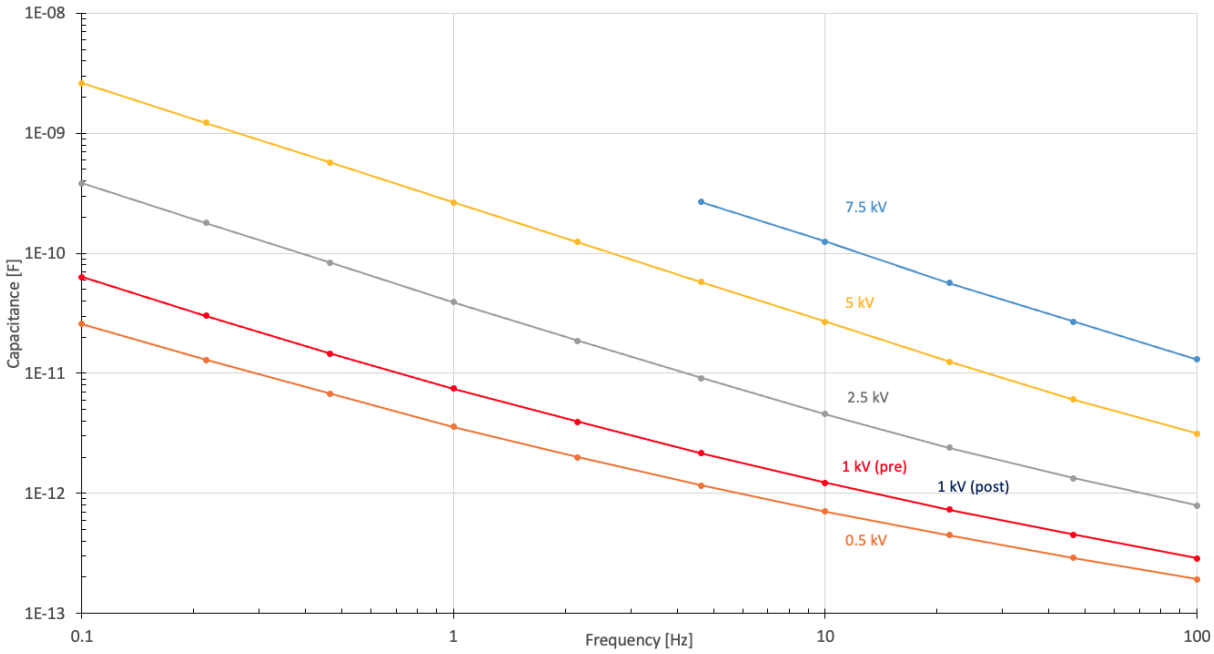

Figure 33: Imaginary part of the capacitance as a function of the frequency measured in measurement number 2 with the new varnish applied to the test object.

When it comes to the dependency of the frequency, the graphs have a similar decreasing shape as for the losses. The capacitance decreases with the increasing frequency. As mentioned in the previous section, the field is influencing the lower frequency region more than the higher frequencies. In addition, it increases the imaginary capacitance with almost one order for each step up in voltage or field. This is influenced by the permittivity and its dependency on the field and frequency.

If all the graphs in the figures from the IDA 200 measurements are considered, the measurements are approximately linear, especially at the low voltages. This means that with both the x-axis and the y-axis logarithmic scaled, the losses and the capacitance of the varnish are mainly dependent on the conductivity.

4.1.3 Field Dependency

No Varnish

The measurement without varnish was performed to see how much the teflon contributed to the losses. As shown in figure 34, the loss values from the teflon are minimal so the losses from the varnish will not be affected.

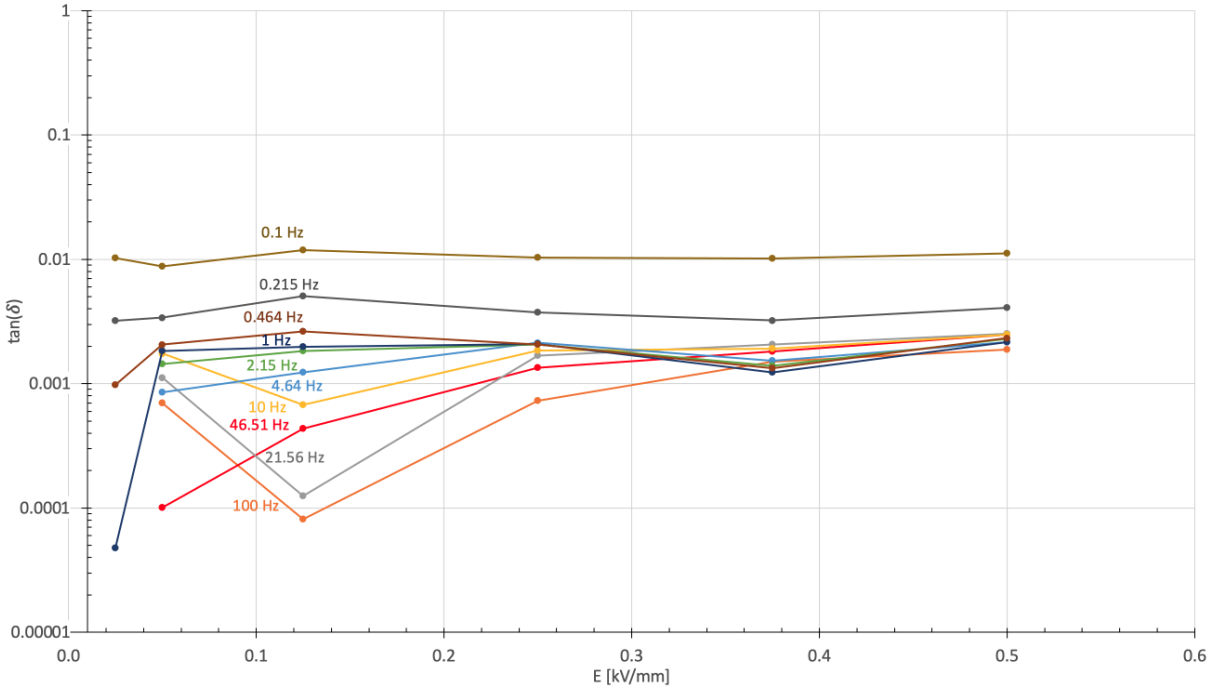

Figure 34: Loss as a function of the electric field measured with no varnish applied to the test object.

Old Varnish

The dependency of the field can be seen in figure 35. The curve of the graphs can be compared to an inverse exponential curve. With an increased electric field, the losses are getting higher. The figure shows that the graphs have an inverse exponential form. The derivative of the graphs decreases and they flatten out. It is also a slight difference in the increase of the losses with the frequency. Together with the increased electric field, the lower frequencies will give an additional increase.

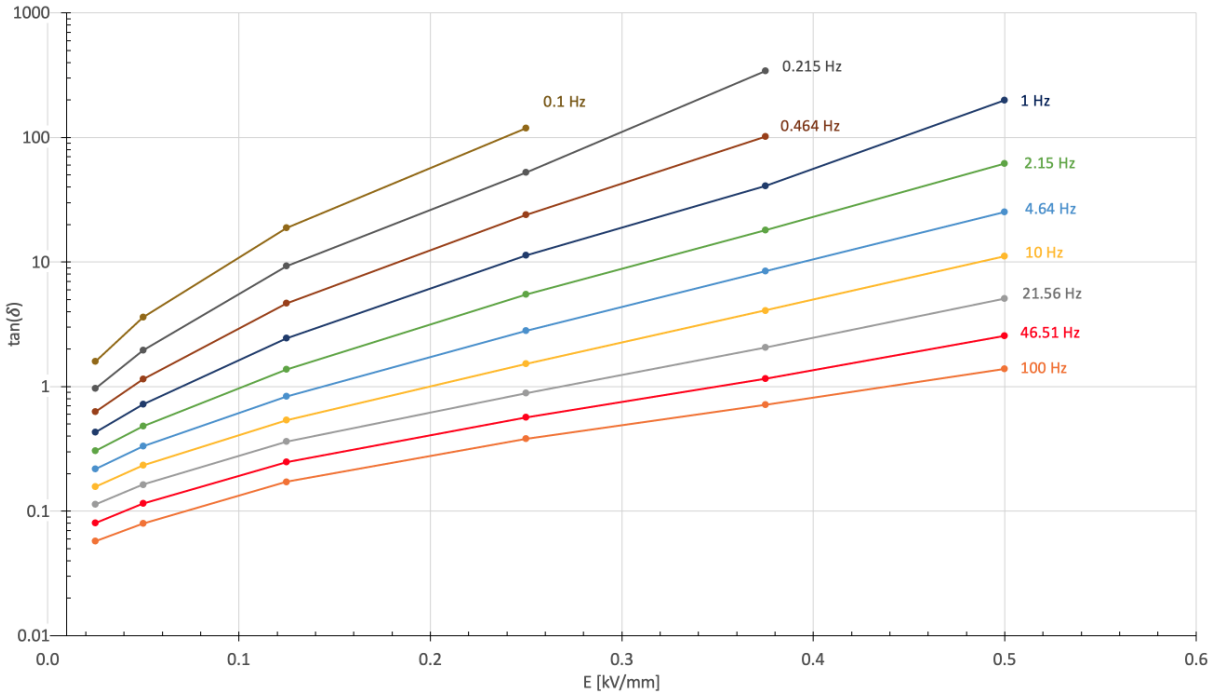

Figure 35: Loss as a function of the electric field measured with the old varnish applied to the test object.

New Varnish

If the measurements from the old and the new varnish are compared, it can be observed that the values from the tests with the new varnish are higher than the ones with the old varnish. With a frequency of 10 Hz and a field of 0.25 kV/mm, the value is 1.52, for the old varnish. For the new varnish with the same conditions, the value is approximately 9.15 from the two measurements. This is a noticeable difference.

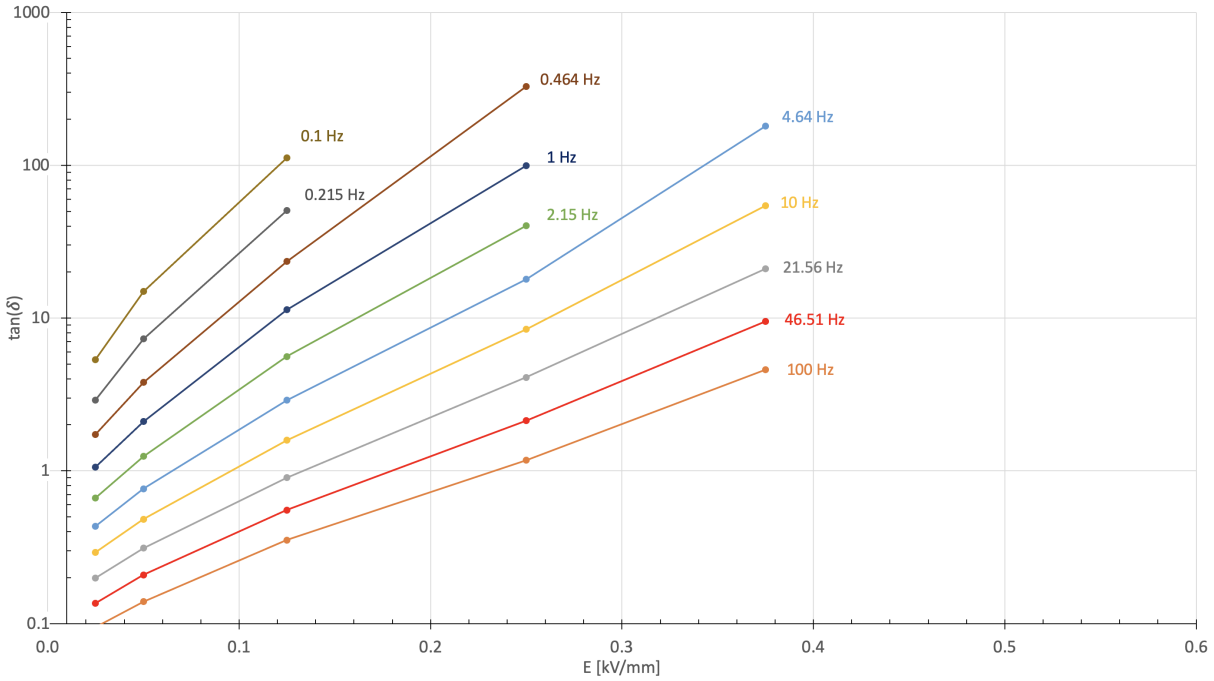

Figure 36: Loss as a function of the electric field measured in measurement number 1 with the new varnish applied to the test object.

For example, the losses at 100 Hz are lower than for the low frequencies. It is normal to assume that this is connected to the polarization mechanisms and the contribution from the permittivity. The conductivity, which is the dominant part of the loss, is dependent on the frequency. From equation 18 the term with the conductivity σ shows that when ω decreases, the loss increases due to the fraction. ω represents the frequency and will explain the difference in losses between the different graphs in the figures in section 4.1.3.

By comparing the results from the new varnish in figure 36 and 37, it is noticed that the values are almost identical. For example, at 10 Hz the graph from measurement 1. has a value of 8.5 with a field of 0.25 kV/mm. The value from measurement 2. is 9.8 with 0.25 kV/mm applied.

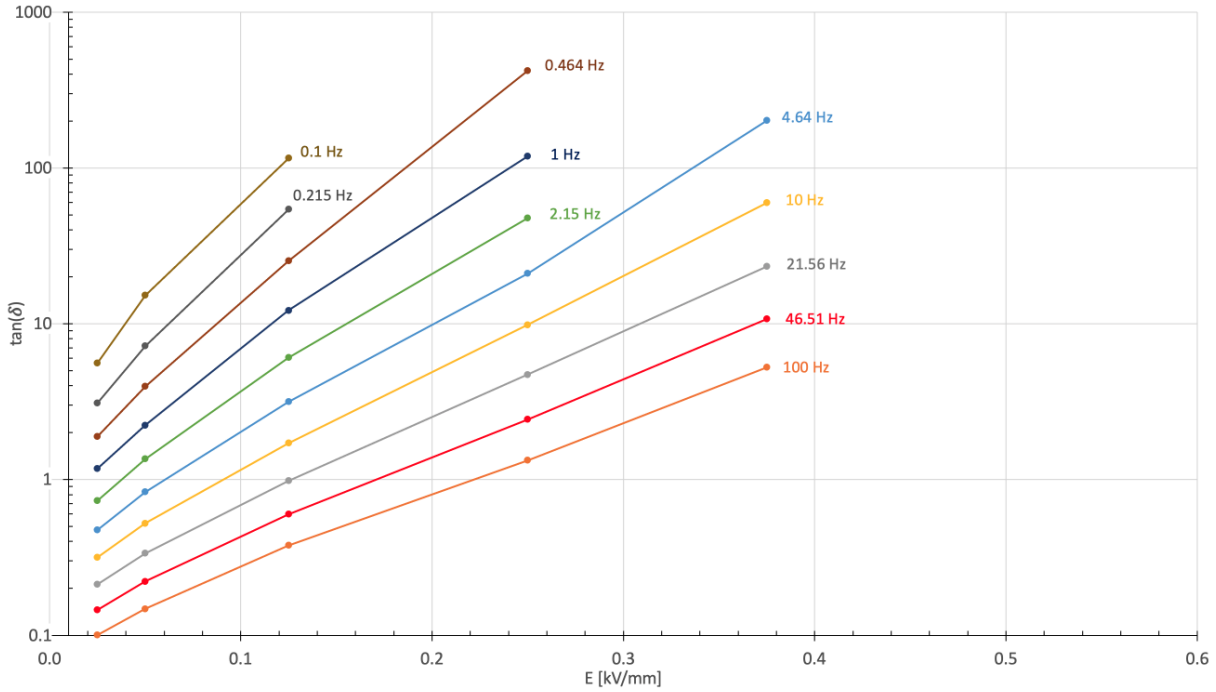

Figure 37: Loss as a function of the electric field measured in measurement number 2 with the new varnish applied to the test object.

4.1.4 Influence on the Current and the Conductivity

With current and voltage measurements from the IDA 200, different graphs could be plotted. These graphs show that the varnish is dependent on the electrical field present.

Old Varnish

In figure 38, 10 kV thus an electric field of 0.5 kV/mm was applied to the old varnish from the previous project. As mentioned, it was more solidified and viscous than the new one.

Figure 38 shows the different harmonic currents measured with the IDA 200. The fundamental frequency of the current is 100 Hz, the highest harmonic measured was the 8th which represented a part of the total current with 800 Hz.

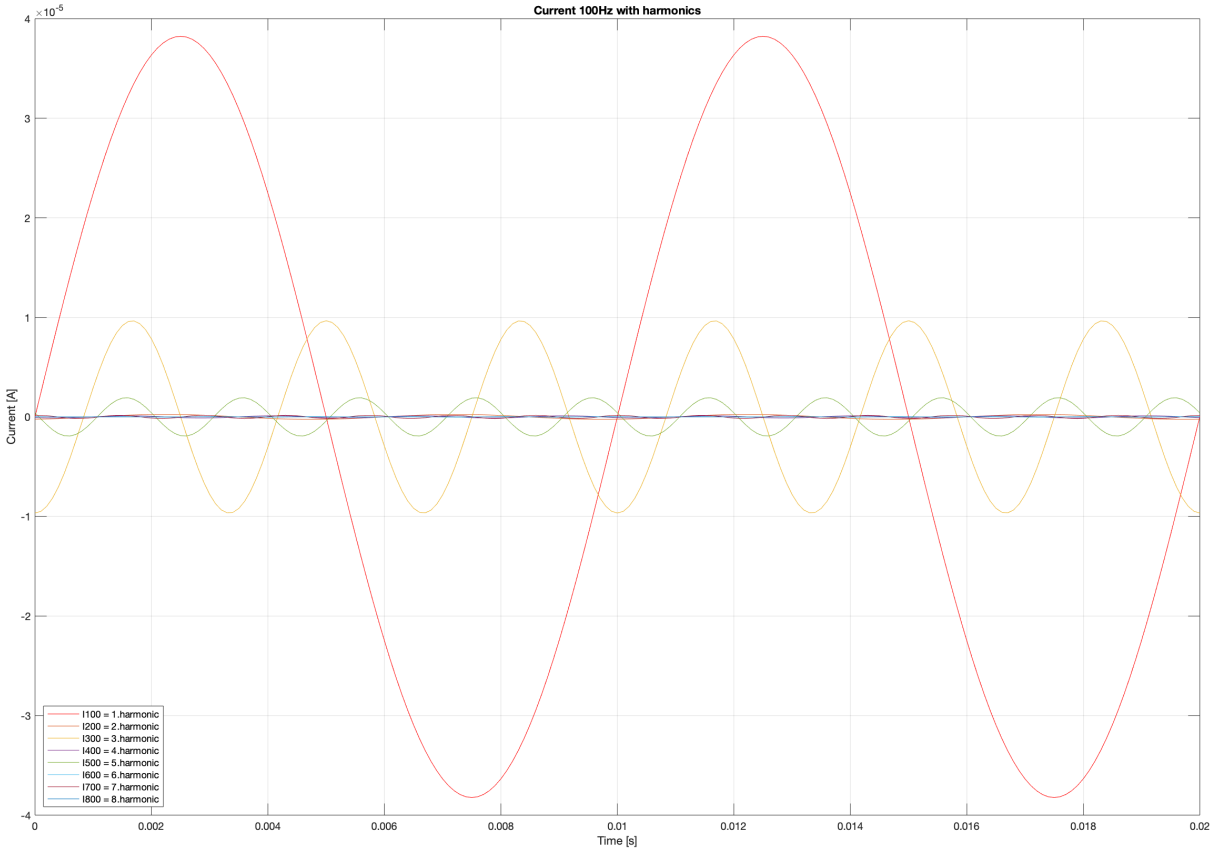

Figure 38: The eight harmonics of the current measured with the IDA 200, with a fundamental frequency of 100Hz. These are results from measurements on the old varnish.(10 kV or 0.5 kV/mm applied)

If the graphs in figure 38 were plotted in their respective windows, the result would look like figure 39. The figure contains four graphs of voltages and four graphs of currents. In the top of the figure are the total voltage and current shown, the three graphs of the most contributing harmonics are shown underneath these two. The total in the top windows of the figure, is a result of the fundamental and all the harmonics added on top of each other. The graphs of the currents were different with higher voltages applied. The total voltage in the top left of the figure, is approximately equal to the fundamental voltage below. The total current on the other hand, in the top right of the figure, is not similar to the fundamental current below. The peak of the sine waves is approximately at the same point. The amplitude of the current is not the same and the sinusoidal shape does not apply in the total current.

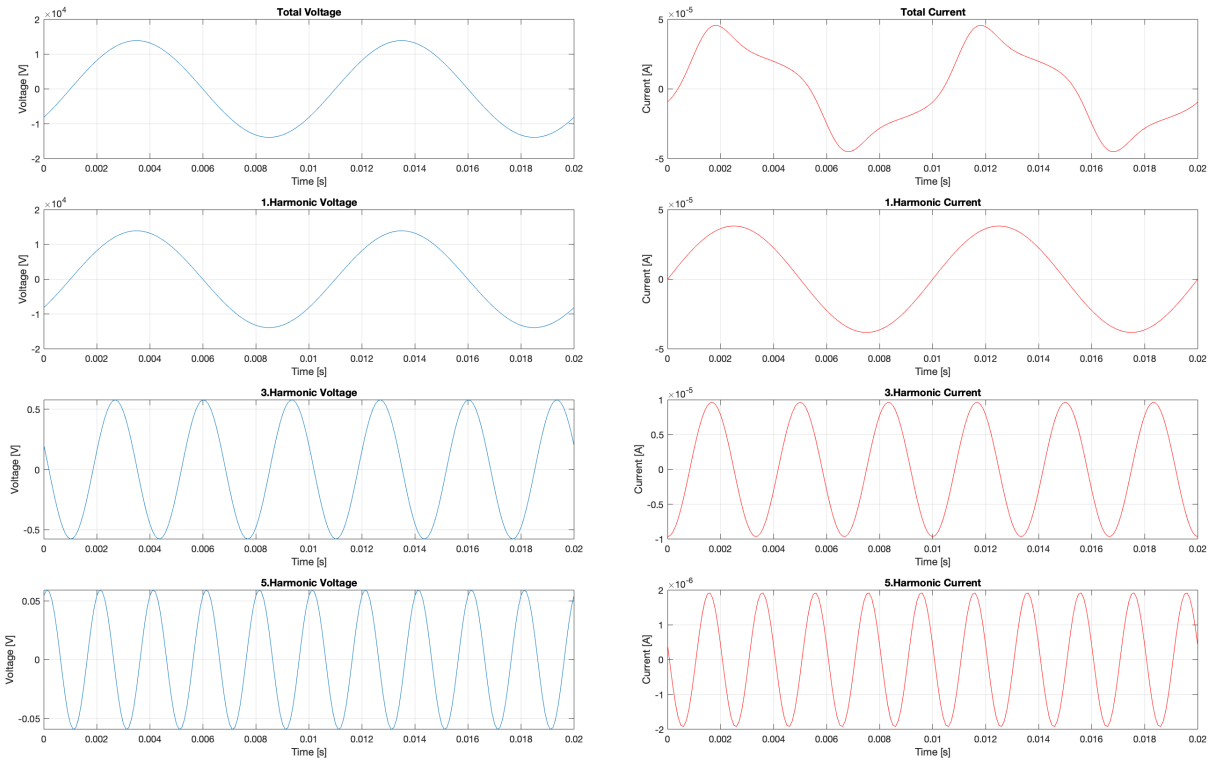

Figure 39: The fundamental frequency, the 3rd and the 5th harmonic of the voltage and the current. In addition the total of both the voltage and the current with all the 8th harmonics included. (10 kV or 0.5 kV/mm applied)

Figure 40 shows the graphs of the total current and voltage. It can be assumed that the varnish was capacitive in these measurements. Since the current is positioned to the left of the voltage, the circuit can be considered capacitive. From the red graph, it can be interpreted that the conductivity of the varnish changes due to the applied electric field. Because of the distortion of the graph, the current is not flowing in a perfect sinusoidal. The distortion is due to the fluctuation of the applied voltage. This means that the conductivity is different with the peak voltage, compared to other positions on the sinusoidal voltage. The results from the measurements can be found in appendix 7.2.

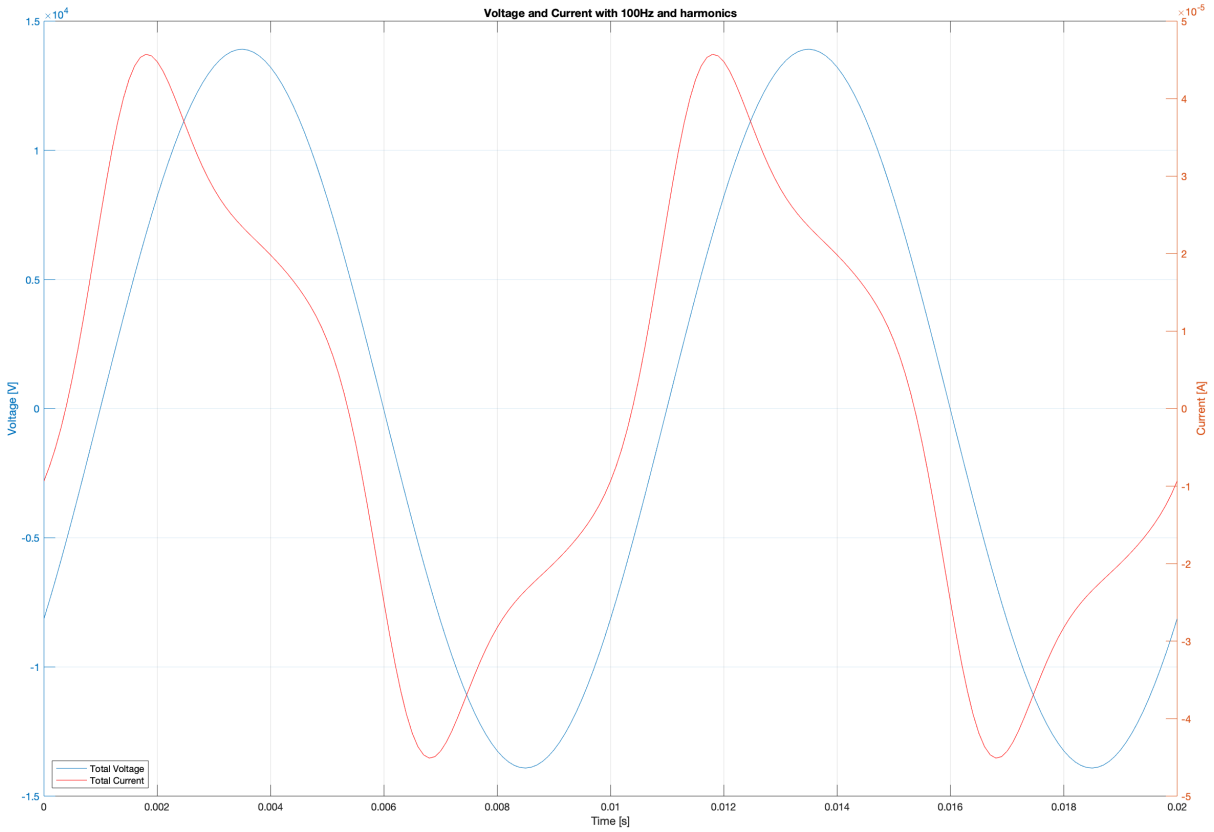

Figure 40: The total voltage and current with all the 8th harmonics included, with a fundamental frequency of 100Hz. (10 kV or 0.5 kV/mm applied)

If the applied electric field was weakened from 0.5 kV/mm to 0.125 kV/mm, the current changed. The shape of the current becomes more sinusoidal and not as distorted as the ones with the stronger fields applied. This is shown in figure 41. If the graphs from figure 40 and 41 are compared, it is clearly a difference between the red graphs. The stronger electric field applied in figure 40 was the only difference, it is therefore the reason for the distortion. If an imaginary line was drawn from the peak of the voltage in figure 41 down to the x-axis, the line would hit the red current graph at zero. This shows that the circuit is capacitive, with the current 90° in front of the voltage.

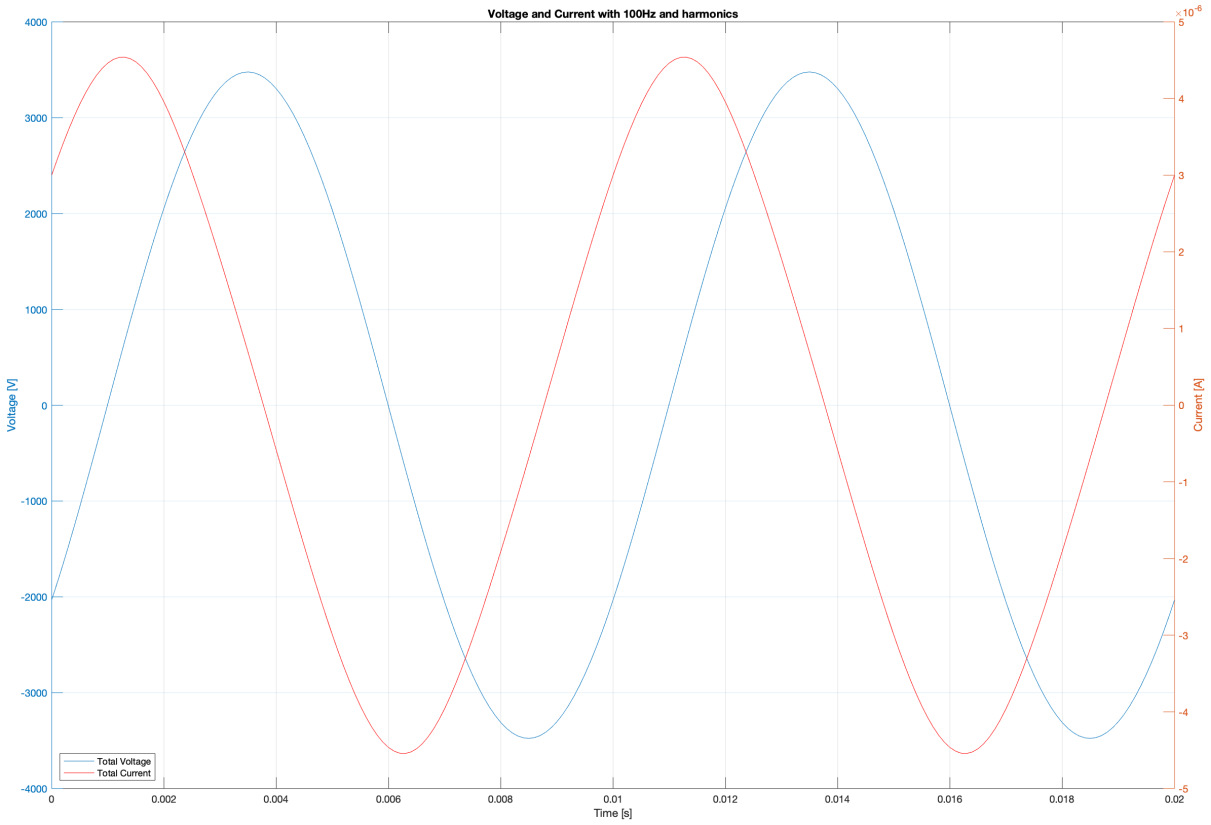

Figure 41: The total voltage and current with all the 8th harmonics included, with a fundamental frequency of 100Hz. (2.5 kV or 0.125 kV/mm applied)

New Varnish

With the new varnish, the graphs from the measurements became different compared to the previous ones. From figure 42, the total current is shown as a more distorted step waveform than the sinusoidal fundamental graph below. The voltage is as with the old varnish almost similar to the fundamental voltage. The sample with the new varnish was also able to accept 10 kV during the measurements. The new varnish was, as mentioned, more liquid and less solidified during the painting process than the old one.

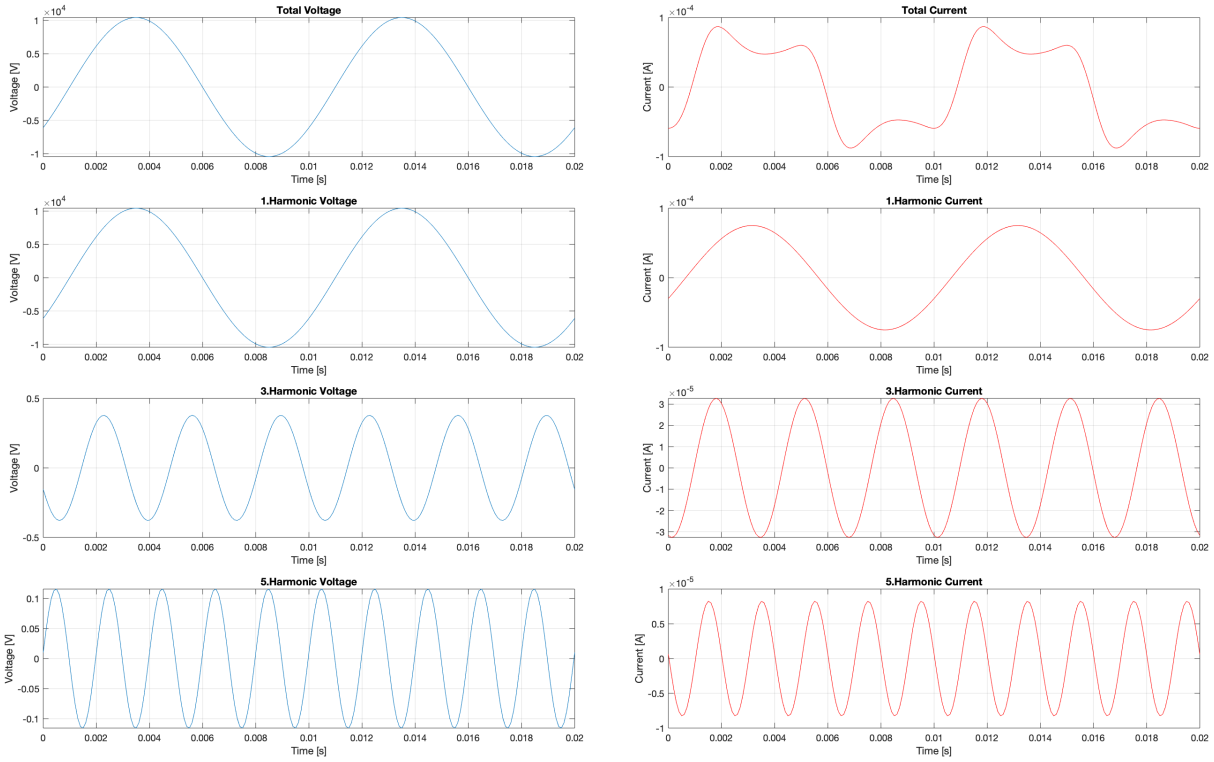

Figure 42: The fundamental frequency, the 3rd and the 5th harmonic of the voltage and the current. In addition the total of both the voltage and the current with all the 8th harmonics included. (10kV or 0.5 kV/mm applied)

With the voltage shaped as an approximately perfect sinusoidal curve, the current makes a dip in the middle where the peak of the voltage is. Figure 43 displays the measurements performed with a field of 0.375 kV/mm. It was not possible to apply a stronger field on the new varnish with to the IDA 200. With this much distortion, it is conceivable that the new varnish is even more dependent on the applied field.

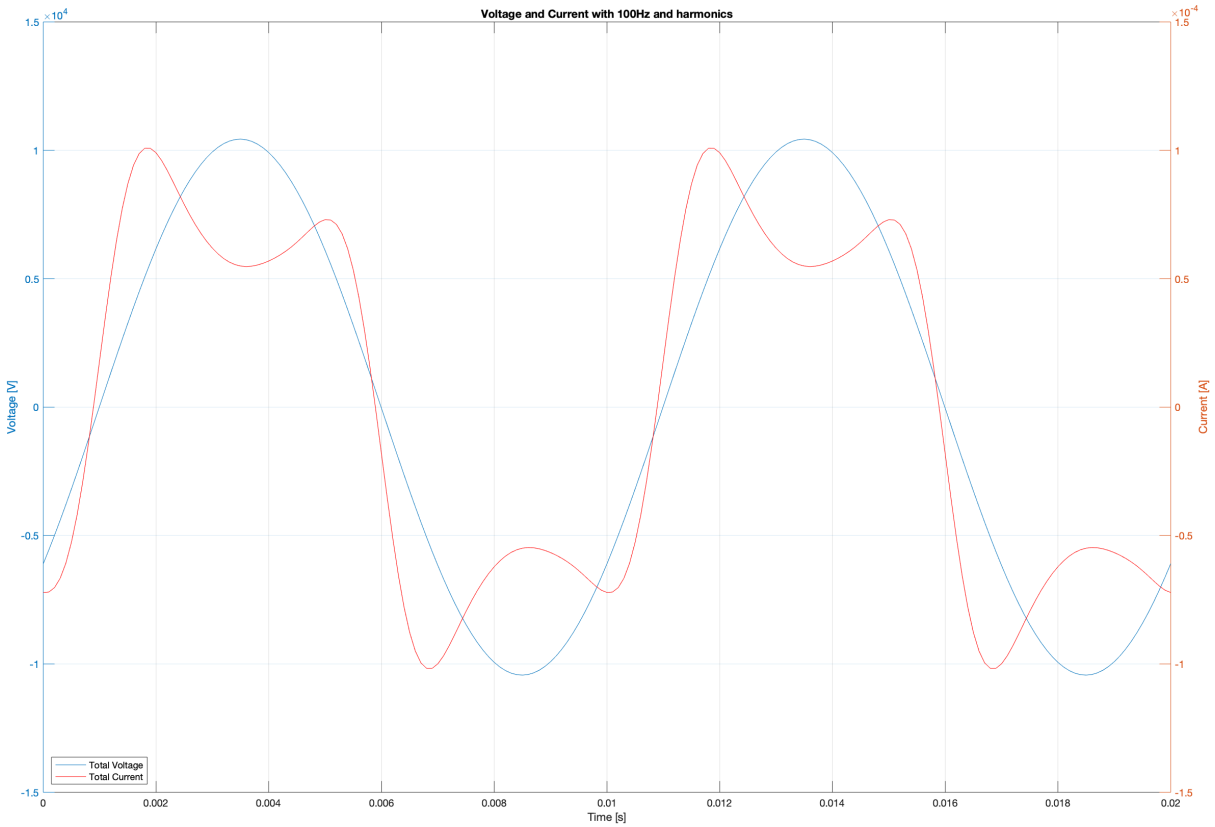

Figure 43: The total voltage and current with all the 8th harmonics included, with a fundamental frequency of 100 Hz. (7.5 kV or 0.375 kV/mm applied)

When the field is reduced from 0.375 to 0.250 kV/mm, the current and voltage changes as shown in figure 44. The shape of the current may resemble the current from the old varnish with a field of 0.5 kV/mm, shown in figure 40. The peak values of the two currents are different, probably due to the difference in the voltage applied.

Considering figure 43, the peak value of the current goes from $1.008 \cdot 10^{-4}$ with 0.375 kV/mm to $2.032 \cdot 10^{-5}$ with 0.250 kV/mm. Which means it decreases almost one order. The distortion is evident when reducing the voltage and thus the electric field, the shape of the current changes.

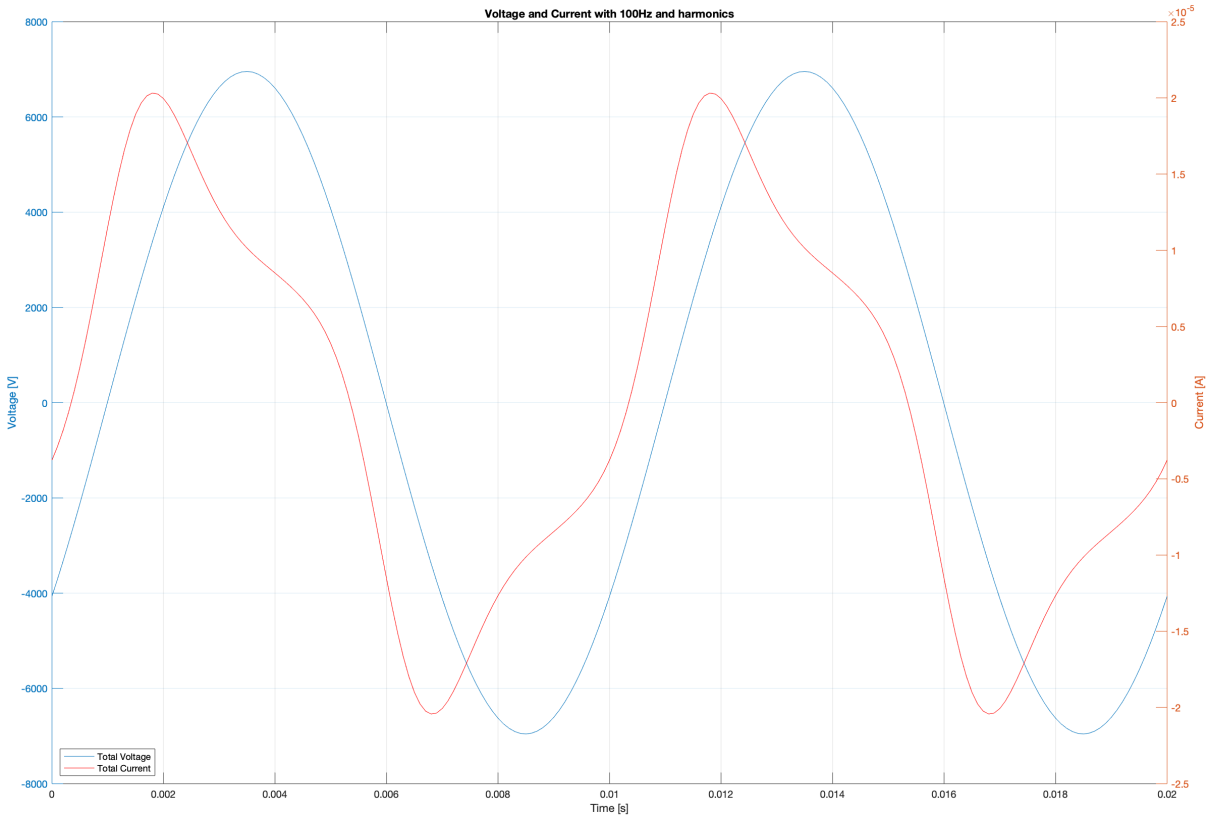

Figure 44: The total voltage and current with all the 8th harmonics included, with a fundamental frequency of 100 Hz.(5kV or 0.25 kV/mm applied)

If the applied field is reduced even more, the current and voltage will look like figure 45. In this figure, the field is 0.125 kV/mm. It is easy to see that the shape of the current has changed again, like with the two previous figures. The shape of the current gradually becomes more like a perfect sinusoidal, with the reduction in the electric field. The peaks of the current are still pointy, the perfectly rounded peaks are not present yet.

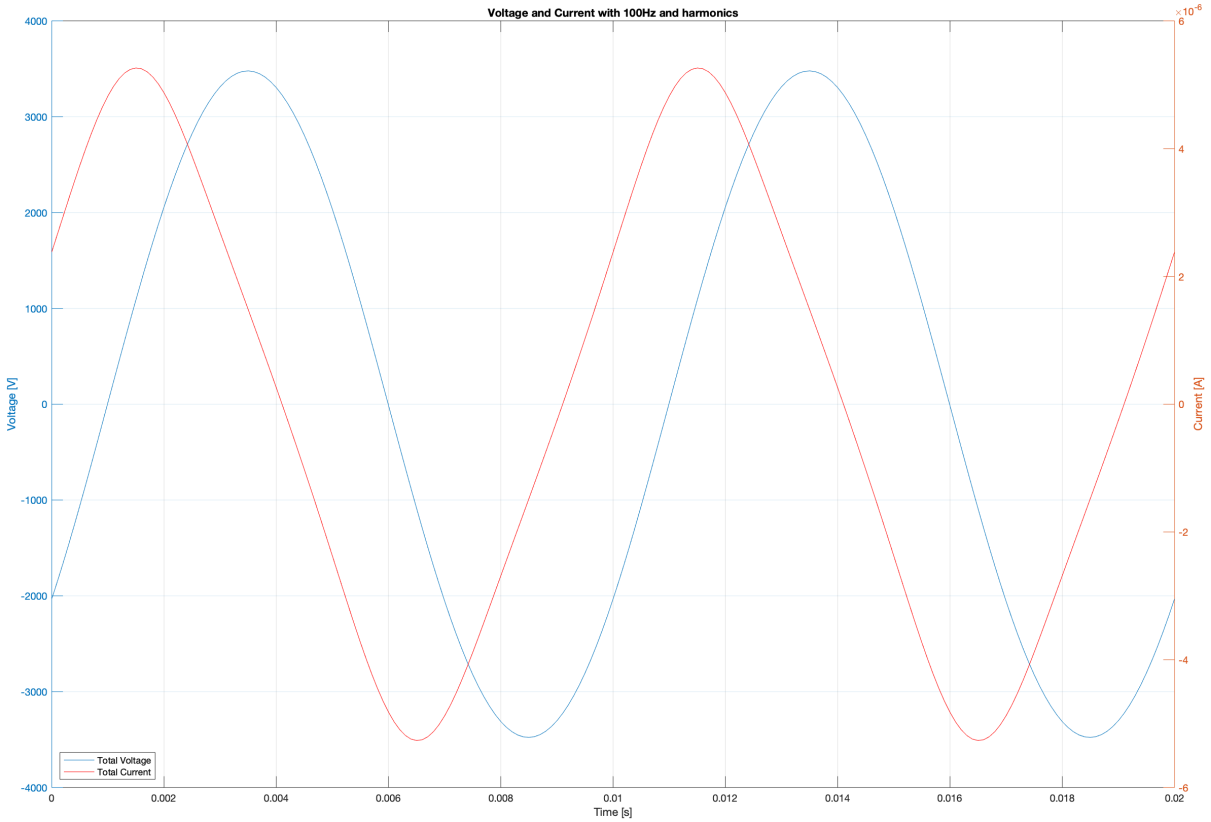

Figure 45: The total voltage and current with all the 8th harmonics included, with a fundamental frequency of 100 Hz. (2.5kV or 0.125 kV/mm applied)

When the field is reduced to 0.05 kV/mm the graphs become almost perfectly sinusoidal. The electric field does not influence the current with this low field strength.

In figure 43, 44, 45 and 46, the different electric fields can show a pattern regarding the current. This means the field is influencing it. For each reduction of the field, the varnish is less affected and therefore less distorted. The dependent conductivity is the reason for the distortion.

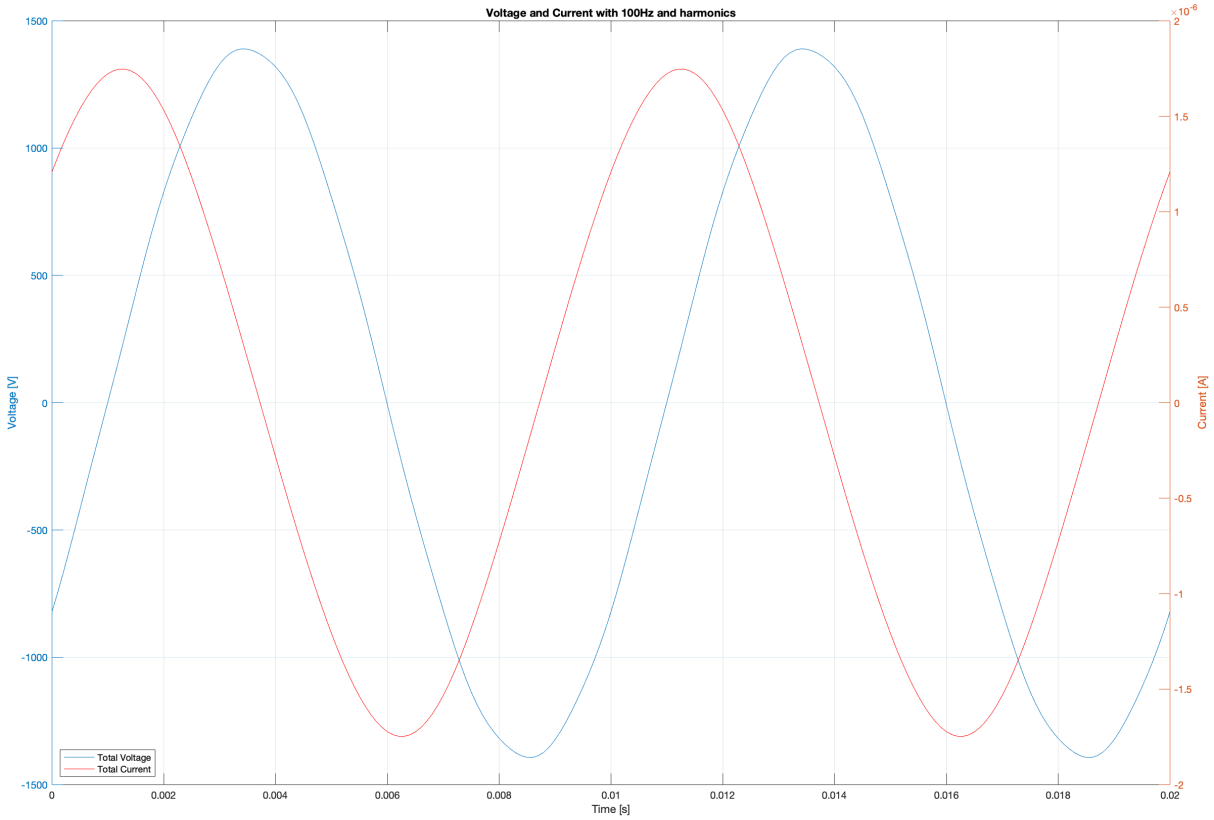

Figure 46: The total voltage and current with all the 8th harmonics included, with a fundamental frequency of 100 Hz. (1kV or 0.05 kV/mm applied)

The different graphs and figures from these measurements are shown in appendix 7.2.

4.2 IDAX 206 Measurements

IDAX 206 had the advantage of a thermal cabinet. The dependency on the temperature could then be investigated. The measurements showed different dependencies and confirmed the results from the IDA. The field strength given from the unit was the concern.

4.2.1 Loss Factor

Only one electric field strength is plotted in figure 47. It shows the different temperatures depending on the frequency, tested with the field strength 0.01 kV/mm.

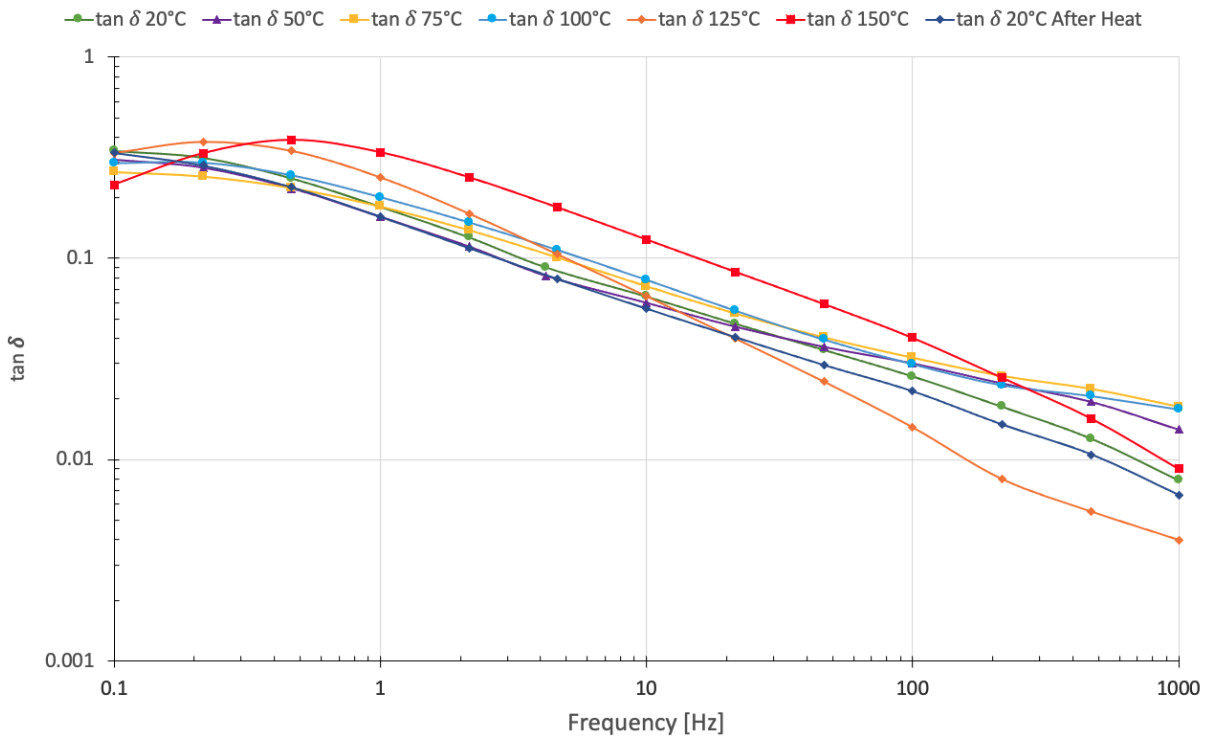

Figure 47: Loss as a function of the frequency from the measurements performed with the IDAX, with an electrical field strength of 0.01 kV/mm.

Figure 47 and 48 consists of measurements performed with the same temperatures. The difference is that the field is four times stronger in figure 48.

The peak of the red graph in both figures are almost similar. The peak is approximately 0.5 and 0.6 Hz in the figures. The loss is not influenced by the small difference in the electric field.

Both figure 47 and 48 show an offset when it comes to the peak of the losses. It seems that this is caused by the temperature. With high temperatures the peak of the losses is shifted

to the right, towards a higher frequency. This is confirmed by the last measurement at 20°C after the thermal stress, where the peak is back at the low frequency region.

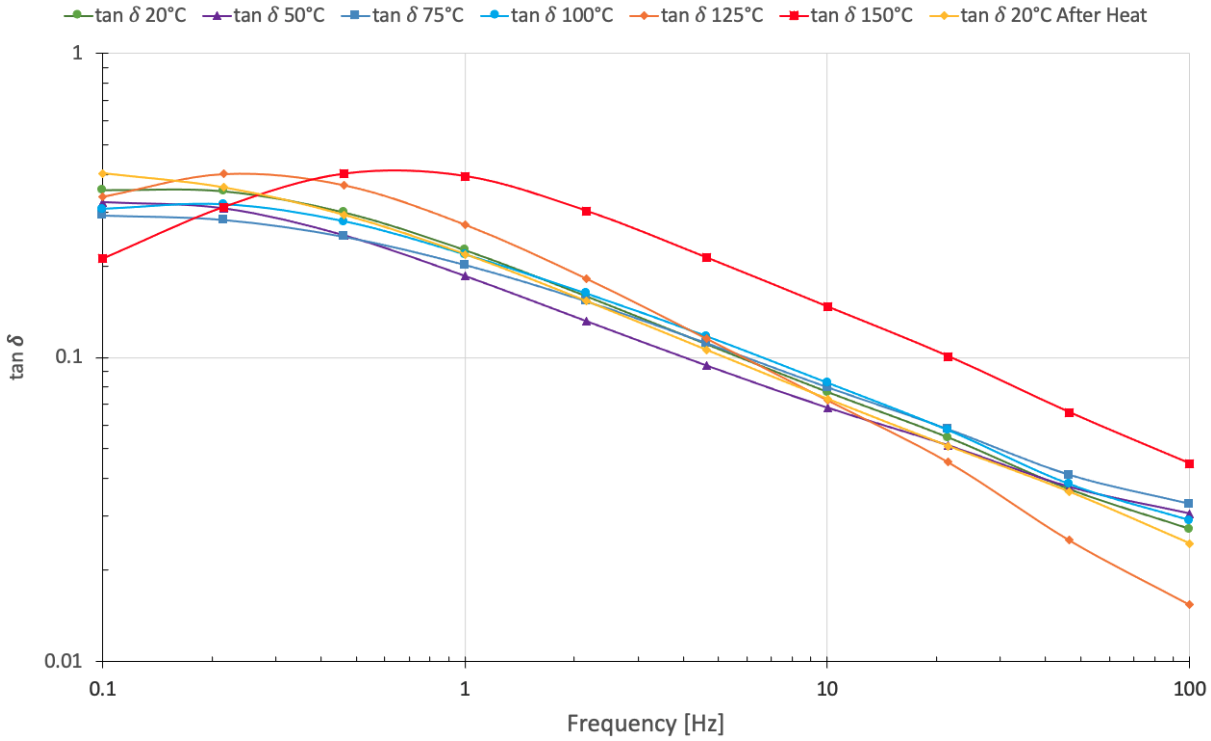

Figure 48: Loss as a function of the frequency from the measurements performed with the IDAX considering the losses and the frequency, with an electrical field strength of 0.04 kV/mm.

Figure 49 shows the results from the measurements performed at 100°C. The four measurements have different field strengths. The interesting thing to observe from this figure is that the fields barely influence the measurements at all. The graphs are almost on top of each other. This can indicate that the fields are not strong enough to make an impact on the varnish. The value of the field where the dependency starts are modeled in 4.4.2.

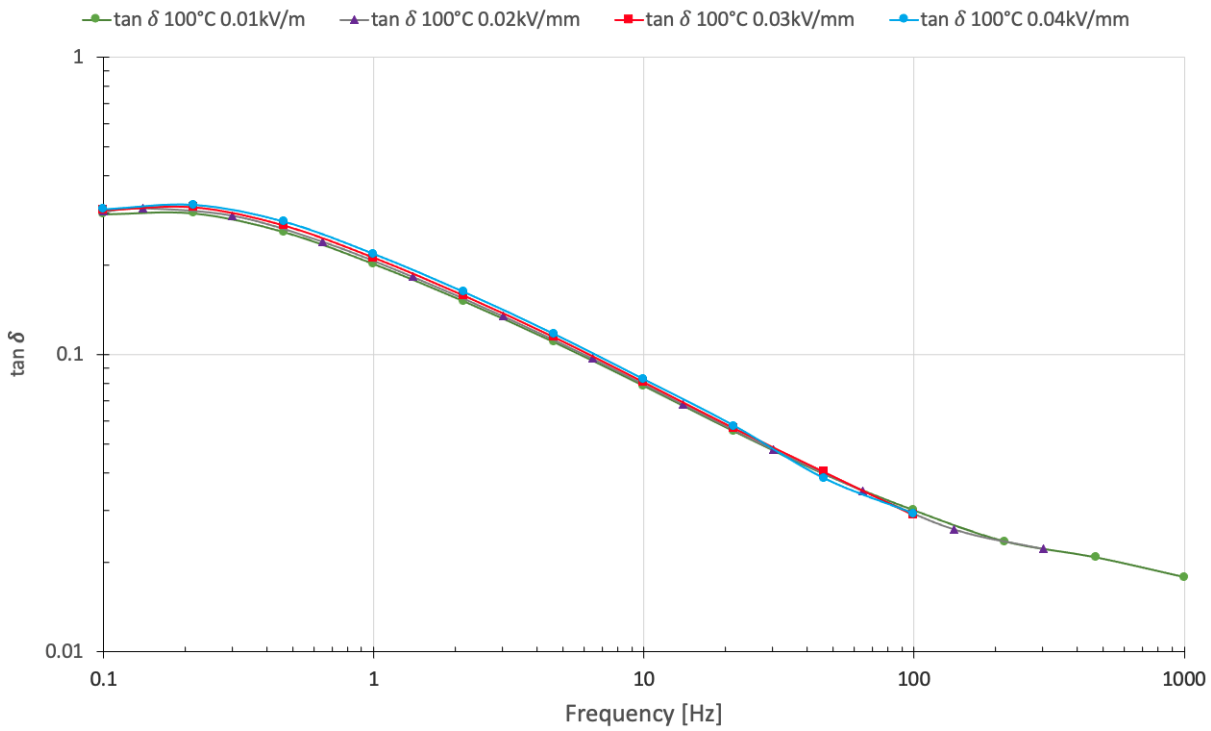

Figure 49: Loss as a function of the frequency from the measurements performed with the IDAX, with an ambient temperature of 100°C.

The figures for the rest of the temperatures with the new varnish are found in appendix 7.1.2. The results from the measurements on the old varnish are found in appendix 7.1.1.

4.2.2 Temperature Dependency

Figure 50, 51, 52 and 53 were made from the same measurement. These figures show the dependency of the temperature and frequency. The last two graphs are shown in 4.2.3. Figure 50 shows the dependency at 100 Hz while 51 shows the dependency at 1 Hz.

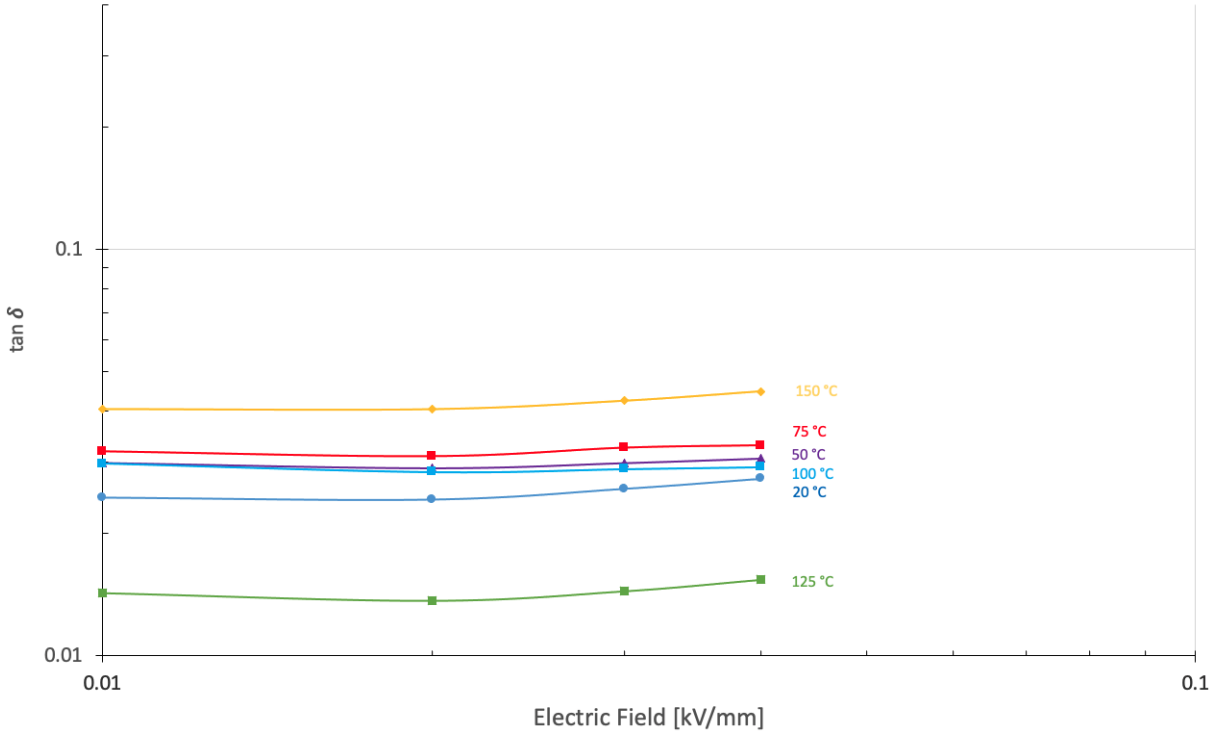

Figure 50: Loss as a function of the frequency from the measurements performed with the IDAX, with a frequency of 100 Hz.

The $tan\delta$ graphs are approximately constant and there is almost no impact with increased field strength. Temperature makes the greatest impact on the loss. At low temperature the results are lower on the y-axis than with higher temperature. The results at 125°C are lower than the rest of the graphs, this could be a miss-reading. The temperatures in the middle are quite similar considering the losses. The graphs of 50, 75 and 100 °C are close and sometimes on top of each other.

If the graphs in figure 50 and 51 are compared, it can be noted that the lower frequency will increase the losses as mentioned earlier. With a frequency of 100 Hz in figure 50 the results are between 0.03 and 0.04. The results in figure 51 at 1 Hz, are between 0.17 and 0.33. These values are approximately one order from each other, due to the frequency. The difference between the results in the figure is of the same order of magnitude. The difference in loss is pretty similar, considering the space between the graphs.

The results of the other frequencies are found in appendix 7.1.3 and 7.1.4, for the old and the new varnish respectively.

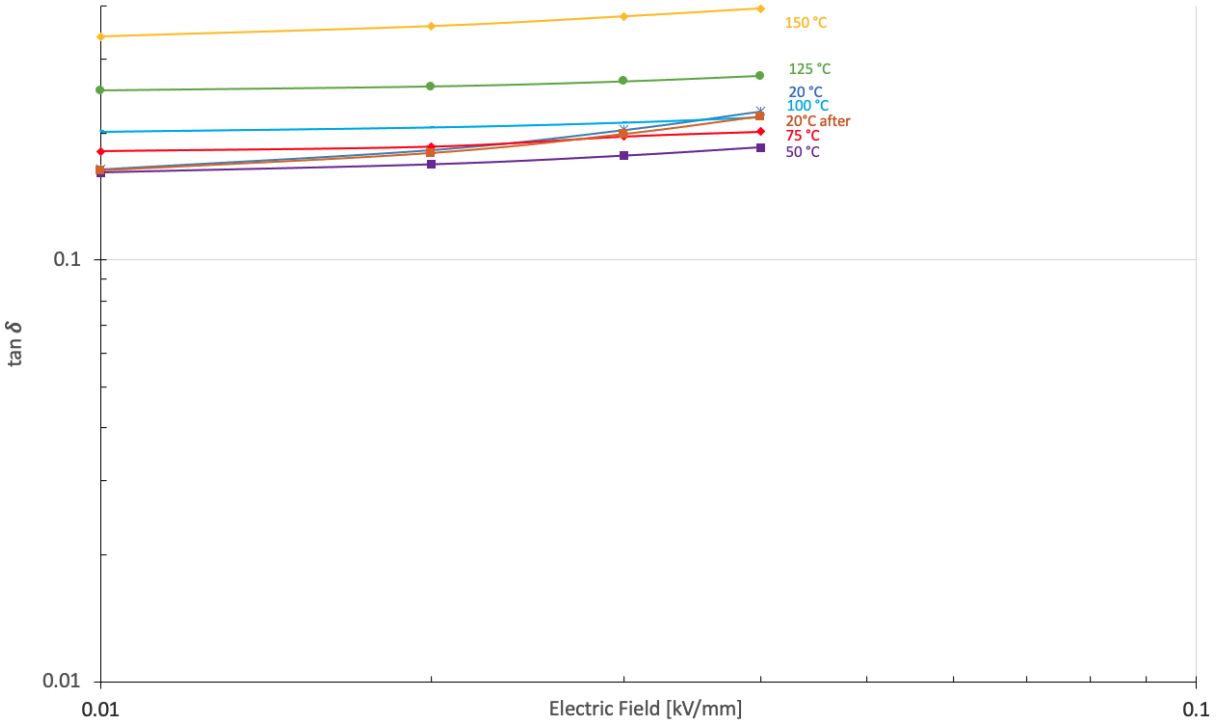

Figure 51: Loss as a function of the frequency from the measurements performed with the IDAX, with a frequency of 1 Hz.

4.2.3 Dependency of Frequency

If the temperatures are replaced with the frequencies in the two previous figures, they will look like figure 52 and 53. They show the dependency with the different frequencies as mentioned in section 4.2.1. The space between the graphs shows that the frequency plays a part in the dependency of the loss. With the same temperature, the results are stable at the given frequency. The increased electric field is not influencing the losses in the varnish. The lower frequencies cause a higher loss. If the graphs are studied closely, the end of them is slightly raising when the field becomes higher. The field is probably not strong enough to affect the varnish. As mentioned, the value where the dependency starts is modeled in 4.4.2.

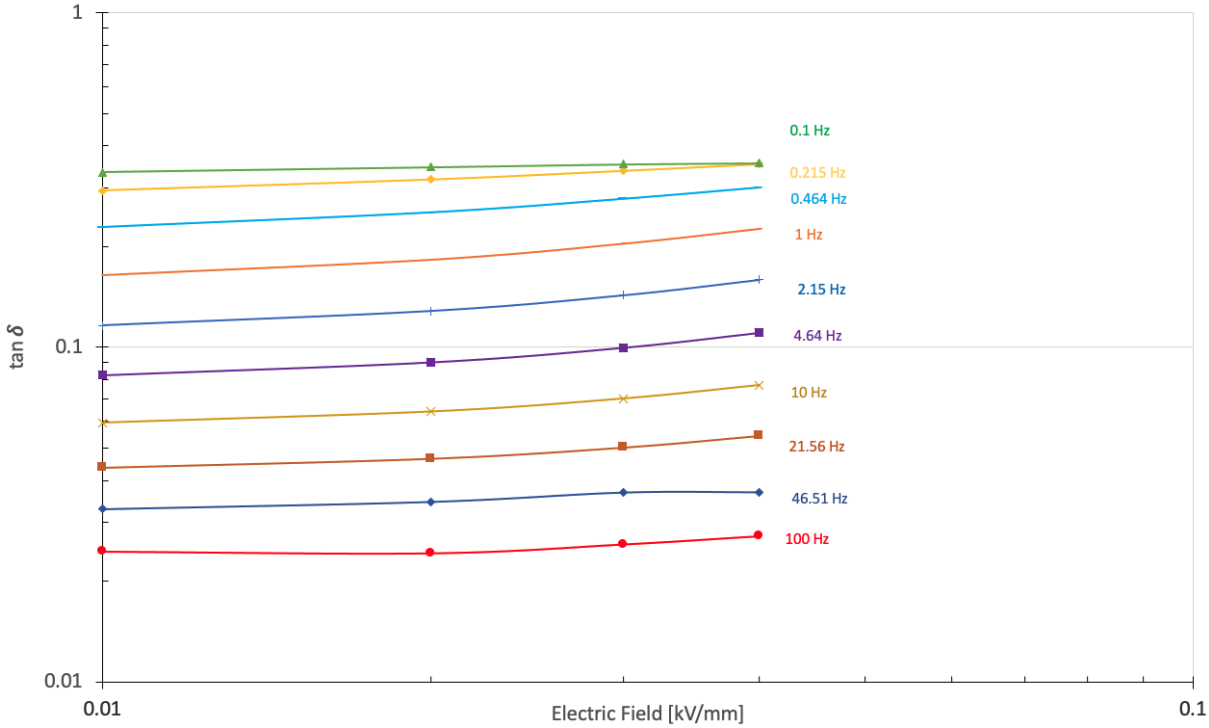

Figure 52: Loss as a function of the electric field from the measurements performed with the IDAX, with a temperature of 20°C. The highest frequency applied is the one with the lowest loss. The lowest frequency is the one with the highest loss. *tan δ* increase with decreasing frequency.

The difference between figure 52 and 53 is small. The results of the lowest frequency have a loss of approximately 0.33 and 0.4 respectively. The results of the highest frequency in figure 52 is approximately 0.023 at 20°C and in figure 53 0.04 at 150°C, which is a bigger difference.

The results with the other temperature, are found in appendix 7.1.5 and 7.1.6. Measurements from the old and the new varnish respectively.

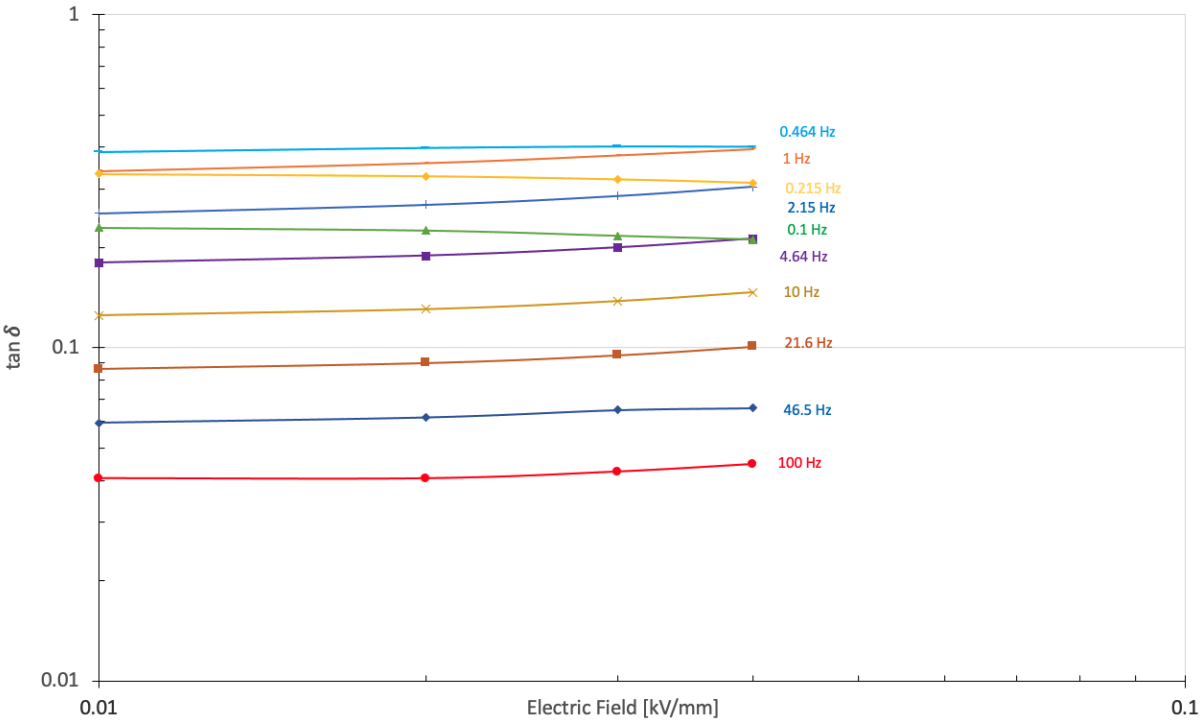

Figure 53: Loss as a function of the electric field from the measurements performed with the IDAX, with a temperature of 150°C. The highest frequency applied is the one with the lowest loss, and the lowest frequency is the one with the highest loss. *tan δ* increase with decreasing frequency.

4.3 Comparison of IDA 200 and IDAX 206 Measurements

The results from the IDA 200 and IDAX 206 are plotted in the same graph, figure 54. The results from the IDAX 206 are almost overlapping. The five graphs from the IDA 200 measurements show that the losses are dependent on the electric field. With an increase in the field, the loss becomes greater. The biggest difference is at the lower frequencies.

If the strength of the electric fields is considered, the position of the graphs is almost correct. The two upper graphs from the IDAX 206 measurements with 0.03 and 0.04 kV/mm are low. These graphs should have been between the two graphs from the IDA 200 measurement with 0.025 and 0.05 kV/mm.

The graph with 0.05 kV/mm from the IDA 200 measurements are found on top of the post-graph of the 0.025 kV/mm measurement. The varnish may have been affected by the different fields applied. The difference between the "pre" and "post" graph shows only a small increase.

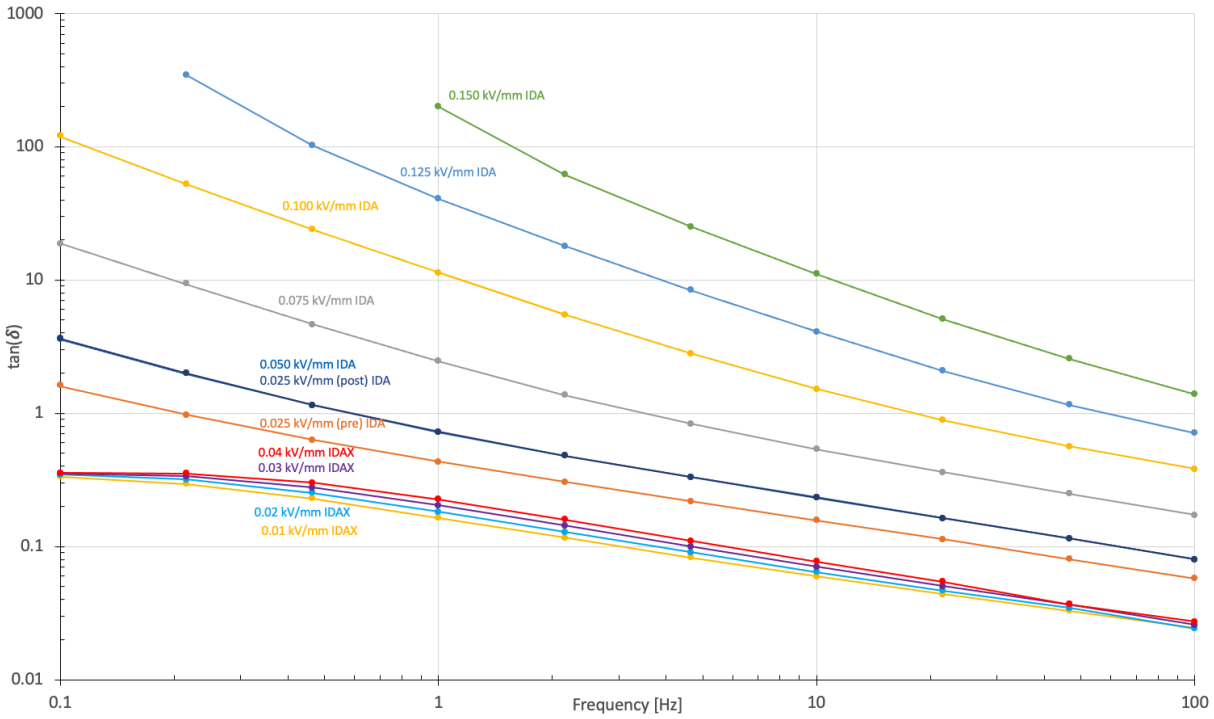

Figure 54: Loss as a function of frequency from the measurements performed with both the IDA 200 and IDAX 206. With a temperature of approximately 20°C.

The difference in frequency from IDA 200 and IDAX 206 are plotted in figure 55. The graphs with the same frequency do not fit each other. With a good fit, the red graphs for example, should have lined up and completed each other. The IDAX gave three frequencies more than the IDA on the old varnish. The difference between the results from the same frequencies is almost one order. For example at 0.1 Hz with the fields of 0.01 and 0.025 kV/mm applied, the loss becomes 0.3 and 1.6. These are the measurements from the tests performed on the old varnish.

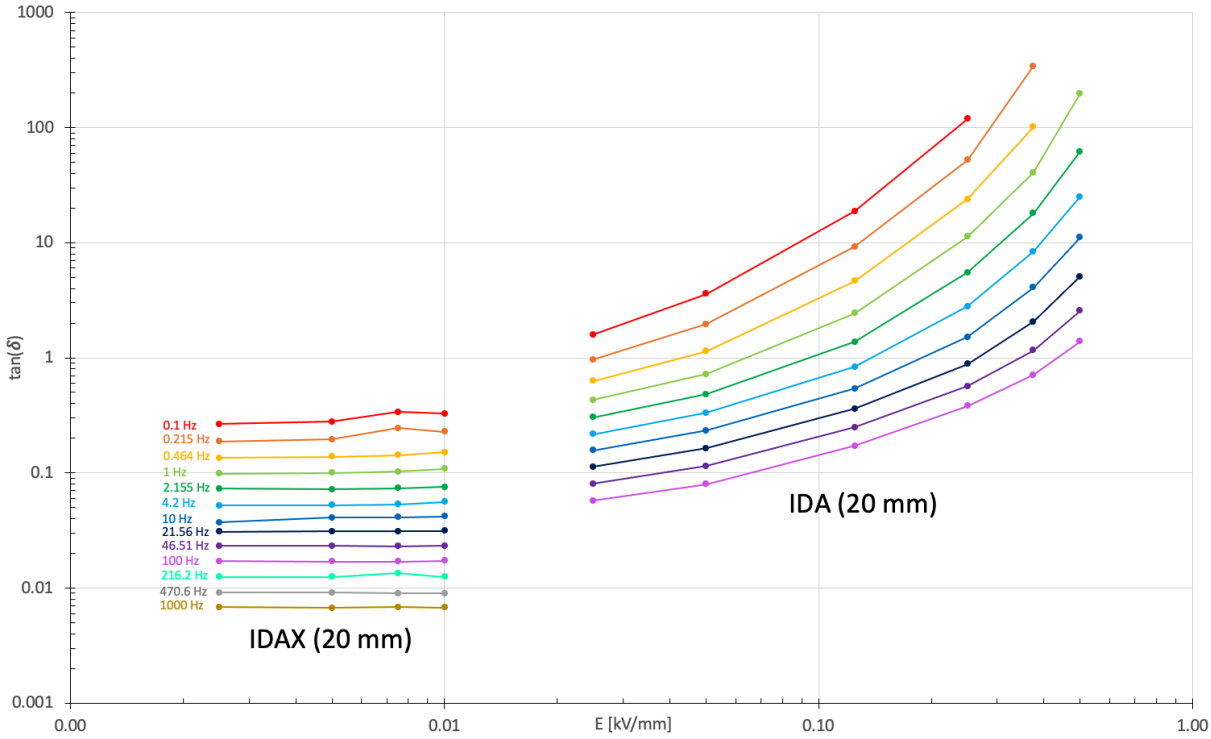

Figure 55: Loss as a function of the electric field, using the 20 mm sample with the IDA 200 and the IDAX 206, both with the old varnish. With a temperature of approximately 20°C.

Figure 56 shows the new varnish. Compared to the old varnish this one consists of results that are much steeper in the IDA section. This means a higher loss due to the fields applied. With an electric field of 0.125 kV/mm, the old varnish had a loss of 18.83 and the new varnish had 111.95 at 0.1 Hz. This is a much higher loss. The new varnish starts with a higher loss and has a steeper curve than the graph of the old varnish.

The measurements from the two different analyzers show a big difference between the loss values. None of the graphs with the same frequency can be connected together or become the continuation of each other. By comparing figure 55 and 56, the results from the IDAX 206 can be seen as similar. The graphs can be seen together in figure 58 and 59.

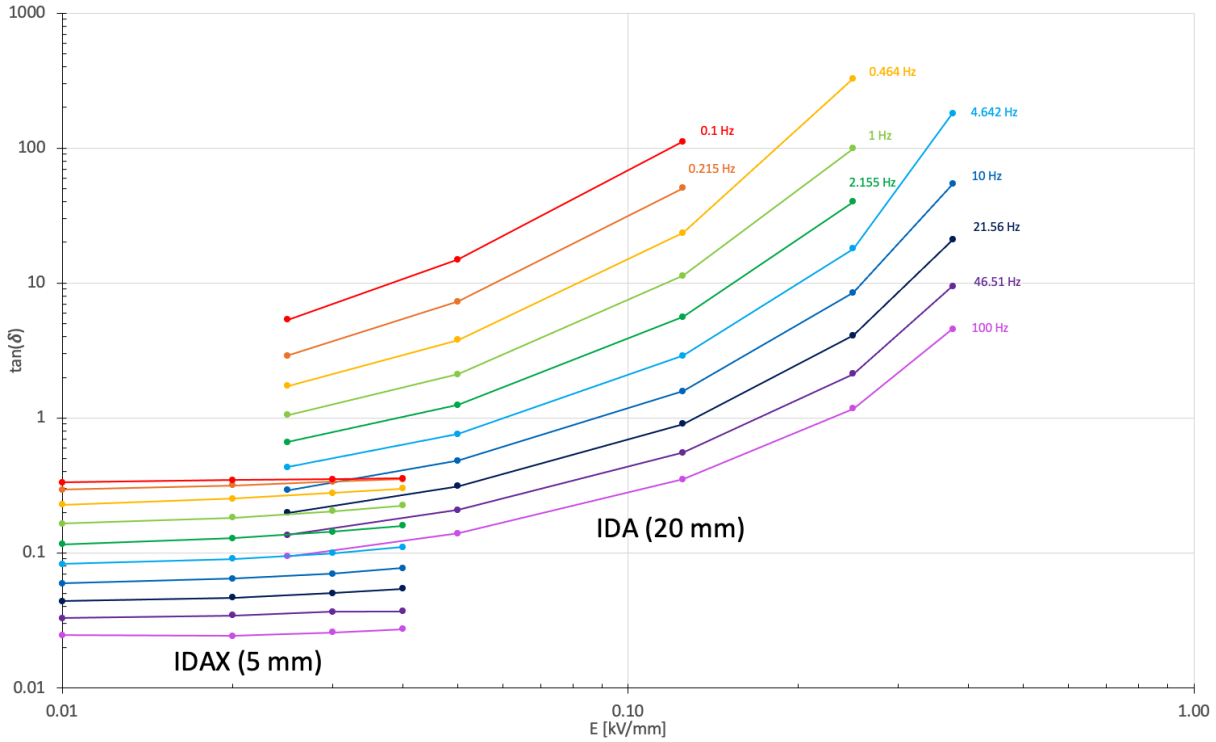

Figure 56: Loss as a function of the electric field (first measurement), using the 20 mm sample with the IDA 200 and the 5 mm sample with the IDAX 206, both with the new varnish. With a temperature of approximately 20°C.

The graphs in figure 56 and 57 are the results from the test on the new varnish. Compared to each other, there is not a big difference between them. The only difference is that the values from the first measurement were a bit lower than the second. For example with 0.1 Hz and 0.125 kV/mm applied, the loss becomes approximately 112 with the first measurement and 116 with the second.

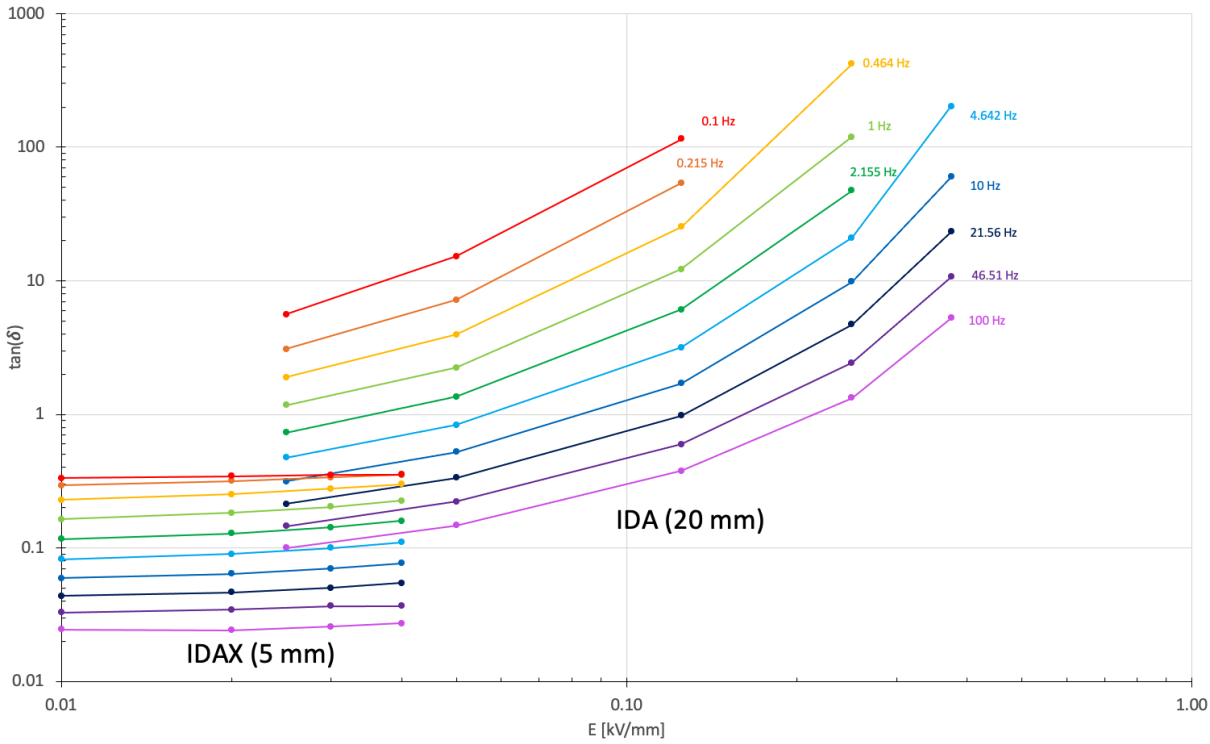

Figure 57: Loss as a function of the electric field (second measurement), using the 20 mm sample with the IDA 200 and the 5 mm sample with the IDAX 206, both with the new varnish. With a temperature of approximately 20°C.

Figure 58 shows the differences and similarities in the results. The graphs from the IDAX 206 measurements with the corresponding frequencies are the only ones that actually match or fit together. There was used a 20 mm teflon spacer instead of a 5 mm on the old sample, the graphs are therefore shifted towards the lower field strengths. This is because the relationship in equation 13 was changed. The electrical field with the 20 mm spacer varied between 0.0025 and 0.01 kV/mm. The field became stronger with the 5 mm spacer. With this test object, it was performed measurements with fields between 0.01 and 0.04 kV/mm. To be able to reach an even stronger field the IDA 200 was needed, it was only used on the 20 mm spacer. The graphs to the right in figure 58 are from these results. The graphs from the IDA 200 do not fit together with the graphs of the same frequency from IDAX 206. Even though the electric field is the same in some areas, the voltage is much higher with the IDA 200. The fact that it was both old and new varnish compared can also have some significance.

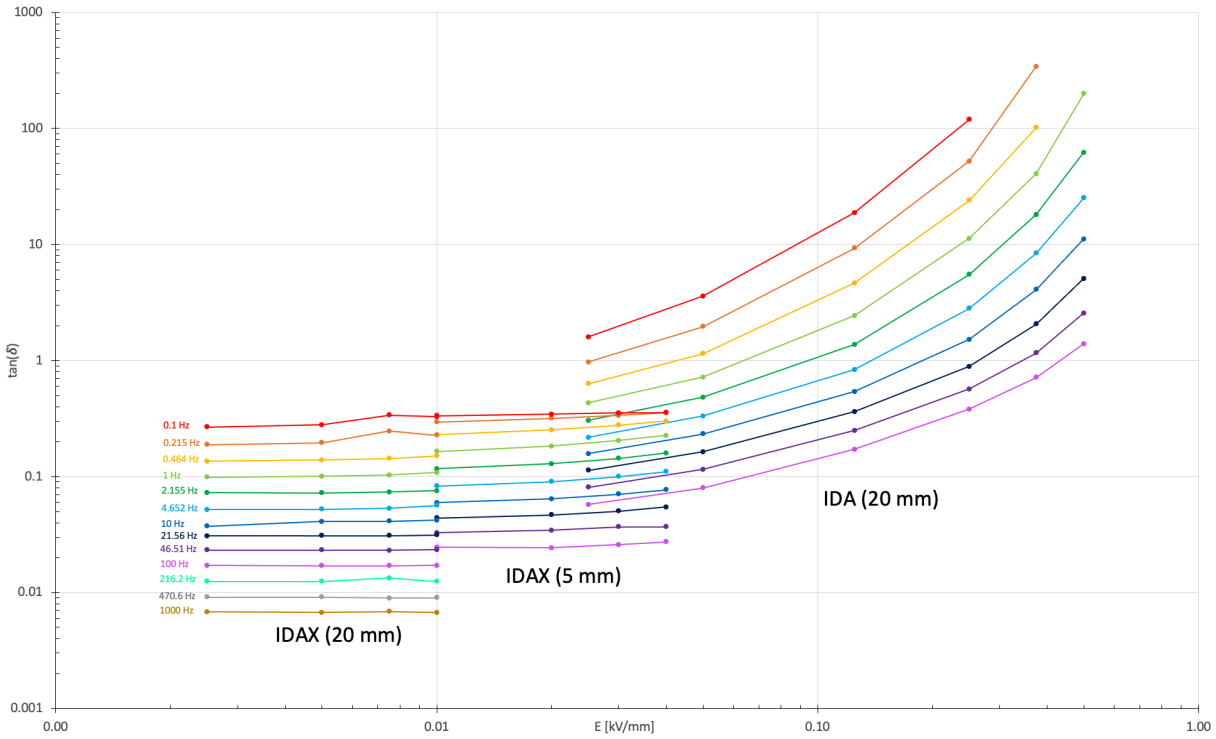

Figure 58: Loss as a function of the electric field from the measurements performed on the 5 mm sample with the IDAX 206 and on the 20 mm sample with both the IDA 200 and the IDAX 206. The varnish on the 5 mm sample was new and the varnish on the 20 mm sample was old. With a temperature of approximately 20°C.

Figure 59 shows the losses, similar to figure 58. The difference is that the 20 mm sample with the old varnish was only used in the IDAX 206 measurement. The IDAX measurements with the 5 mm sample and the IDA measurement with the 20 mm sample were with the new varnish.

The biggest difference between figure 58 and 59 is the results from the IDA 200. With

the minimum frequency and the weakest field, the red graph from IDA starts at 1.6 with the old varnish in 58. With the same prerequisites the red graph from IDA shows 5.35 in 59, this is not a significant difference.

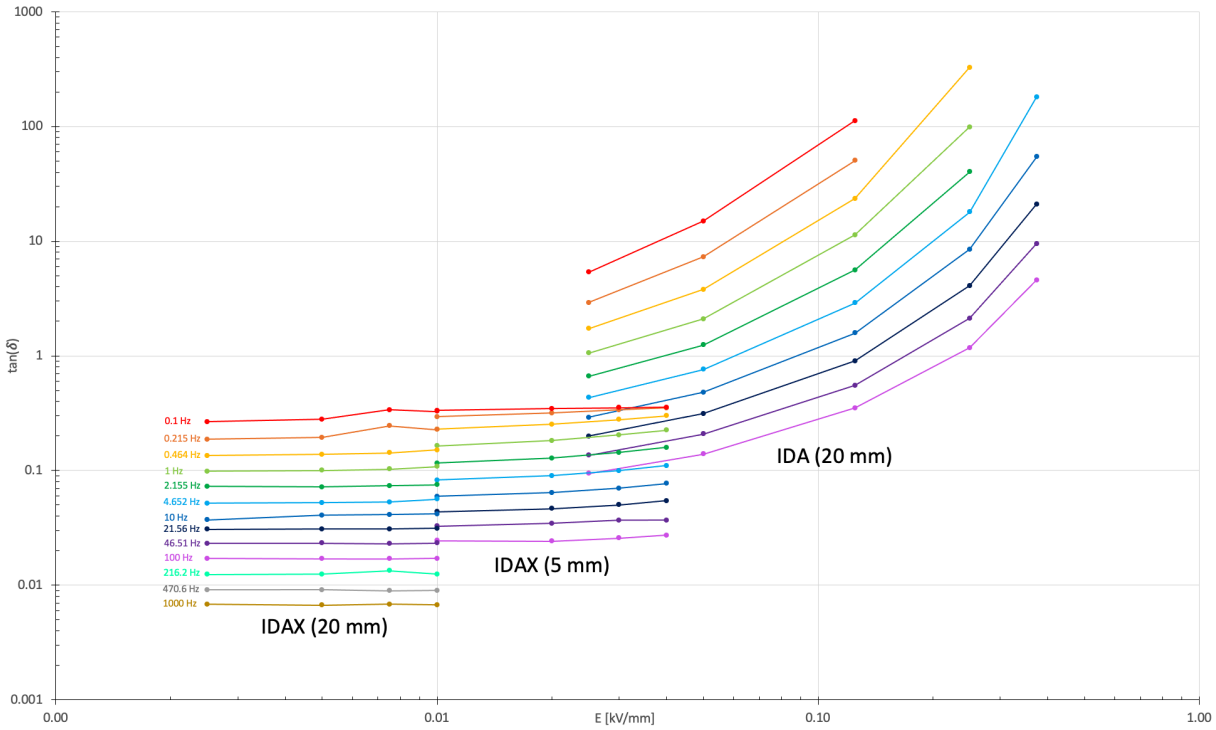

Figure 59: Loss as a function of the electric field from the measurements performed on the 5 mm sample with the IDAX 206 and on the 20 mm sample with both the IDA 200 and the IDAX 206. The varnish on the 5 mm sample was new and the varnish on the 20 mm sample was both old and new, for the IDAX and the IDA respectively. With a temperature of approximately 20°C.

4.4 Megging with Polarization and Depolarization

The megohmmeter needed a long time to stabilize the current and resistance. The polarization test was therefore chosen to measure for 50 minutes, before depolarization. The most interesting about this work was the steady state values of the polarization current and resistance.

4.4.1 Polarization Resistance

Figure 60 shows the resistance measured during a polarization with the megger. The values used for the calculations of the conductivity are from the steady area after approximately 50 minutes or 3000 seconds. To calculate two of the points in figure 61, the resistances 12880 MΩ and 76900 MΩ were used. These resistances belong to the field strengths 0.25 and 0.125 kV/mm respectively. These values are as mentioned taken from the steady measurement in figure 60. With equation 22, two of the points in the blue graph in figure 61 were calculated.

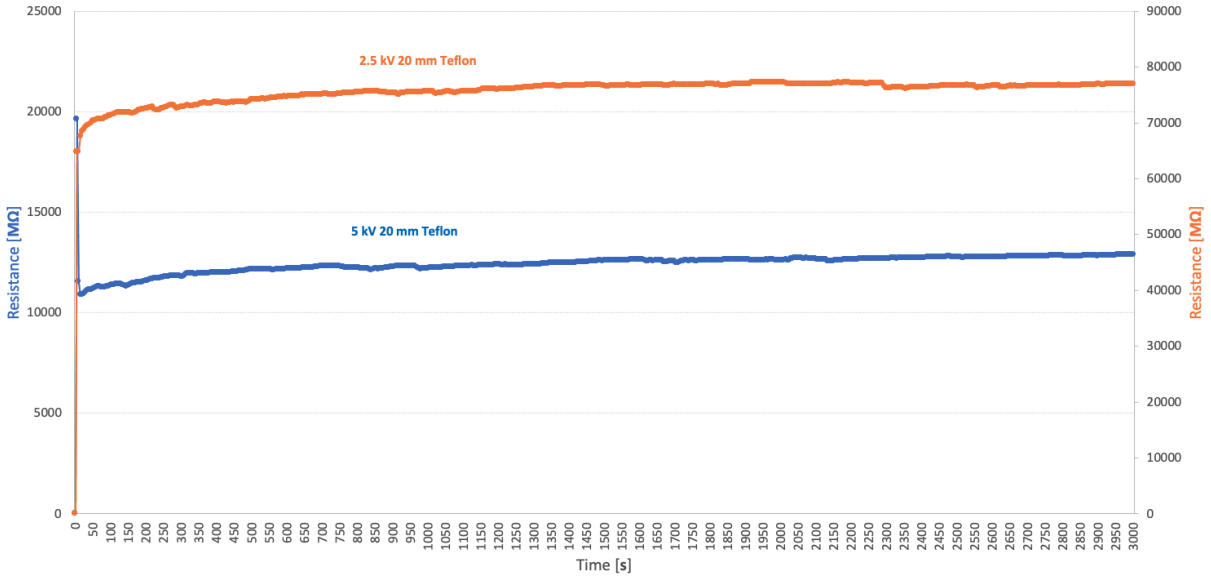

Figure 60: Examples of the resistance measured during the polarization with the megger, with a temperature of approximately 20°C. In this case, a voltage of 5 kV and thus 0.25 kV/mm was used in addition to 2.5 kV and 0.125 kV/mm. The values from these graphs are from megging the test sample with 20 mm spacer and new varnish that had been exposed to heat.

From megging the test objects, the resistance values were found and noted. The values were used together with the dimensions of the varnish to calculate the conductivity σ. The product of the calculations was plotted in figure 61 below, as a function of the applied electric field.

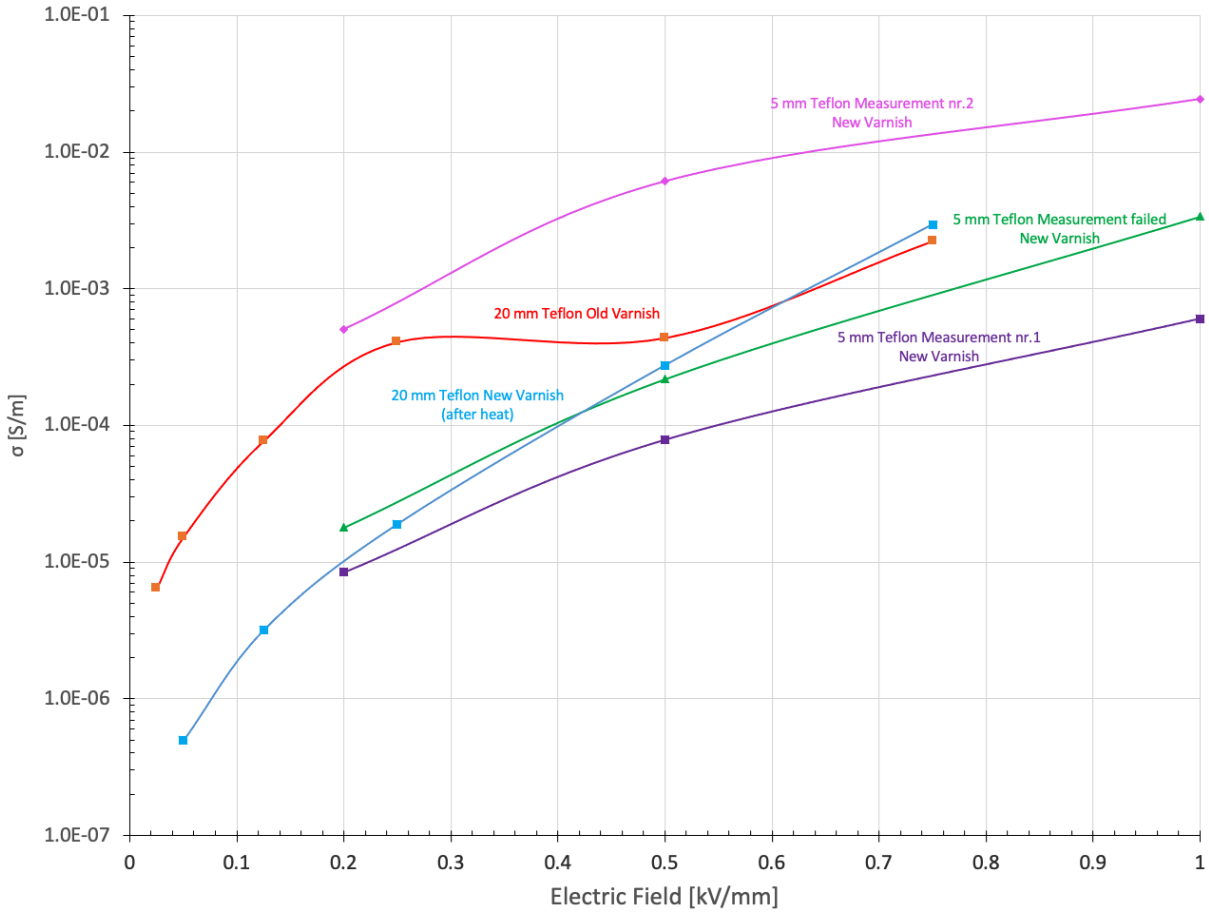

Figure 61: Conductivity as a function of the electric field from the calculations performed with the values measured with the megger, with a temperature of approximately 20°C.

The red and blue graphs are found from megging the cylindrical test object with the 20 mm teflon spacer. The rest of the graphs are found using the test sample with a 5 mm teflon spacer.

As mentioned, to be able to calculate the conductivity of the varnish, physical measurements of the varnish were needed. The thickness of the varnish on the test sample with 20 mm teflon spacer was measured to 1 mm. The varnish with 5 mm teflon spacer was measured to 0.6 mm. The resulting cross-section of the varnish was $81.68mm^2$ and $47.88mm^2$, respectively with these values and the radii.

One sample with new varnish failed during the last measurement with an electric field of 1 kV/mm applied, represented by the green graph in figure 61. The pink and purple graphs are two separate test objects made the same way. It is therefore normal to expect a pretty similar result from the two samples. This is not the case here. The easiest explanation for this would be that the varnish did not get a good enough connection to the electrodes around the cylinder. This is likely to happen, especially during the mounting of the finished set-up. The red line is from the previous project [1] and is therefore measured using two different meggers. One from 0.5 to 5 kV (0.025 to 0.25 kV/mm) and another

from 10 to 15 kV (0.25 to 0.75 kV/mm). Observed in the graph at 0.5 kV/mm. If the same megger had been used during all the measurements, the graph should have been more straight like the other results.

The blue graph represents the new varnish with the 20 mm teflon spacer, exposed to thermal stress in advance. By comparing the red and blue graph, the exposure of the high temperatures clearly makes the conductivity much lower. This means that the varnish had become more brittle and cured. The sample had gone through a test earlier with the IDAX 206, where it was exposed to 20, 50, 75, 100, 125 and 150°C for 24 hours on each temperature. It looks like the main difference is where the electric field is low, when the field is 0.5 kV/mm and above there is not a big difference in the conductivity.

4.4.2 Modeling

By using equation 4 from the theory in 2.1.3, the yellow graph in figure 63 could be calculated and plotted. Calculations are shown on the next page. The expression 4 had four parameters that were necessary before modeling. The first value needed was the base conductivity, found during megging with a low electric field applied. This was to avoid influence from the field during the measurement. The second value needed was the α, for the nonlinear section of the expression. To calculate α several parameters were needed, two current densities and their corresponding electrical fields. The field values were taken from the nonlinear section of the calculated graphs in figure 61. J were found by calculation, using these field values. The calculation of the two current densities is shown on the next page. The values used were the cross-section of the varnish and the polarization current. The dimensions were from the sample with the 20mm teflon spacer. The currents were found from the polarization measurements with the two fields of the nonlinear section, 0.125 and 0.250 kV/mm. These can be seen in the calculations below and in figure 62. The current densities were found by dividing the measured current on the cross-section of the conducting material. The subscript of the current densities represents the applied voltage in kilovolts.

Insertion of values into equation 4 is shown in expression 23. The constants for both the switching and the saturation field strength were trial and error. According to the graphs and their shapes from figure 61, some ideas of the values were thought through. The used values made the yellow graph look like the other graphs. With the E_1 and E_2 value equal to 0.045 and 1.0 kV/mm respectively, the yellow graph resembled the others in the figure. These values were therefore used in the modeling. The saturation field of the varnish is around 1 kV/mm and the dependency on the field starts at approximately 0.045 kV/mm.

$$A = \pi \cdot r^2$$

$$A = (\pi \cdot (\frac{27mm}{2})^2) - (\pi \cdot (\frac{25mm}{2})^2) = 81.68mm^2$$

$$\sigma_0 = 6.4435 \cdot 10^{-6}[S/m]$$

$$J_5 = \frac{I_5}{A} = \frac{0.397\mu A}{81.68mm^2} = 4.86 \cdot 10^{-3}[A/m^2]$$

$$J_{2.5} = \frac{I_{2.5}}{A} = \frac{0.0332\mu A}{81.68mm^2} = 4.065 \cdot 10^{-4}[A/m^2]$$

$$\alpha = (\frac{\lg(J_b/J_a)}{\lg(E_b/E_a)}) = (\frac{\lg(\frac{4.86 \cdot 10^{-3}}{4.065 \cdot 10^{-4}})}{\lg(\frac{0.250}{0.125})}) = 3.58$$

$$\sigma(E) = \sigma_0 \cdot \frac{1 + (\frac{E}{E_1})^{\alpha-1}}{1 + (\frac{E}{E_2})^{\alpha-1}} = 6.4435 \cdot 10^{-6} \cdot \frac{1 + (\frac{E}{0.045})^{3.58-1}}{1 + (\frac{E}{1.0})^{3.58-1}} \tag{23}$$

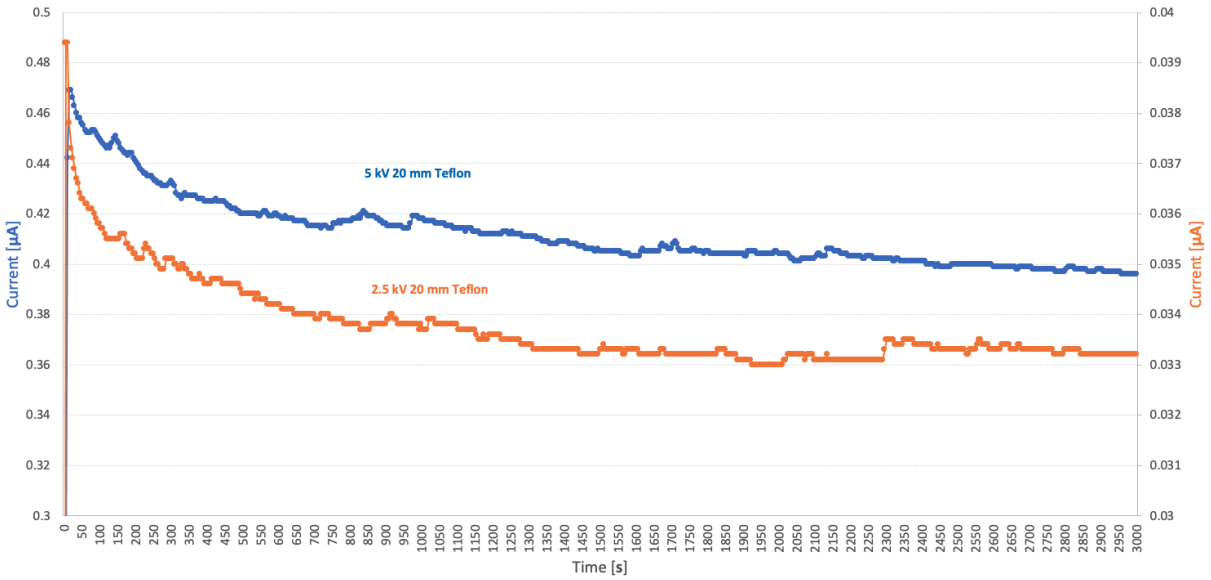

Figure 62: Current measurements from the polarisation of the test object with the new varnish. With a temperature of approximately 20°C. The corresponding fields was 0.25 and 0.125 kV/mm respectively with 5 and 2.5 kV applied.

The polarization currents above show the values measured with a field of 0.25 and 0.125 kV/mm. These fields are assumed as a part of the nonlinear section of the yellow σ-E -graph that is modeled.

In figure 63 the modeled graph from expression 23 is plotted together with the graphs from the previous figure.

The shape of the calculated lines is approximately similar to the yellow graph from the modeling, but the values are not similar for all of them. The yellow graph is similar to pink and red. The red had been even closer if one megger was used. The dip in the graph would then have been avoided.

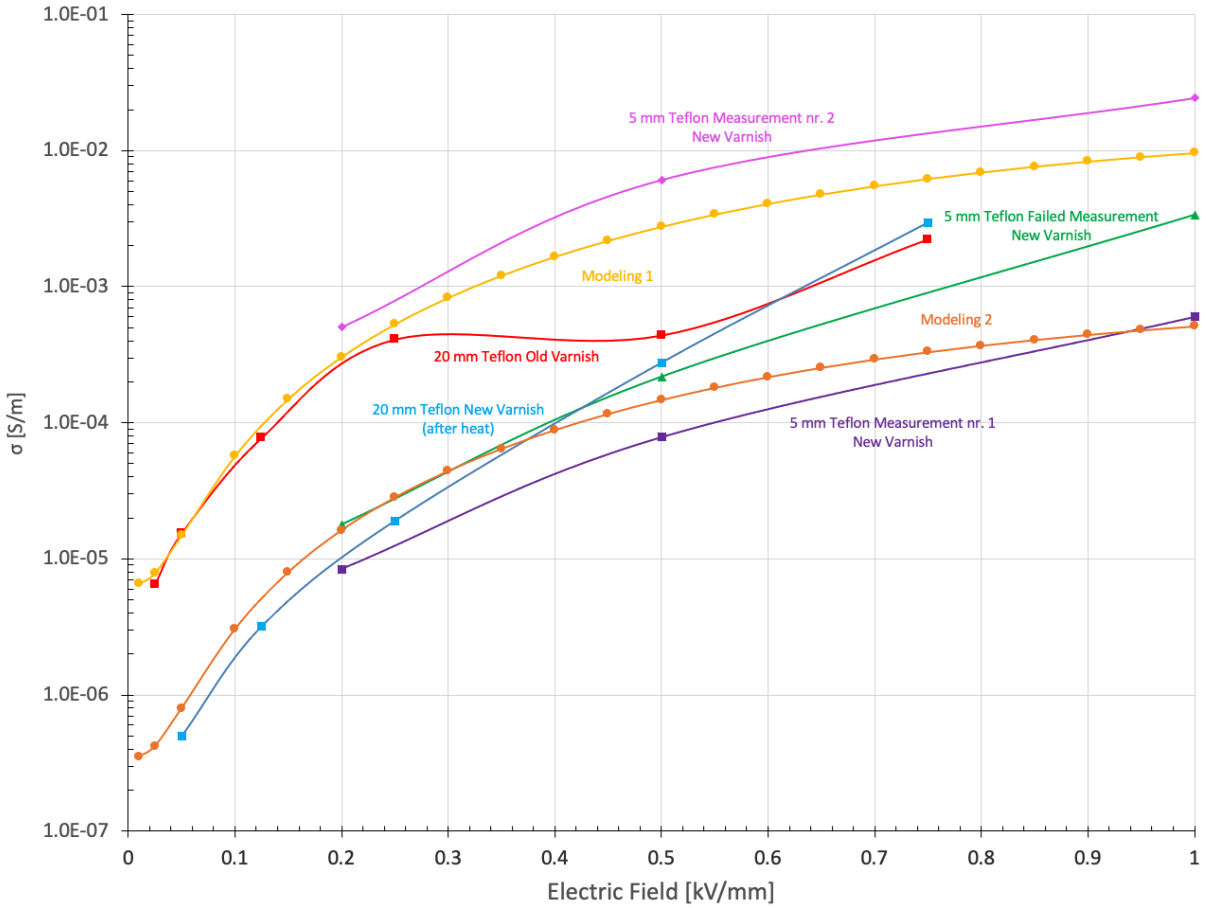

Figure 63: Graphs from the calculations performed with the values measured with the megger, considering the conductivity and the strength of the field, with a temperature of approximately 20°C. In addition the modeled graphs from expression 4 is plotted for comparison.

In addition to the yellow, the orange graph in the figure was modeled. This was done to make another graph that fitted the lower graphs in the figure. The orange graph resembled the blue, green and purple graphs better. The difference between the orange and the yellow modeling was mainly the base conductivity. It was changed from $6.58 \cdot 10^{-6}$

to $3.51 \cdot 10^{-7}$ S/m, the switching and the saturation field strength was kept constant. The two modeled expressions are shown below:

$$\sigma(E) = 6.4435 \cdot 10^{-6} \cdot \frac{1 + (\frac{E}{0.045})^{3.58-1}}{1 + (\frac{E}{1.0})^{3.58-1}}$$

$$\sigma(E) = 3.4435 \cdot 10^{-7} \cdot \frac{1 + (\frac{E}{0.045})^{3.58-1}}{1 + (\frac{E}{1.0})^{3.58-1}}$$

If the graphs are compared to figure 6 from the theory, some similarities are observed. The saturation of the electric field, E_2, is clearly shown in figure 63. The switching field strength is shown as a short section in the low field region. The nonlinear section of the graphs is found between 0.05 kV/mm and 0.25 kV/mm. Even though the conductivity values of the graphs are different, can the three recognizable sections be found in the same areas considering the electric field. All the graphs have the same switching section, nonlinear section and saturation section on the x-axis. The only difference is that they are shifted up and down vertically relative to the y-axis.

If the current graphs from the IDA measurements are inspected, the dependency stops at a given point. It stops between 0.125 and 0.05 kV/mm used in figure 45 and 46. According to the graphs above, the flat uninfluenced section of the curves is between 0 and 0.01 kV/mm. This suggests that the current in figure 46 could be affected. The distortion is hard to perceive in this figure. With the field of 0.05 kV/mm from 46, the conductivity of the varnish is barely inside the nonlinear section in figure 63. This can be the reason that the distortion is hard to see.

4.5 Potential Measurements with the Electrostatic Voltmeter

Potential measurements were done by wrapping a measuring steel wire snugly around the test object, the potential values were then found. The graphs could easily be compared with the data sheet of the varnish.

4.5.1 Cylindrical Test Object

The test object shown in figure 21 was used for the first measurements considering the potential distribution. The length of the sample goes parallel with the x-axis in figure 64. The section with varnish was 11.5 cm and the measurements were started and stopped 0.25 cm before the outer ends of the section. This gave 11 cm with one measurement for each centimeter. The potential is applied on the right side of the test object at 11.5 cm. High voltage was measured at 11.25 cm because it is close to the electrode with the applied potential. The first measurement was 0.25 cm from the ground electrode. It was therefore almost no potential measured by the electrostatic voltmeter at this point. From figure 64 there are shown four even graphs, with approximately the same forms.

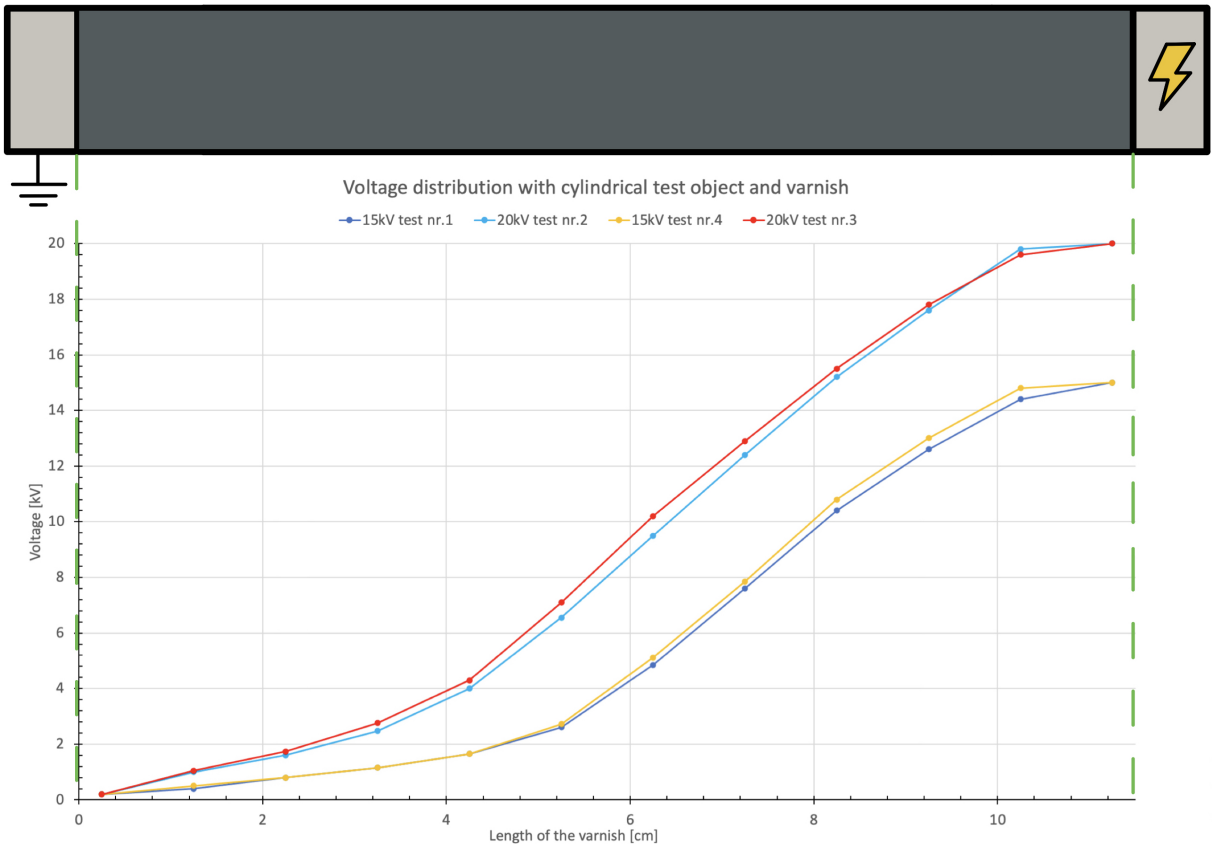

Figure 64: Potential measurements were performed with the Electrostatic voltmeter, considering the strength of the field and its distribution along the surface of the varnish on the cylindrical test object. The test object is shown at the top as a reference to the distribution. Assuming that the voltage was applied on the right side of the cylinder above the graph window. Measurements were performed with a temperature of approximately 20°C.

The red and the yellow line are from the measurements with the same test object but with two different voltages applied, the same goes for the two blue lines which belong to test object number two. The two lines with 20 kV are almost identical, the same goes for the two lines with 15 kV applied. This makes the two test objects look quite similar.

4.5.2 Generator Bars

The four figures below show the results from the measurements performed on the generator bars. There were performed measurements in both ends of the bars, with two different voltages, these are presented by the four graphs in figure 65, 66, 67 and 68. The ends of the new bar were given the numbers 1 and 2, the heat exposed bar was given the numbers 3 and 4 for the bar ends. As mentioned in section 3.3.2, the conductive layer of the new bar was removed and measurements were performed at 6.4 and 11 kV. These voltages were used during measurements on both bar ends, with and without varnish. The field

controlling section of the generator bar is represented by the x-axis of the four figures 65, 66, 67 and 68. This area is illustrated on the top of the figures, which is where the distribution of the potential was measured. The relationship between the potential and its distribution on the test object is shown in the figures. Ground potential was found at 0 cm and the conductor at 15 cm. This means that the section for measuring and field grading went from 0 to 15 cm. The area used for measuring was 15 cm even though the varnish was 15.5 cm. The overlap of 0.5 cm was found behind the 0 cm mark in figure 66 and 67. The overlapping varnish goes 0.5 cm to the left of the left dotted line in the figures. The additional 0.5 cm was due to the overlap of the conductive section in the middle. The reason for this was explained in section 2.1.2 and shown in figure 5.

The potential measured on the surface of the bar without varnish was stable. Figure 65 shows that the values start changing right before the end, near the ground potential. The small variations from 2 cm to 14 cm are probably due to the uneven surface of the insulation measured. Near the ground potential, where the stator core is simulated, the increase of the potential is steep. The electric field becomes strong rapidly from 0 cm when looking at the values towards the conductor of the generator bar.

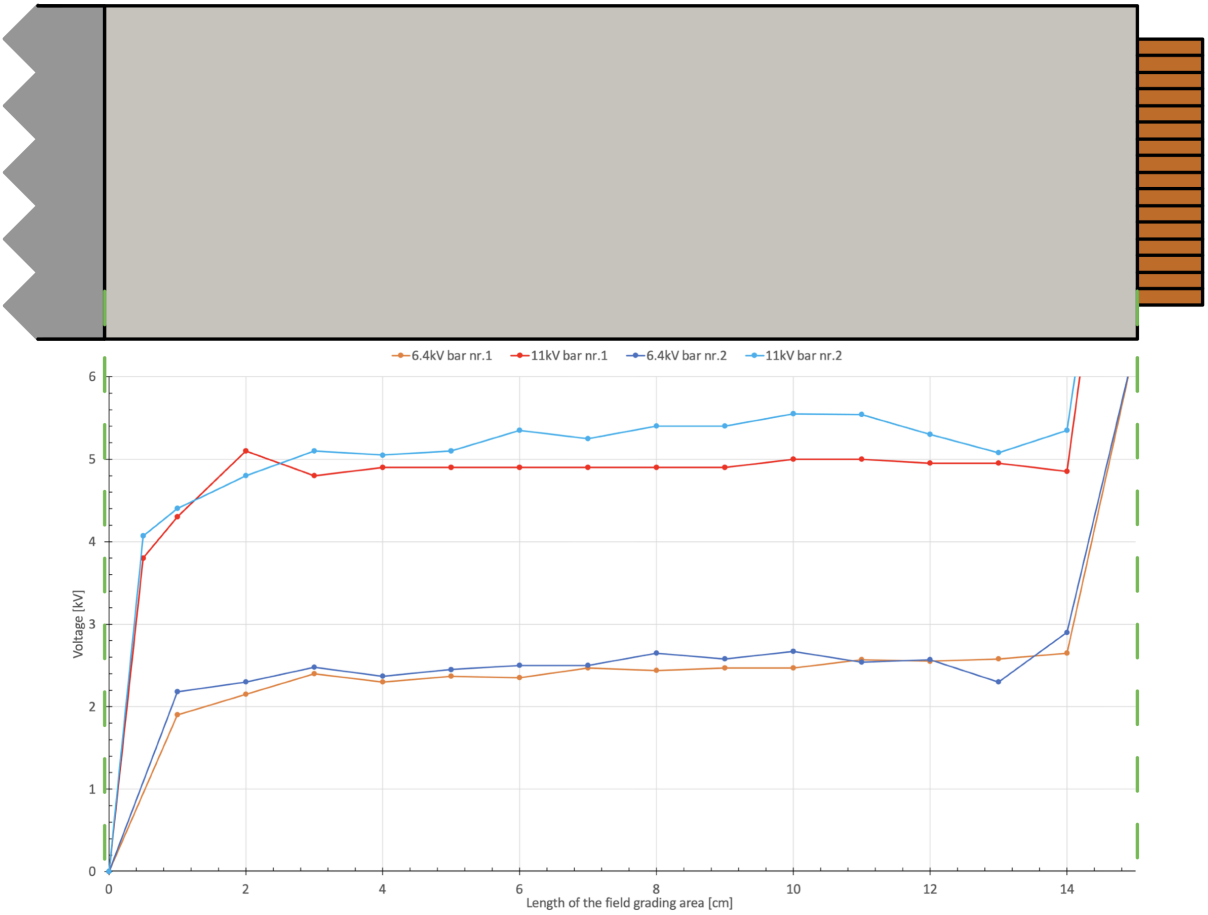

Figure 65: Potential measurements were performed on the insulation with the Electrostatic voltmeter, considering the strength of the field and its distribution along the surface of the bar´s field grading section. Considering bar end numbers 1 and 2. The field grading section without varnish is shown at the top as a reference to the distribution. Assuming that the voltage was applied to the conductor on the right side of the figure above the graph window. The measurements were performed with approximately 20°C.

As mentioned, the x-axis starts at 0 cm at the "grounded stator core", and goes towards the tip of the insulation, near the conductor, at 15 cm. This makes it possible to imagine the distribution of the potential along the field grading section. The graphs in figure 65 can be compared with the black graph in figure 16, collected from the data sheet [7]. This graph represents the potential distribution on a section without a field grading varnish. The shape of the black graph is steep until the peak and flat after. This shape resembles the graphs in figure 65. This indicates that the measurements are valid and can be trusted.

Figure 66 shows the results from measurements on a generator bar applied with a thin layer of varnish to its field grading section. The graphs show a stable potential from the tip of the conductor towards the grounded area. The decrease in potential starts at 5 cm and goes towards 0 cm. The small differences in the measurements from 5 to 14 cm may be caused by an uneven varnish surface, uneven insulation underneath, or bad precision

considering the electrostatic voltmeter.

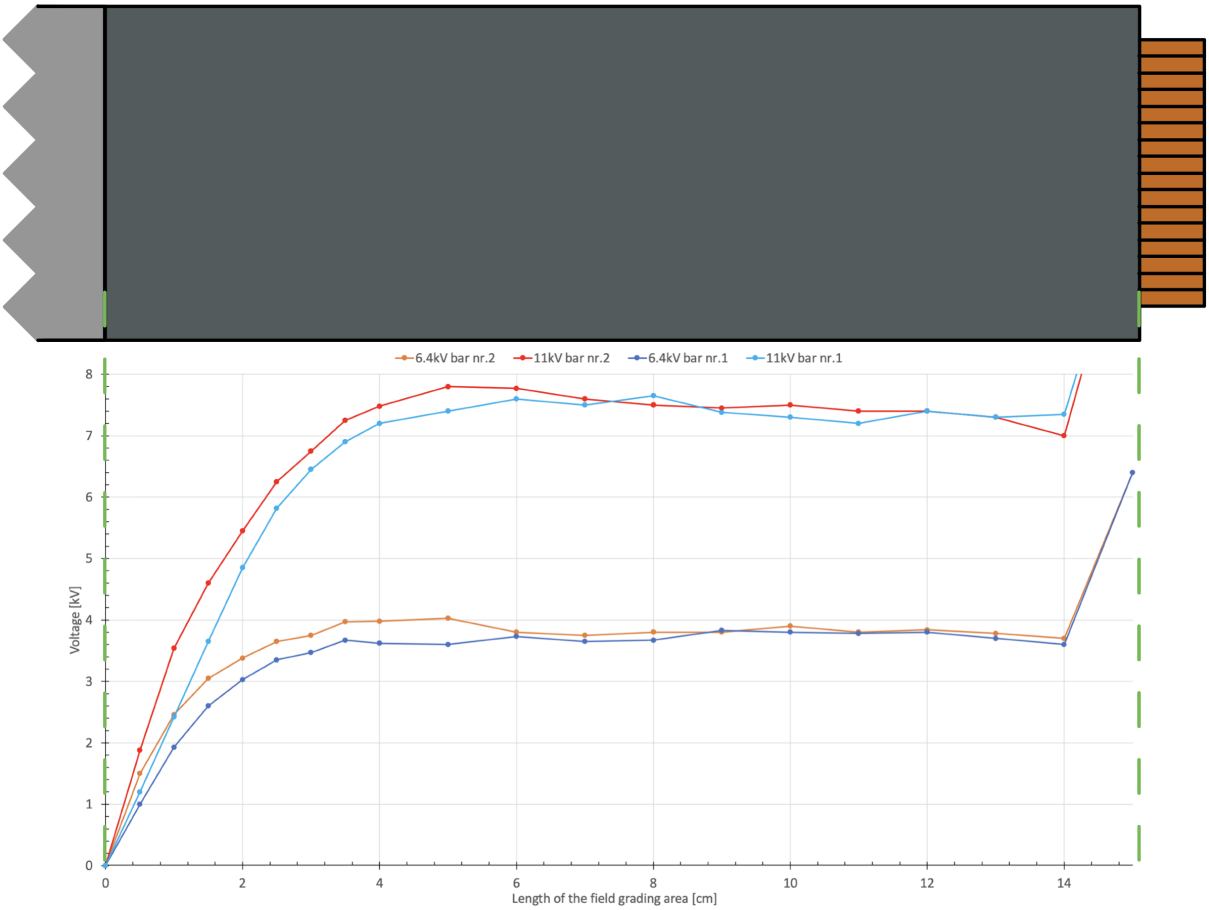

Figure 66: Potential measurements were performed on the thin varnish with the Electrostatic voltmeter, considering the strength of the field and its distribution along the surface of the varnish on the generator bars. Considering bar end numbers 1 and 2. The field grading section with varnish is shown at the top as a reference to the distribution. Assuming that the voltage was applied to the conductor on the right side of the figure above the graph window. Measurements were performed with a temperature of approximately 20°C.

By comparing figure 66 to 16, some similarities is observed. The measured potential distribution, with a thin varnish applied, has the same shape as the green graph from 16. The steep section of the graph in figure 65, towards the grounded area, is more flat with the thin varnish applied. The peak is also shifted and a little higher than without varnish. The peak of the potential is higher, rounded and further away from the "grounded stator core". The shape of the measured graph became more similar to the green graph in figure 16 when the thin layer of varnish was applied. The difference between figure 65 and 66 is noticeable, the increase and curvature of the graphs are way smoother with the varnish.

Figure 67 shows the measured values on the surface of the varnish with the most amount of layers, approximately 1 mm of varnish. The graphs are smoother and the peak is even

more flat. Compared to the green reference graph from the data sheet in figure 16, the even, shifted and rounded peak is quite similar. Compared to figure 66 with only half the layers, the graphs in figure 67 are smoother and more rounded. From the peak and towards the tip of the conductor at 15 cm, more even values are measured compared to the thin varnish. The peak of the potential also got reduced due to the thicker varnish. With 11 kV applied, the potential went from 7.8 with the thin varnish to 7.6 kV with the thick varnish. With 6.4 kV applied there is not a difference in the measured values, both are measured to 3.9 kV. By comparing the two graphs from the results with 6.4 and 11.0 kV, there is not any significant difference between the two ends of the generator bars. For example, the red and the light blue graph are almost similar. The difference between the results from the test of the thin and the thick layer is also minimal. The purpose of the varnish is obtained with the thin layer. The recommended thickness of the finished varnish from the data sheet [7] was between 0.2 and 0.5 mm. This strengthens the theory that a thin layer is enough.

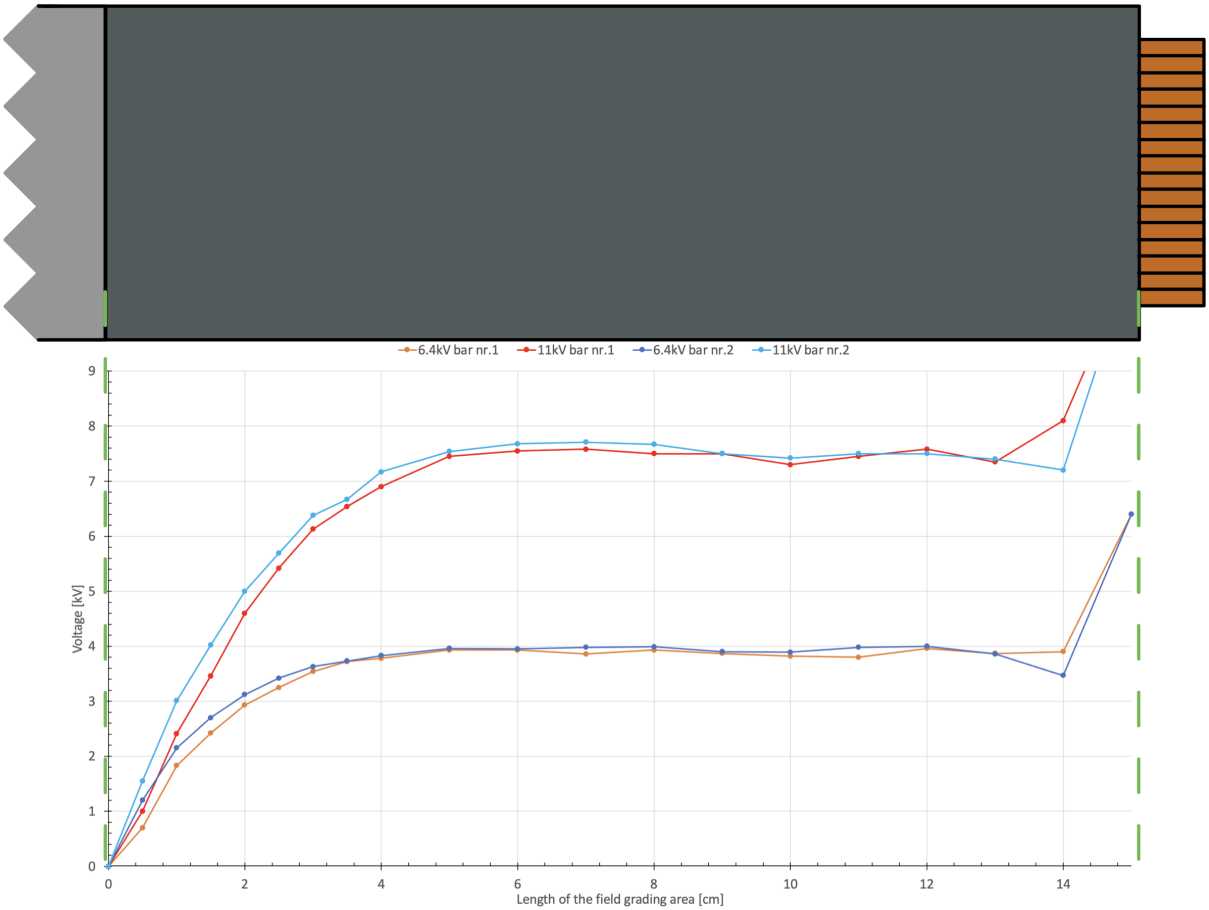

Figure 67: Potential measurements were performed on the thick varnish with the Electrostatic voltmeter, considering the strength of the field and its distribution along the surface of the varnish on the generator bars. Considering bar end numbers 1 and 2. The field grading section with varnish is shown at the top as a reference to the distribution. Assuming that the voltage was applied to the conductors on the right side of the figure, above the graph window. The measurements were performed with approximately 20°C.

The generator bar with the varnish exposed to thermal stress, was measured with the same potentials applied and the same set-up. The only difference was the length of the field grading area which was 10 cm instead of 15 cm. In figure 68 the results from the measurements are shown. The stable value measured along the surface of the bar from 3 to 8 cm is almost similar to the values from the two previous measurements. With 11 kV, several of the measured values on the surface of the varnish were steady at 6.6 kV. With 6.4 kV applied, the steady value was about 3.2 kV. The bar with the new varnish, that was not exposed to thermal stress, had a stable potential of 7.5 and 3.9 kV. The potential values measured were lower with cured varnish. It could also be because another person made the sample earlier and the procedure may have been performed in another way.

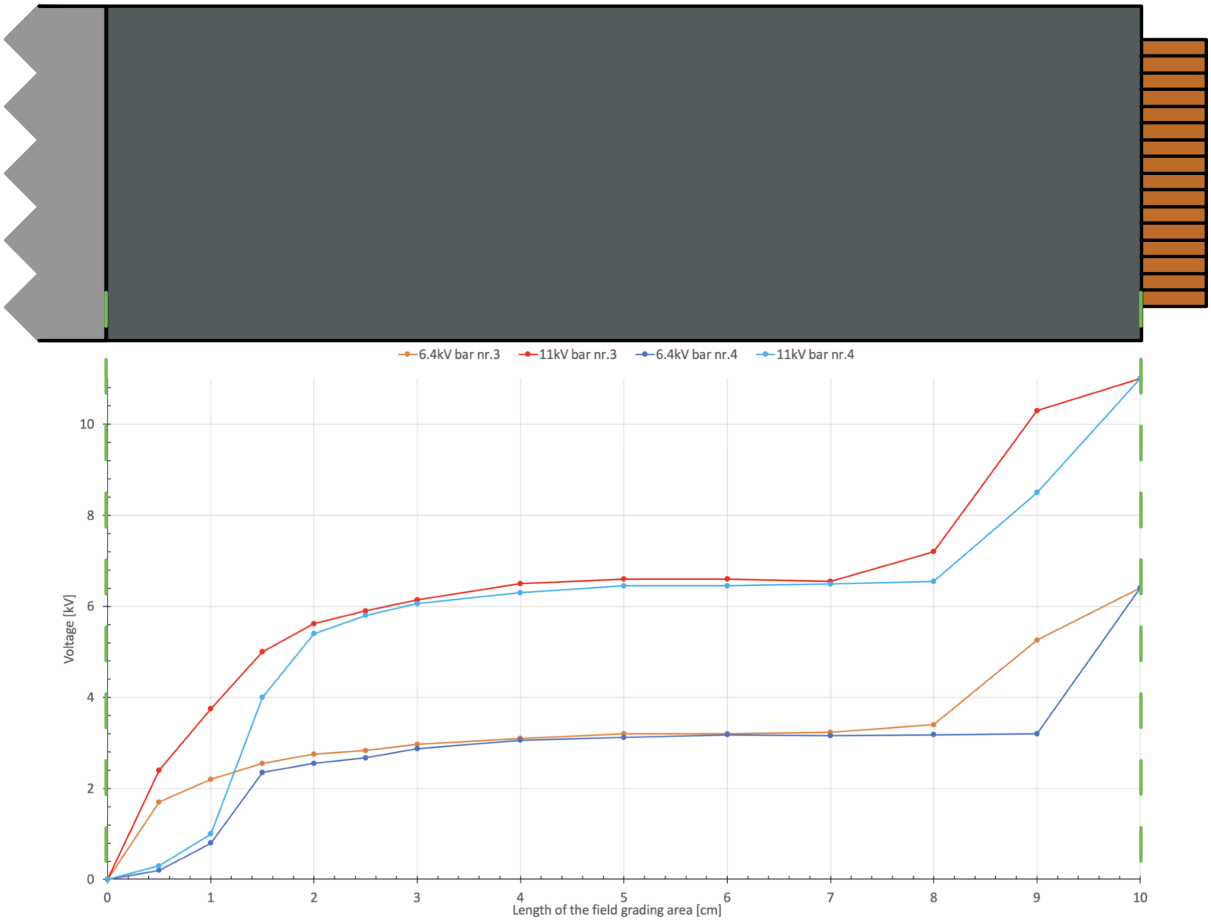

Figure 68: Potential measurements were performed on the old heat exposed varnish with the Electrostatic voltmeter, considering the strength of the field and its distribution along the surface of the varnish on the generator bar. Considering bar end numbers 3 and 4. The field grading section with varnish is shown at the top as a reference to the distribution. Assuming that the voltage was applied to the conductors on the right side of the figure, above the graph window. The measurements were performed with approximately 20°C.

Figure 68 shows that one of the two generator bar ends was different from the other. The shape of the green graph in figure 16 is not similar to the blue graphs in 68. The blue

graphs from bar end number 4 had a weird shape in the section closest to the grounded area at 0 cm. Between 0 cm and 2 cm, there is a difference from bar end number 3. This could be caused by the underlying insulation or the preparation of the layers and area. After this bad section of the generator bar, the measured values start to go back towards the graphs that belong to bar end number 3. They then become quite similar toward the conductor at 10 cm.

5 Conclusion

The desired outcome of this thesis was to increase the knowledge around the behavior of the field grading varnish. The dependency of the temperature, frequency and electric field was considered in this work. The different measuring methods performed through this work gave several different types of results. All the dependencies were confirmed present during the testing.

From the IDA 200 measurements, the graphs presented, clearly shows the dependency of the frequencies. At higher frequencies, the loss factor decreases. The same goes for the imaginary part of the capacitance. The results also showed that the higher fields gave higher losses. The carefully measured current confirmed the influence of the field, by showing a more distorted current with higher fields.

With the fairly similar IDAX, the fields obtained were too weak to show any interesting results. The outcome that gave interesting values from this measuring method, was the different graphs with the different temperatures. It was possible to see that the higher temperatures gave higher losses. In addition, the dependency of the frequency was confirmed with the results from this analyzer. If the frequency increased, the loss factor decreased. With little consistency, these dependencies were hard to pinpoint exactly.

By comparing the results from the two analyzers, a more complete overview of the dependencies was found. The complete figure showed graphs from 0.0025 to 0.5 kV/mm with frequencies from 0.1 Hz to 100 Hz. The transition between the IDAX and IDA measurements is not as desired, these should complete each other.

Two graphs were made out of the results from the megger. The stable values of the stationary current and resistance were used to produce the graphs. The modeled graphs represent the dependency of the conductivity on the electric field. The only disadvantage is that these are fitted graphs and not as precise as a totally measured curve. Because of the varying graphs from the measurements, the modeled graphs needed to be adapted. The graphs showed that the dependency of the electric field started around 0.01 kV/mm. The nonlinear section was found between 0.05 and 0.25 kV/mm.

The measurements done with the electrostatic voltmeter confirmed the given effect of the varnish from the manufacturer. The curves of the potential distribution were found in the data sheet. The graphs that showed the measured potential on the surface of the varnish resemble the ones in the data sheet.

6 Further Work

To get more information and knowledge around this varnish and its properties, further tests and characterizations can be performed. From the results and the conclusion some suggestion for further work are:

- Perform more detailed modeling. Show the dependency of the field, temperature and frequency. This would give a more complete overview of the behavior of the varnish.
- Measure with higher frequencies. With the IDA 200 and IDAX 206, only frequencies between 0.1 and 1000 Hz were used. It would have been interesting and more complementary to measure with frequencies up to a few kHz.
- The modeling needs verification. This can be done with measurements, to make this possible a measuring probe is needed. To measure the electric field of the surface of the test object.
- A sample with a smaller spacer than 20 mm, to be able to make even stronger fields in the measurements of the IDA 200

References

[1] Sagøy O.H., Dielectric Characterization of Semi Conducting Field Grading Varnish for Hydro Generators. Project report in TET5500 Elkraftteknikk, Trondheim: Department of Electric Power Engineering, NTNU; 2020 [Cited: 23.April 2021].

[2] getmyuni.com [Internet]. [Cited: 16. Oct 2020]. Available from: https://d13mk4zmvuctmz.cloudfront.net/assets/main/study-material/notes/electrical-engineering_engineering_electrical-machine-design_design-of-synchronous-machines_notes.pdf

[3] Ildstad E. TET4160 Insulation Materials for High voltage Applications. Trondheim: Department of Electric Power Engineering, NTNU; 2019 [Cited: 16. Nov 2020].

[4] Programma Electrics AB. IDA 200, Insulation Diagnostic System User´s Manual. 2002 [Cited: 27. Apr 2021].

[5] Cigre. TB794, Field grading in electrical insulation systems. March 2020 [Cited:May 2021].

[6] Chapman M., Bruetsch R. Suppression of partial discharges in high-voltage rotating machines. 2009 IEEE Electrical Insulation Conference. Montreal, QC, Canada: VonRoll, IEEE; 2009. p. 338-342.

[7] Von Roll data-sheet. Available from: https://www.bag-distribution.com/corona-shield-p8001-in-1-kg-can-c2x17676759

[8] Nysveen A. Power-points from Von Roll obtained with E-mail correspondence.

[9] Secklehner, M.; Hussain, R.; Hinrichsen, V.: Tailoring of new Field Grading Materials for HVDC Systems. INSUCON 2017, Birmingham, 16th to 18th may, 2017

[10] 2006 Pax Diagnostics. IDAX-206 User´s Manual. [Cited 31. Apr. 2021]

7 Appendix

7.1 Appendix A

7.1.1 IDAX 206 Measurements of The Old Varnish, Field Dependency

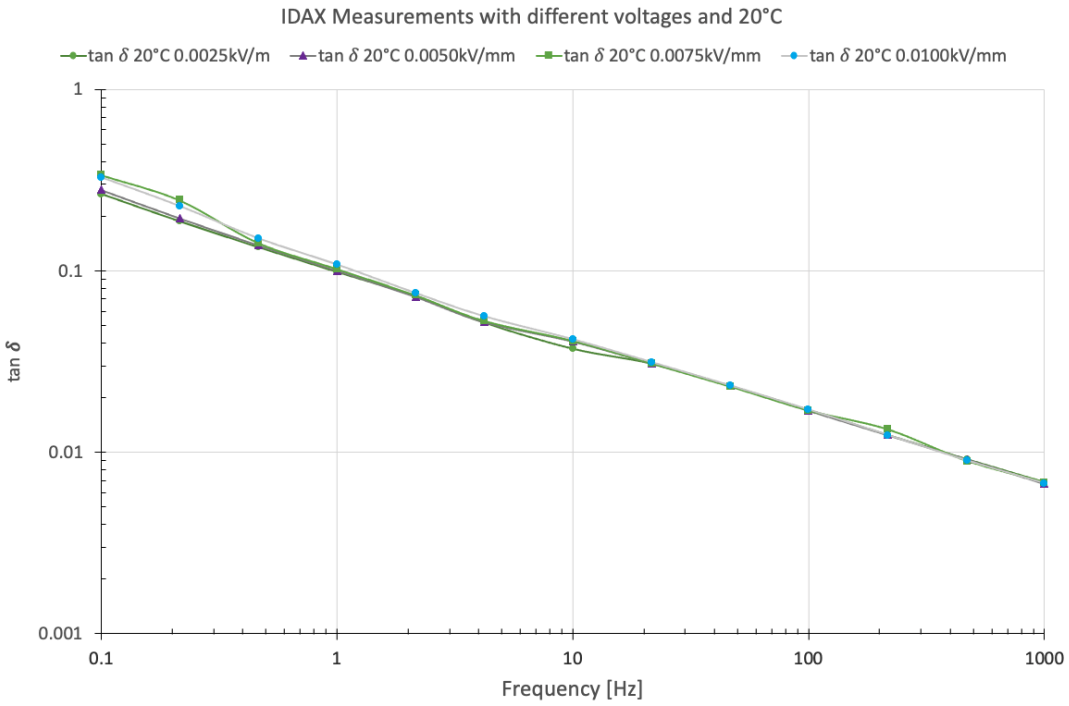

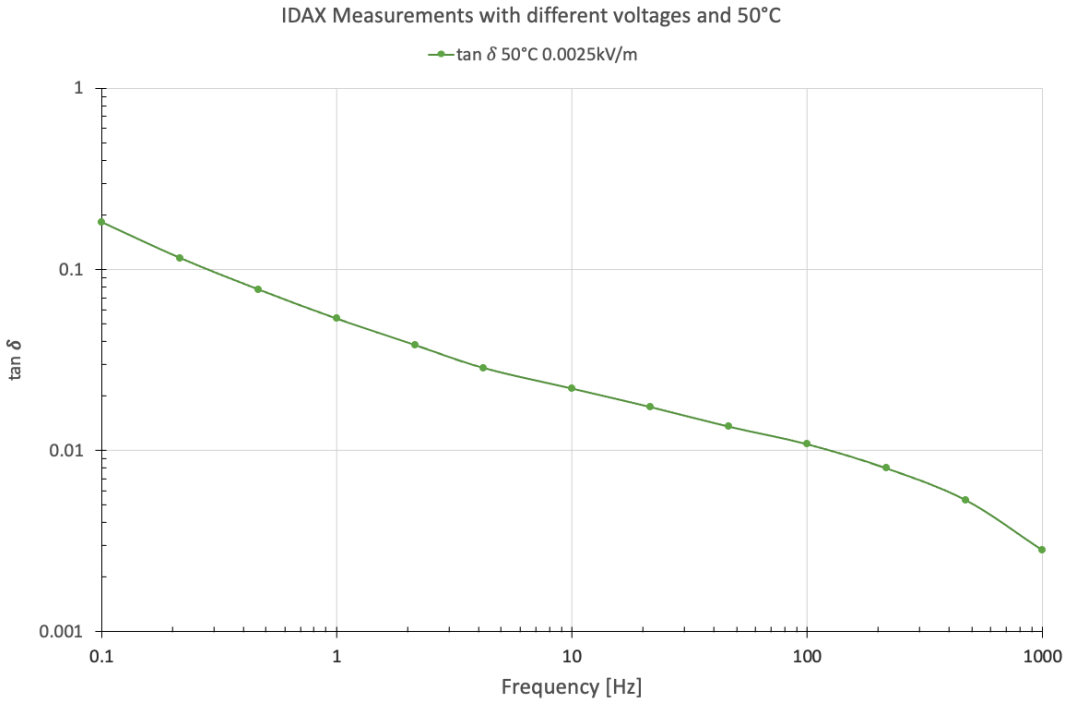

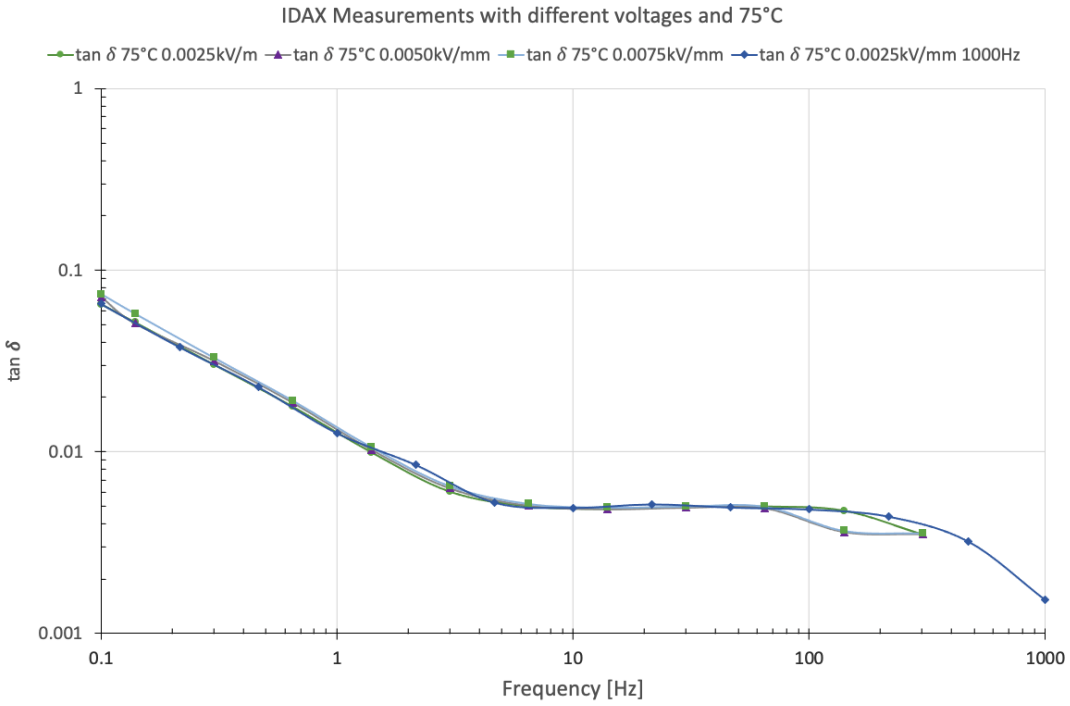
IDAX Measurements with different voltages and 75°C
tan δ 75°C 0.0025kV/m
tan δ 75°C 0.0050kV/mm
tan δ 75°C 0.0075kV/mm
tan δ 75°C 0.0025kV/mm 1000Hz
tan δ
1
0.1
0.01
0.001
0.1
1
10
100
1000
Frequency [Hz]

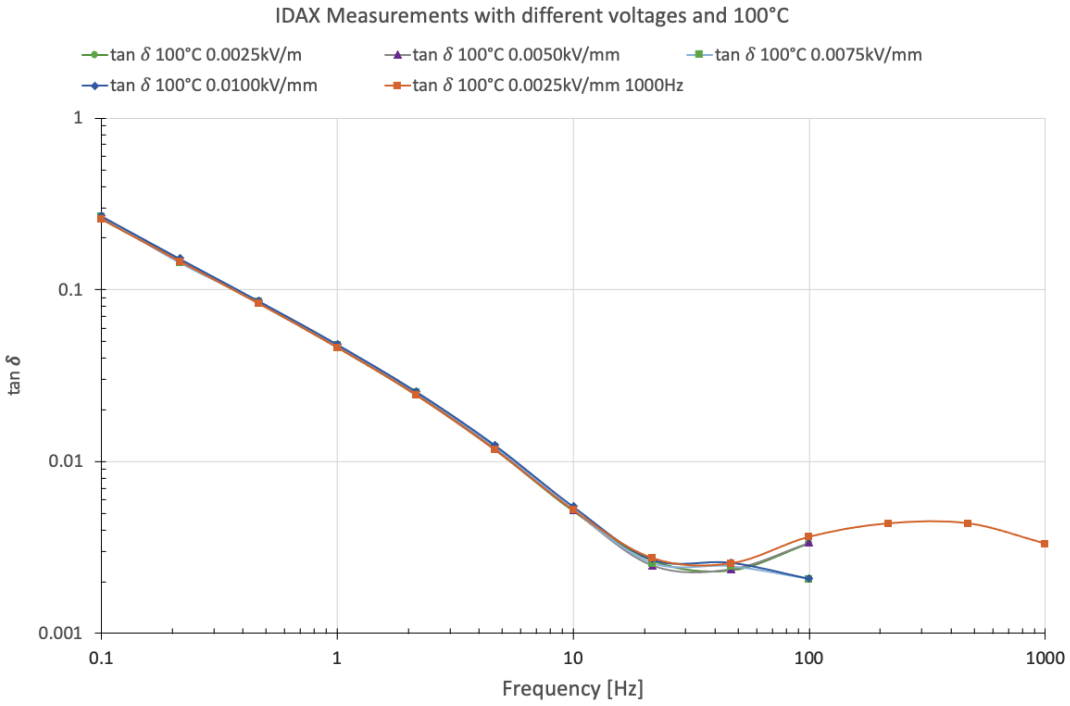
IDAX Measurements with different voltages and 100°C
tan δ 100°C 0.0025kV/m
tan δ 100°C 0.0050kV/mm
tan δ 100°C 0.0075kV/mm
tan δ 100°C 0.0100kV/mm
tan δ 100°C 0.0025kV/mm 1000Hz
tan δ
1
0.1
0.01
0.001
0.1
1
10
100
1000
Frequency [Hz]

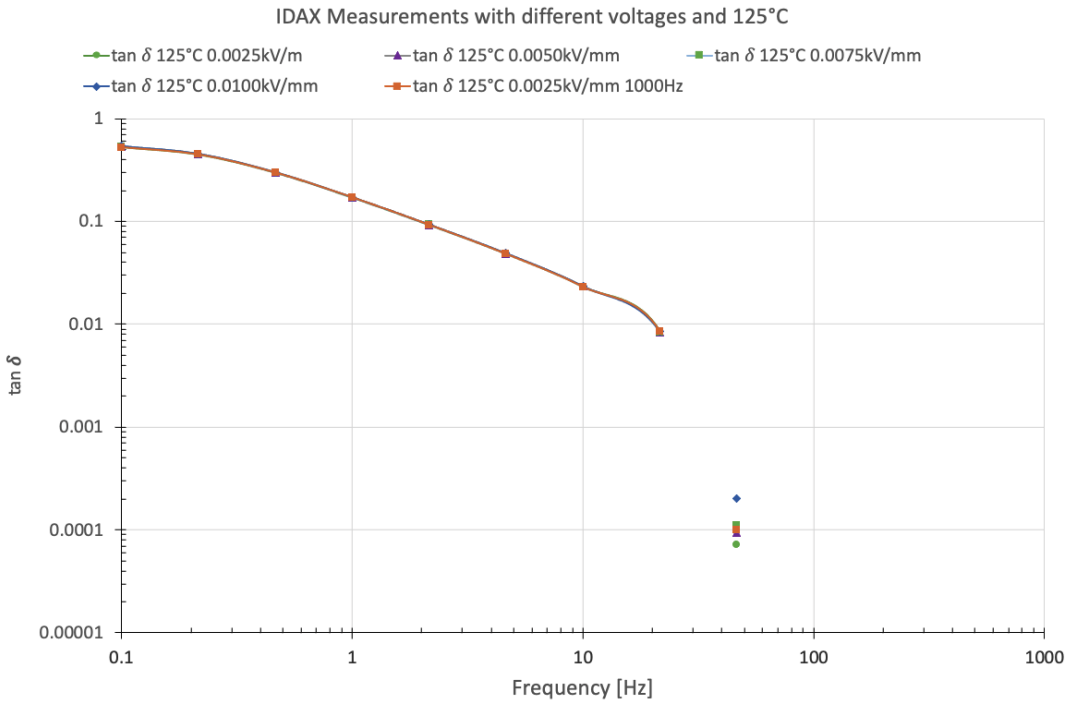
IDAX Measurements with different voltages and 125°C
tan δ 125°C 0.0025kV/m
tan δ 125°C 0.0050kV/mm
tan δ 125°C 0.0075kV/mm
tan δ 125°C 0.0100kV/mm
tan δ 125°C 0.0025kV/mm 1000Hz
tan δ
1
0.1
0.01
0.001
0.0001
0.00001
0.1
1
10
100
1000
Frequency [Hz]

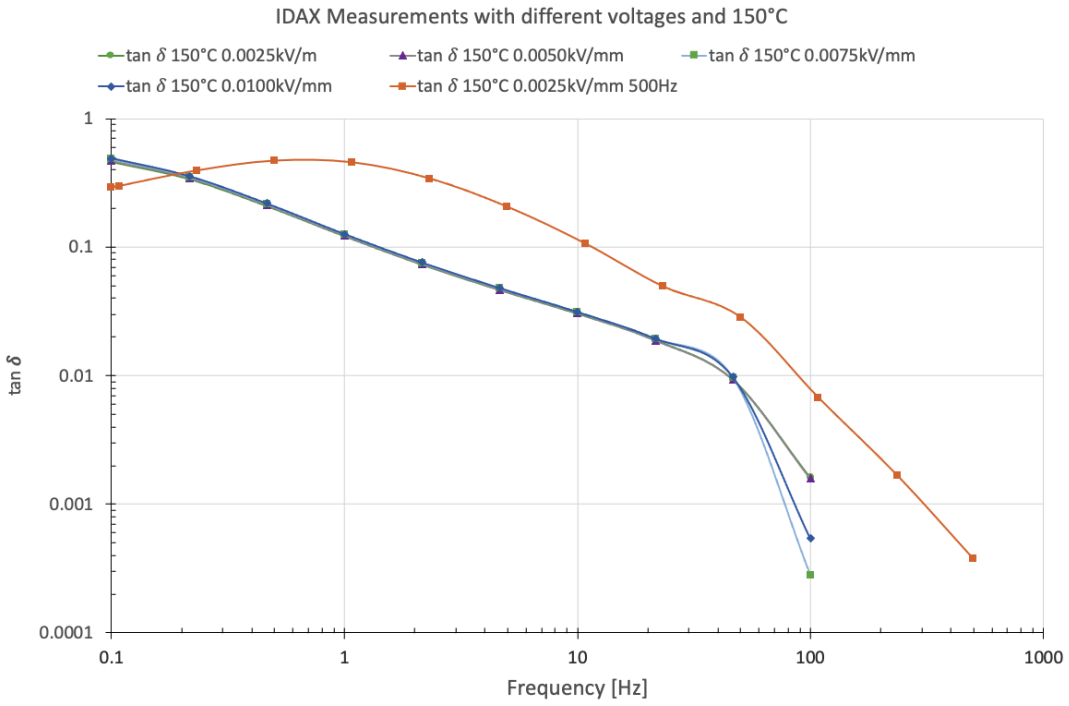
IDAX Measurements with different voltages and 150°C
tan δ 150°C 0.0025kV/m
tan δ 150°C 0.0050kV/mm
tan δ 150°C 0.0075kV/mm
tan δ 150°C 0.0100kV/mm
tan δ 150°C 0.0025kV/mm 500Hz
tan δ
1
0.1
0.01
0.001
0.0001
0.1
1
10
100
1000
Frequency [Hz]

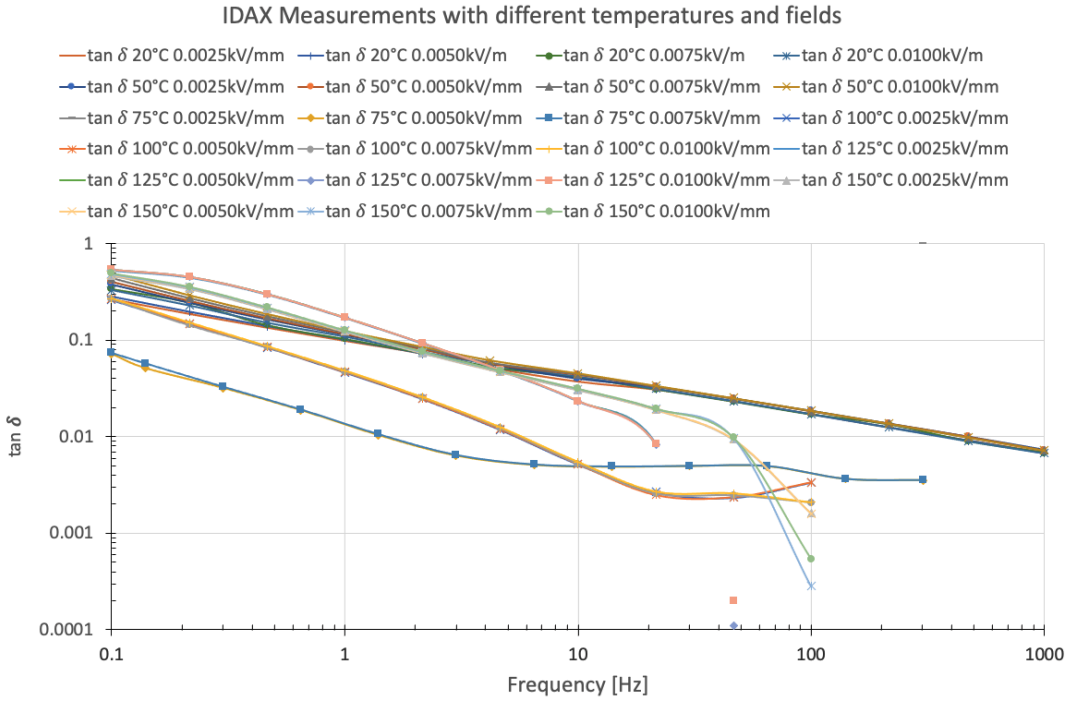
IDAX Measurements with different temperatures and fields
tan δ 20°C 0.0025kV/mm
tan δ 20°C 0.0050kV/m
tan δ 20°C 0.0075kV/m
tan δ 20°C 0.0100kV/m
tan δ 50°C 0.0025kV/mm
tan δ 50°C 0.0050kV/mm
tan δ 50°C 0.0075kV/mm
tan δ 50°C 0.0100kV/mm
tan δ 75°C 0.0025kV/mm
tan δ 75°C 0.0050kV/mm
tan δ 75°C 0.0075kV/mm
tan δ 100°C 0.0025kV/mm
tan δ 100°C 0.0050kV/mm
tan δ 100°C 0.0075kV/mm
tan δ 100°C 0.0100kV/mm
tan δ 125°C 0.0025kV/mm
tan δ 125°C 0.0050kV/mm
tan δ 125°C 0.0075kV/mm
tan δ 125°C 0.0100kV/mm
tan δ 150°C 0.0025kV/mm
tan δ 150°C 0.0050kV/mm
tan δ 150°C 0.0075kV/mm
tan δ 150°C 0.0100kV/mm
1
0.1
0.01
0.001
0.0001
tan δ
0.1
1
10
100
1000
Frequency [Hz]

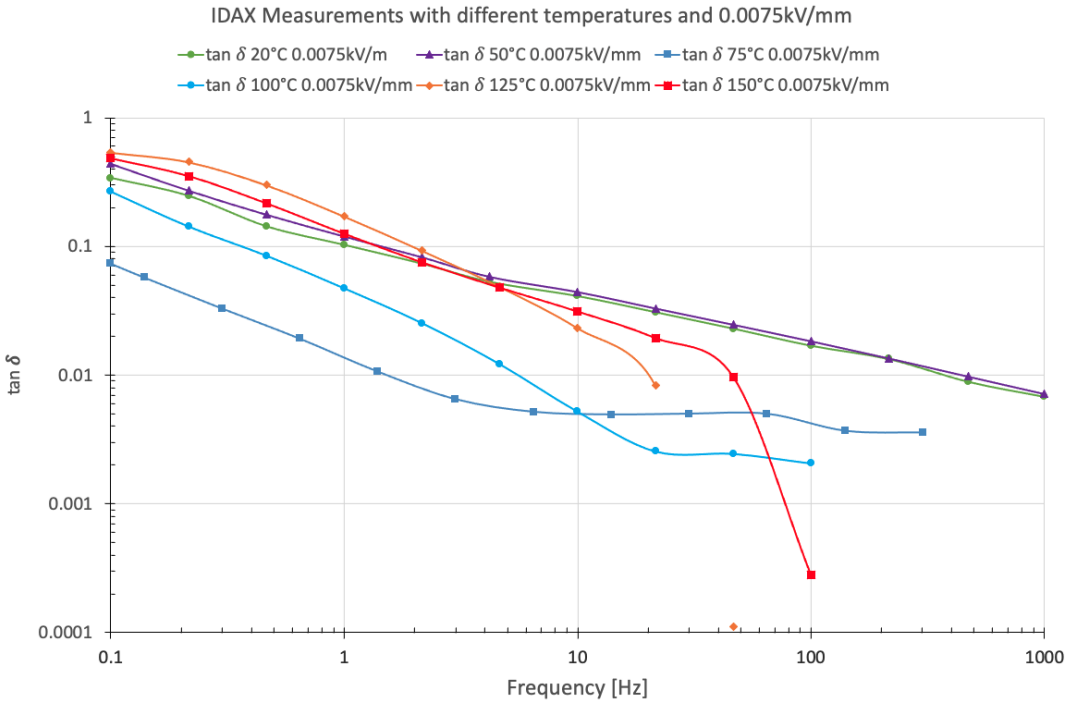
IDAX Measurements with different temperatures and 0.0075kV/mm
tan δ 20°C 0.0075kV/m
tan δ 50°C 0.0075kV/mm
tan δ 75°C 0.0075kV/mm
tan δ 100°C 0.0075kV/mm
tan δ 125°C 0.0075kV/mm
tan δ 150°C 0.0075kV/mm
1
0.1
0.01
0.001
0.0001
tan δ
0.1
1
10
100
1000
Frequency [Hz]

7.1.2 IDAX 206 Measurements of The New Varnish, Field Dependency

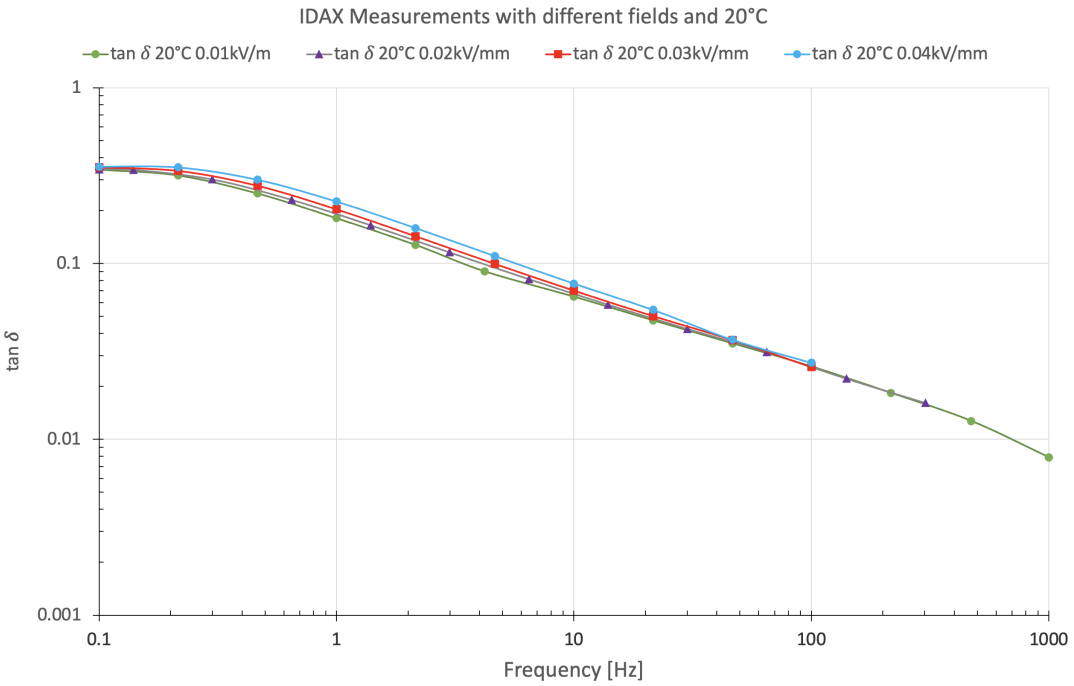

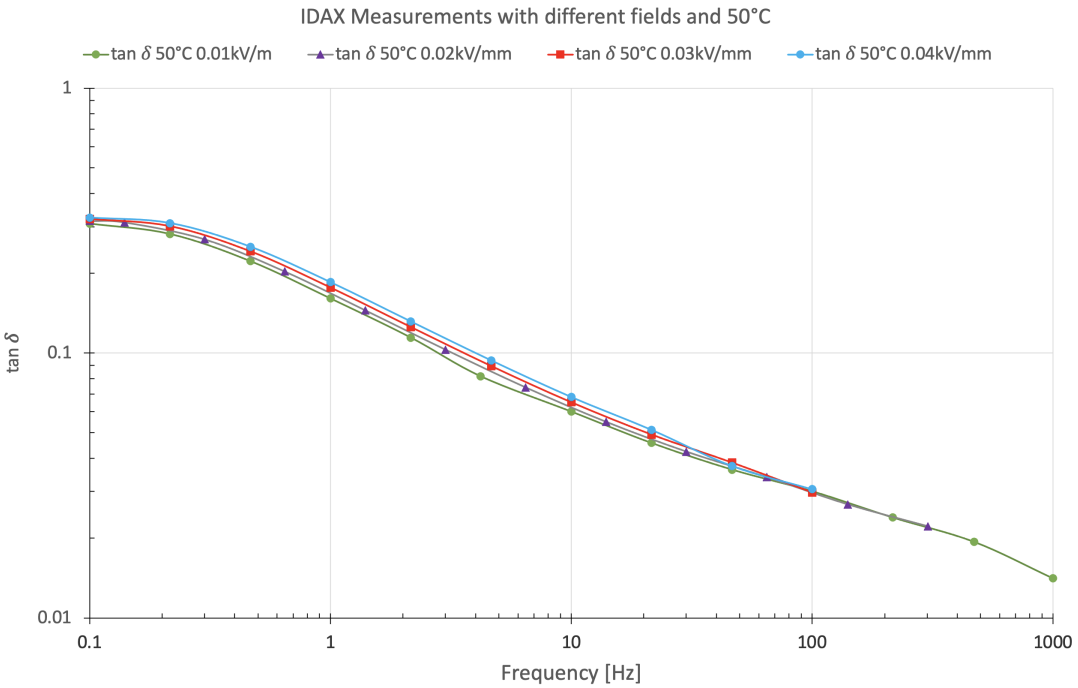

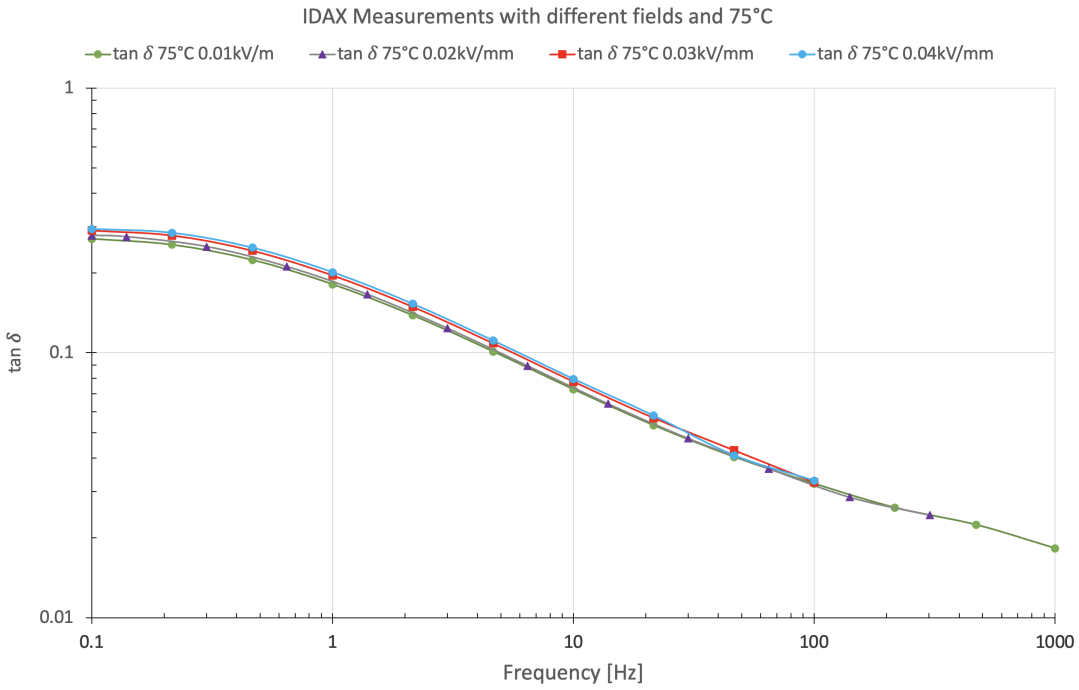
IDAX Measurements with different fields and 75°C
tan δ 75°C 0.01kV/m
tan δ 75°C 0.02kV/mm
tan δ 75°C 0.03kV/mm
tan δ 75°C 0.04kV/mm
tan δ
1
0.1
0.01
0.1
1
10
100
1000
Frequency [Hz]

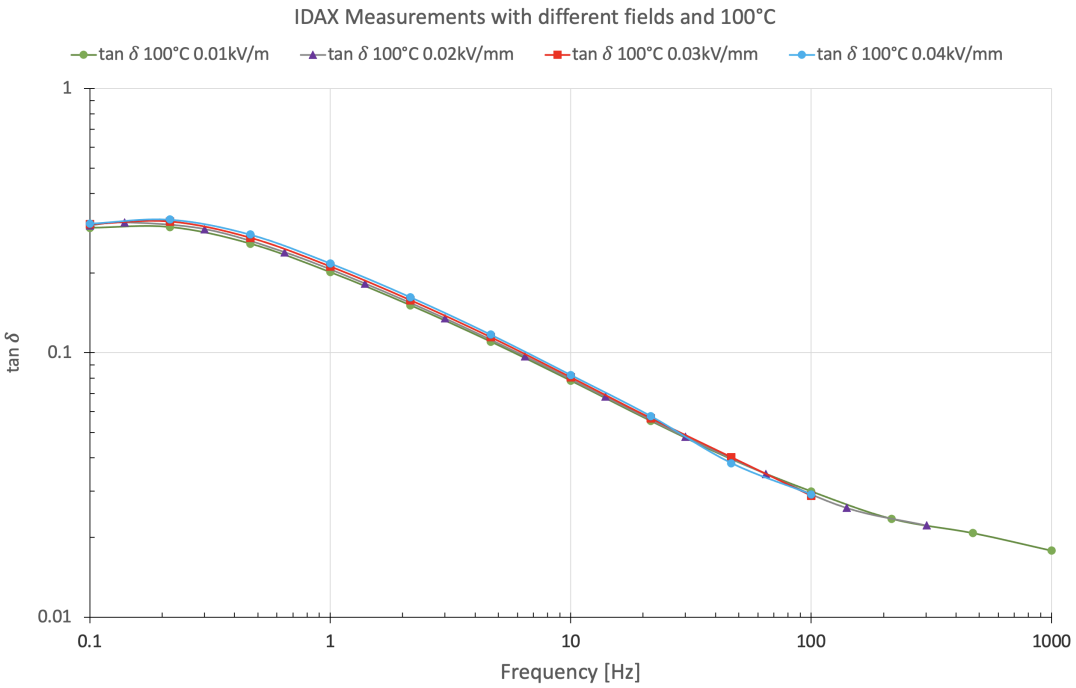
IDAX Measurements with different fields and 100°C
tan δ 100°C 0.01kV/m
tan δ 100°C 0.02kV/mm
tan δ 100°C 0.03kV/mm
tan δ 100°C 0.04kV/mm
tan δ
1
0.1
0.01
0.1
1
10
100
1000
Frequency [Hz]

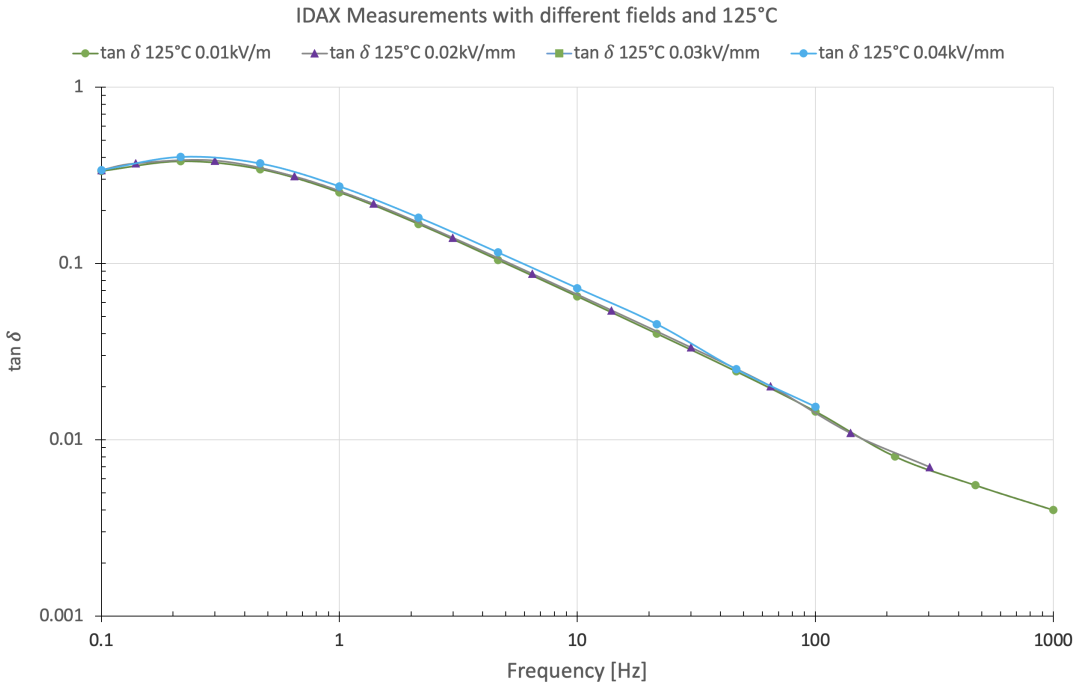
IDAX Measurements with different fields and 125°C
tan δ 125°C 0.01kV/m
tan δ 125°C 0.02kV/mm
tan δ 125°C 0.03kV/mm
tan δ 125°C 0.04kV/mm
1
0.1
0.01
0.001
tan δ
0.1
1
10
100
1000
Frequency [Hz]

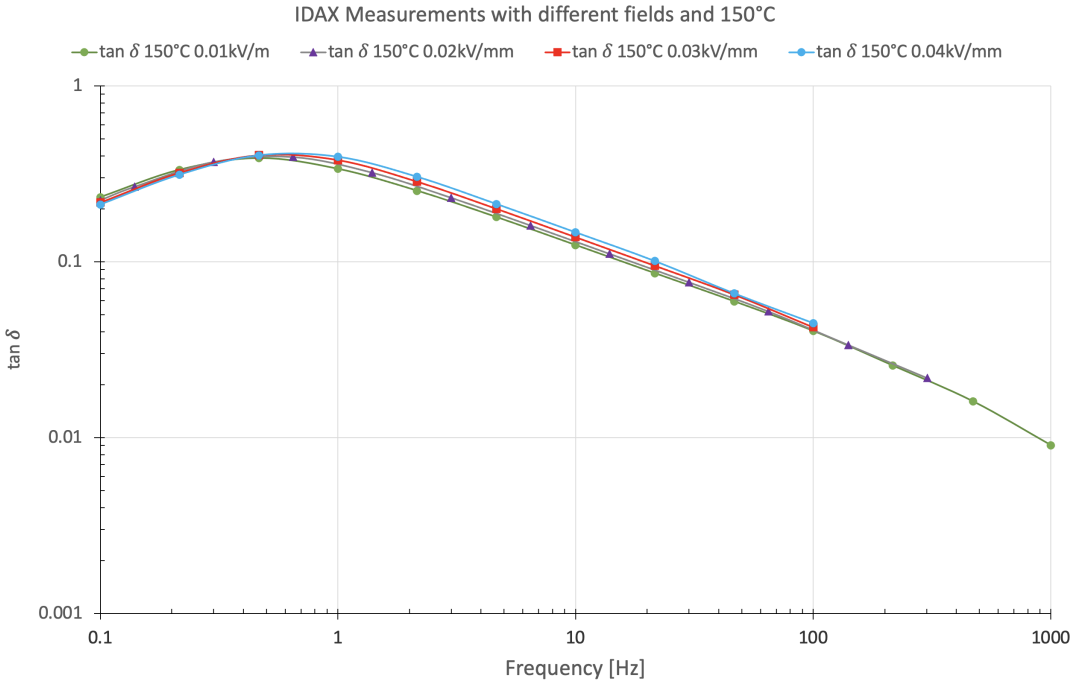
IDAX Measurements with different fields and 150°C
tan δ 150°C 0.01kV/m
tan δ 150°C 0.02kV/mm
tan δ 150°C 0.03kV/mm
tan δ 150°C 0.04kV/mm
1
0.1
0.01
0.001
tan δ
0.1
1
10
100
1000
Frequency [Hz]

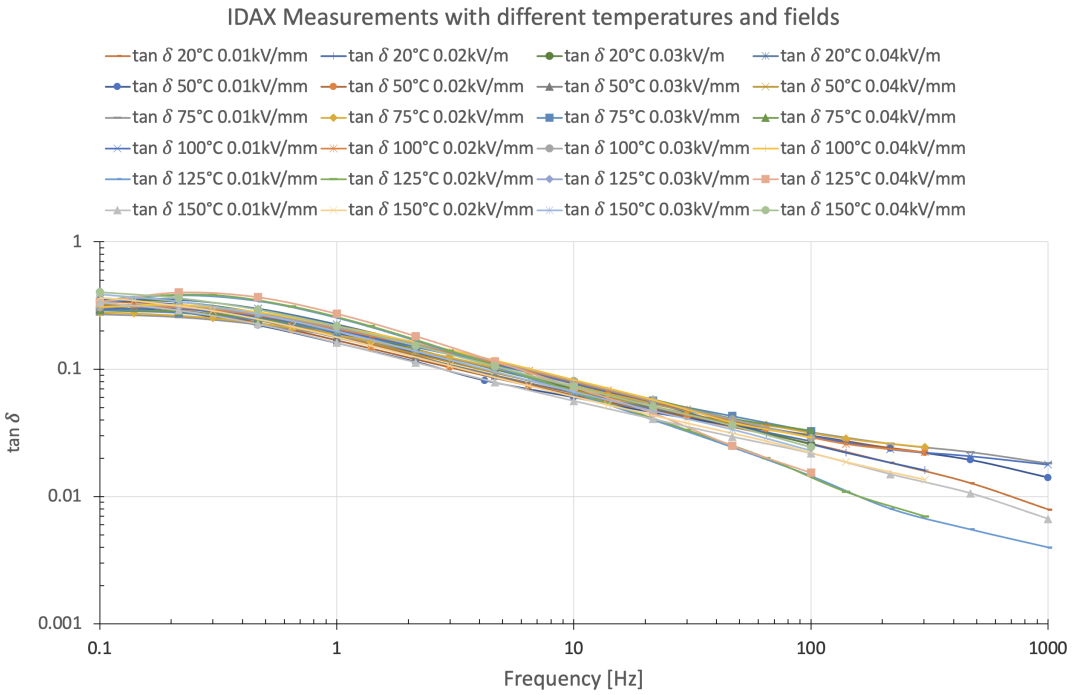
IDAX Measurements with different temperatures and fields
tan δ 20°C 0.01kV/mm
tan δ 20°C 0.02kV/m
tan δ 20°C 0.03kV/m
tan δ 20°C 0.04kV/m
tan δ 50°C 0.01kV/mm
tan δ 50°C 0.02kV/mm
tan δ 50°C 0.03kV/mm
tan δ 50°C 0.04kV/mm
tan δ 75°C 0.01kV/mm
tan δ 75°C 0.02kV/mm
tan δ 75°C 0.03kV/mm
tan δ 75°C 0.04kV/mm
tan δ 100°C 0.01kV/mm
tan δ 100°C 0.02kV/mm
tan δ 100°C 0.03kV/mm
tan δ 100°C 0.04kV/mm
tan δ 125°C 0.01kV/mm
tan δ 125°C 0.02kV/mm
tan δ 125°C 0.03kV/mm
tan δ 125°C 0.04kV/mm
tan δ 150°C 0.01kV/mm
tan δ 150°C 0.02kV/mm
tan δ 150°C 0.03kV/mm
tan δ 150°C 0.04kV/mm
1
0.1
0.01
0.001
tan δ
0.1
1
10
100
1000
Frequency [Hz]

7.1.3 IDAX 206 Measurements of The Old Varnish, Temperature Dependency

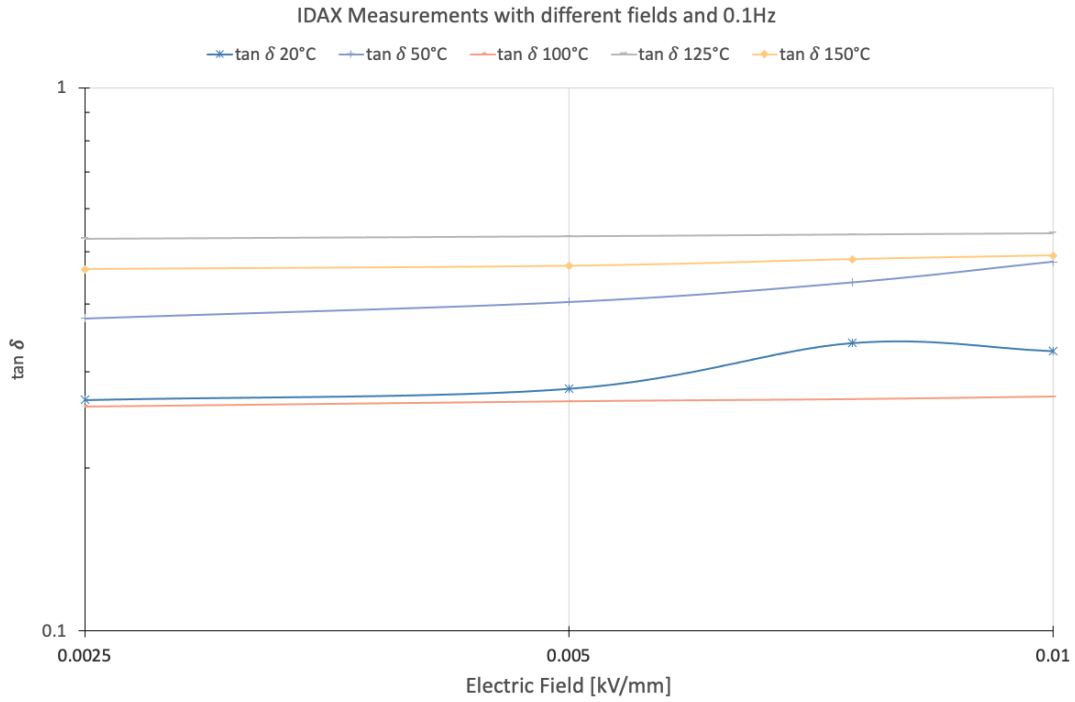

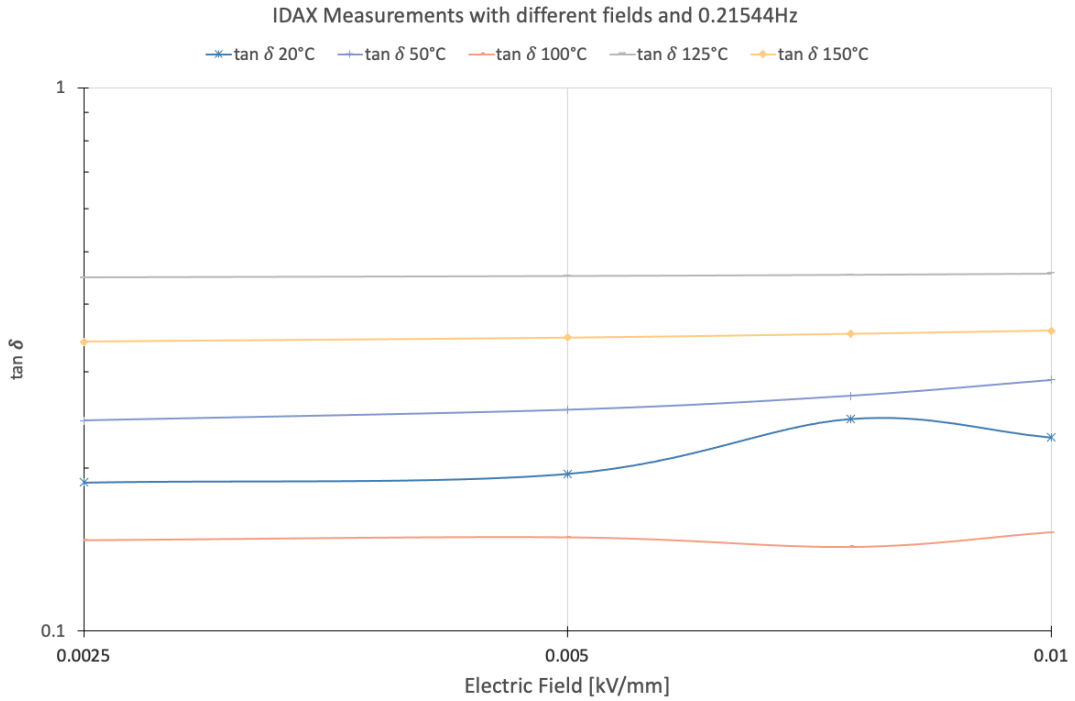

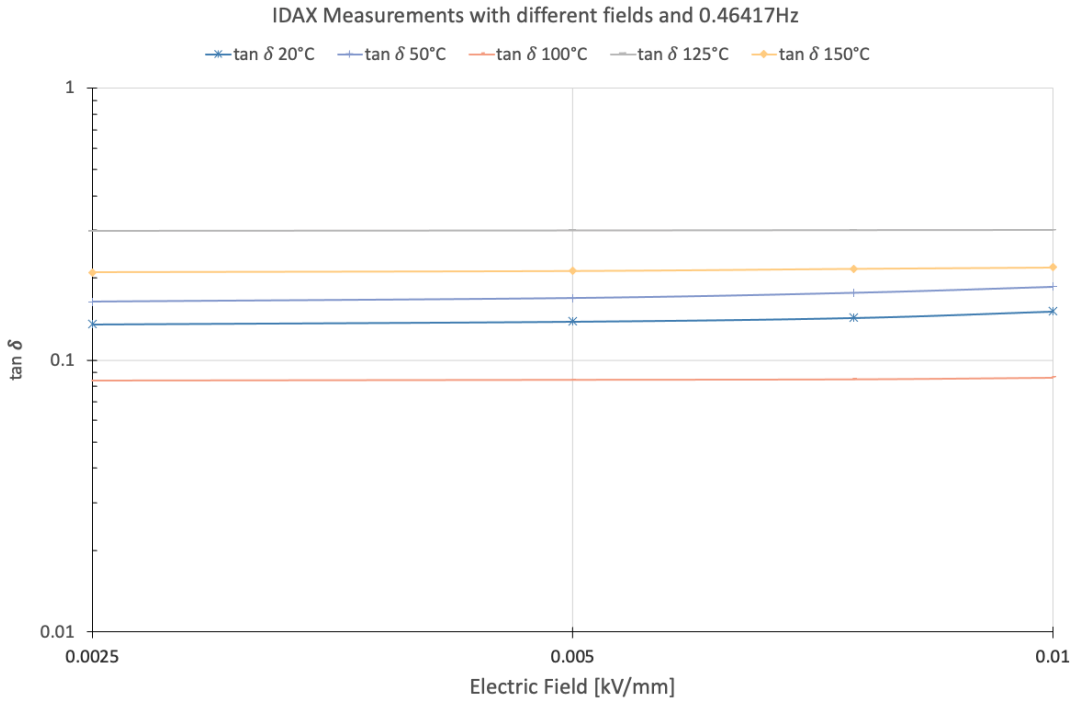
IDAX Measurements with different fields and 0.46417Hz
tan δ 20°C
tan δ 50°C
tan δ 100°C
tan δ 125°C
tan δ 150°C
1
0.1
0.01
tan δ
0.0025
0.005
0.01
Electric Field [kV/mm]

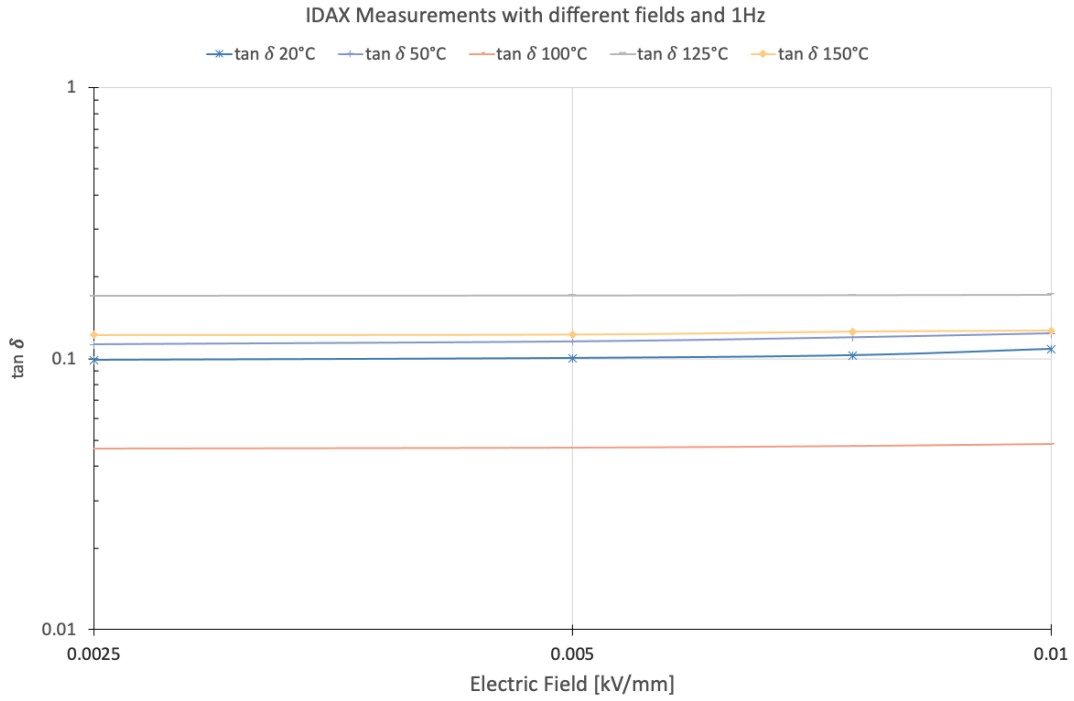
IDAX Measurements with different fields and 1Hz
tan δ 20°C
tan δ 50°C
tan δ 100°C
tan δ 125°C
tan δ 150°C
1
0.1
0.01
tan δ
0.0025
0.005
0.01
Electric Field [kV/mm]

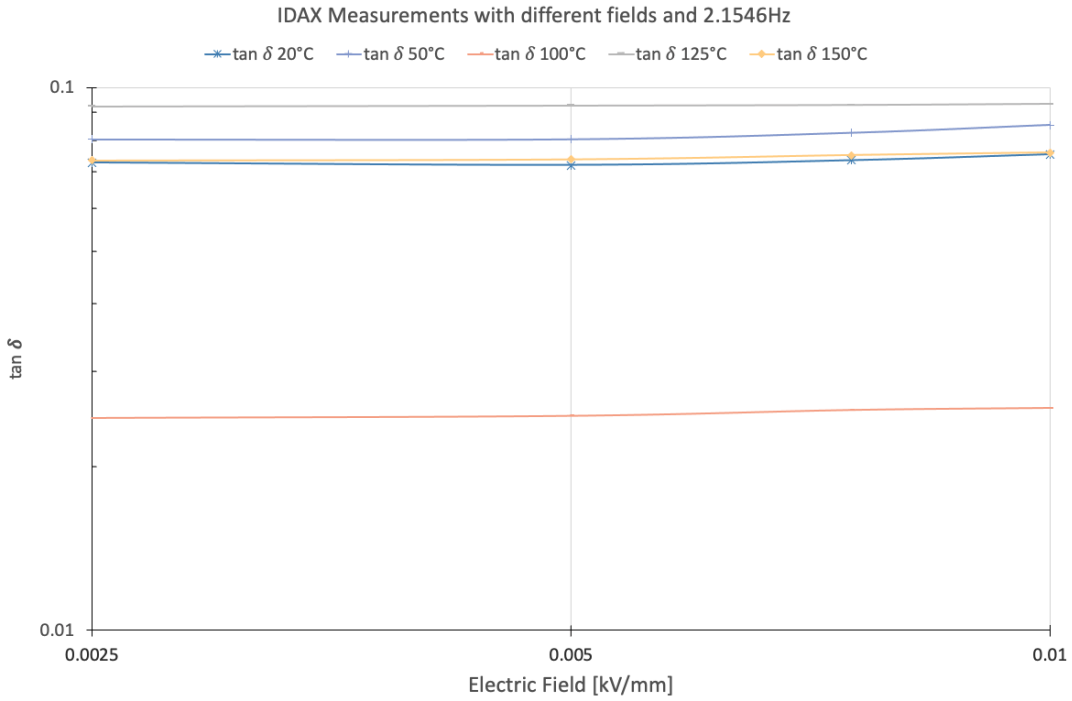
IDAX Measurements with different fields and 2.1546Hz
tan δ 20°C
tan δ 50°C
tan δ 100°C
tan δ 125°C
tan δ 150°C
0.1
0.01
tan δ
0.0025
0.005
0.01
Electric Field [kV/mm]

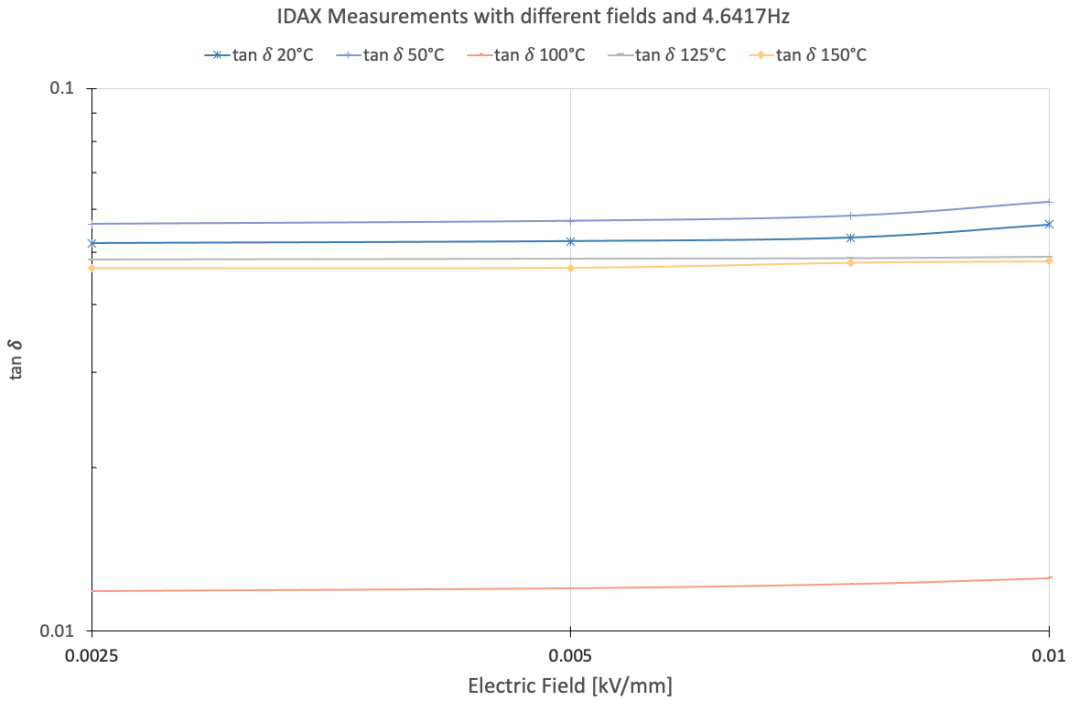
IDAX Measurements with different fields and 4.6417Hz
tan δ 20°C
tan δ 50°C
tan δ 100°C
tan δ 125°C
tan δ 150°C
0.1
0.01
tan δ
0.0025
0.005
0.01
Electric Field [kV/mm]

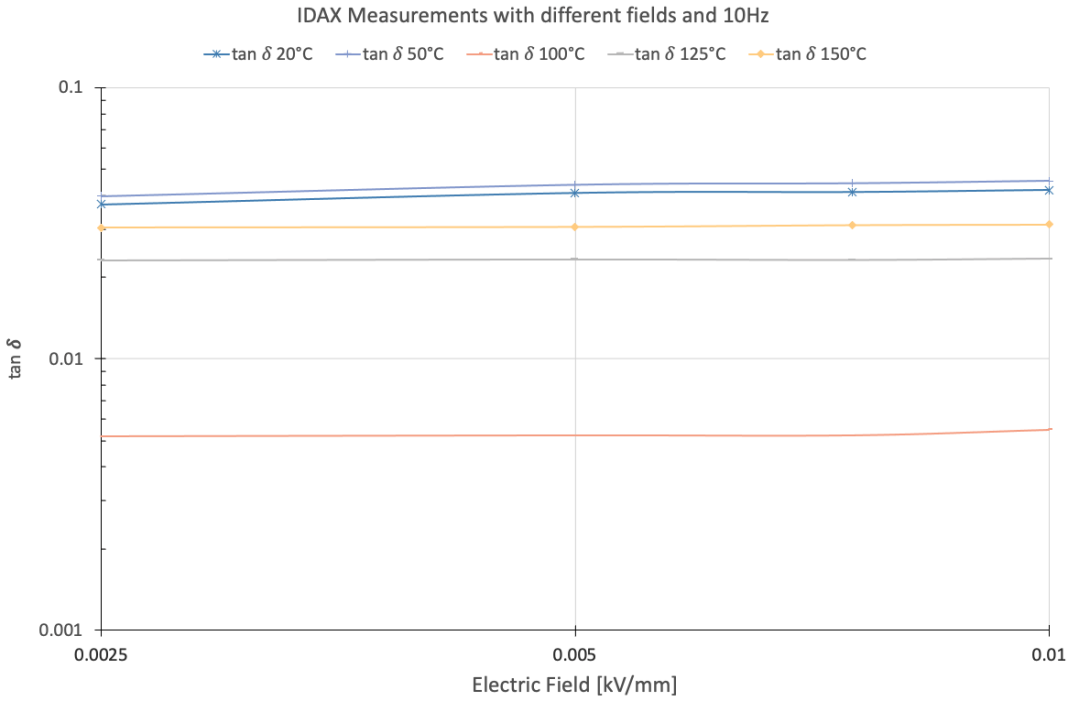
IDAX Measurements with different fields and 10Hz
tan δ 20°C
tan δ 50°C
tan δ 100°C
tan δ 125°C
tan δ 150°C
0.1
0.01
0.001
tan δ
0.0025
0.005
0.01
Electric Field [kV/mm]

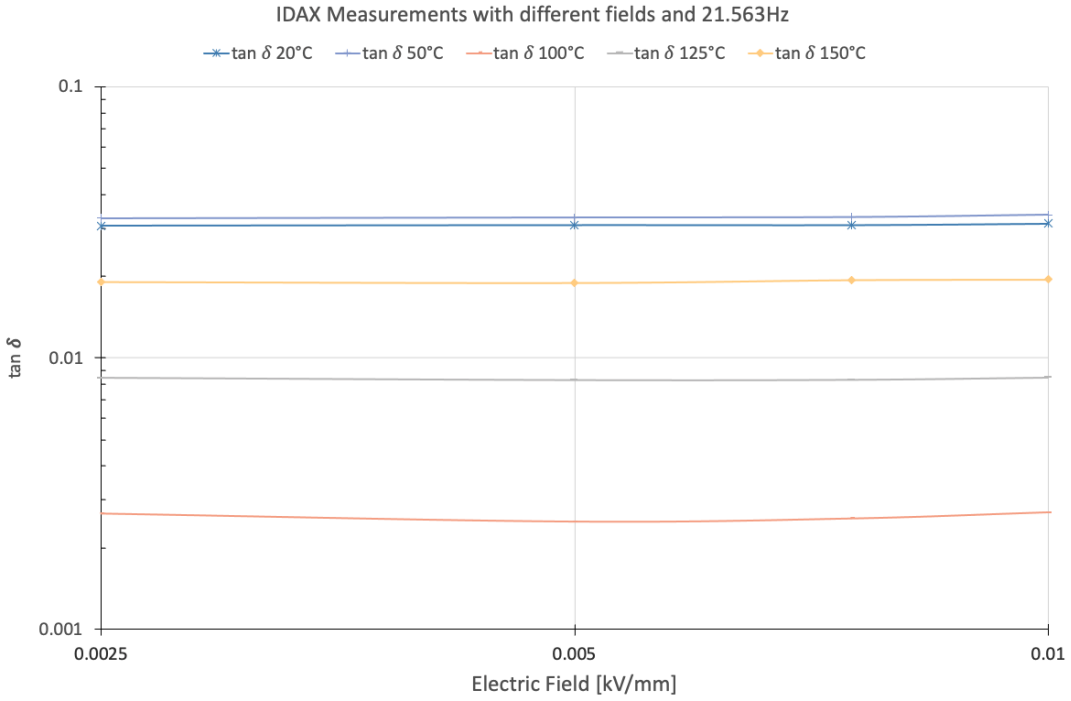
IDAX Measurements with different fields and 21.563Hz
tan δ 20°C
tan δ 50°C
tan δ 100°C
tan δ 125°C
tan δ 150°C
0.1
0.01
0.001
tan δ
0.0025
0.005
0.01
Electric Field [kV/mm]

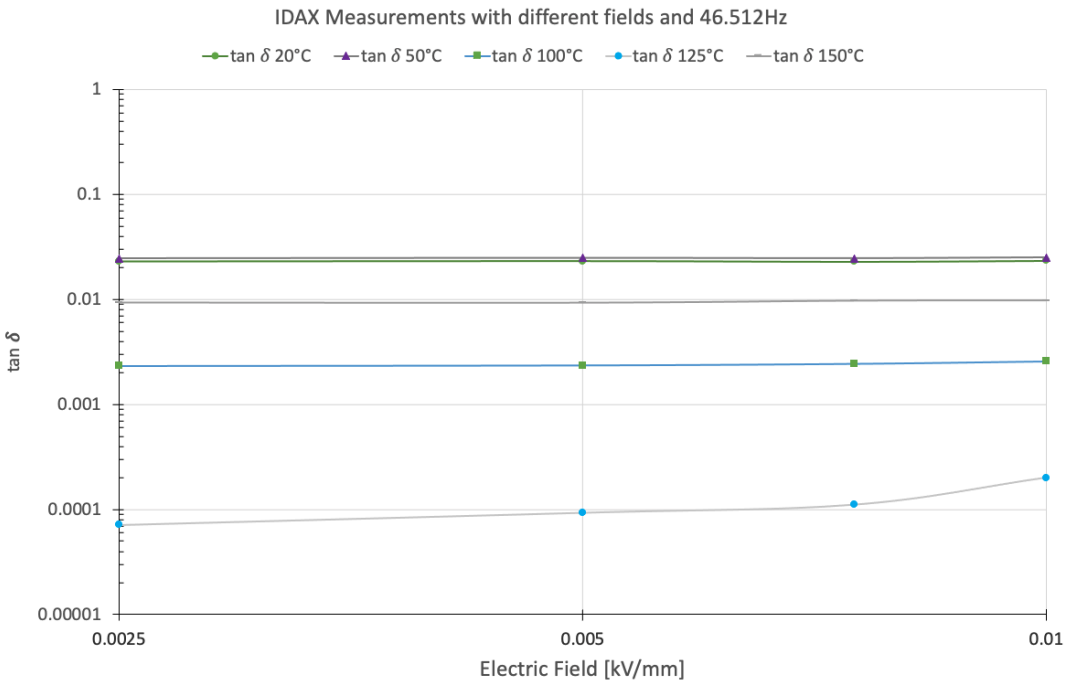
IDAX Measurements with different fields and 46.512Hz
tan δ 20°C
tan δ 50°C
tan δ 100°C
tan δ 125°C
tan δ 150°C
1
0.1
0.01
0.001
0.0001
0.00001
tan δ
0.0025
0.005
0.01
Electric Field [kV/mm]

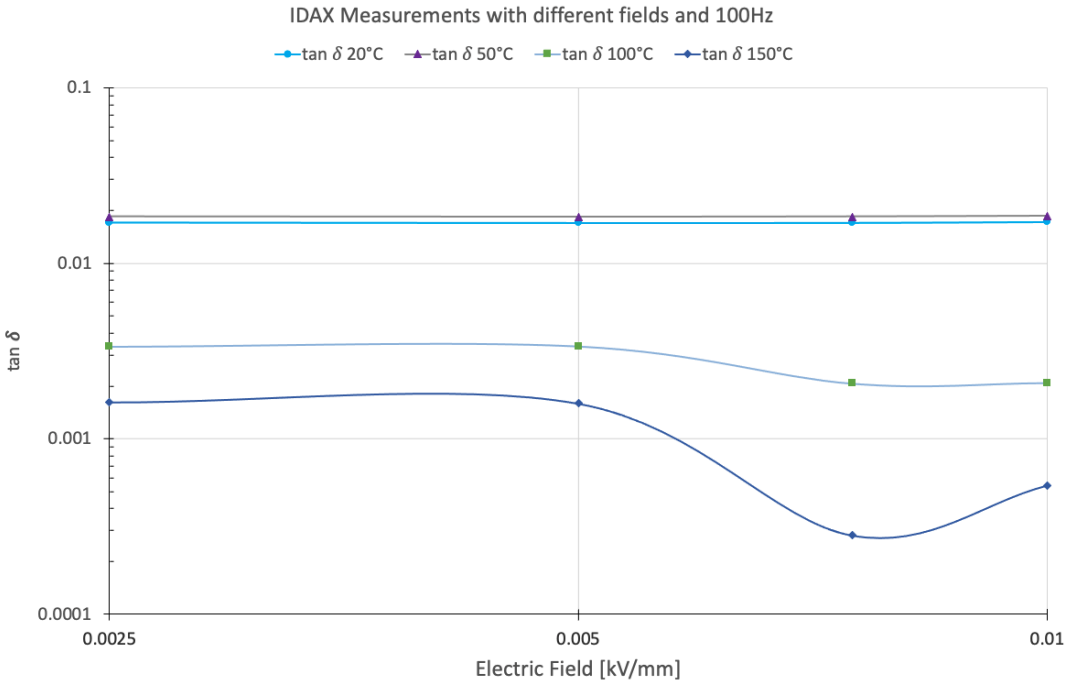
IDAX Measurements with different fields and 100Hz
tan δ 20°C
tan δ 50°C
tan δ 100°C
tan δ 150°C
0.1
0.01
0.001
0.0001
tan δ
0.0025
0.005
0.01
Electric Field [kV/mm]

7.1.4 IDAX 206 Measurements of The New Varnish, Temperature Dependency

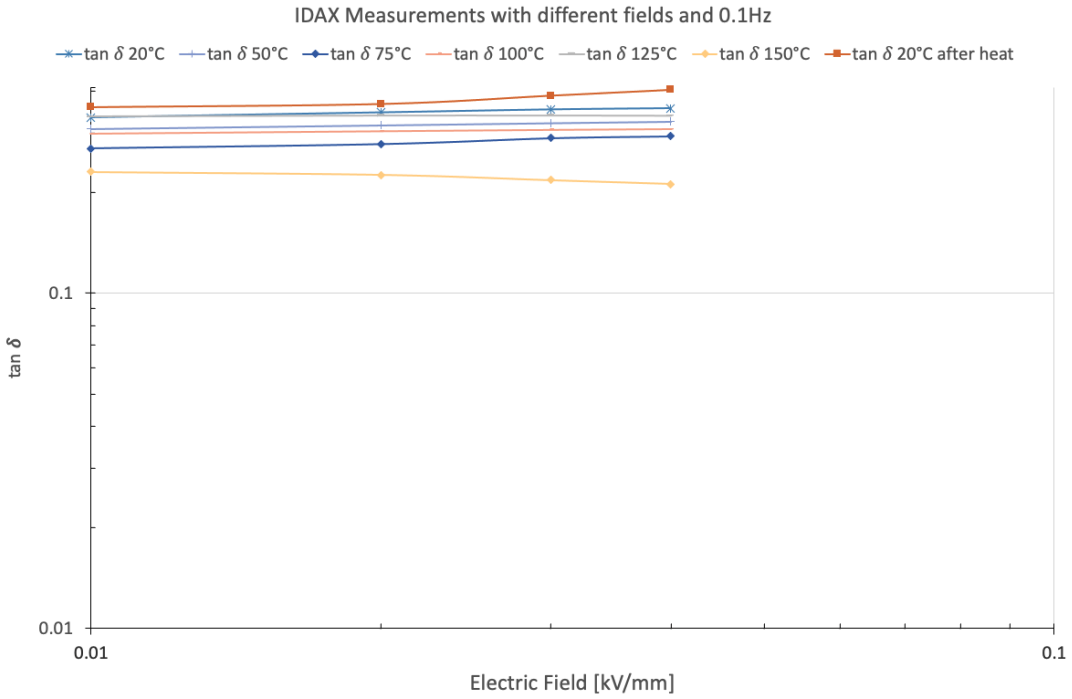

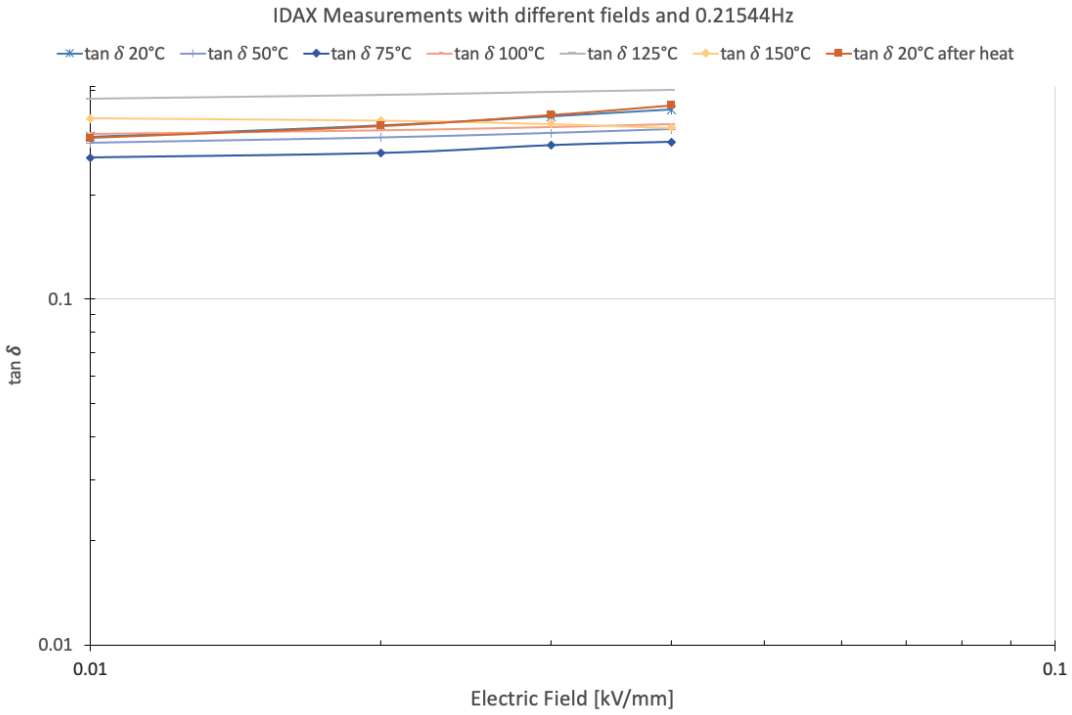

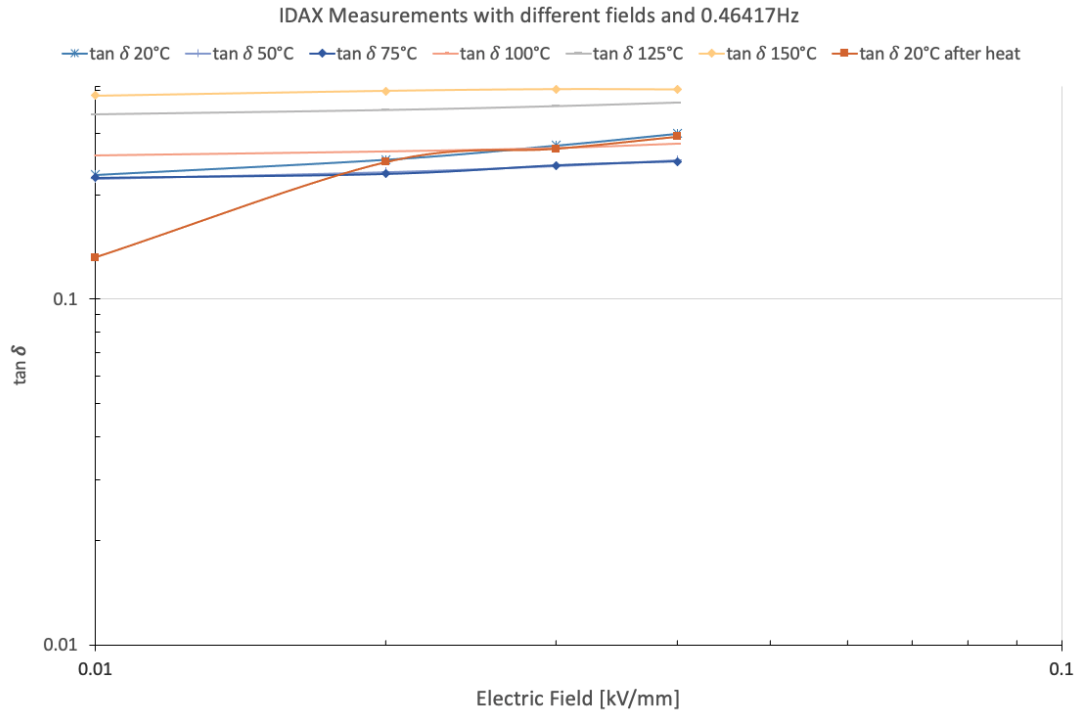
IDAX Measurements with different fields and 0.46417Hz
tan δ 20°C
tan δ 50°C
tan δ 75°C
tan δ 100°C
tan δ 125°C
tan δ 150°C
tan δ 20°C after heat
tan δ
0.1
0.01
0.01
0.1
Electric Field [kV/mm]

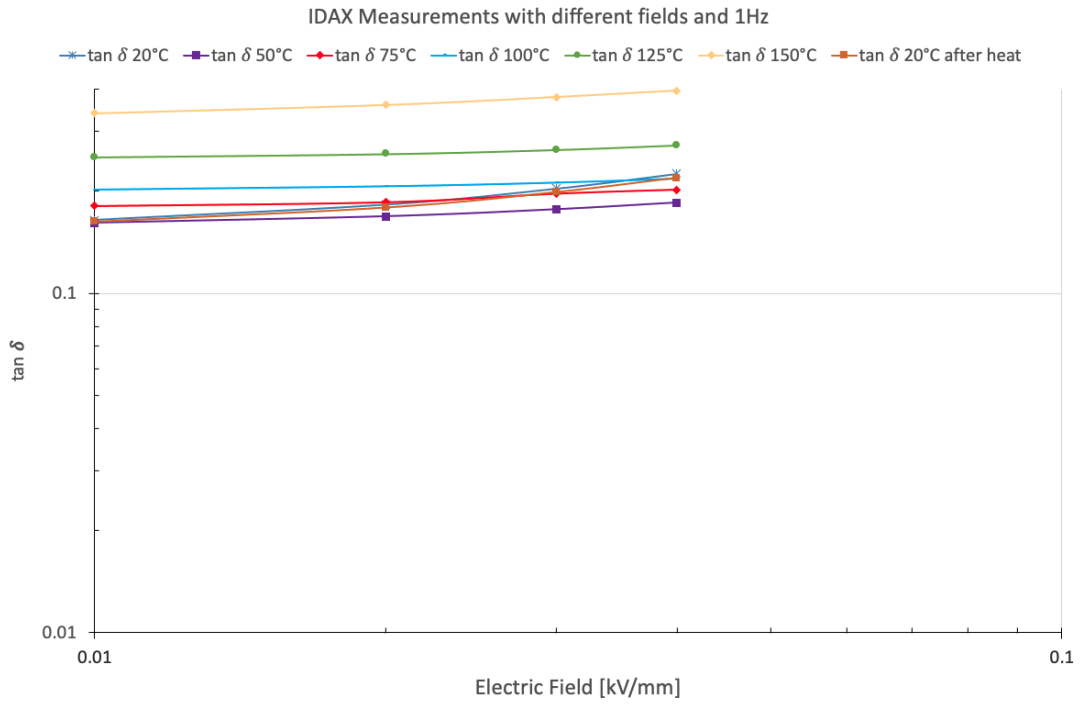
IDAX Measurements with different fields and 1Hz
tan δ 20°C
tan δ 50°C
tan δ 75°C
tan δ 100°C
tan δ 125°C
tan δ 150°C
tan δ 20°C after heat
tan δ
0.1
0.01
0.01
0.1
Electric Field [kV/mm]

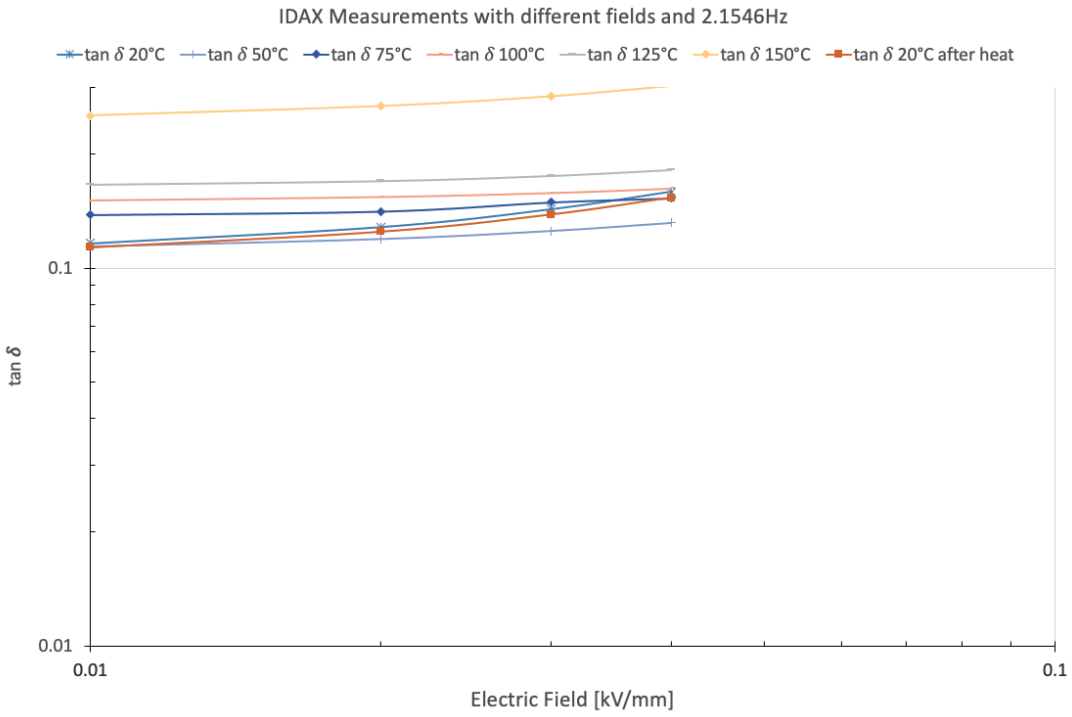
IDAX Measurements with different fields and 2.1546Hz
tan δ 20°C
tan δ 50°C
tan δ 75°C
tan δ 100°C
tan δ 125°C
tan δ 150°C
tan δ 20°C after heat
0.1
0.01
tan δ
0.01
0.1
Electric Field [kV/mm]

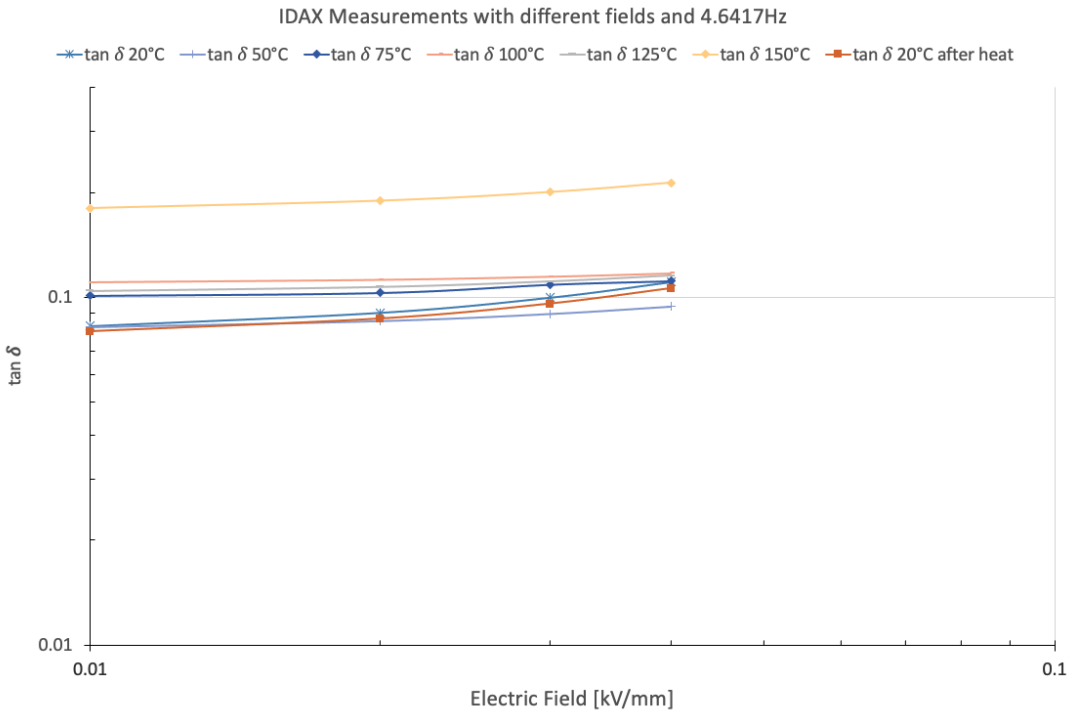
IDAX Measurements with different fields and 4.6417Hz
tan δ 20°C
tan δ 50°C
tan δ 75°C
tan δ 100°C
tan δ 125°C
tan δ 150°C
tan δ 20°C after heat
0.1
0.01
tan δ
0.01
0.1
Electric Field [kV/mm]

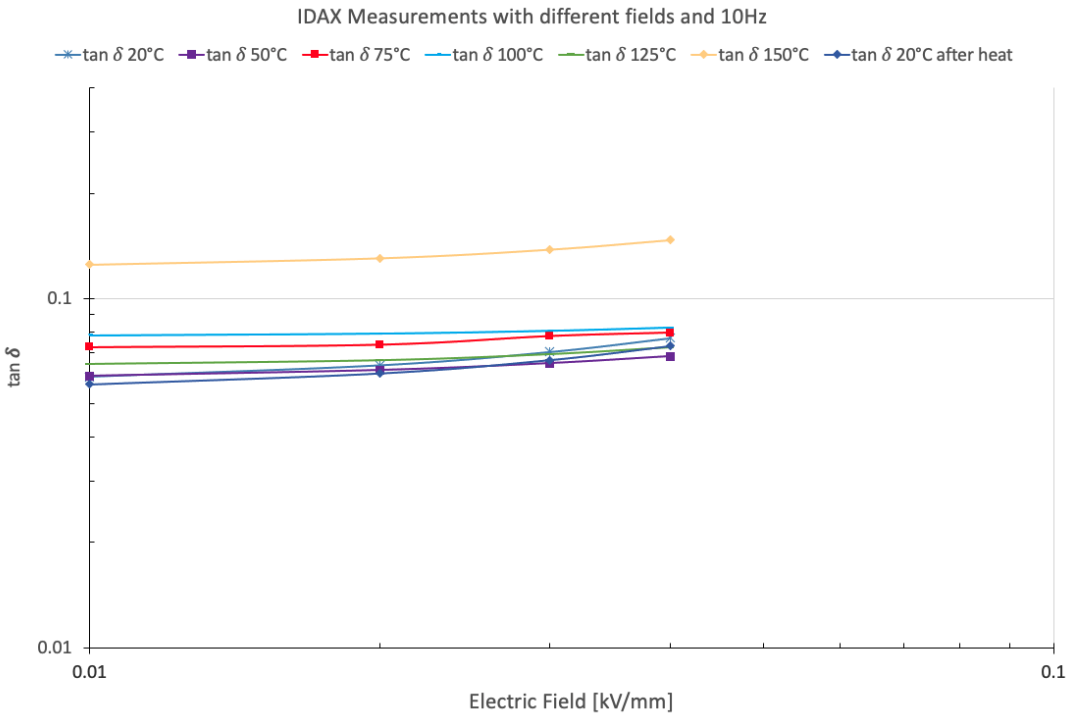
IDAX Measurements with different fields and 10Hz
tan δ 20°C
tan δ 50°C
tan δ 75°C
tan δ 100°C
tan δ 125°C
tan δ 150°C
tan δ 20°C after heat
0.1
0.01
tan δ
0.01
0.1
Electric Field [kV/mm]

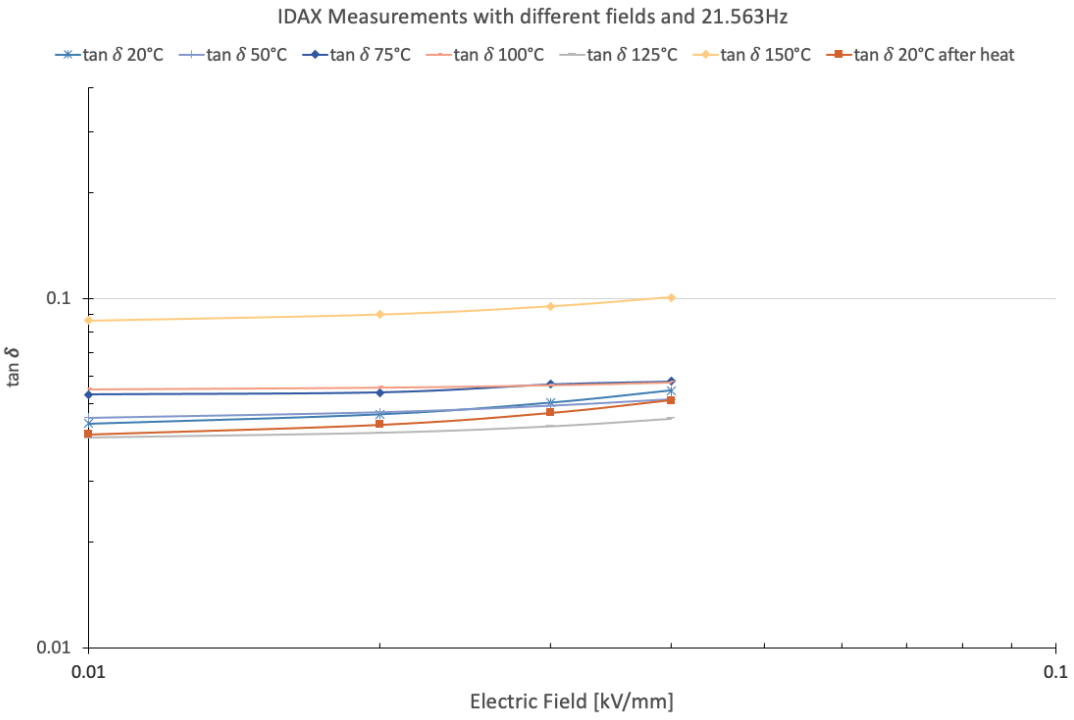
IDAX Measurements with different fields and 21.563Hz
tan δ 20°C
tan δ 50°C
tan δ 75°C
tan δ 100°C
tan δ 125°C
tan δ 150°C
tan δ 20°C after heat
0.1
0.01
tan δ
0.01
0.1
Electric Field [kV/mm]

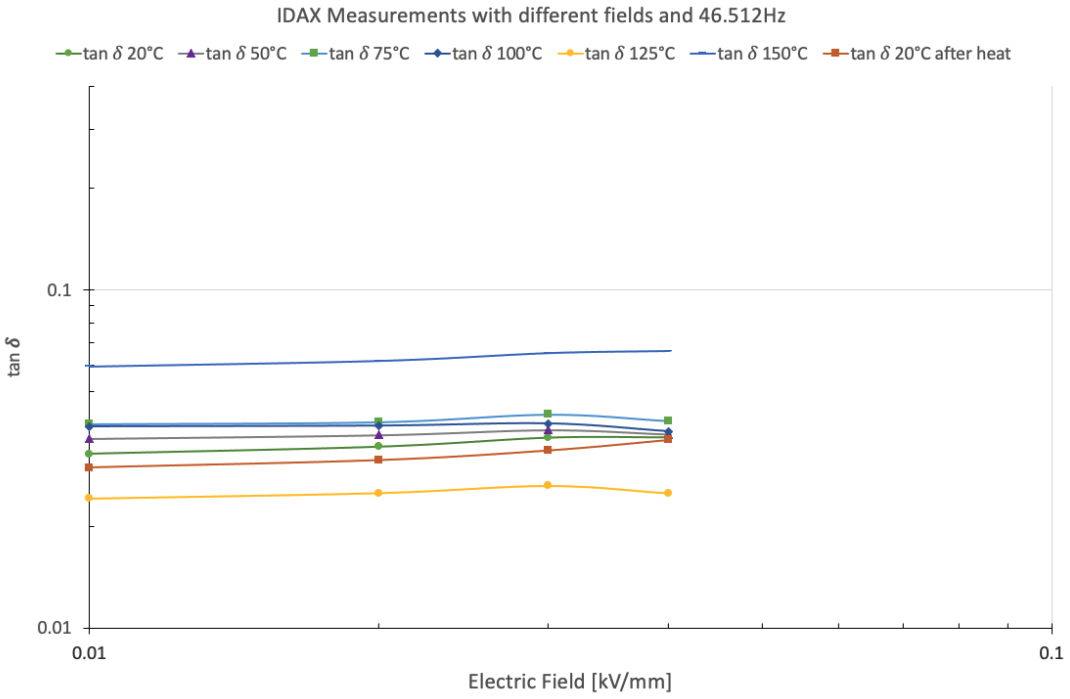
IDAX Measurements with different fields and 46.512Hz
tan δ 20°C
tan δ 50°C
tan δ 75°C
tan δ 100°C
tan δ 125°C
tan δ 150°C
tan δ 20°C after heat
tan δ
0.1
0.01
0.01
0.1
Electric Field [kV/mm]

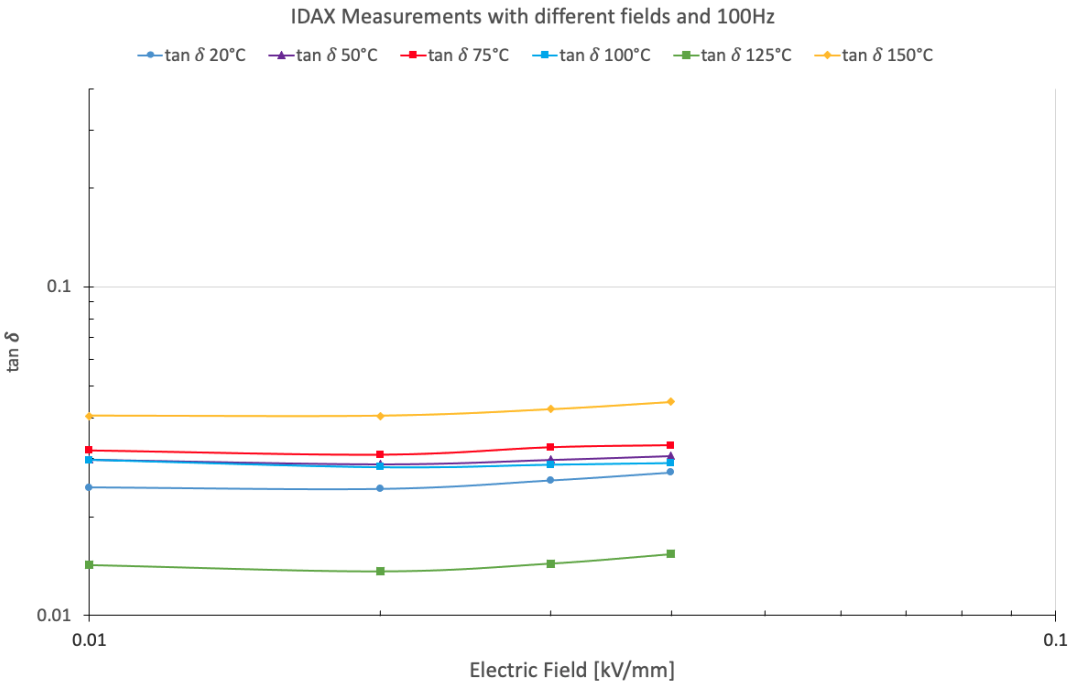
IDAX Measurements with different fields and 100Hz
tan δ 20°C
tan δ 50°C
tan δ 75°C
tan δ 100°C
tan δ 125°C
tan δ 150°C
tan δ
0.1
0.01
0.01
0.1
Electric Field [kV/mm]

7.1.5 IDAX 206 Measurements of The Old Varnish, Frequency Dependency

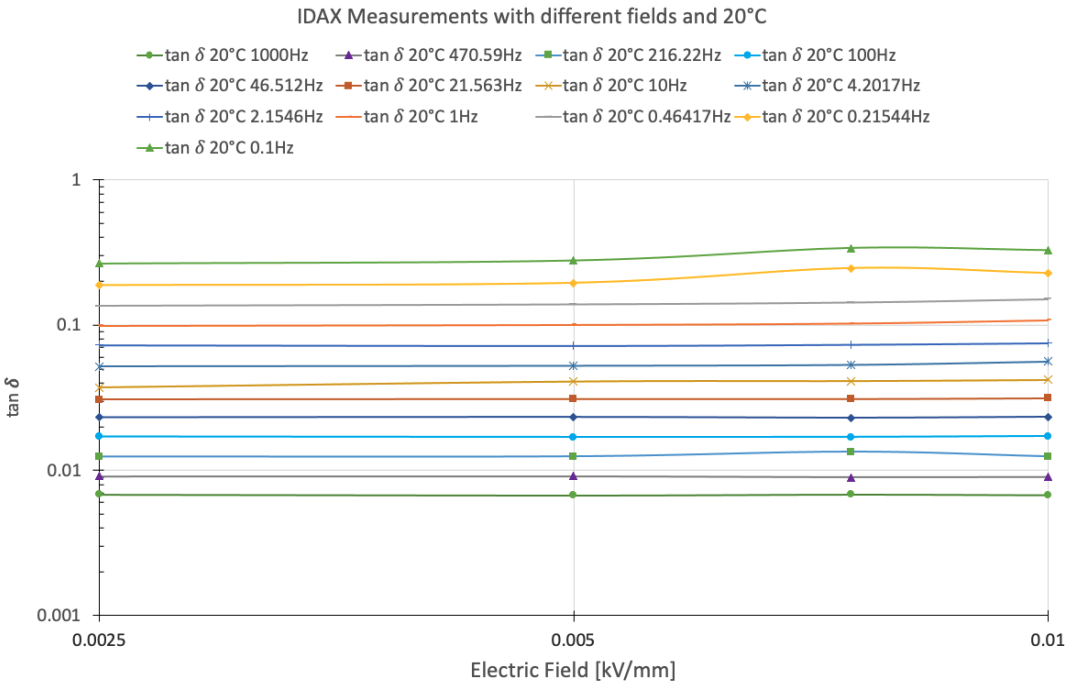

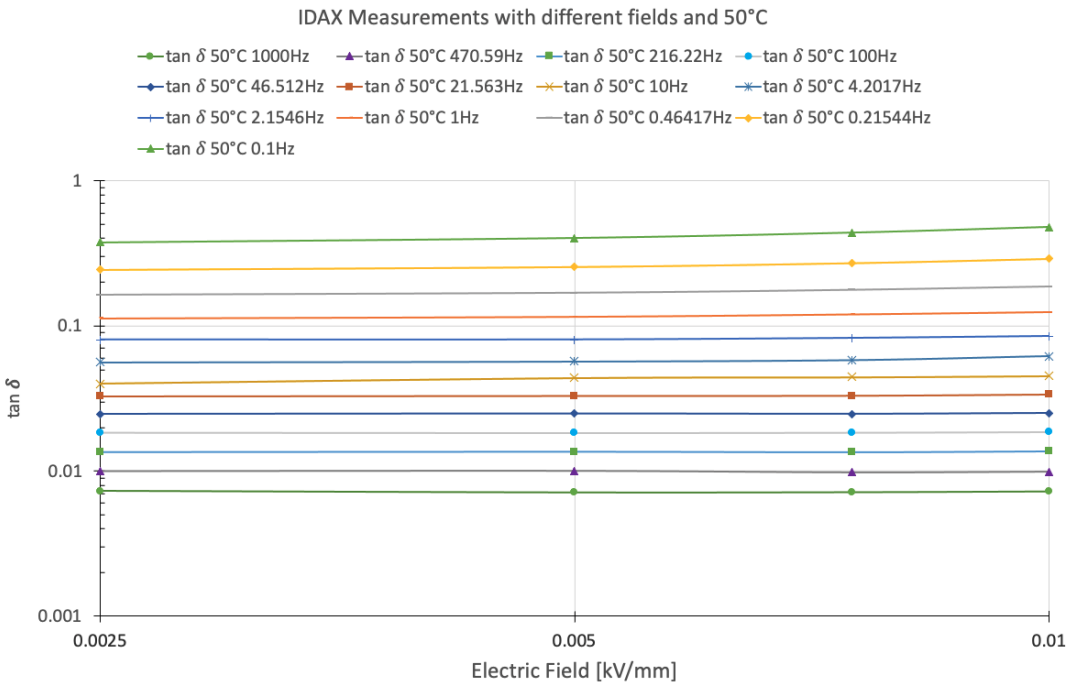

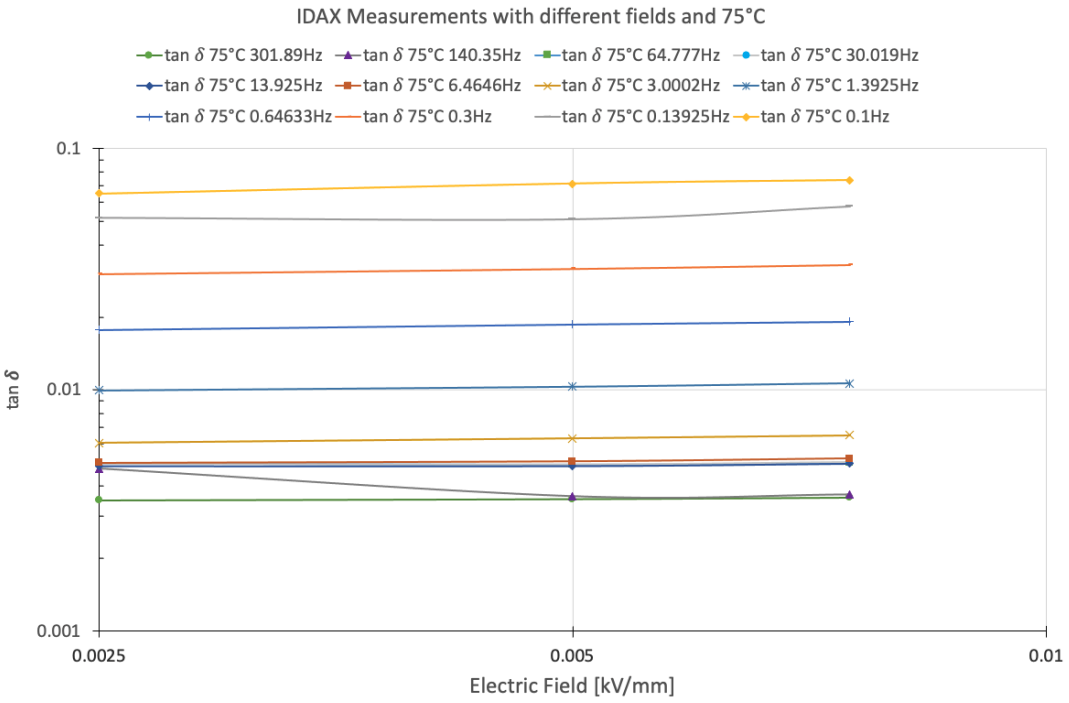
IDAX Measurements with different fields and 75°C
tan δ 75°C 301.89Hz
tan δ 75°C 140.35Hz
tan δ 75°C 64.777Hz
tan δ 75°C 30.019Hz
tan δ 75°C 13.925Hz
tan δ 75°C 6.4646Hz
tan δ 75°C 3.0002Hz
tan δ 75°C 1.3925Hz
tan δ 75°C 0.64633Hz
tan δ 75°C 0.3Hz
tan δ 75°C 0.13925Hz
tan δ 75°C 0.1Hz
0.1
0.01
0.001
tan δ
0.0025
0.005
0.01
Electric Field [kV/mm]

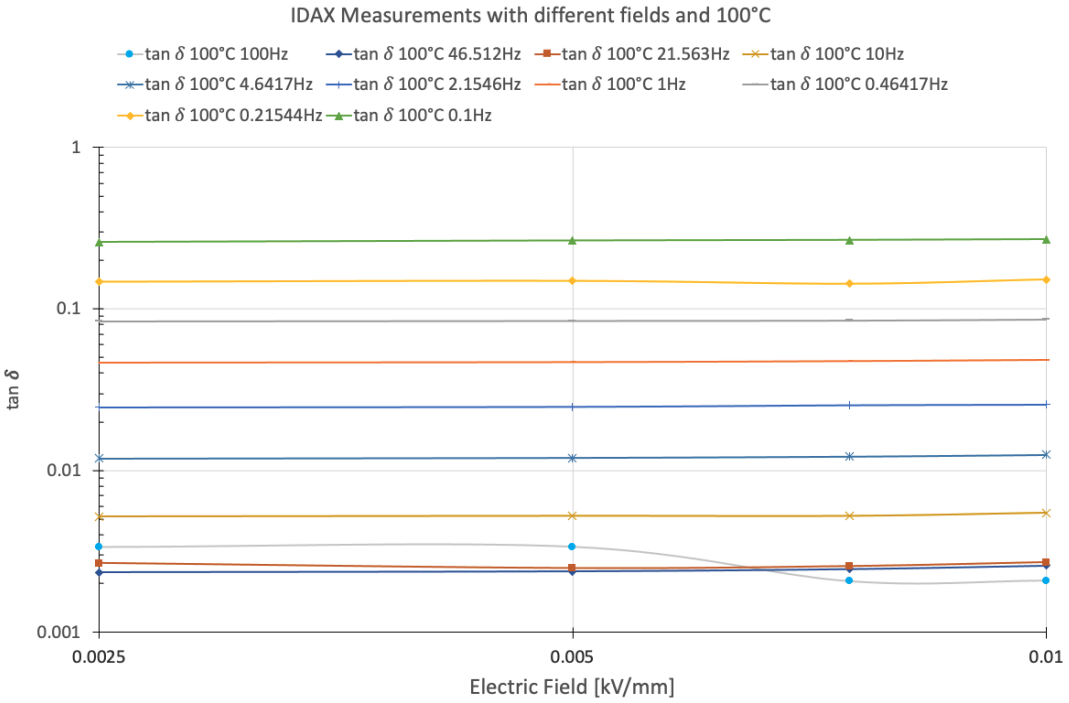
IDAX Measurements with different fields and 100°C
tan δ 100°C 100Hz
tan δ 100°C 46.512Hz
tan δ 100°C 21.563Hz
tan δ 100°C 10Hz
tan δ 100°C 4.6417Hz
tan δ 100°C 2.1546Hz
tan δ 100°C 1Hz
tan δ 100°C 0.46417Hz
tan δ 100°C 0.21544Hz
tan δ 100°C 0.1Hz
1
0.1
0.01
0.001
tan δ
0.0025
0.005
0.01
Electric Field [kV/mm]

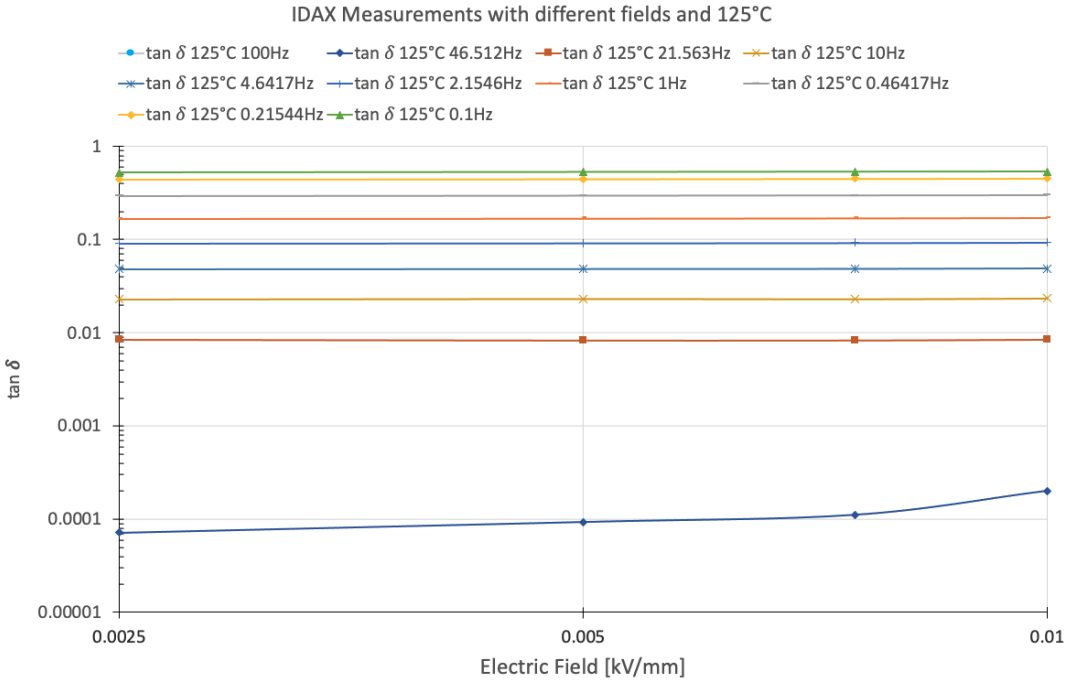
IDAX Measurements with different fields and 125°C
tan δ 125°C 100Hz
tan δ 125°C 46.512Hz
tan δ 125°C 21.563Hz
tan δ 125°C 10Hz
tan δ 125°C 4.6417Hz
tan δ 125°C 2.1546Hz
tan δ 125°C 1Hz
tan δ 125°C 0.46417Hz
tan δ 125°C 0.21544Hz
tan δ 125°C 0.1Hz
1
0.1
0.01
0.001
0.0001
0.00001
tan δ
0.0025
0.005
0.01
Electric Field [kV/mm]

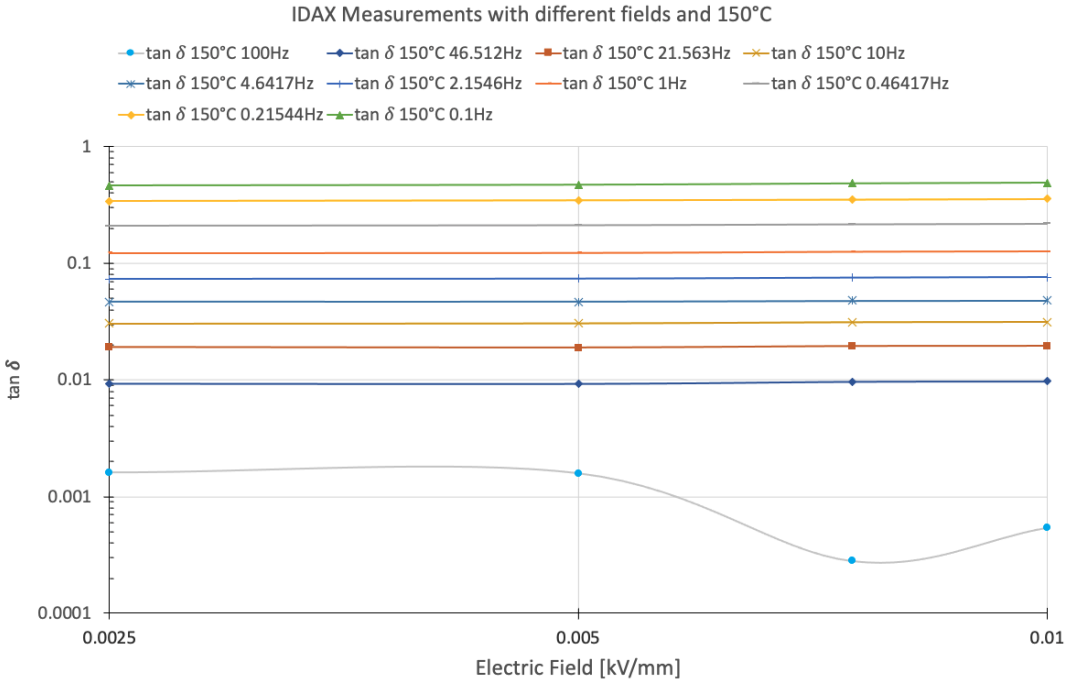
IDAX Measurements with different fields and 150°C
tan δ 150°C 100Hz
tan δ 150°C 46.512Hz
tan δ 150°C 21.563Hz
tan δ 150°C 10Hz
tan δ 150°C 4.6417Hz
tan δ 150°C 2.1546Hz
tan δ 150°C 1Hz
tan δ 150°C 0.46417Hz
tan δ 150°C 0.21544Hz
tan δ 150°C 0.1Hz
1
0.1
0.01
0.001
0.0001
tan δ
0.0025
0.005
0.01
Electric Field [kV/mm]

7.1.6 IDAX 206 Measurements of The New Varnish, Frequency Dependency

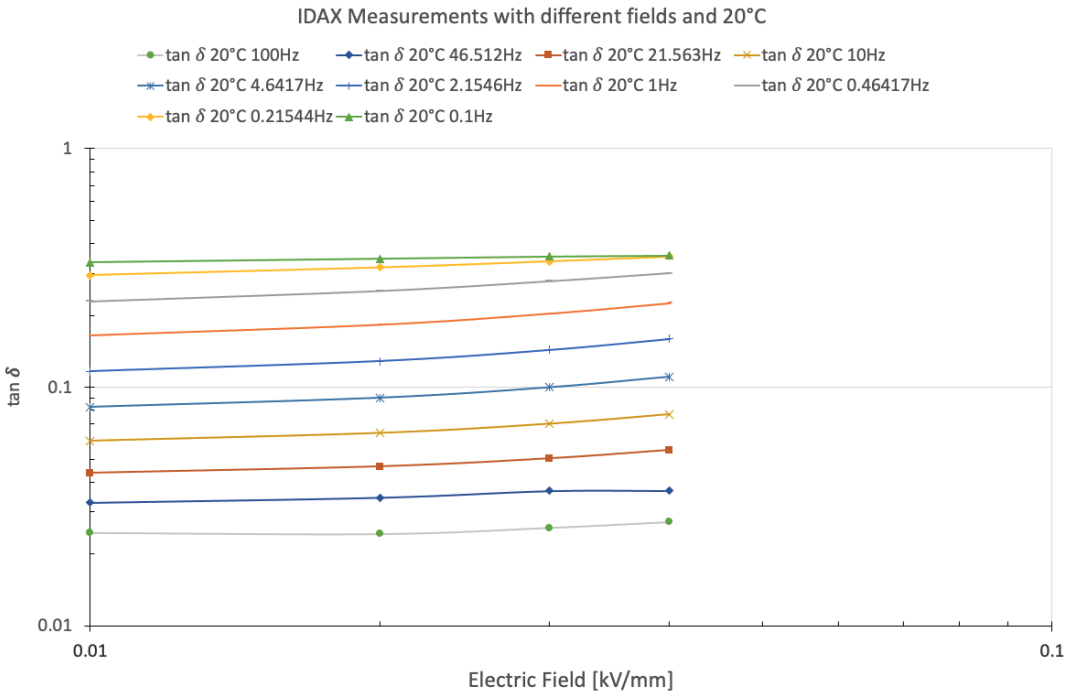

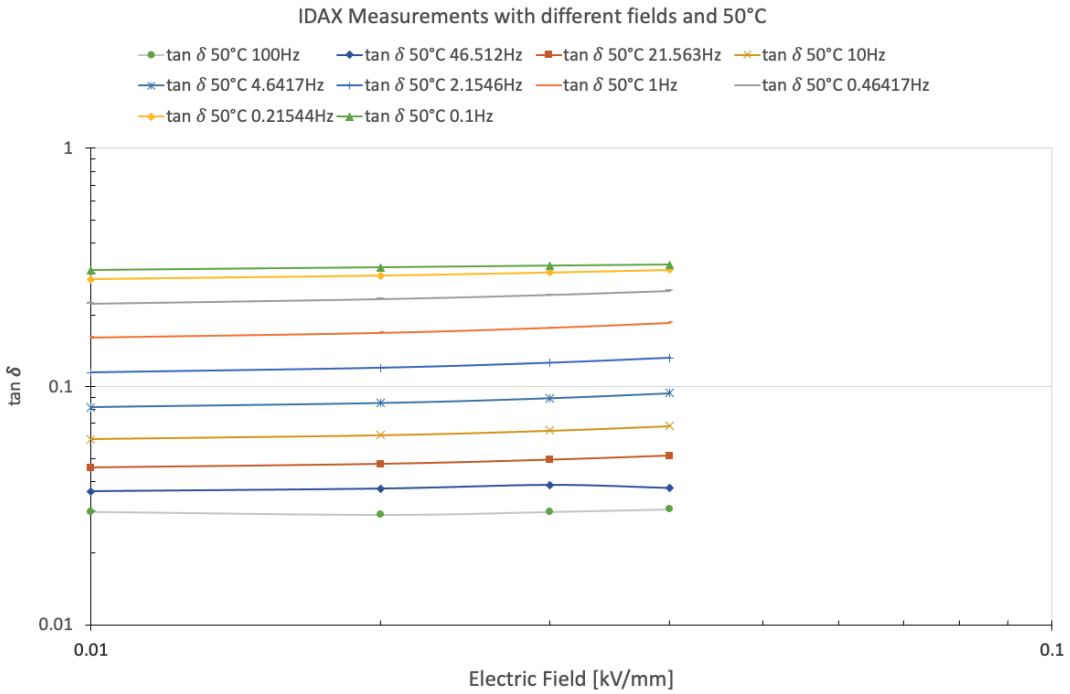

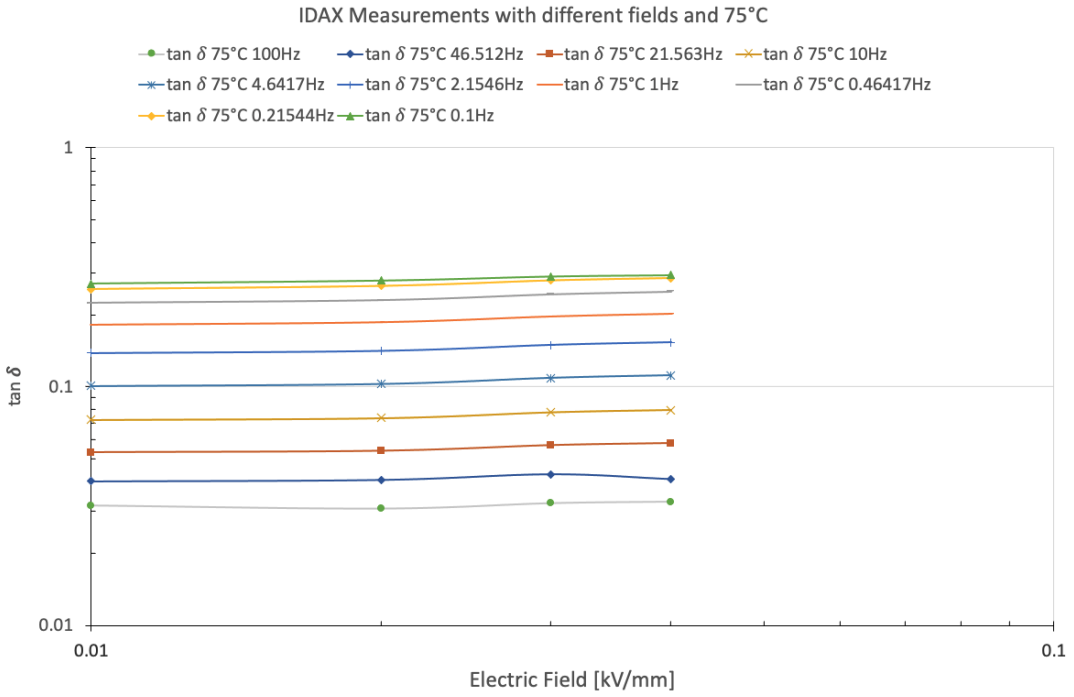
IDAX Measurements with different fields and 75°C
tan δ 75°C 100Hz
tan δ 75°C 46.512Hz
tan δ 75°C 21.563Hz
tan δ 75°C 10Hz
tan δ 75°C 4.6417Hz
tan δ 75°C 2.1546Hz
tan δ 75°C 1Hz
tan δ 75°C 0.46417Hz
tan δ 75°C 0.21544Hz
tan δ 75°C 0.1Hz
1
0.1
0.01
tan δ
0.01
0.1
Electric Field [kV/mm]

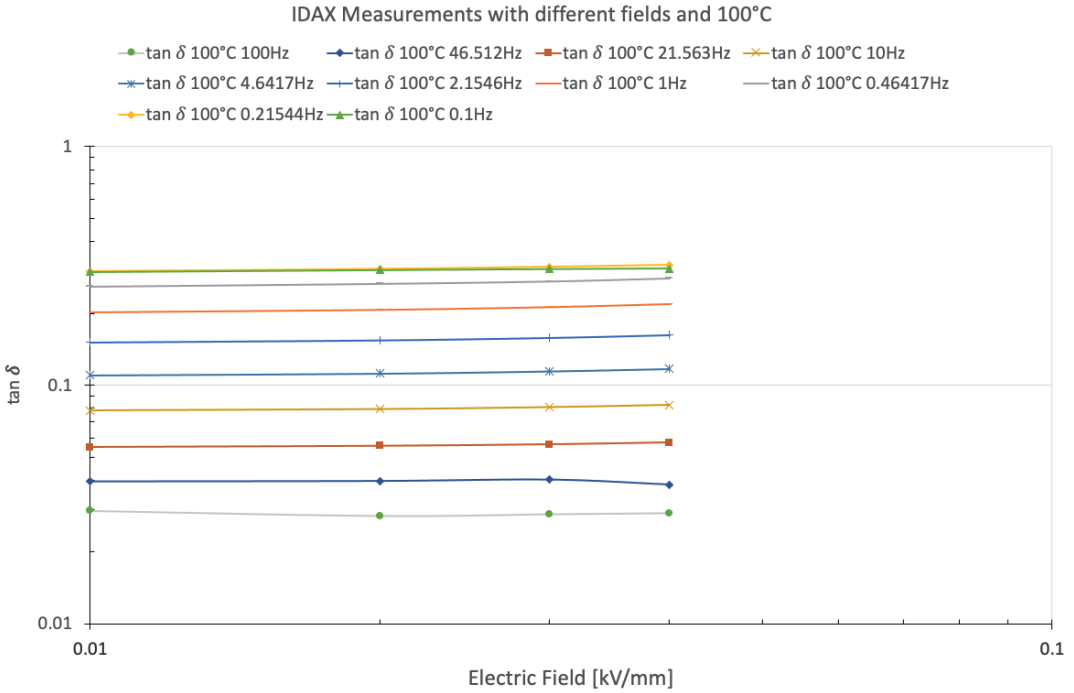
IDAX Measurements with different fields and 100°C
tan δ 100°C 100Hz
tan δ 100°C 46.512Hz
tan δ 100°C 21.563Hz
tan δ 100°C 10Hz
tan δ 100°C 4.6417Hz
tan δ 100°C 2.1546Hz
tan δ 100°C 1Hz
tan δ 100°C 0.46417Hz
tan δ 100°C 0.21544Hz
tan δ 100°C 0.1Hz
1
0.1
0.01
tan δ
0.01
0.1
Electric Field [kV/mm]

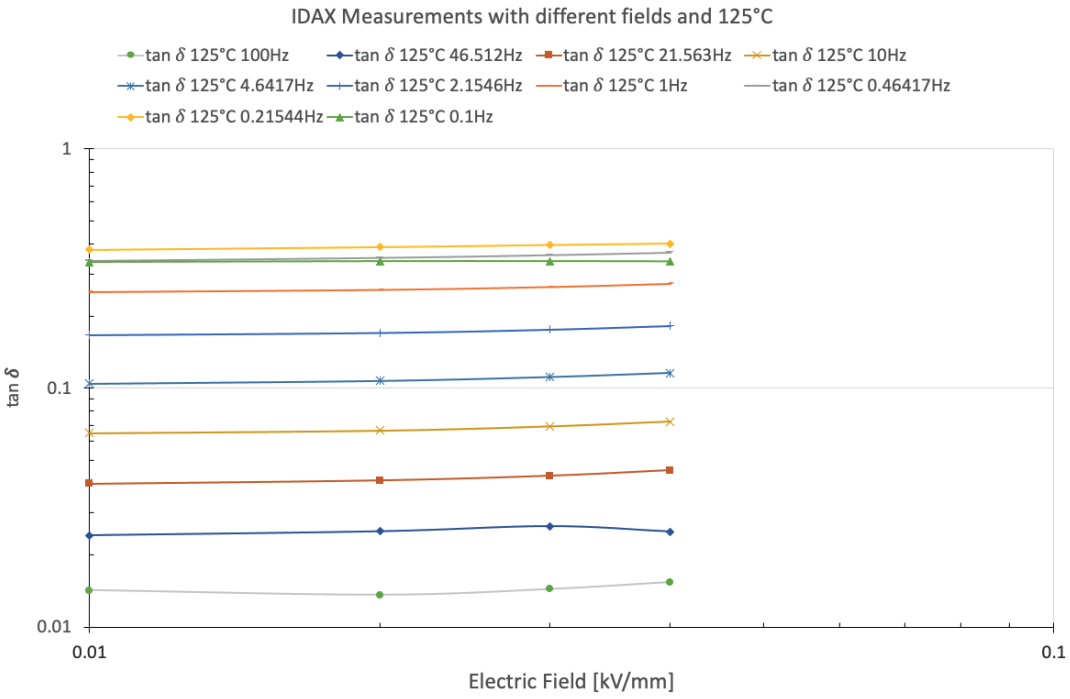
IDAX Measurements with different fields and 125°C
tan δ 125°C 100Hz
tan δ 125°C 46.512Hz
tan δ 125°C 21.563Hz
tan δ 125°C 10Hz
tan δ 125°C 4.6417Hz
tan δ 125°C 2.1546Hz
tan δ 125°C 1Hz
tan δ 125°C 0.46417Hz
tan δ 125°C 0.21544Hz
tan δ 125°C 0.1Hz
1
0.1
0.01
tan δ
0.01
0.1
Electric Field [kV/mm]

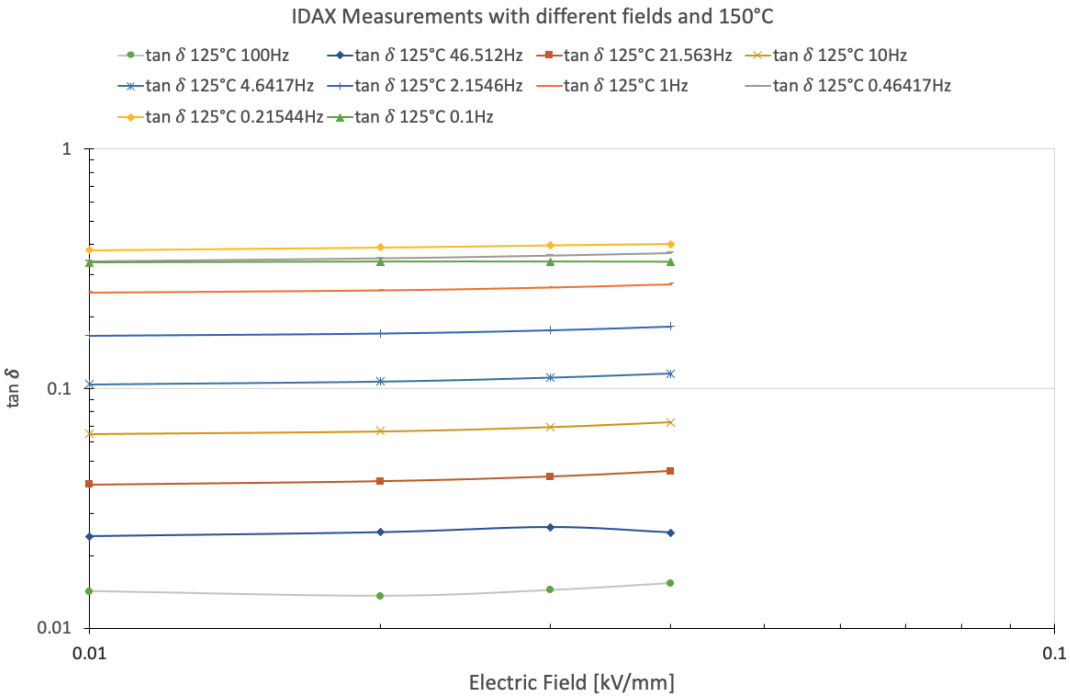
IDAX Measurements with different fields and 150°C
tan δ 125°C 100Hz
tan δ 125°C 46.512Hz
tan δ 125°C 21.563Hz
tan δ 125°C 10Hz
tan δ 125°C 4.6417Hz
tan δ 125°C 2.1546Hz
tan δ 125°C 1Hz
tan δ 125°C 0.46417Hz
tan δ 125°C 0.21544Hz
tan δ 125°C 0.1Hz
1
0.1
0.01
tan δ
0.01
0.1
Electric Field [kV/mm]

7.2 Appendix B

7.2.1 Measurements of The Old Varnish with IDA 200, with 10kV or 0.5kV/mm applied.

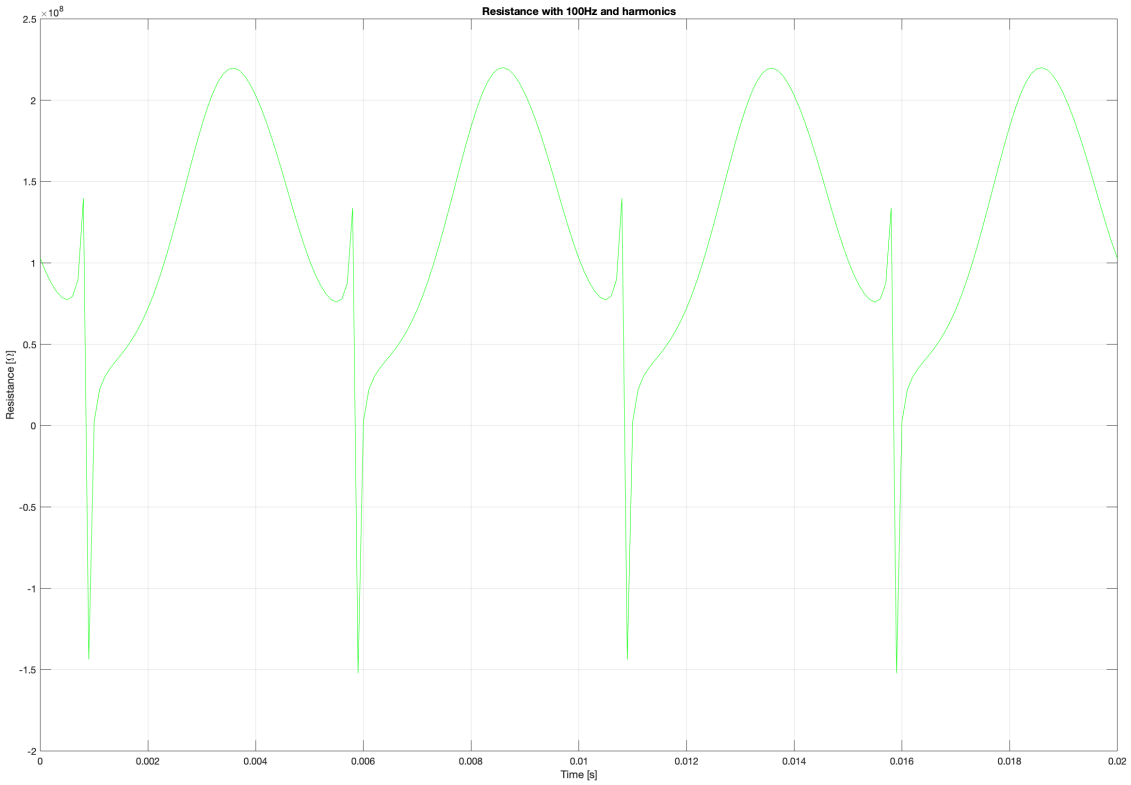

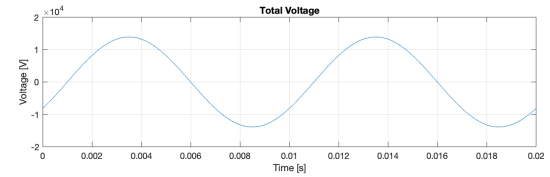

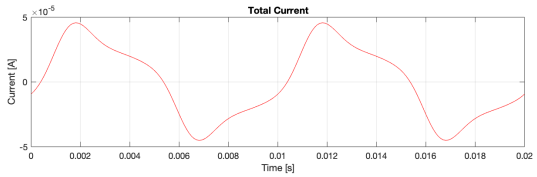

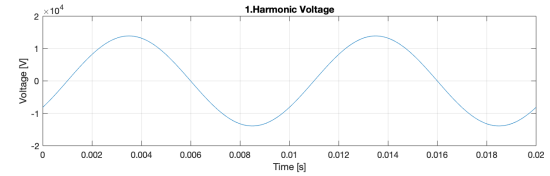

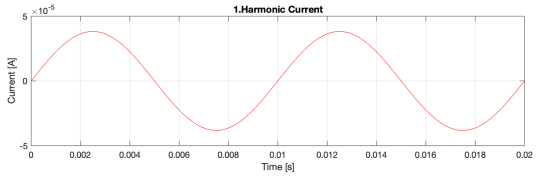

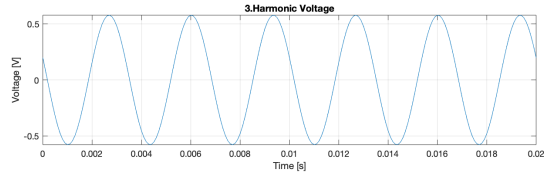

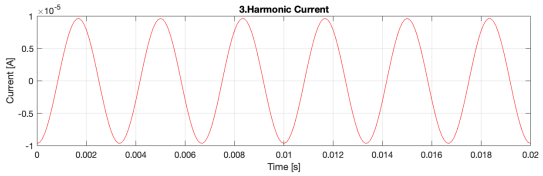

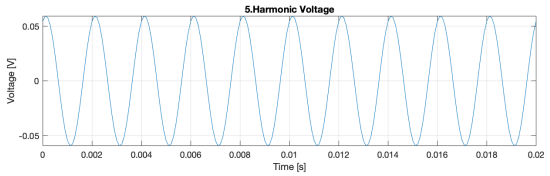

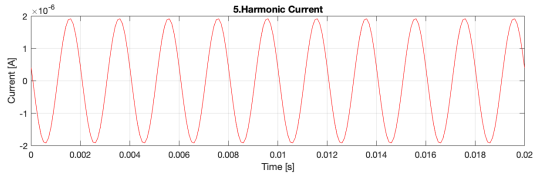

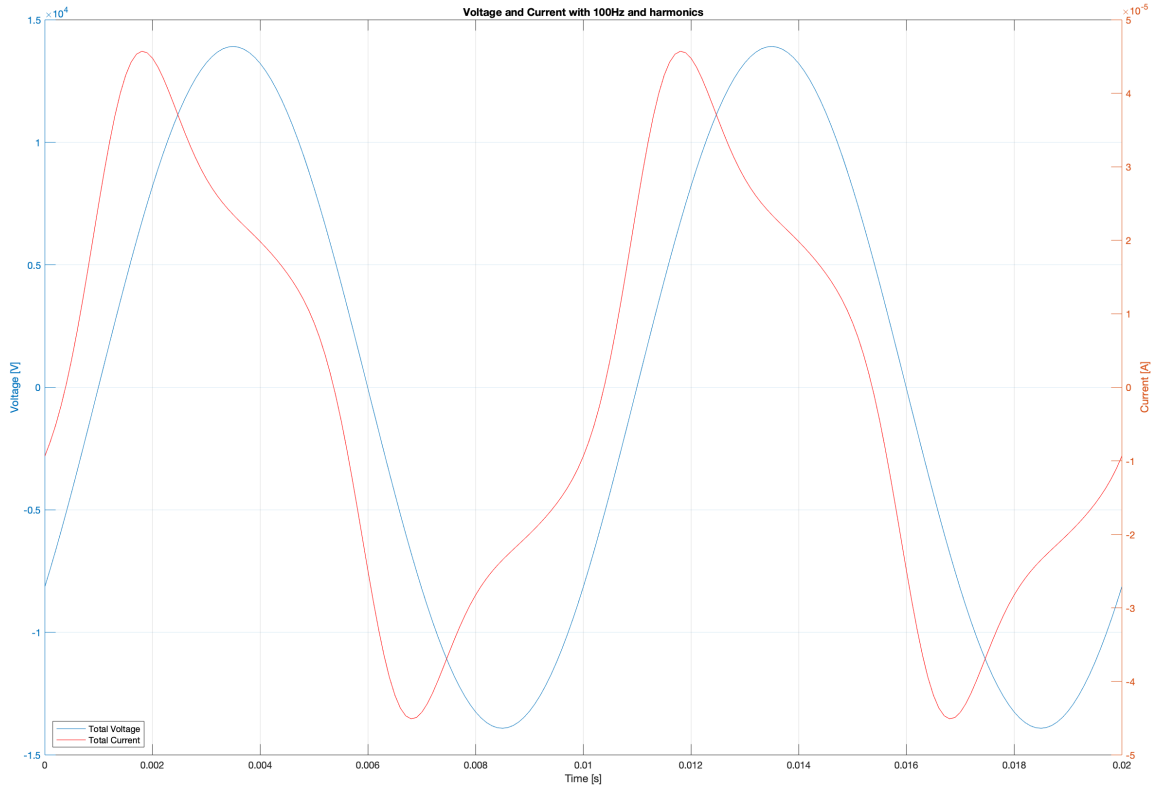
Voltage and Current with 100Hz and harmonics
Voltage [V]
Current [A]
Time [s]
Total Voltage
Total Current

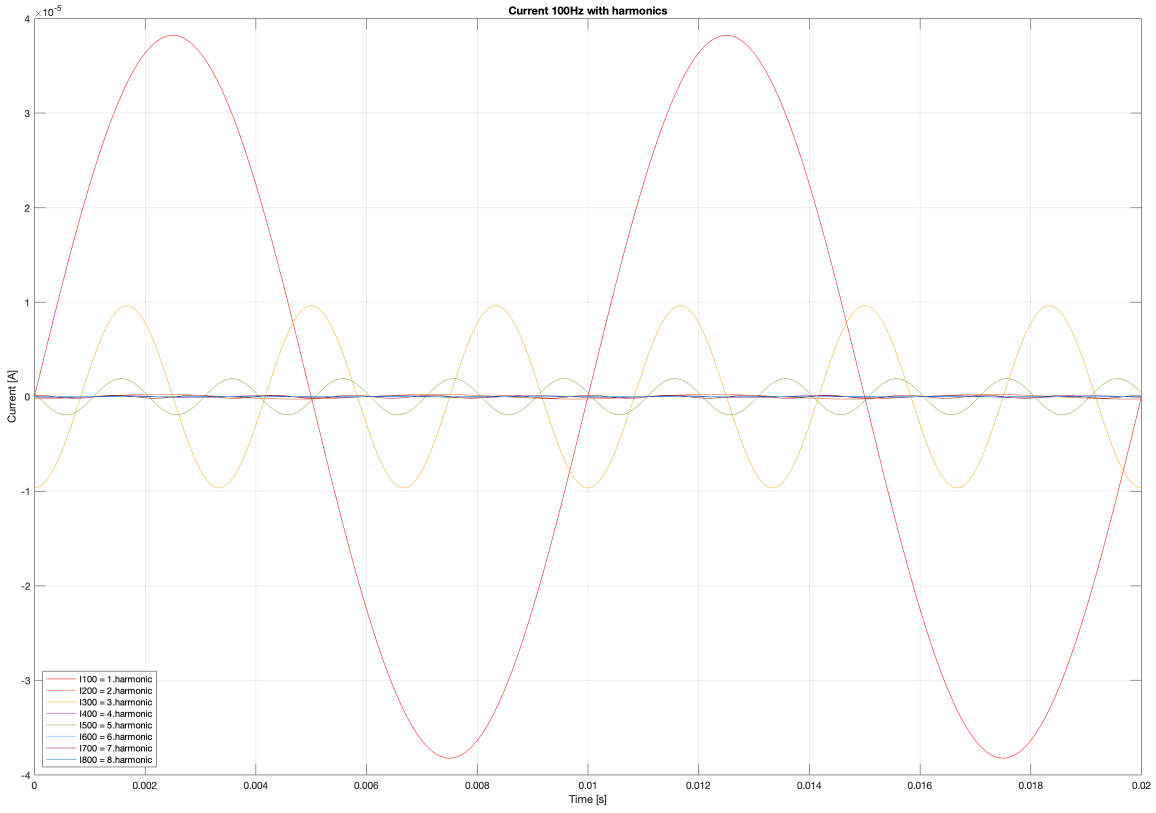
Current 100Hz with harmonics
Current [A]
Time [s]
I100 = 1.harmonic
I200 = 2.harmonic
I300 = 3.harmonic
I400 = 4.harmonic
I500 = 5.harmonic
I600 = 6.harmonic
I700 = 7.harmonic
I800 = 8.harmonic

7.2.2 Measurement Number 1 and 2 of The New Varnish with IDA 200, with 10kV or 0.5kV/mm applied.

Measurement nr.1

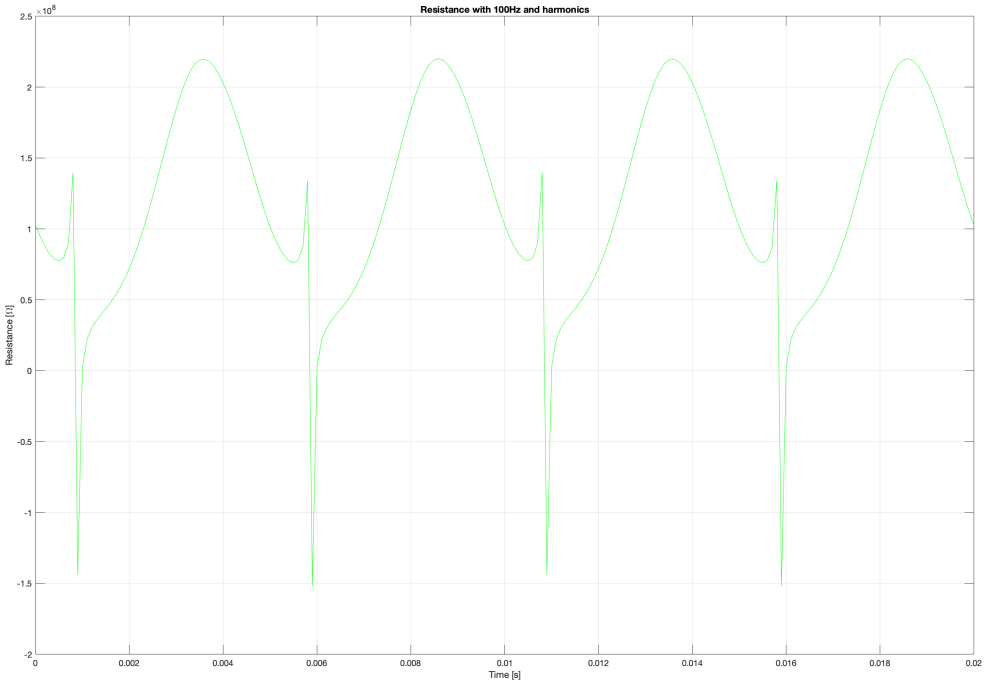

Measurement nr.2

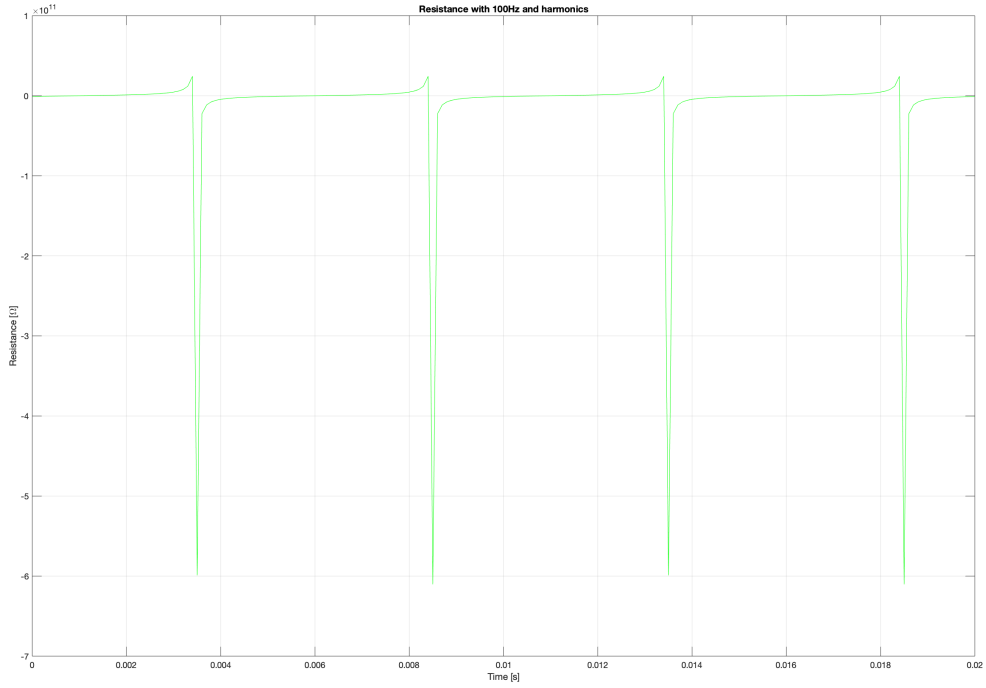

Measurement nr.1

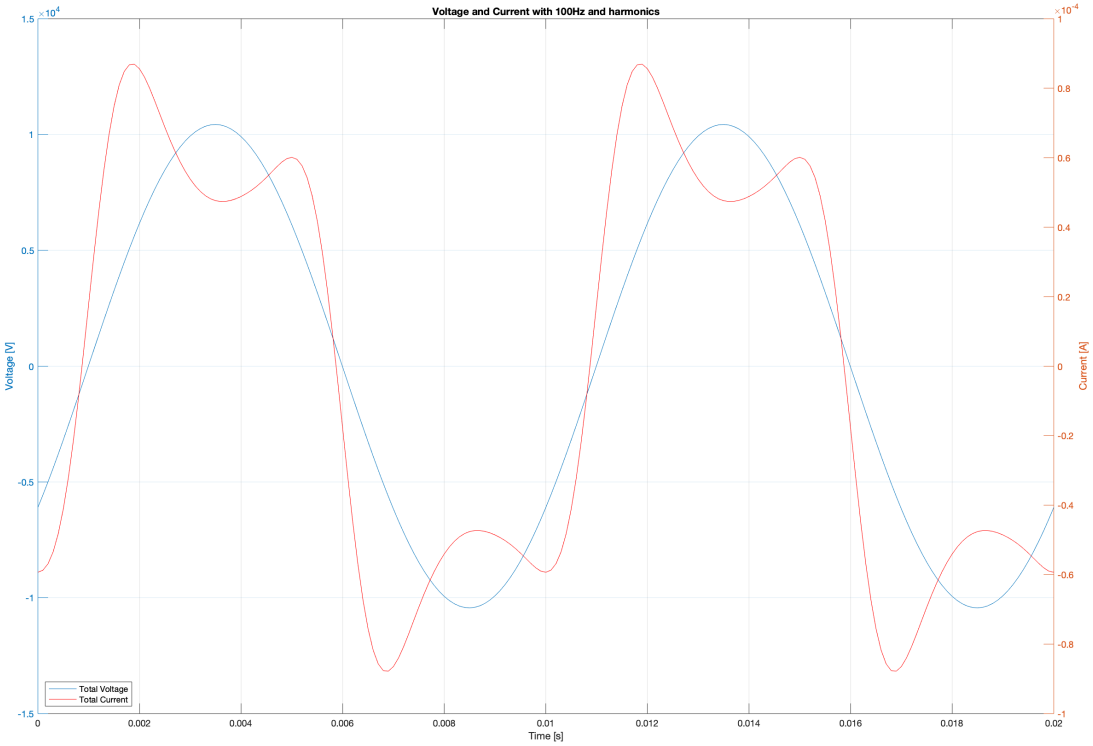

Measurement nr.2

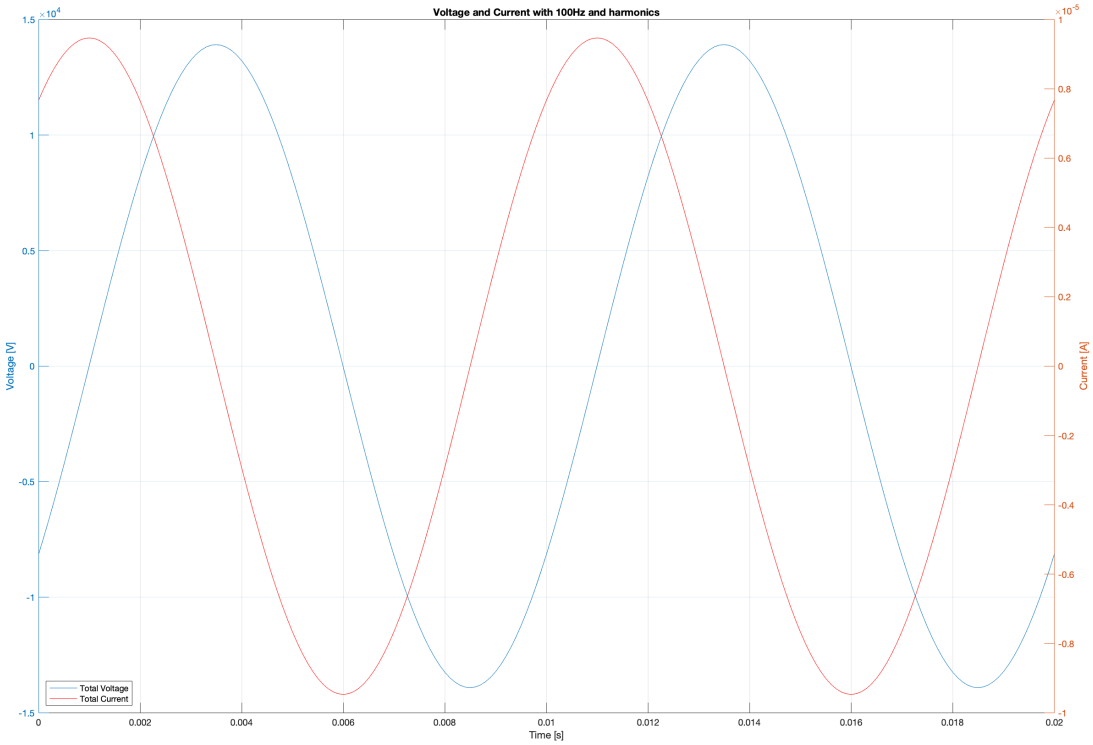

Measurement nr.1

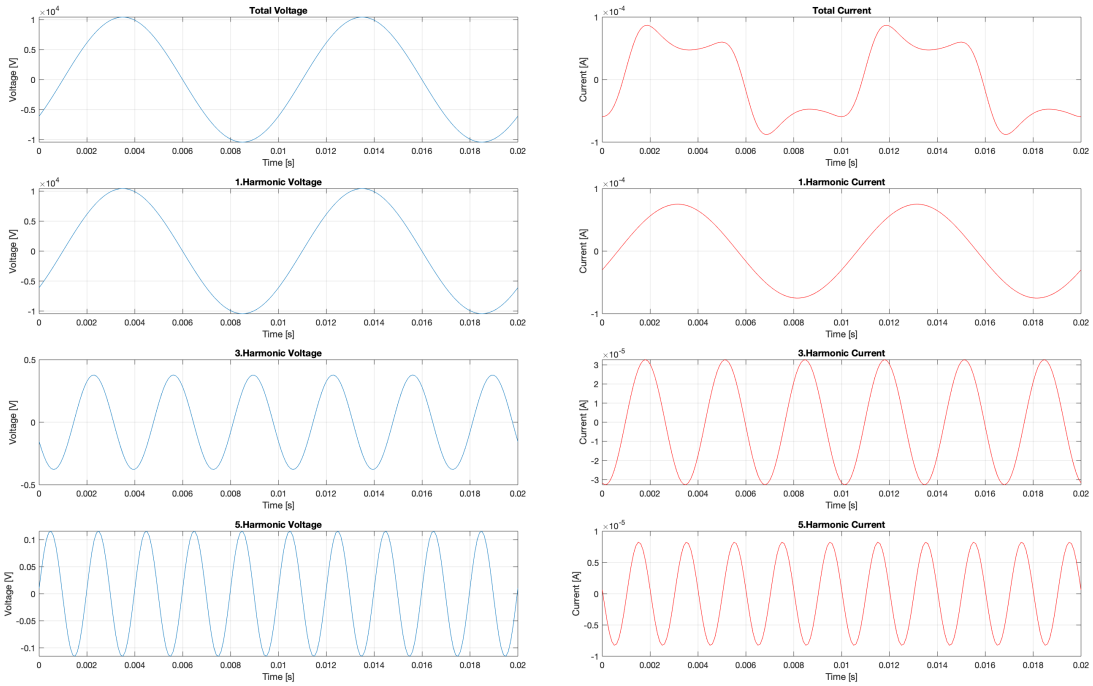

Measurement nr.2

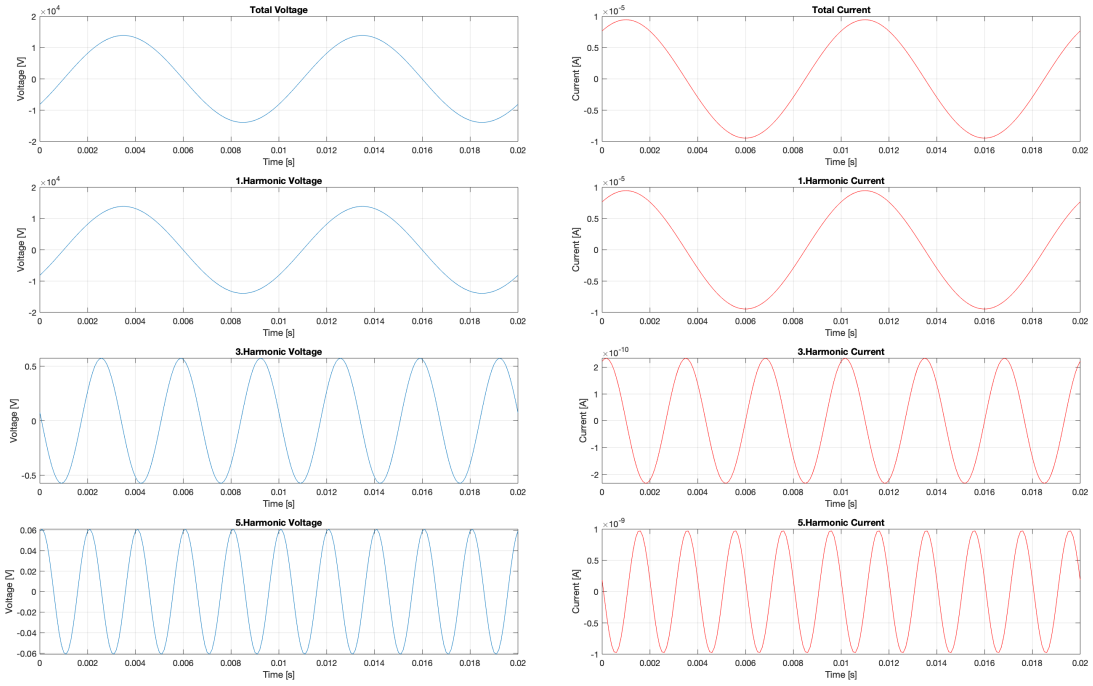

Measurement nr.1

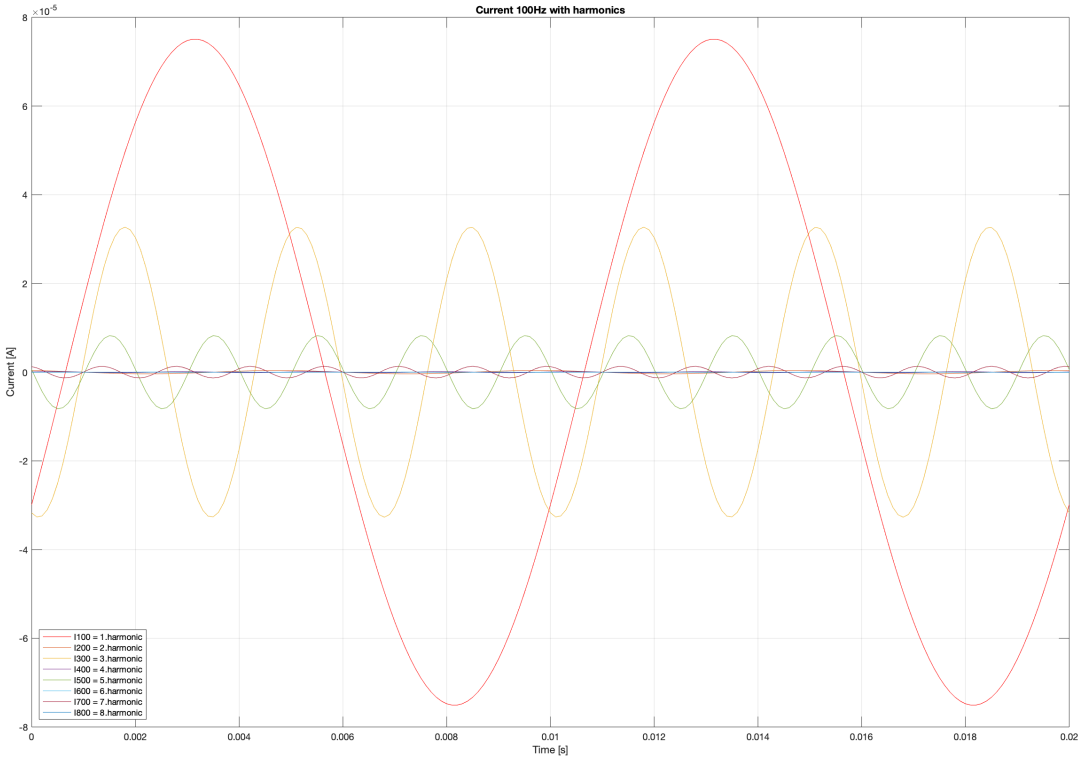

Measurement nr.2

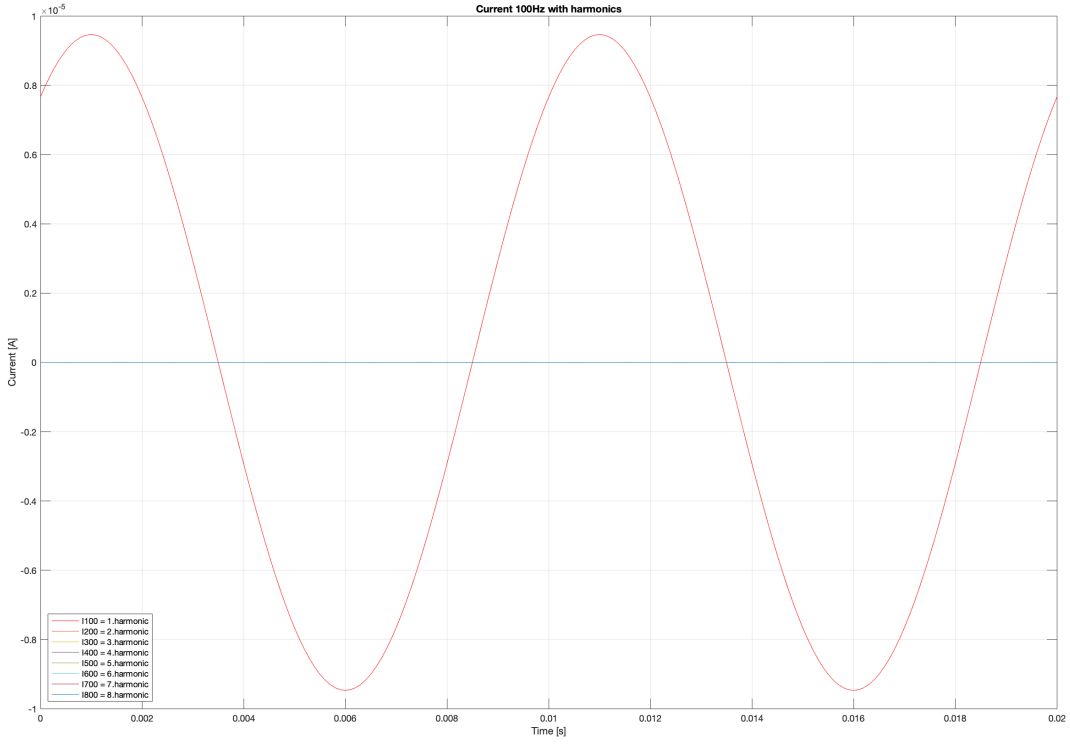

7.2.3 Measurements of The Old Varnish with IDA 200, with 7.5kV or 0.375kV/mm applied.

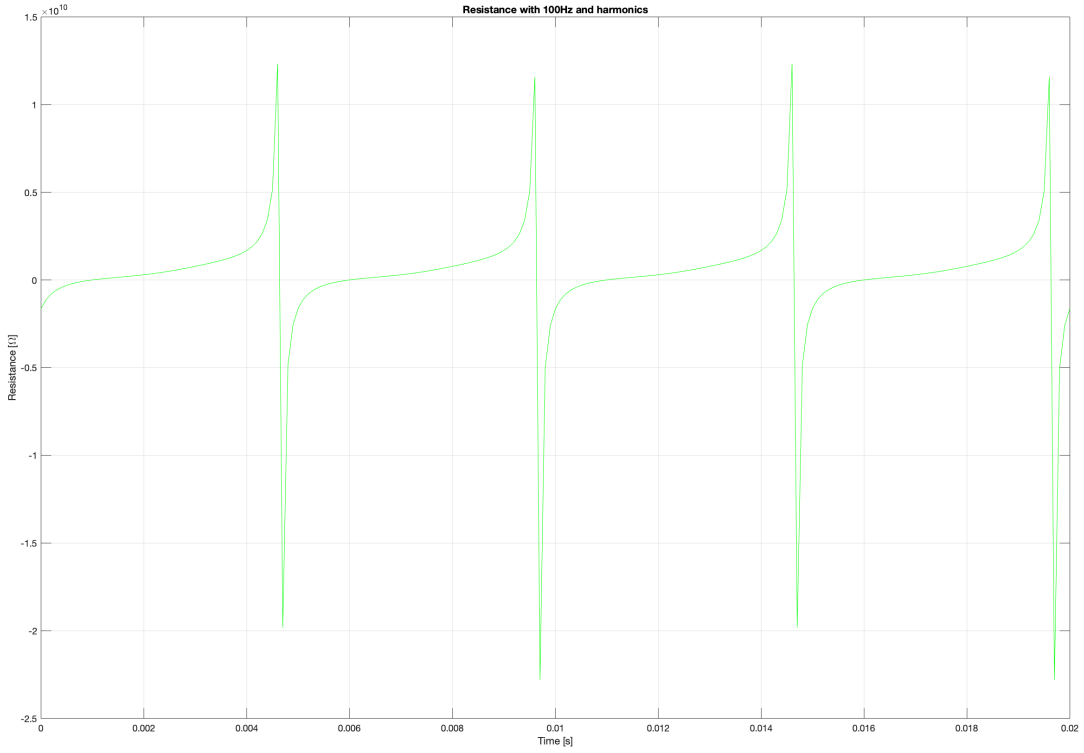

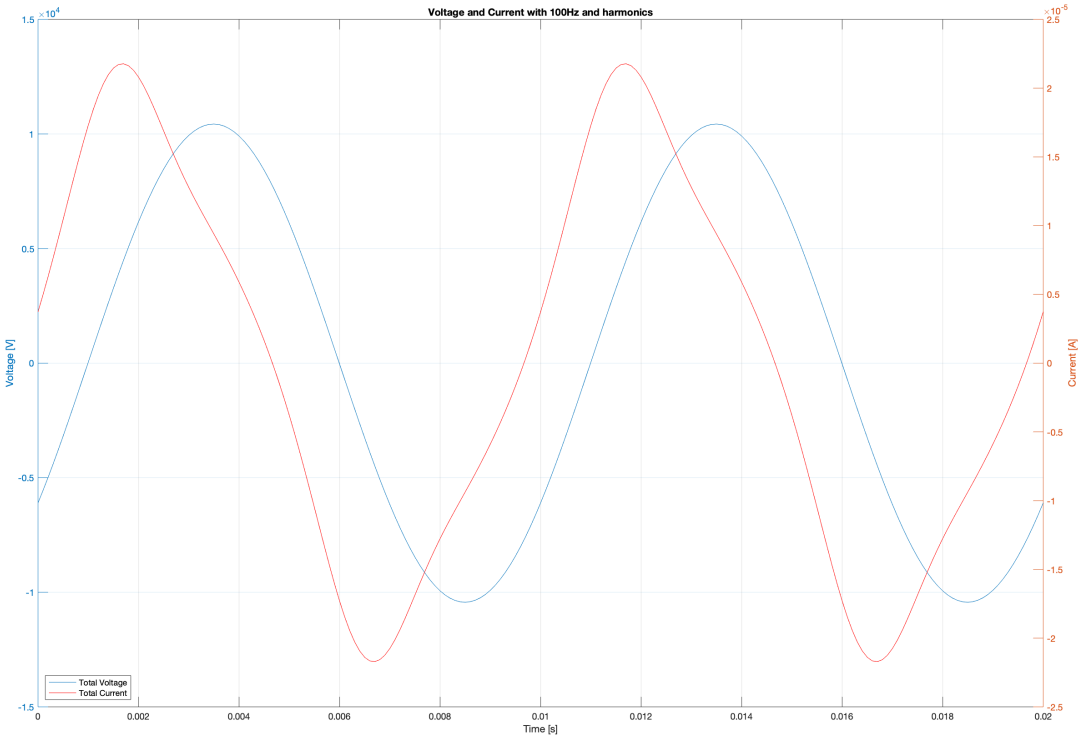

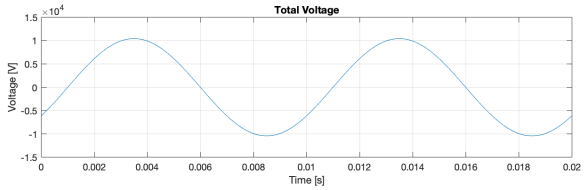
Total Voltage
Voltage [V]
Time [s]

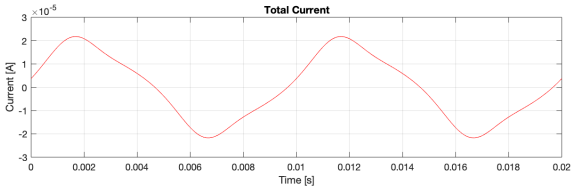
Total Current
Current [A]
Time [s]

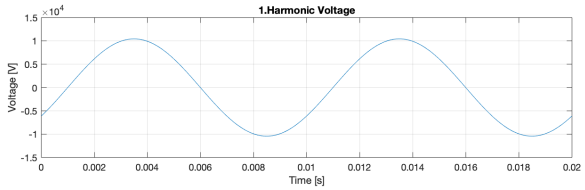
1.Harmonic Voltage
Voltage [V]
Time [s]

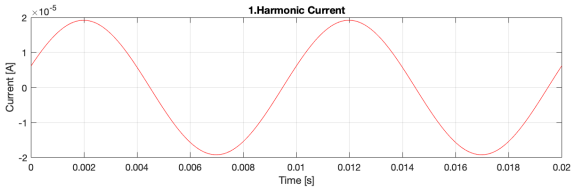
1.Harmonic Current
Current [A]
Time [s]

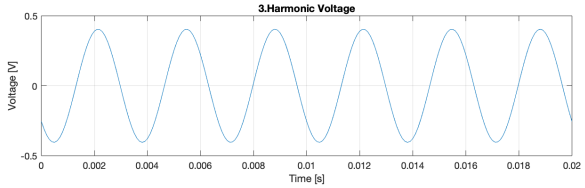
3.Harmonic Voltage
Voltage [V]
Time [s]

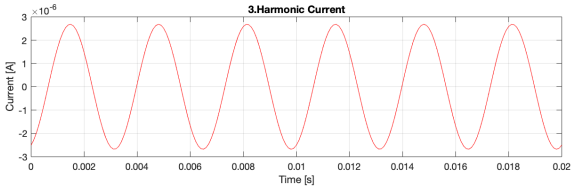
3.Harmonic Current
Current [A]
Time [s]

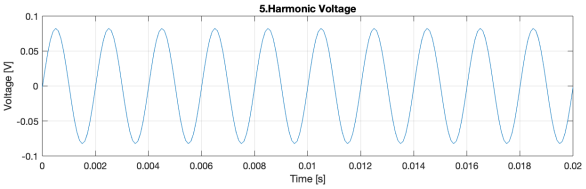
5.Harmonic Voltage
Voltage [V]
Time [s]

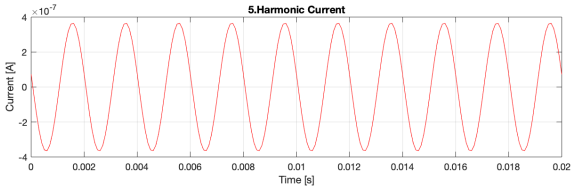
5.Harmonic Current
Current [A]
Time [s]

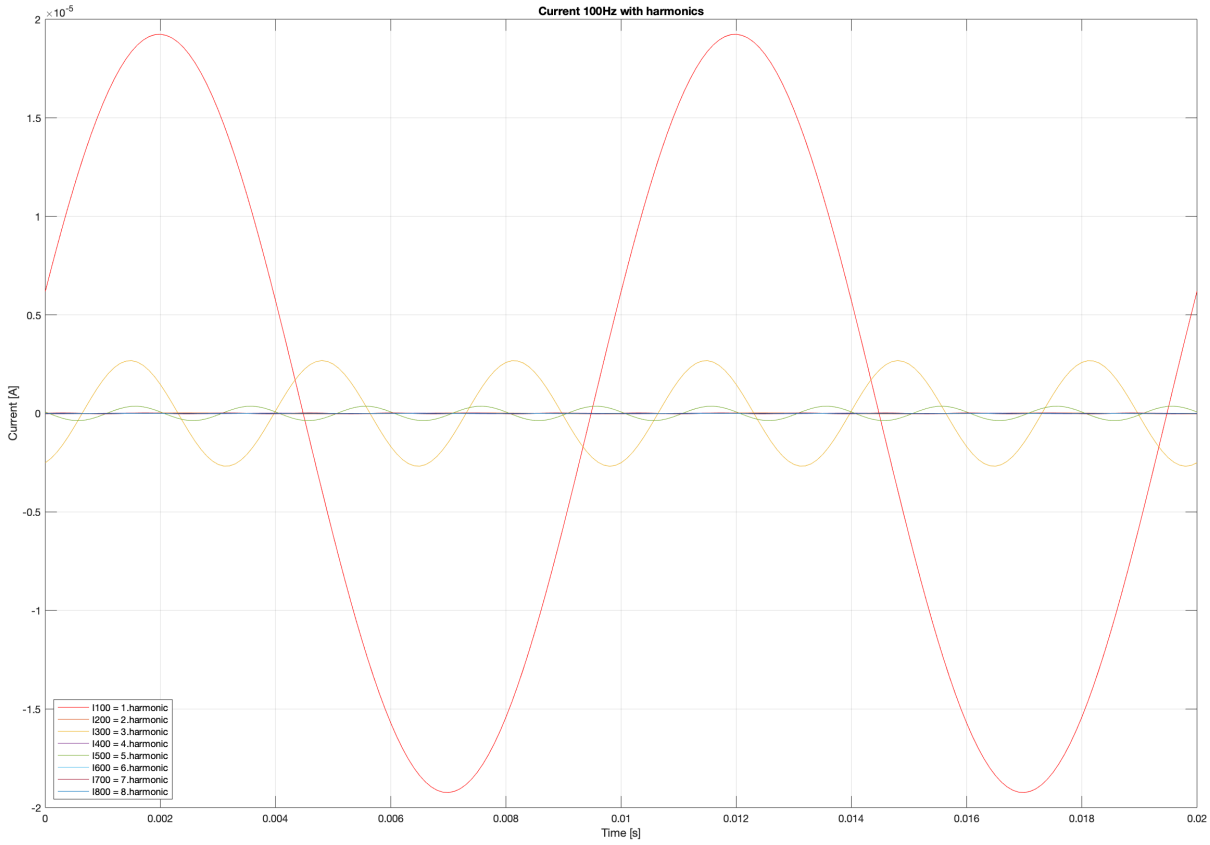
Current 100Hz with harmonics
Current [A]
Time [s]
I100 = 1.harmonic
I200 = 2.harmonic
I300 = 3.harmonic
I400 = 4.harmonic
I500 = 5.harmonic
I600 = 6.harmonic
I700 = 7.harmonic
I800 = 8.harmonic

7.2.4 Measurement Number 1 and 2 of The New Varnish with IDA 200, with 7.5kV or 0.375kV/mm applied.

Measurement nr.1

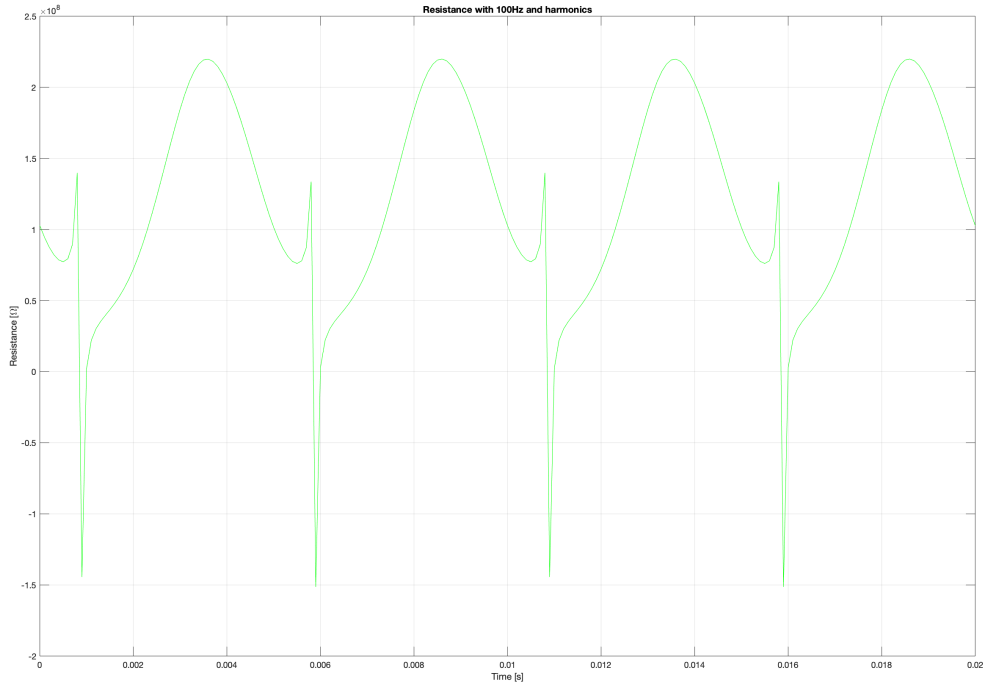

Measurement nr.2

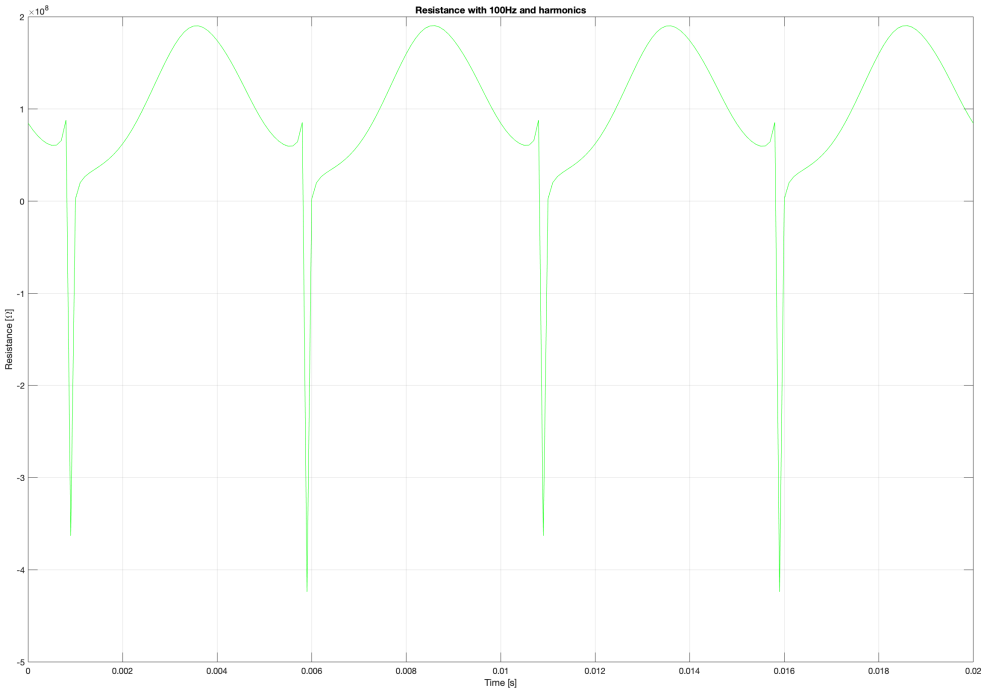

Measurement nr.1

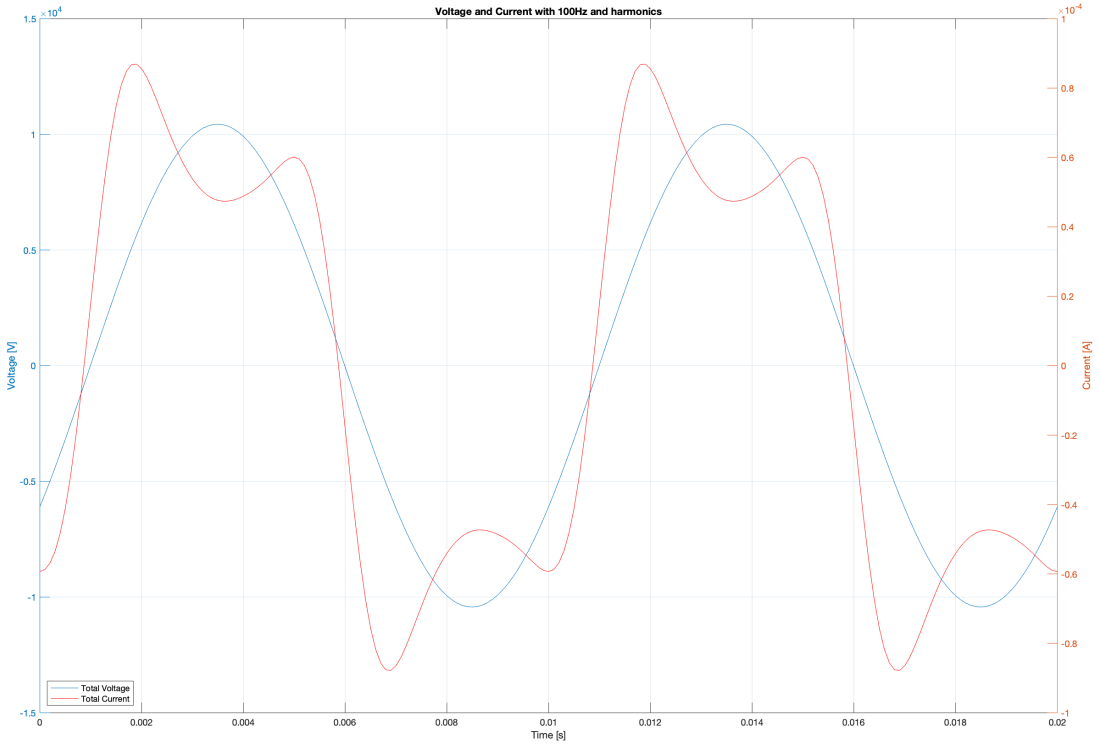

Measurement nr.2

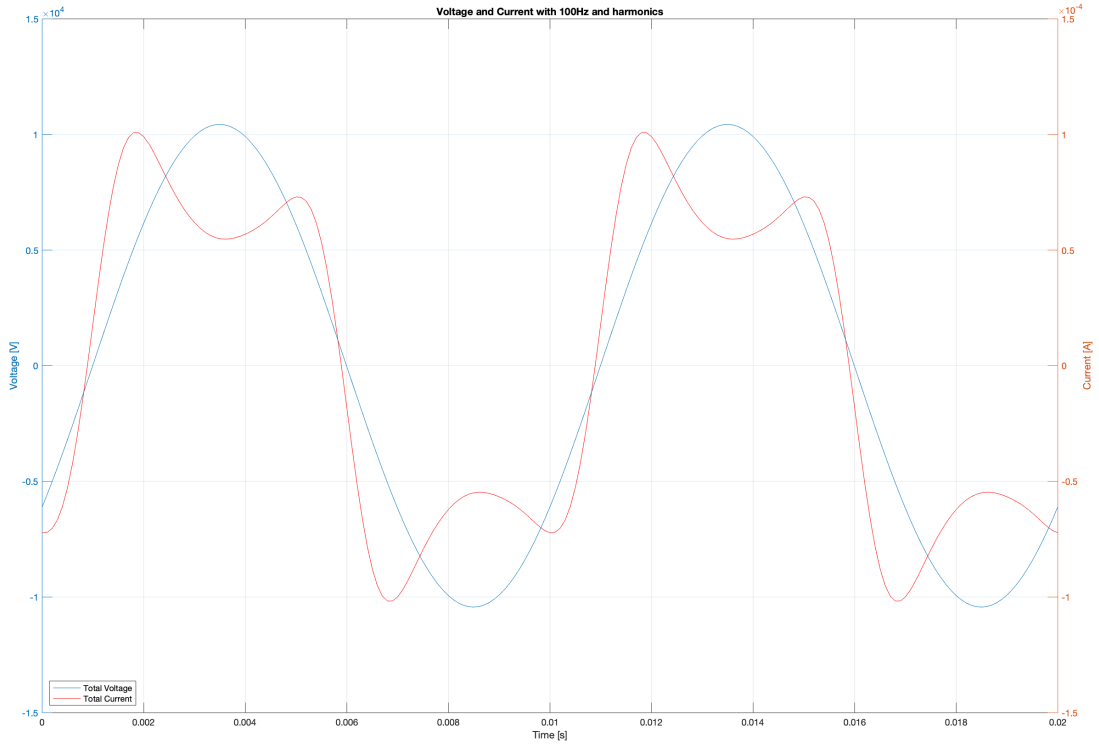

Measurement nr.1

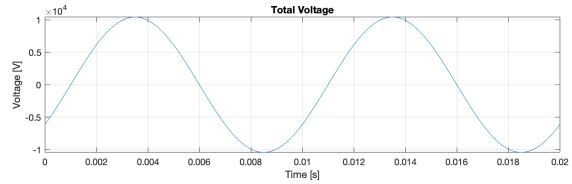

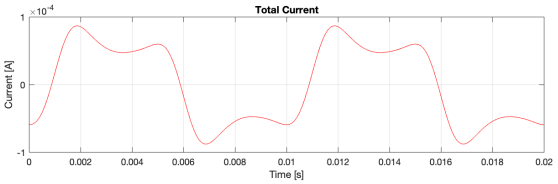

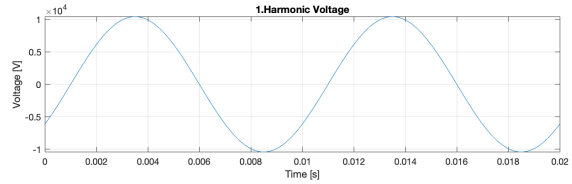

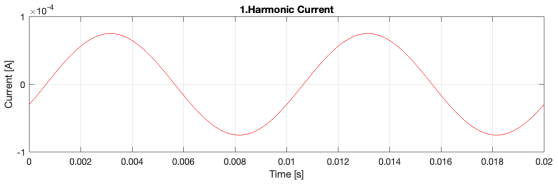

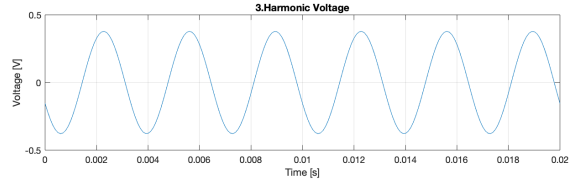

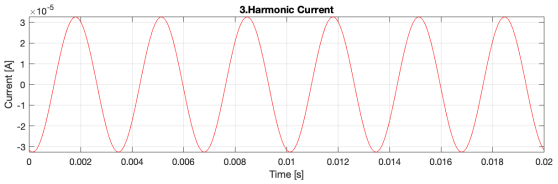

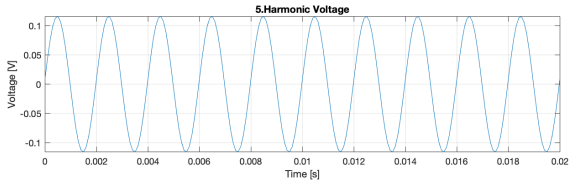

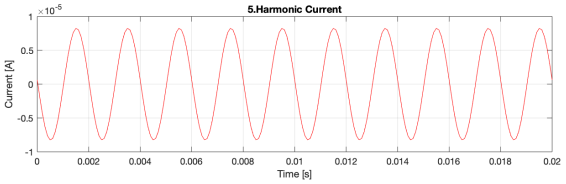

Measurement nr.2

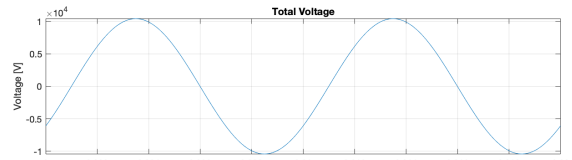

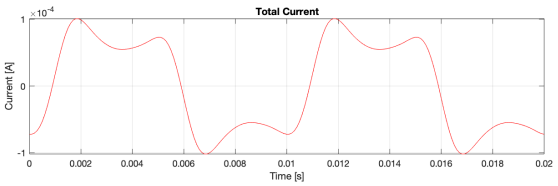

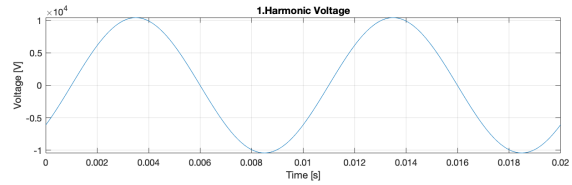

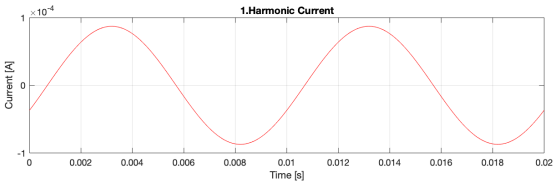

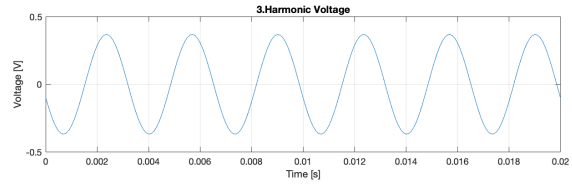

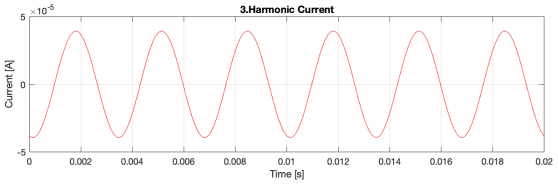

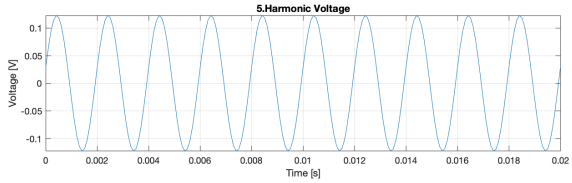

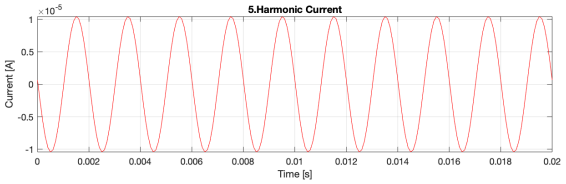

Measurement nr.1

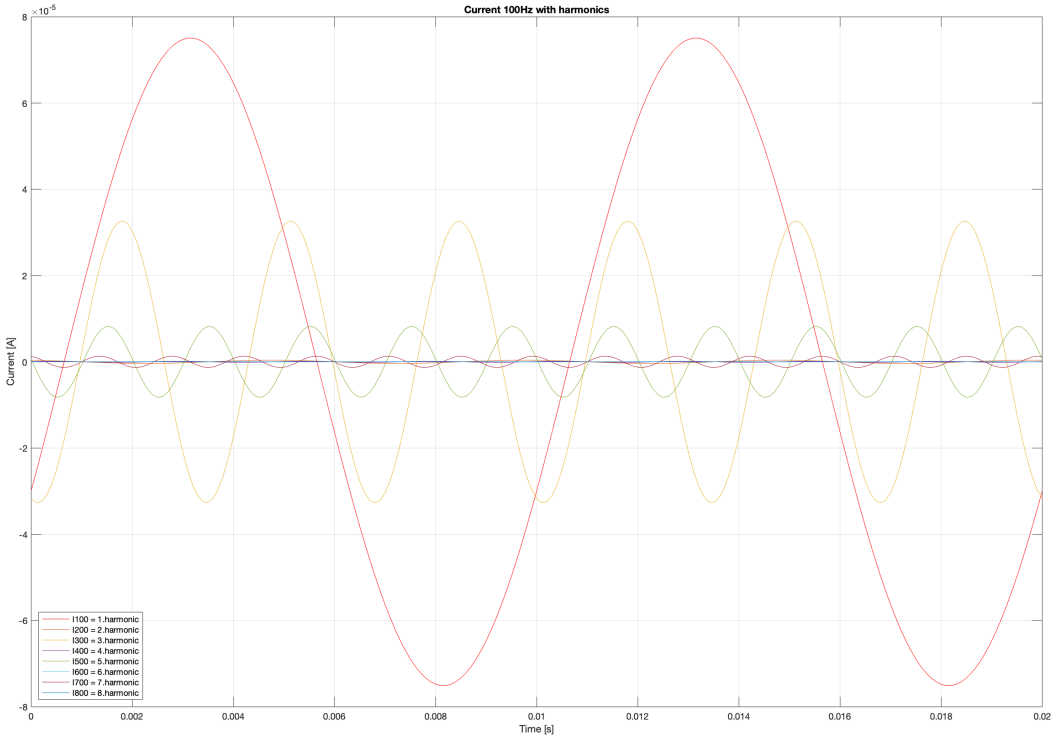

Measurement nr.2

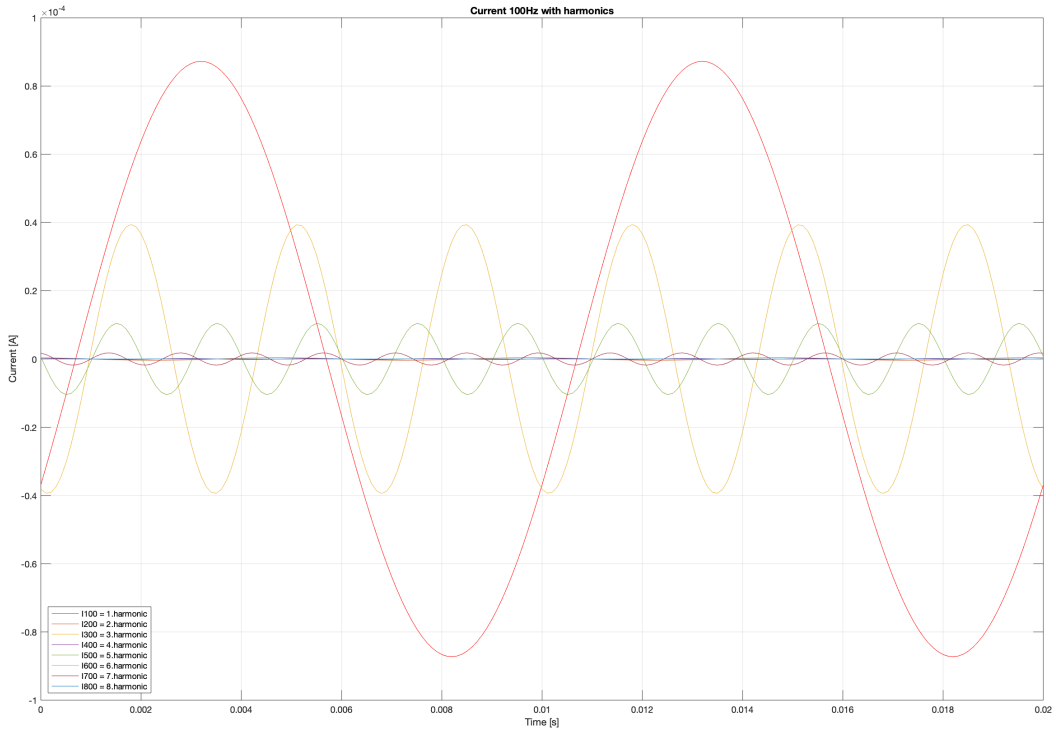

7.2.5 Measurements of The Old Varnish with IDA 200, with 5kV or 0.250kV/mm applied.

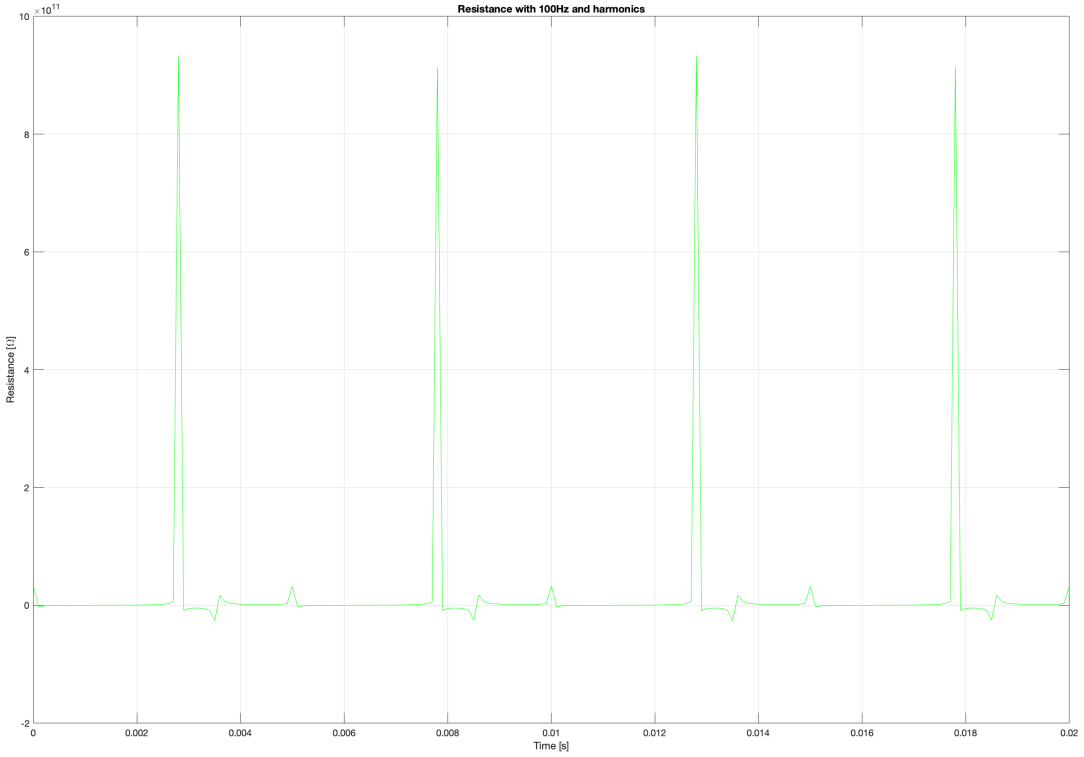

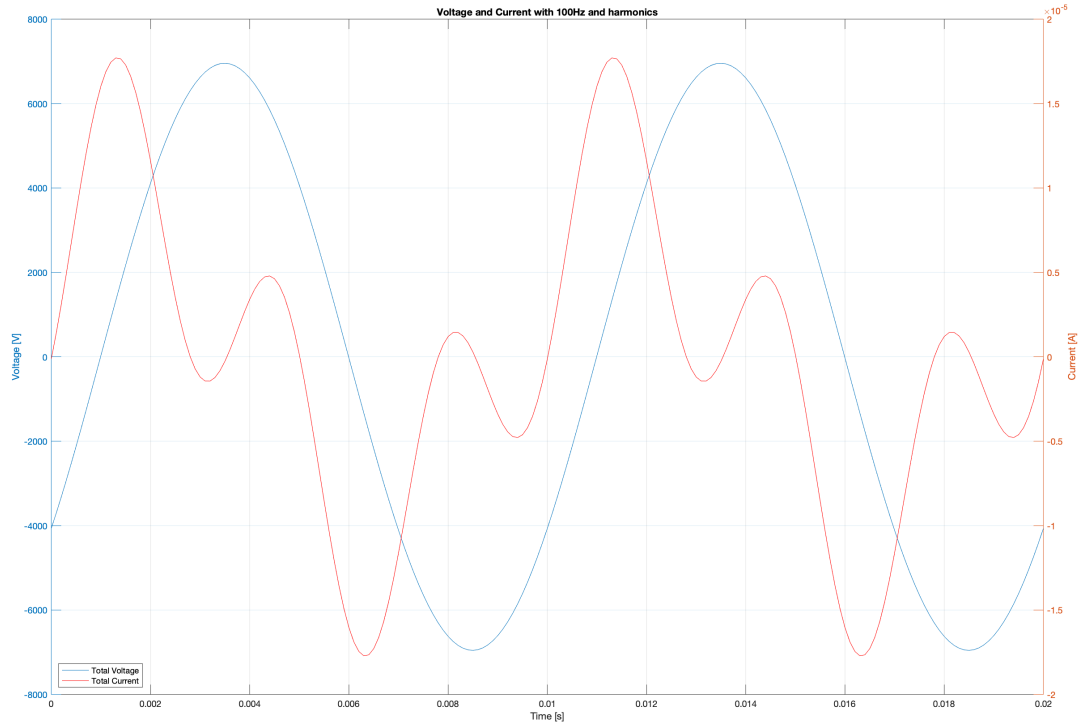

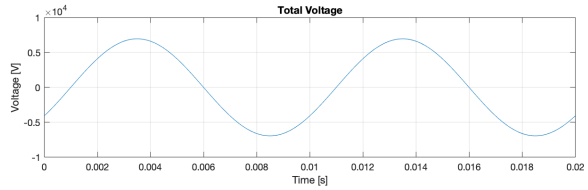
Total Voltage
Voltage [V]
Time [s]

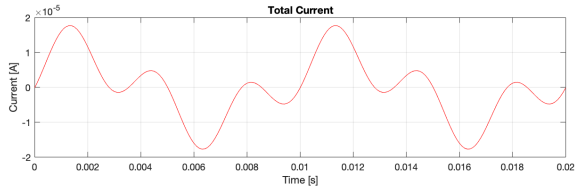
Total Current
Current [A]
Time [s]

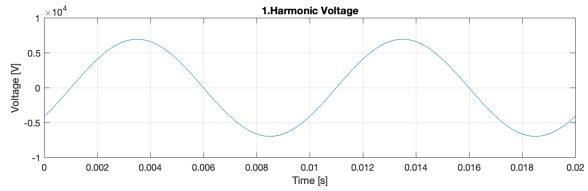
1.Harmonic Voltage
Voltage [V]
Time [s]

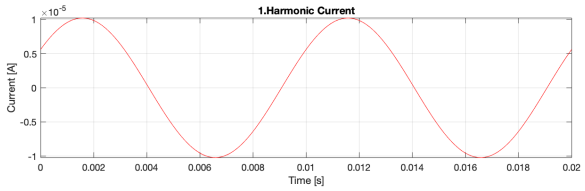
1.Harmonic Current
Current [A]
Time [s]

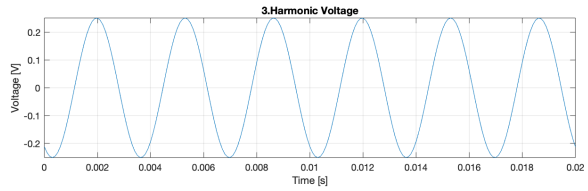
3.Harmonic Voltage
Voltage [V]
Time [s]

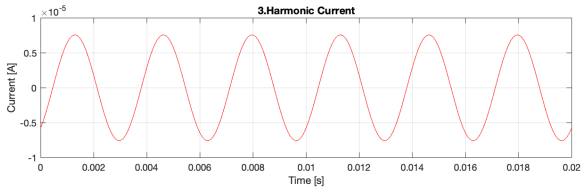
3.Harmonic Current
Current [A]
Time [s]

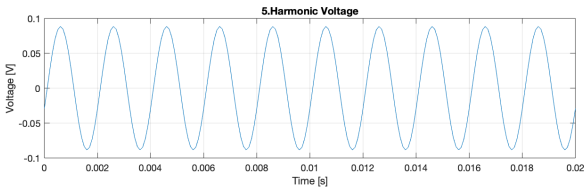
5.Harmonic Voltage
Voltage [V]
Time [s]

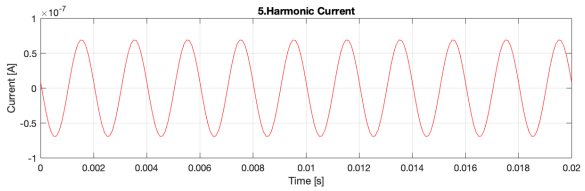
5.Harmonic Current
Current [A]
Time [s]

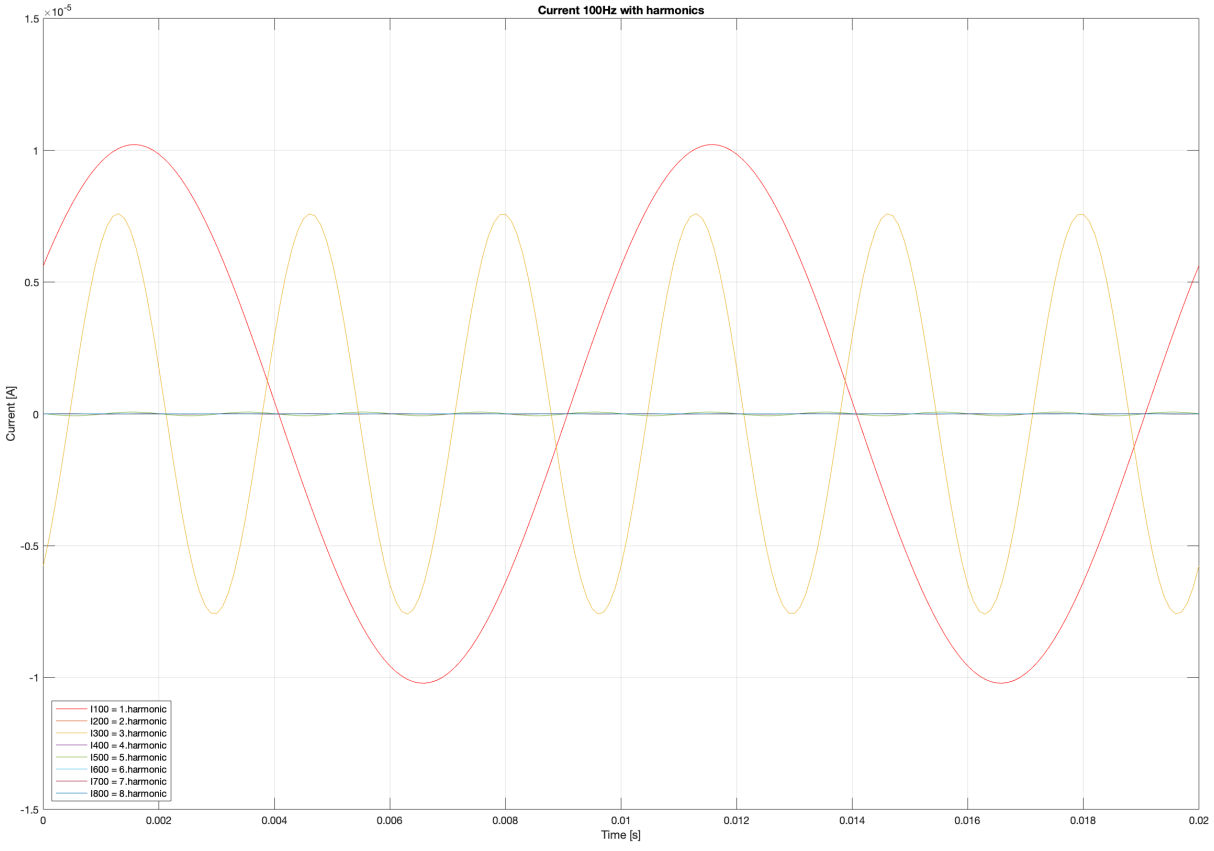
Current 100Hz with harmonics
Current [A]
Time [s]
I100 = 1.harmonic
I200 = 2.harmonic
I300 = 3.harmonic
I400 = 4.harmonic
I500 = 5.harmonic
I600 = 6.harmonic
I700 = 7.harmonic
I800 = 8.harmonic

7.2.6 Measurement Number 1 and 2 of The New Varnish with IDA 200, with 5kV or 0.250kV/mm applied.

Measurement nr.1

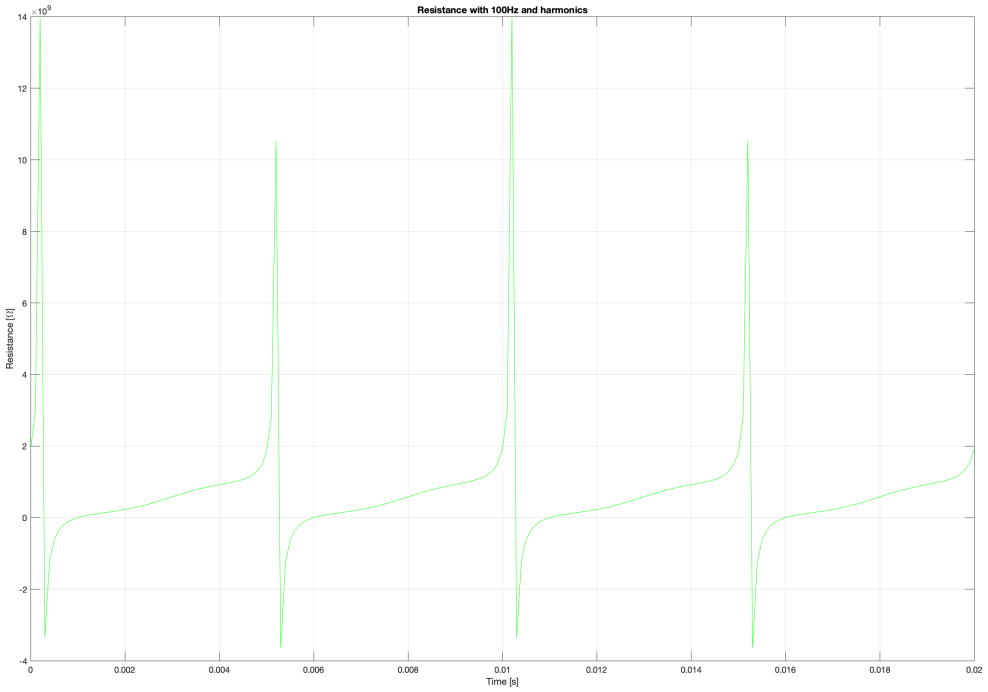

Measurement nr.2

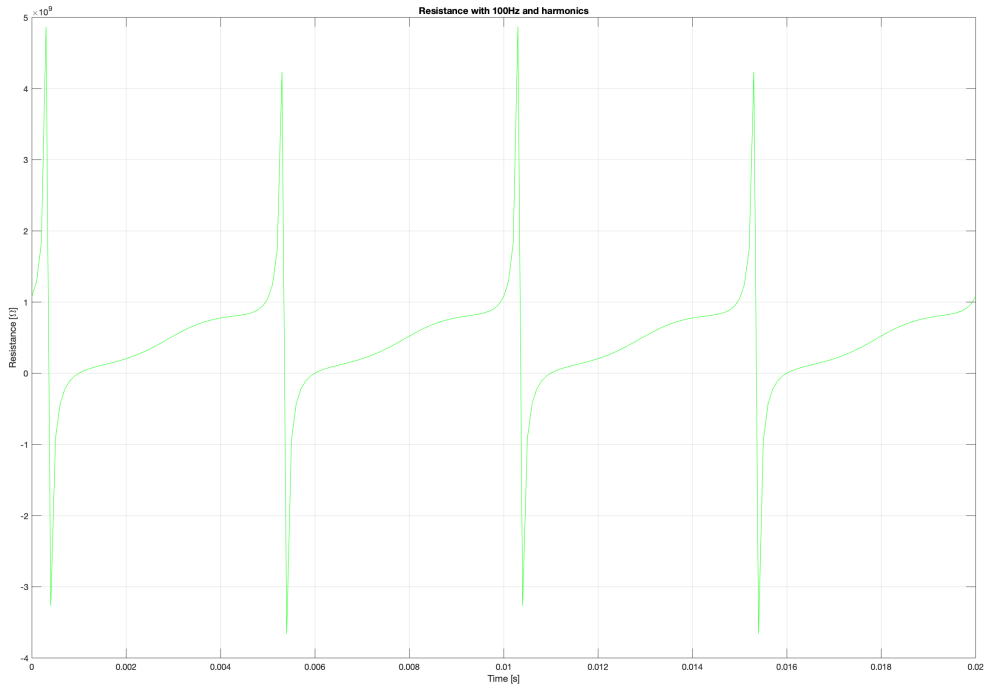

Measurement nr.1

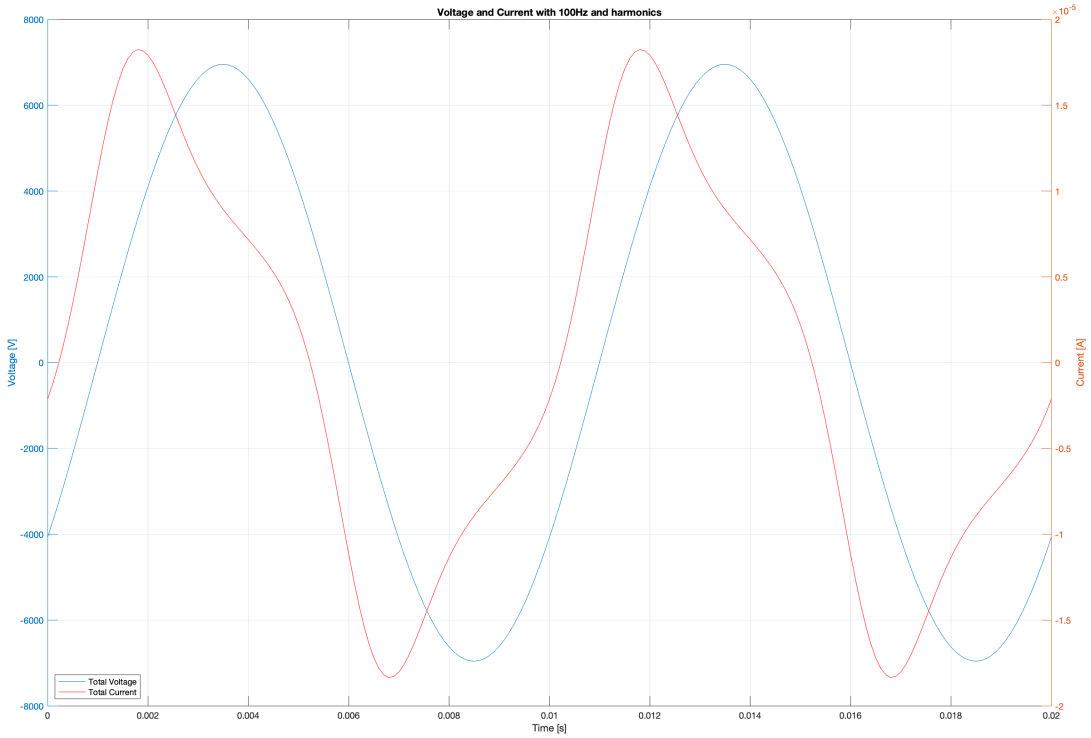

Measurement nr.2

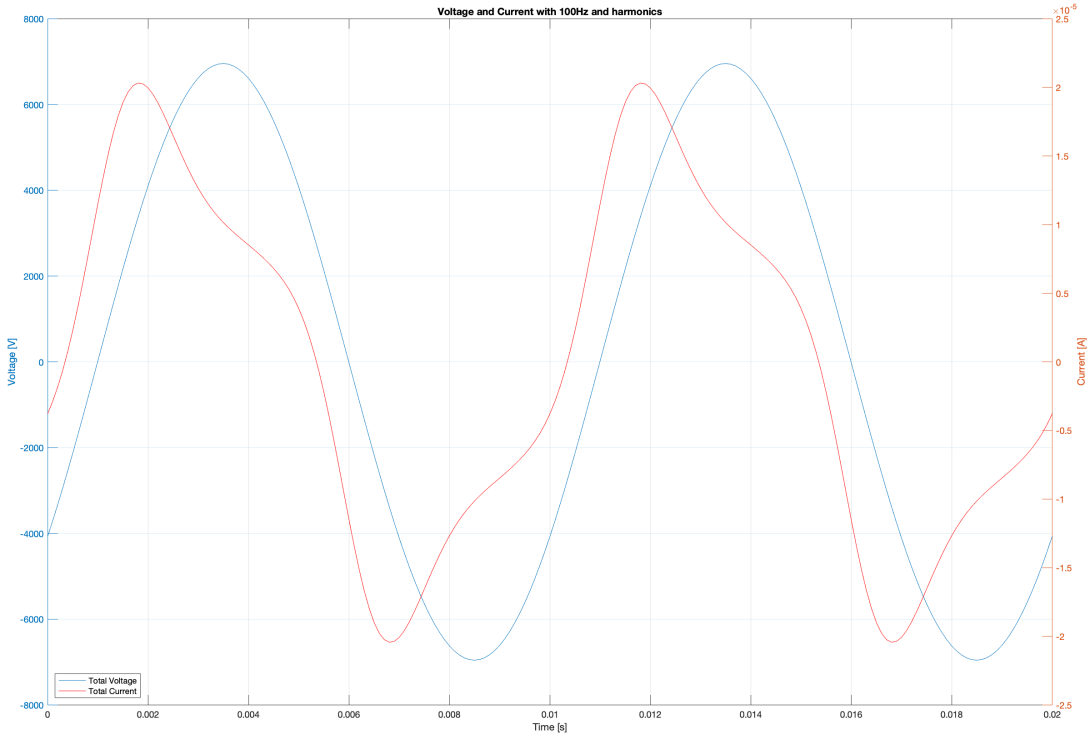

Measurement nr.1

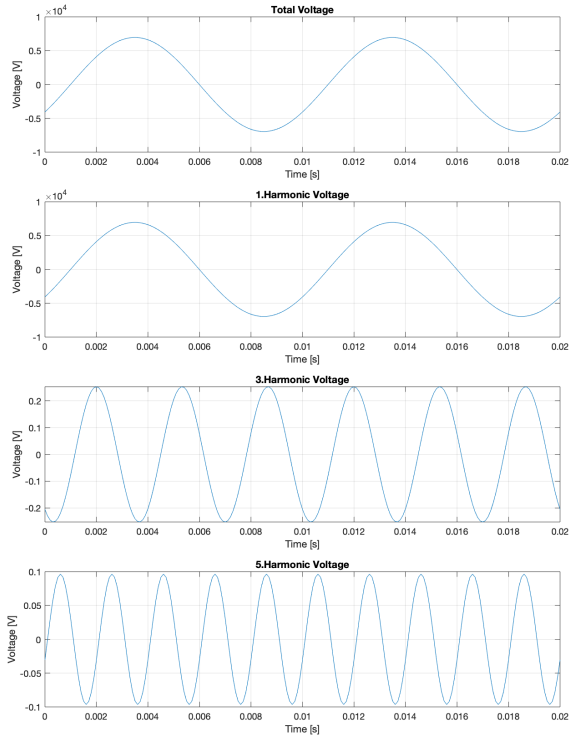

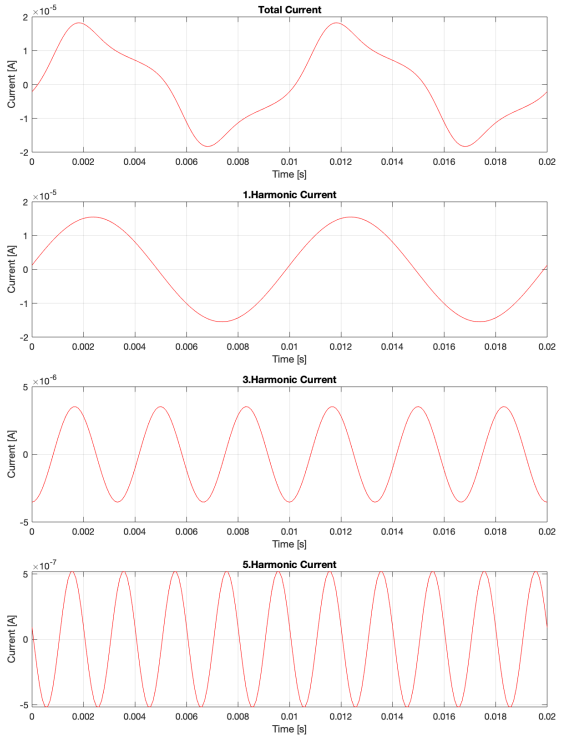

Measurement nr.2

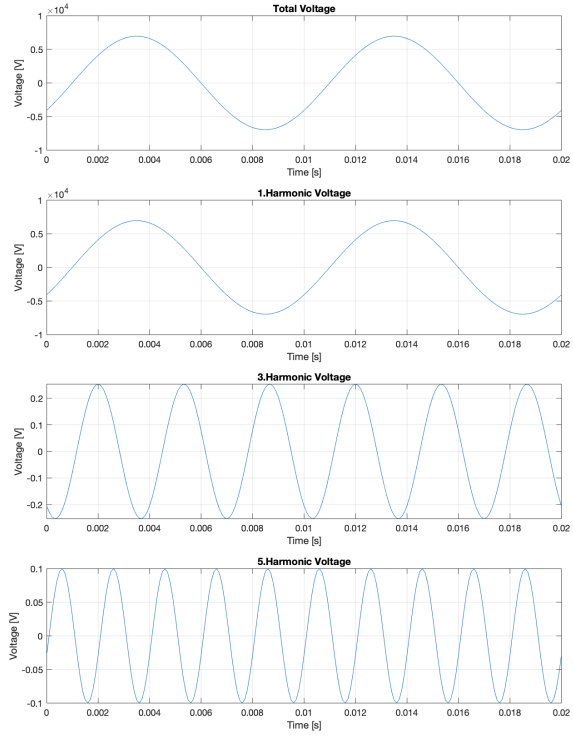

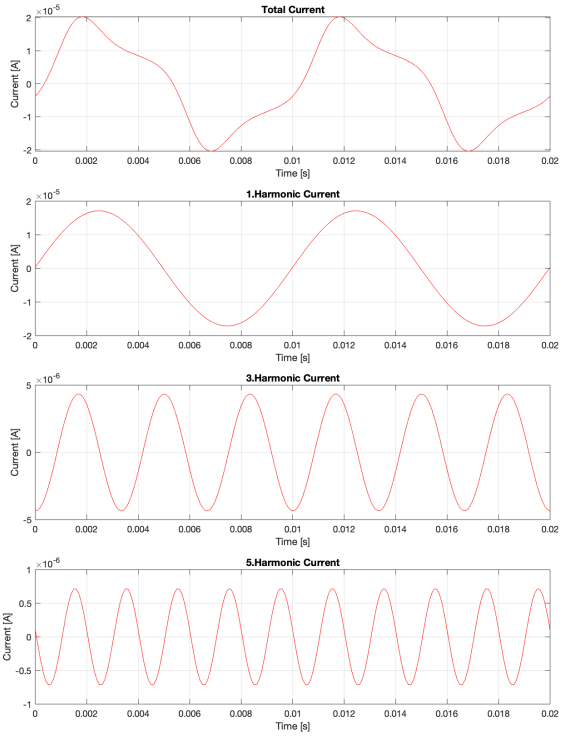

Measurement nr.1

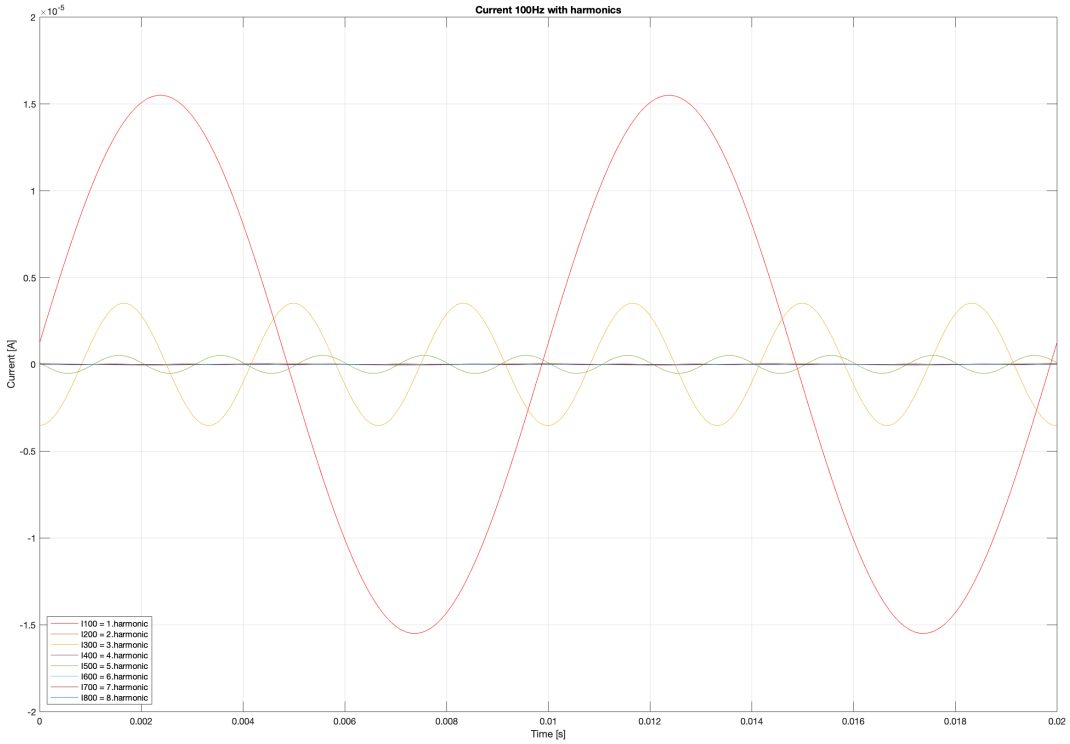

Measurement nr.2

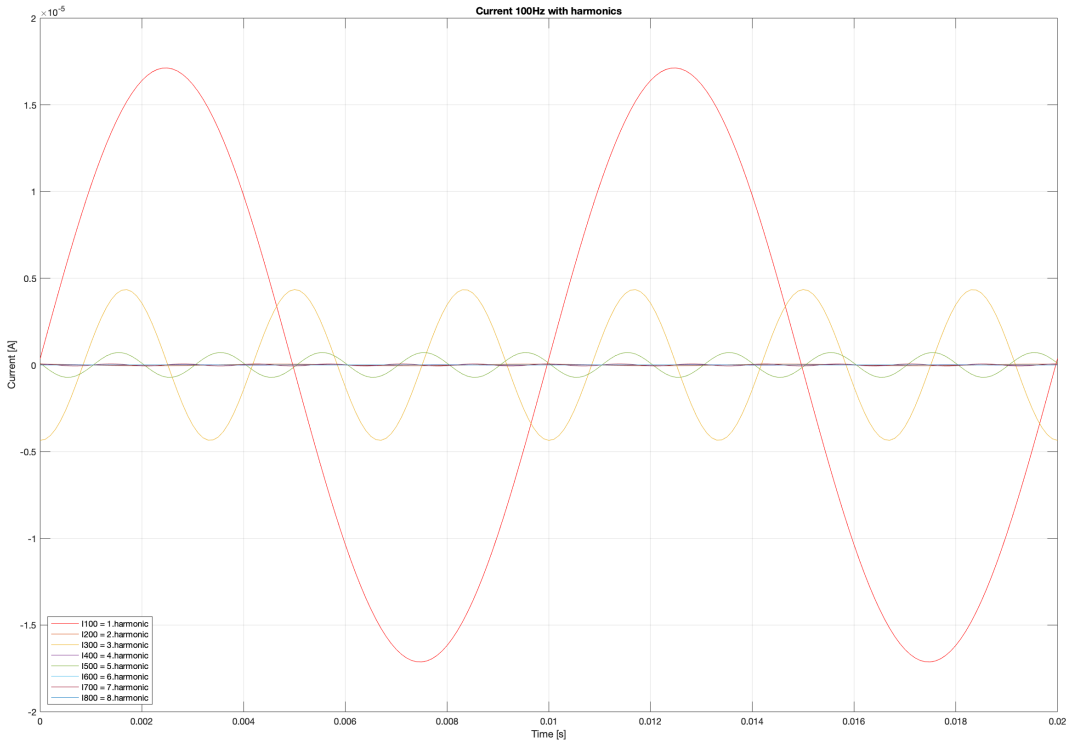

7.2.7 Measurements of The Old Varnish with IDA 200, with 2.5kV or 0.125kV/mm applied.

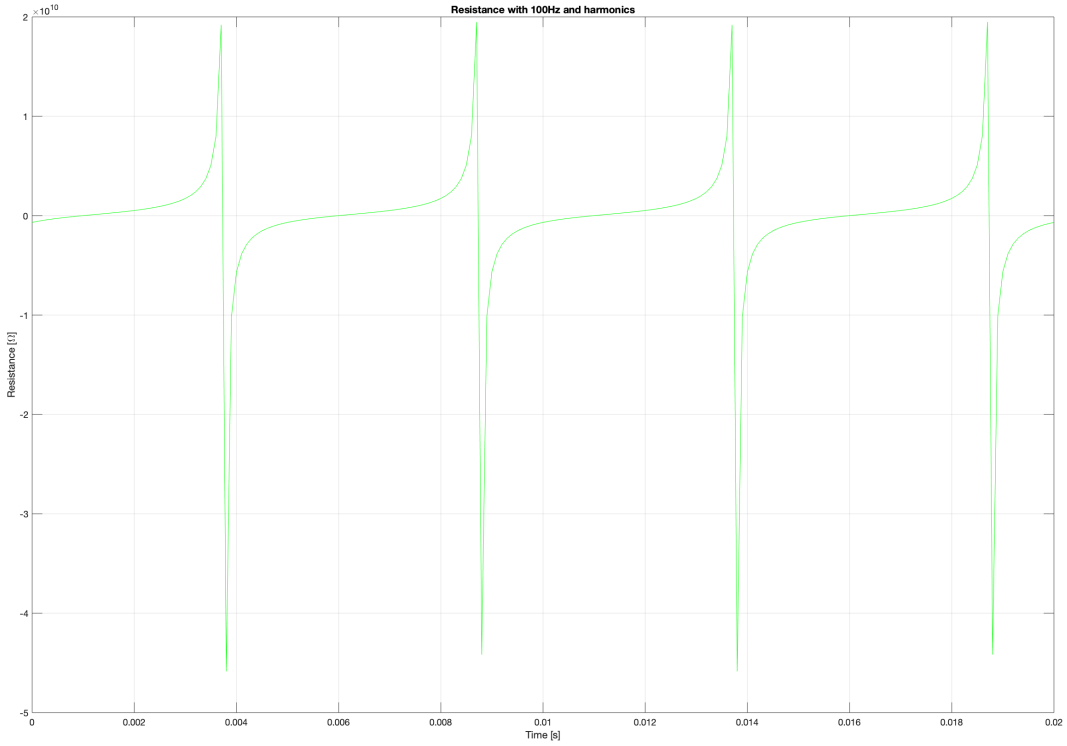

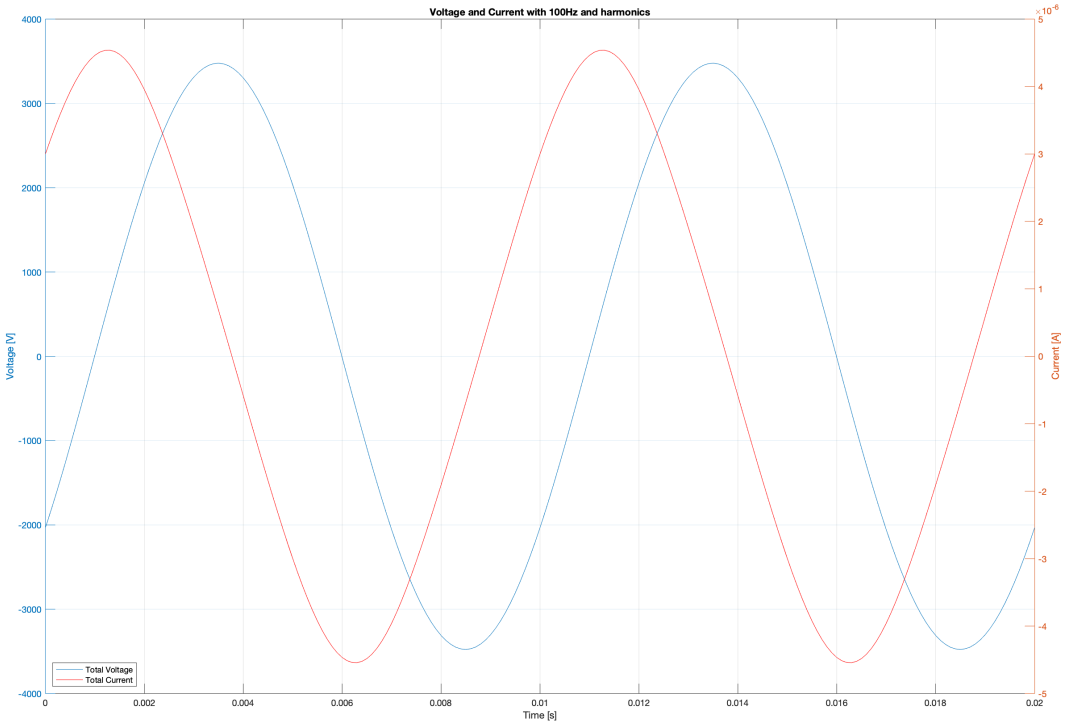

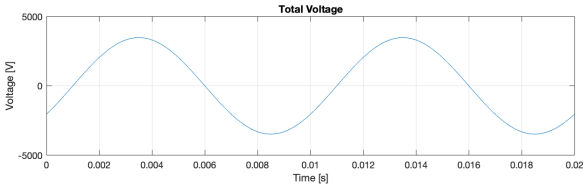
Total Voltage
Voltage [V]
Time [s]

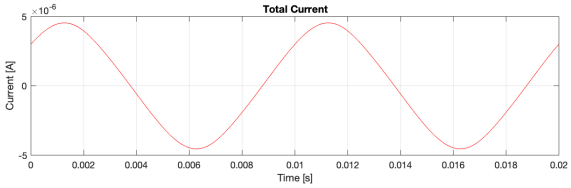
Total Current
Current [A]
Time [s]

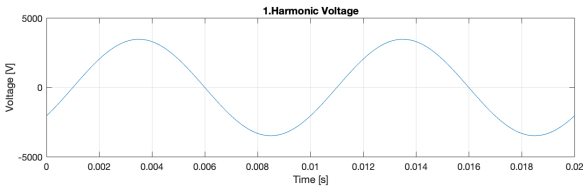
1.Harmonic Voltage
Voltage [V]
Time [s]

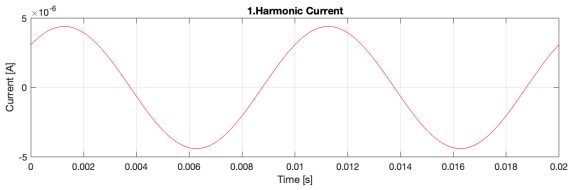
1.Harmonic Current
Current [A]
Time [s]

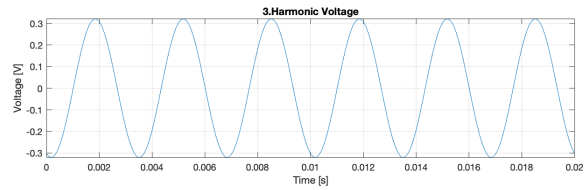
3.Harmonic Voltage
Voltage [V]
Time [s]

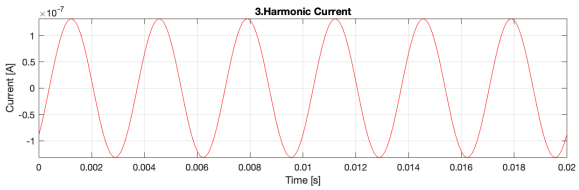
3.Harmonic Current
Current [A]
Time [s]

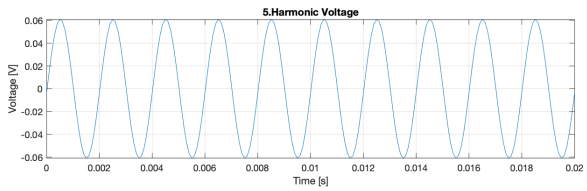
5.Harmonic Voltage
Voltage [V]
Time [s]

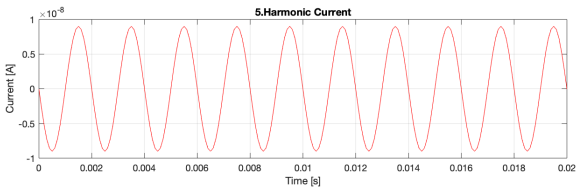
5.Harmonic Current
Current [A]
Time [s]

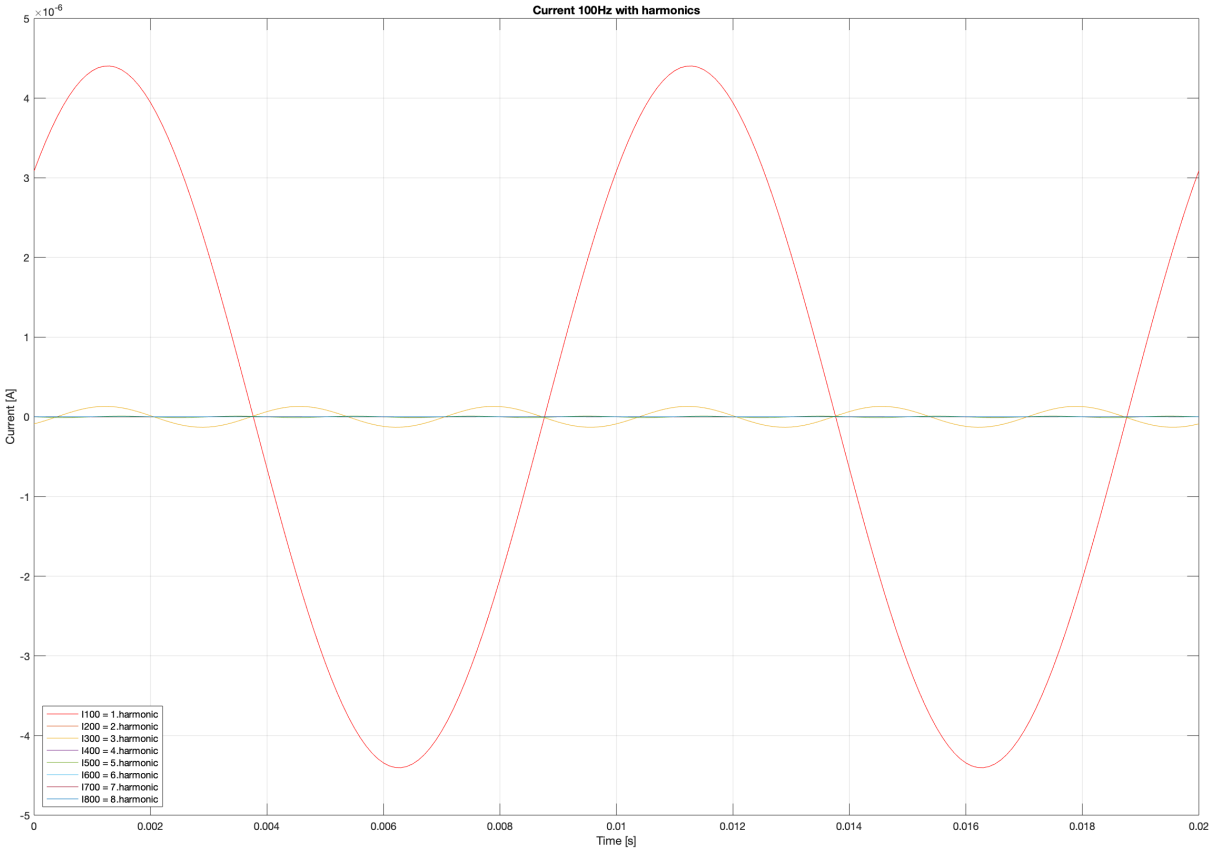
Current 100Hz with harmonics
Current [A]
Time [s]
I100 = 1.harmonic
I200 = 2.harmonic
I300 = 3.harmonic
I400 = 4.harmonic
I500 = 5.harmonic
I600 = 6.harmonic
I700 = 7.harmonic
I800 = 8.harmonic

7.2.8 Measurement Number 1 and 2 of The New Varnish with IDA 200, with 2.5kV or 0.125kV/mm applied.

Measurement nr.1

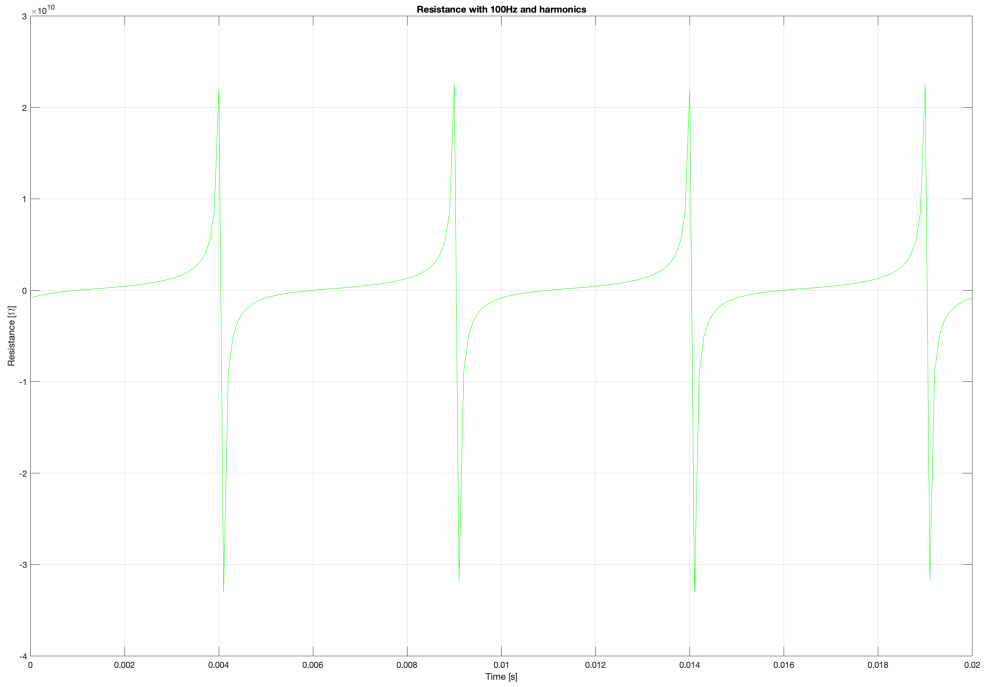

Measurement nr.2

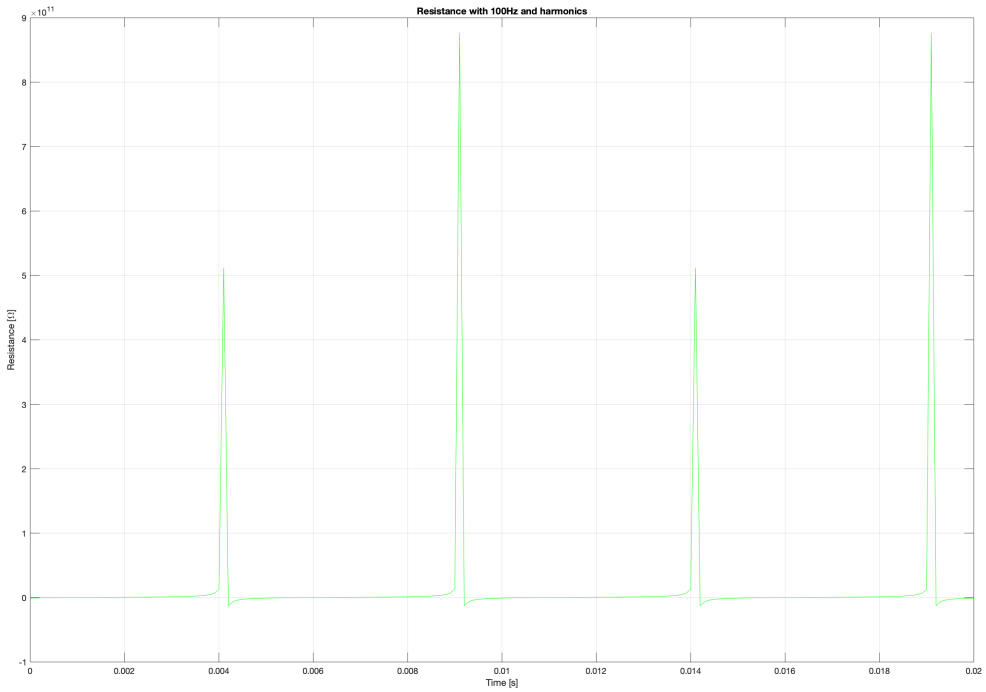

Measurement nr.1

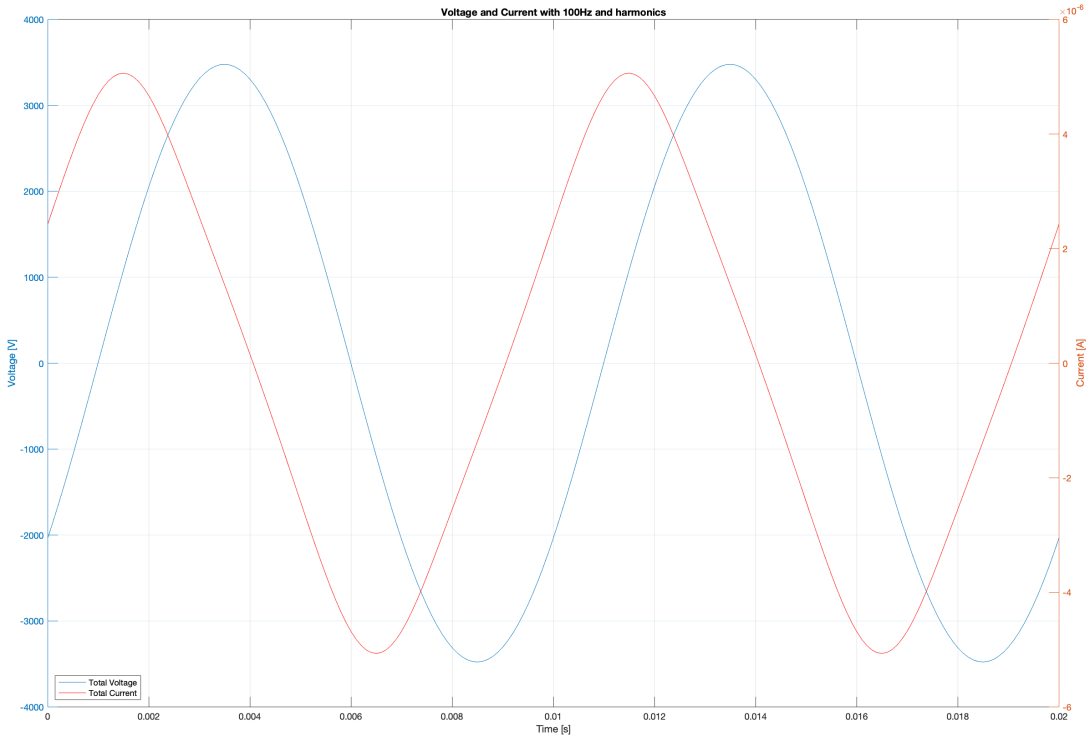

Measurement nr.2

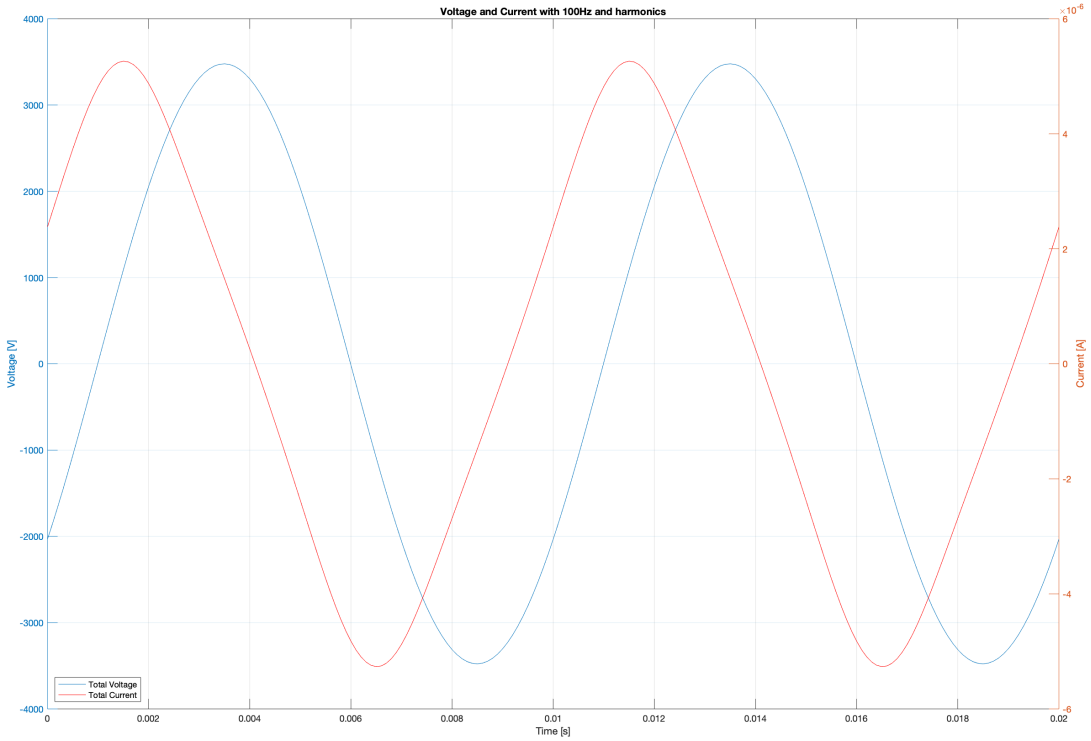

Measurement nr.1

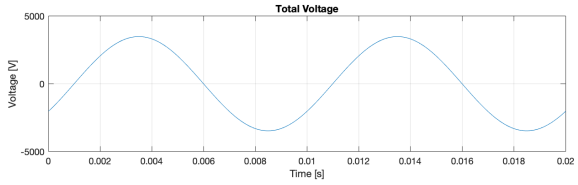

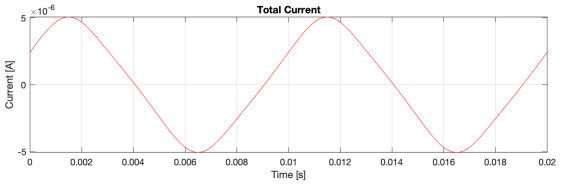

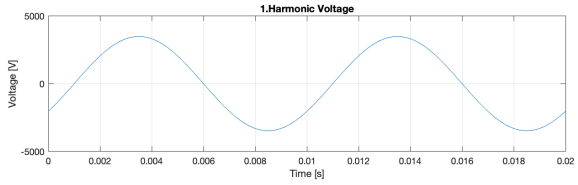

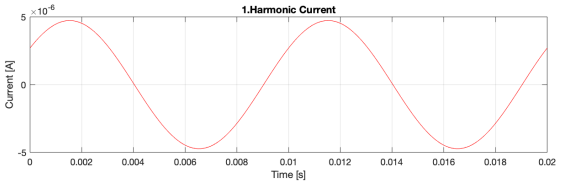

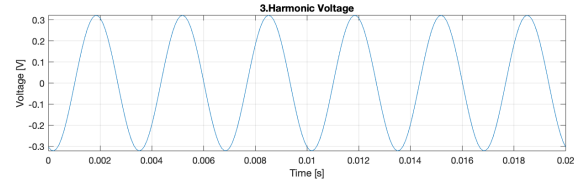

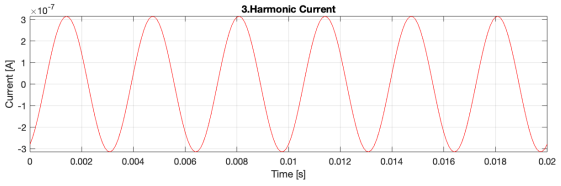

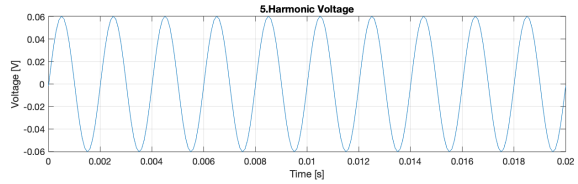

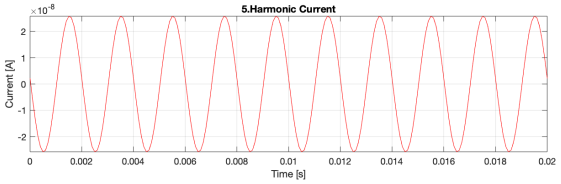

Measurement nr.2

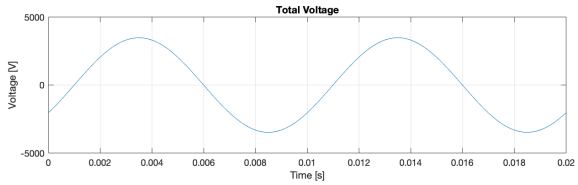

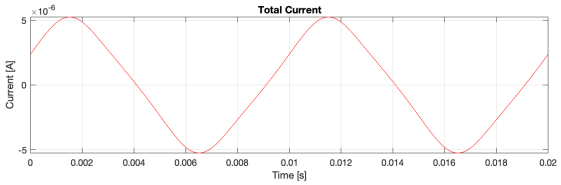

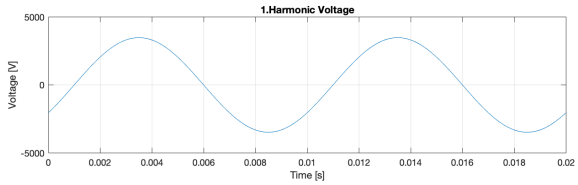

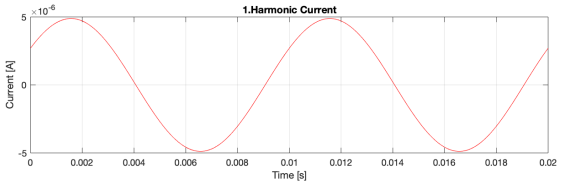

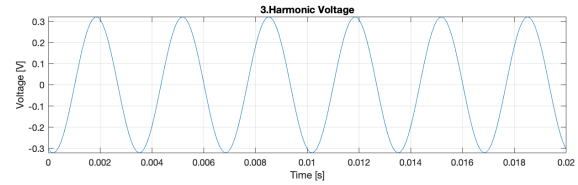

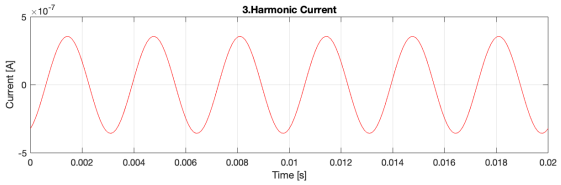

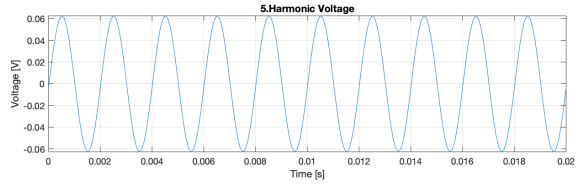

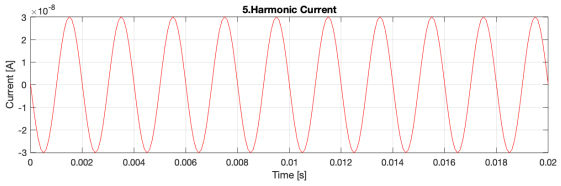

Measurement nr.1

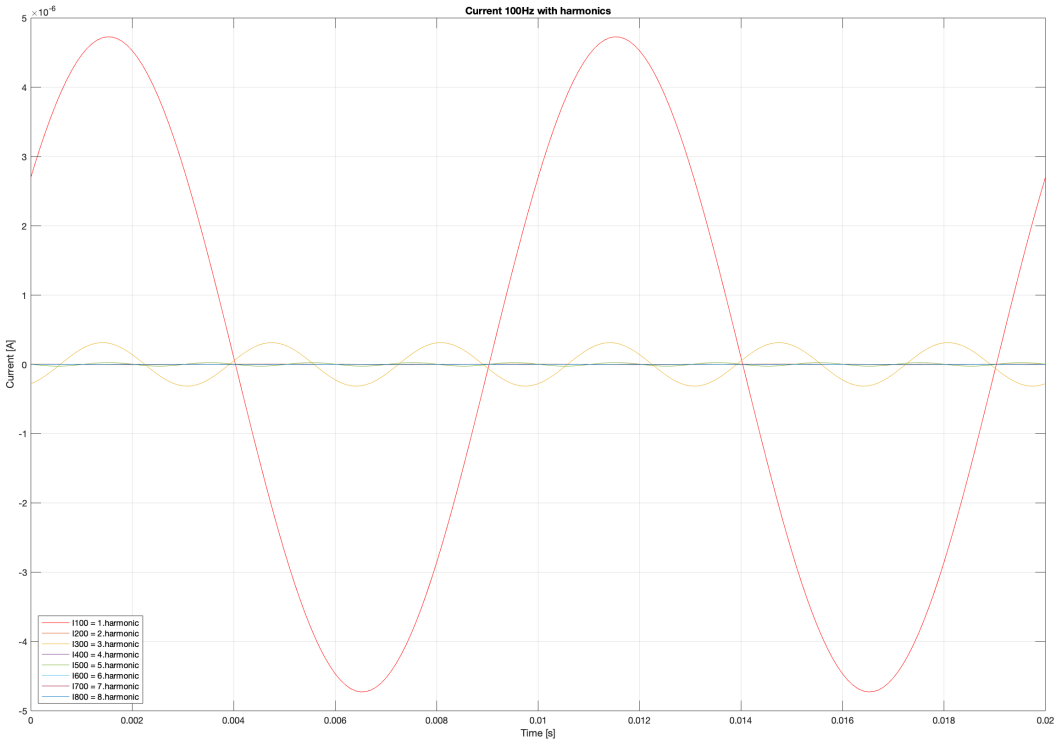

Measurement nr.2

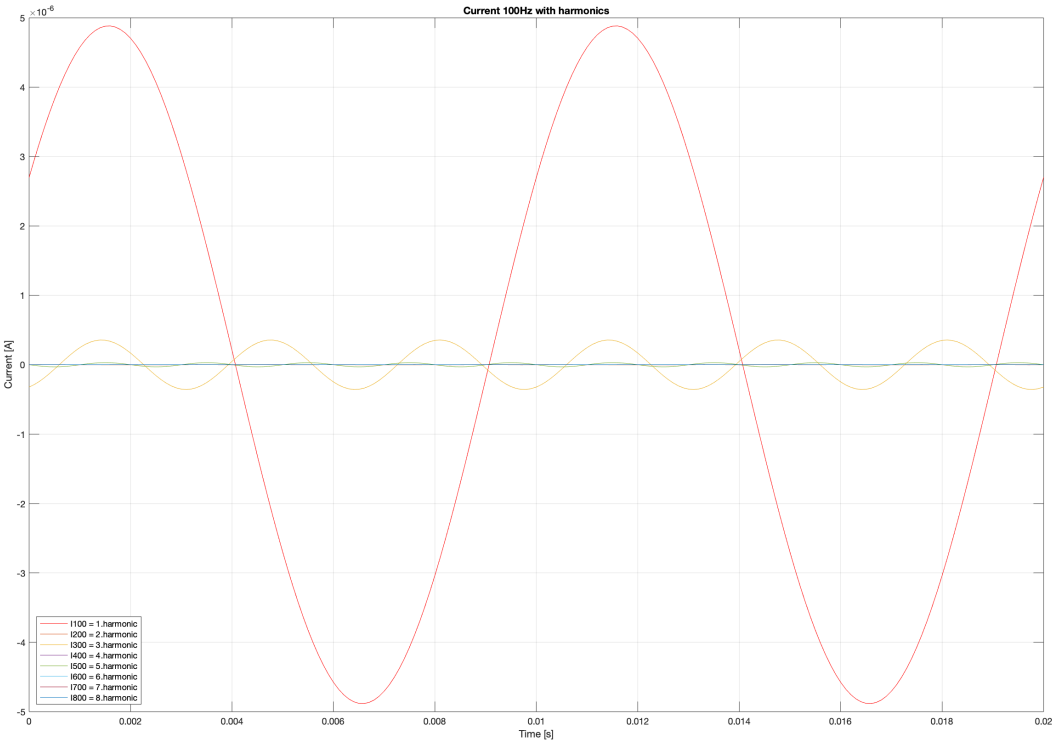

7.2.9 Measurements of The Old Varnish with IDA 200, with 500V or 0.025kV/mm applied.

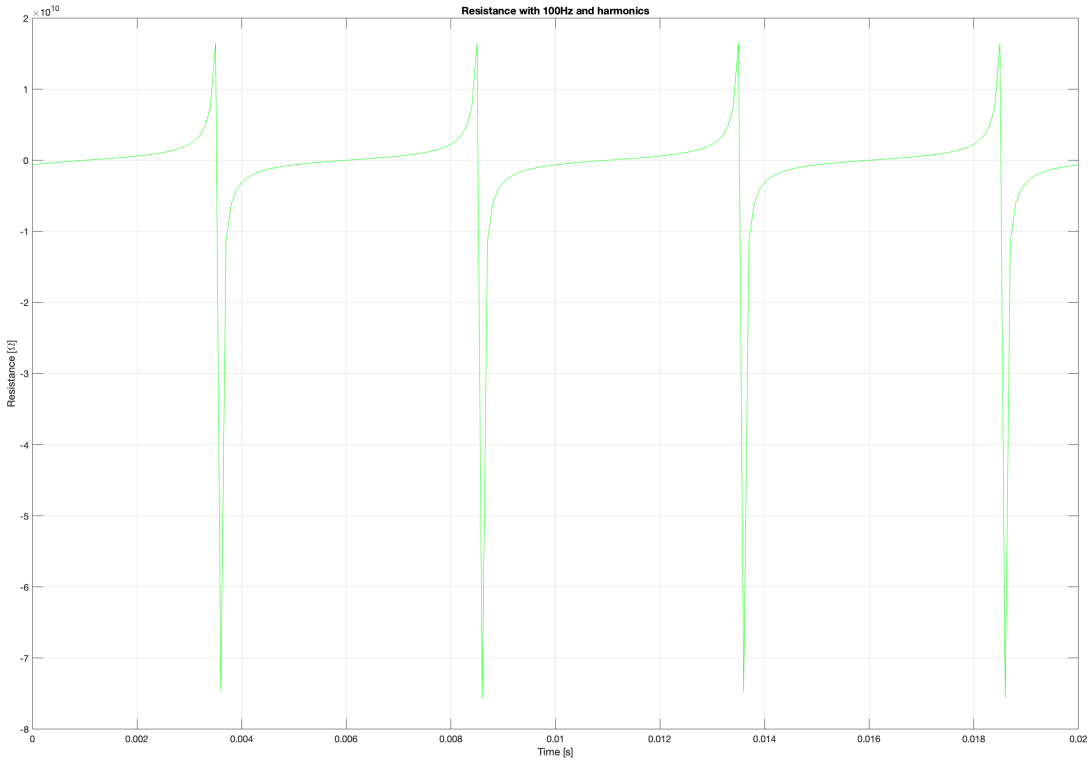

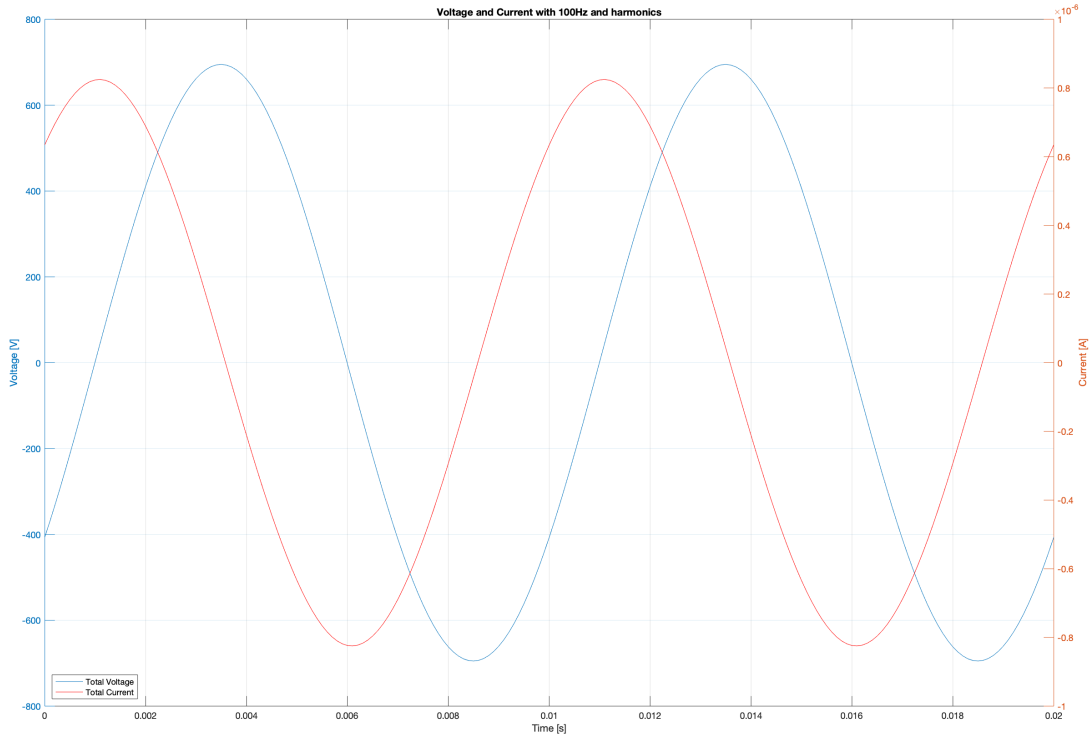

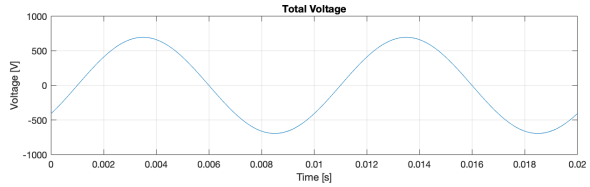
Total Voltage
Voltage [V]
Time [s]

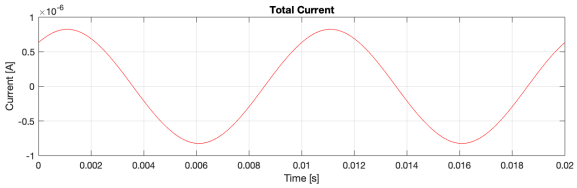
Total Current
Current [A]
Time [s]

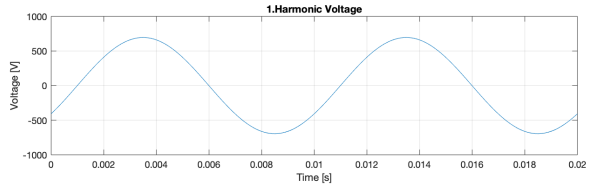
1.Harmonic Voltage
Voltage [V]
Time [s]

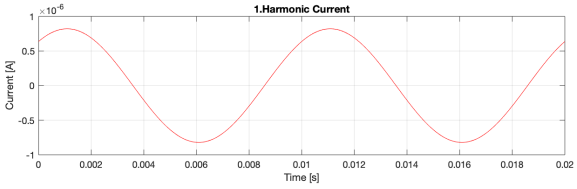
1.Harmonic Current
Current [A]
Time [s]

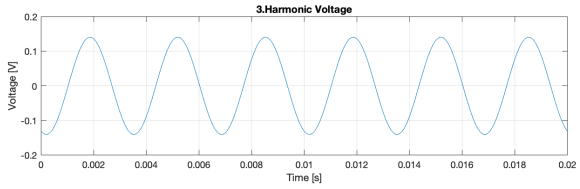
3.Harmonic Voltage
Voltage [V]
Time [s]

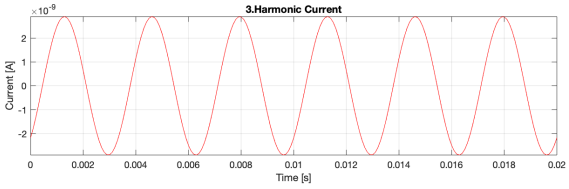
3.Harmonic Current
Current [A]
Time [s]

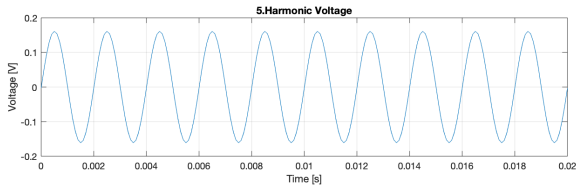
5.Harmonic Voltage
Voltage [V]
Time [s]

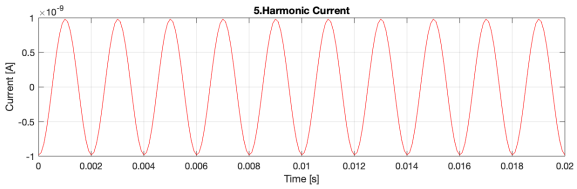
5.Harmonic Current
Current [A]
Time [s]

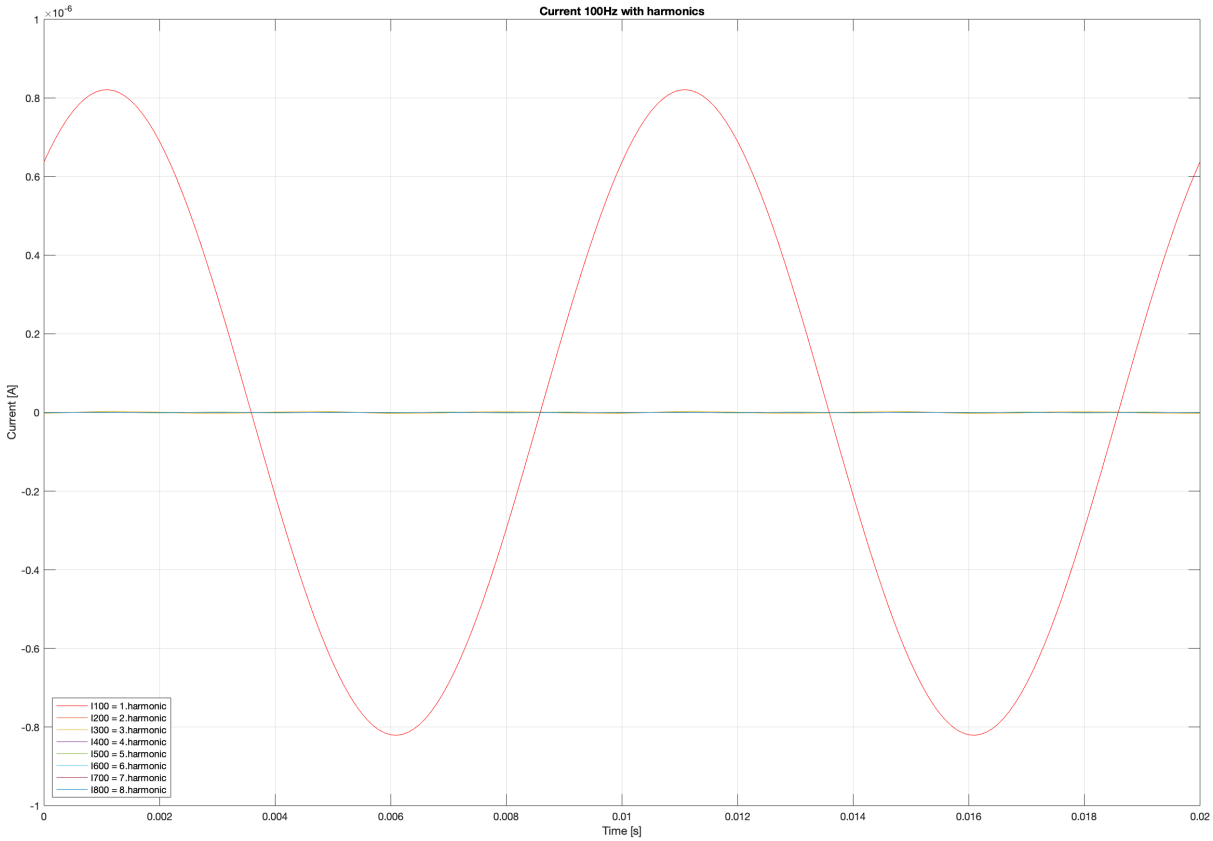
Current 100Hz with harmonics
Current [A]
Time [s]
I100 = 1.harmonic
I200 = 2.harmonic
I300 = 3.harmonic
I400 = 4.harmonic
I500 = 5.harmonic
I600 = 6.harmonic
I700 = 7.harmonic
I800 = 8.harmonic

7.2.10 Measurement Number 1 and 2 of The New Varnish with IDA 200, with 500V or 0.025kV/mm applied.

Measurement nr.1

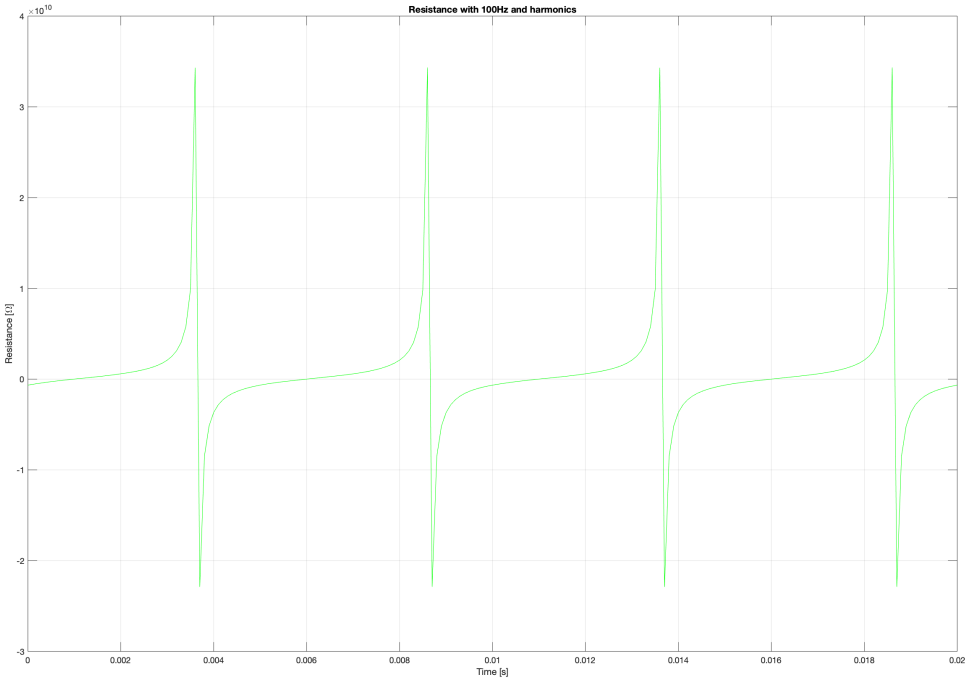

Measurement nr.2

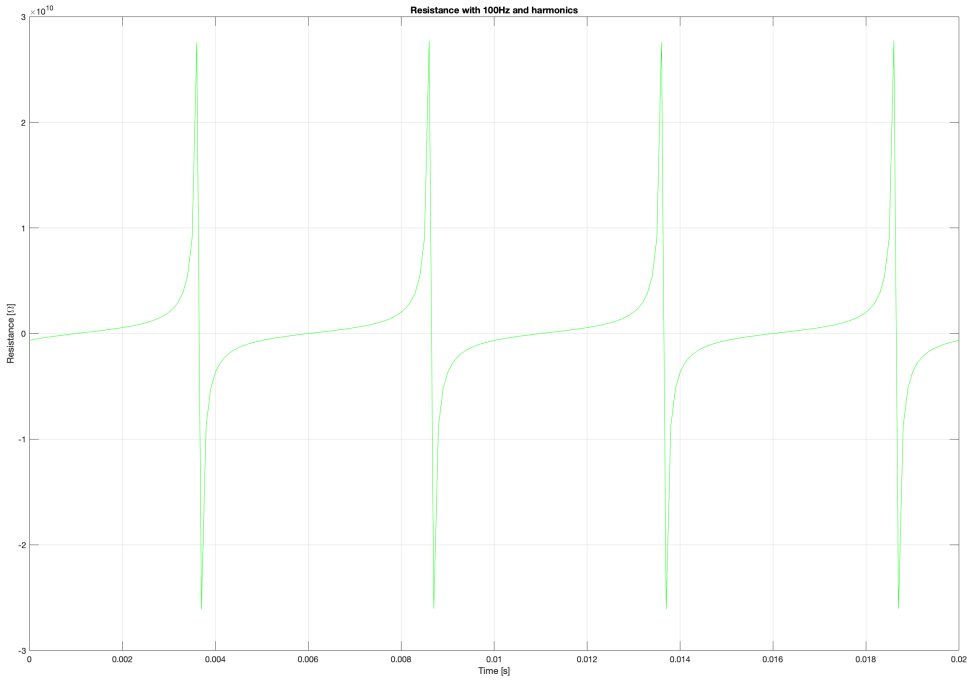

Measurement nr.1

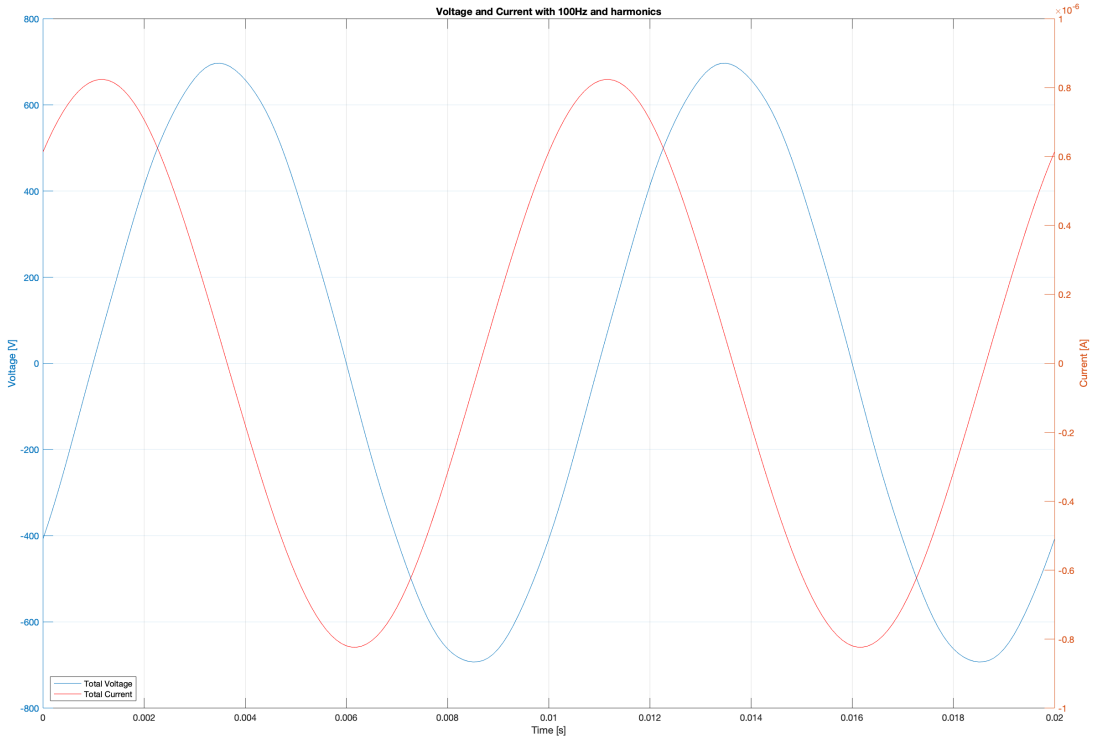

Measurement nr.2

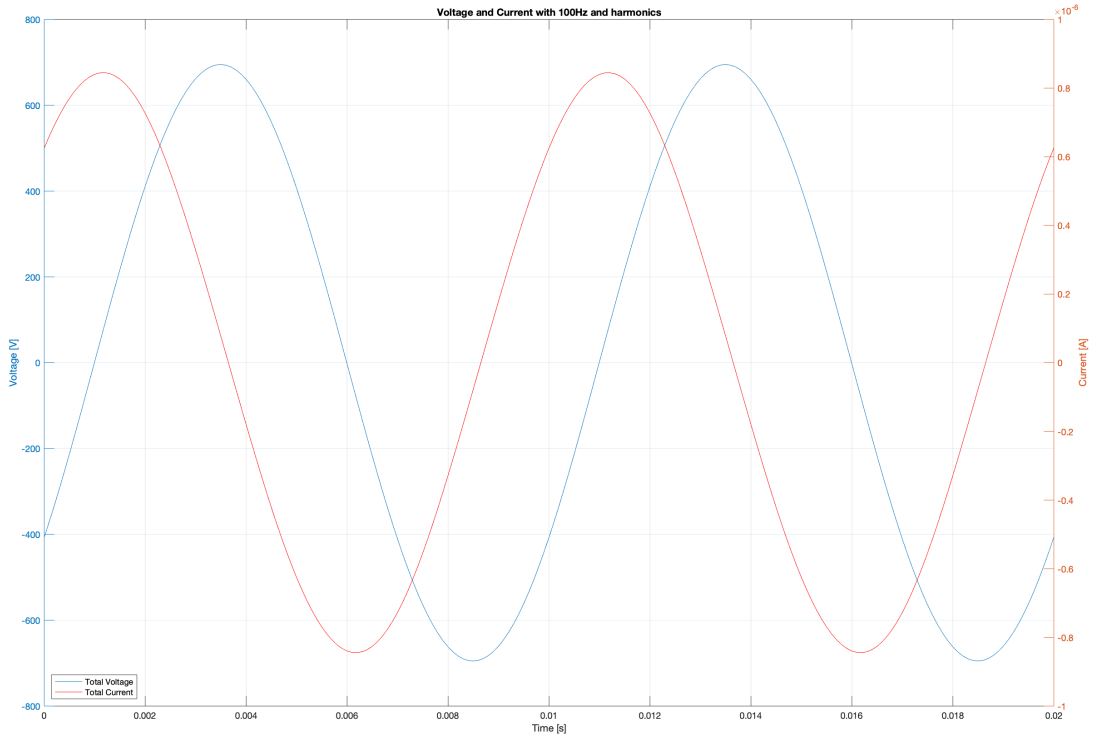

Measurement nr.1

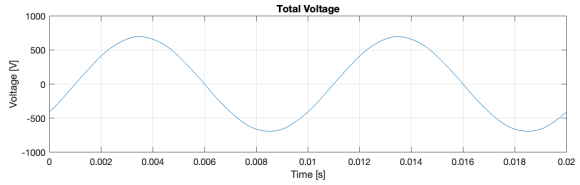

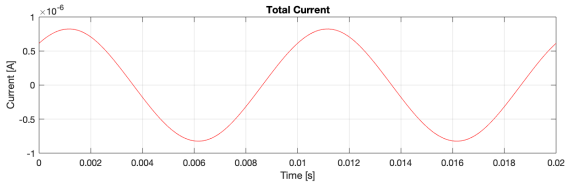

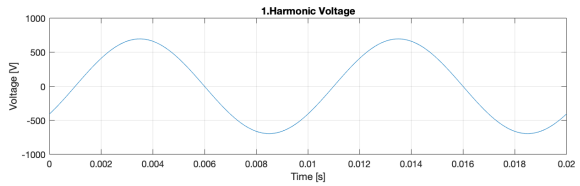

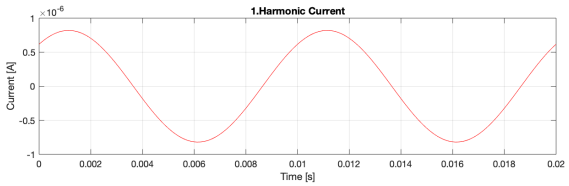

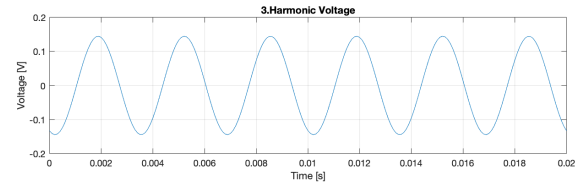

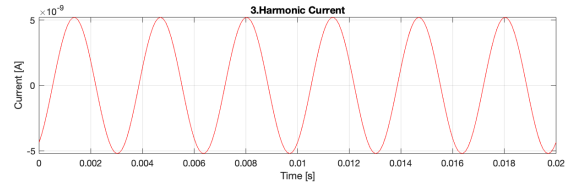

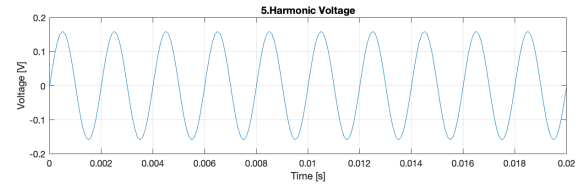

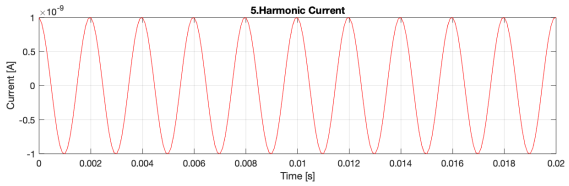

Measurement nr.2

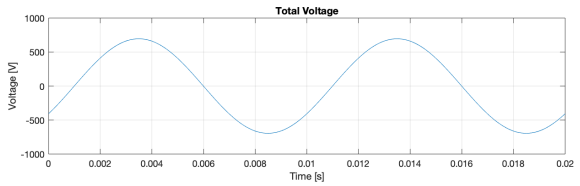

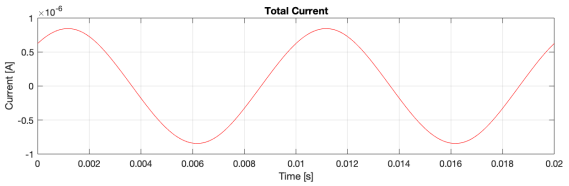

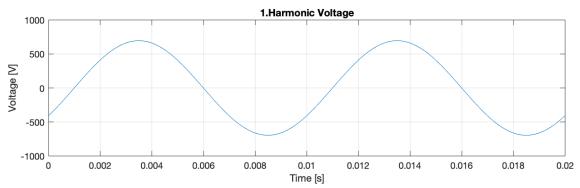

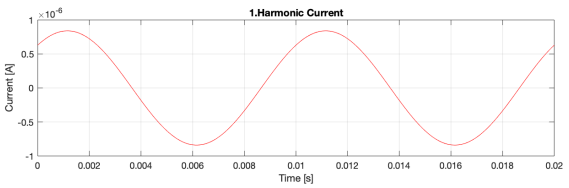

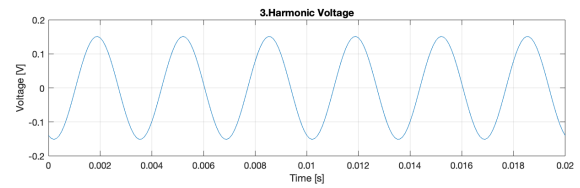

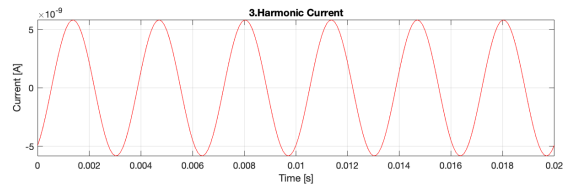

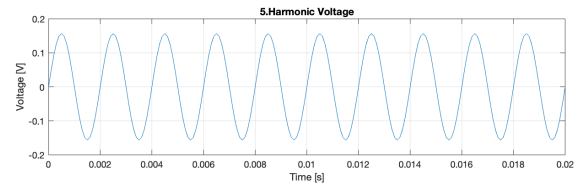

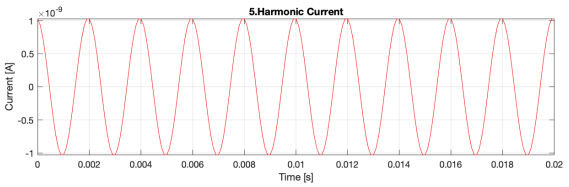

Measurement nr.1

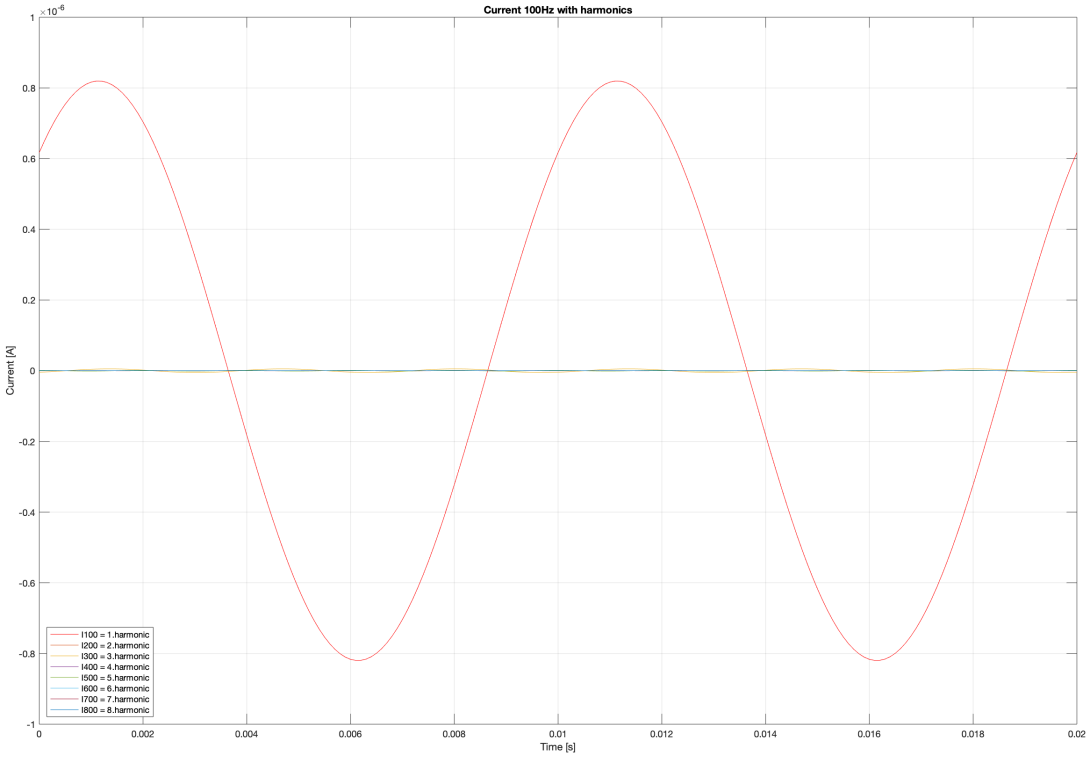

Measurement nr.2

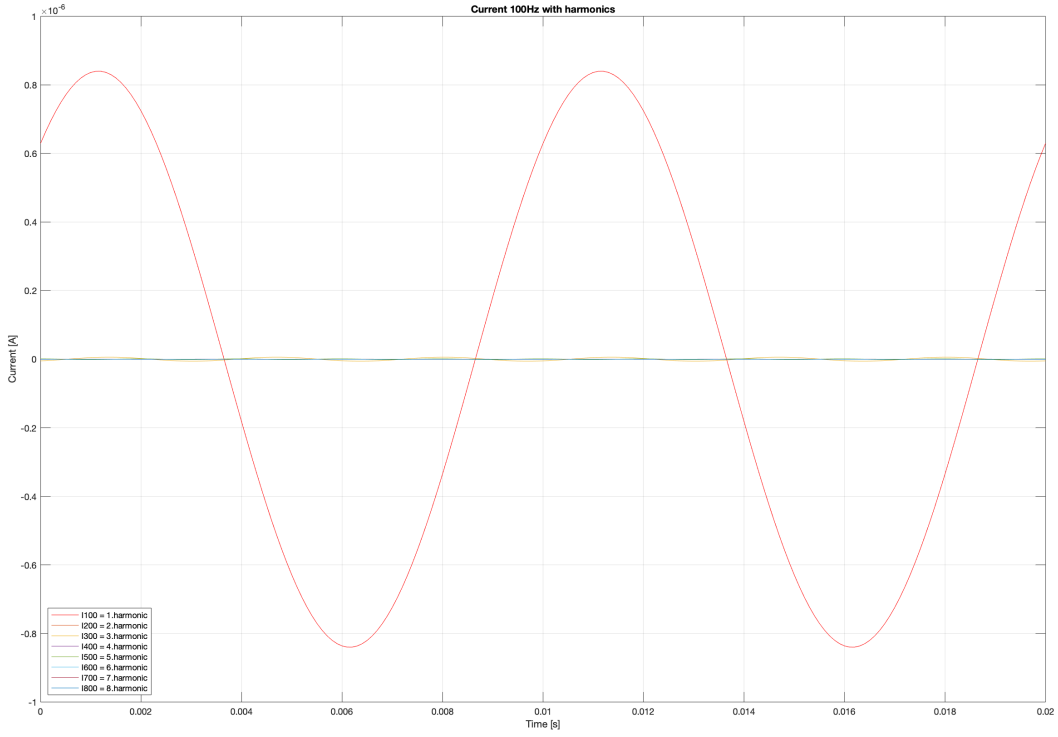

7.3 Appendix C

7.3.1 Data Sheet Field Grading Varnish

Anti corona

CoronaShield® P 8001

- **Semi conductive varnish for end corona protection (stress grading)**
- **Strong stress-grading characteristic**
- **Becomes hard after thermal aging**
- **Suitable for RR as well as VPI**
- **Compatible with epoxy anhydride systems**

General description
CoronaShield® P 8001 is a modified phenolic resin with a semi conductive filler, for use up to class F (155°C), suitable for Resin Rich and can also be used for VPI processed machines.

Impact Shock test

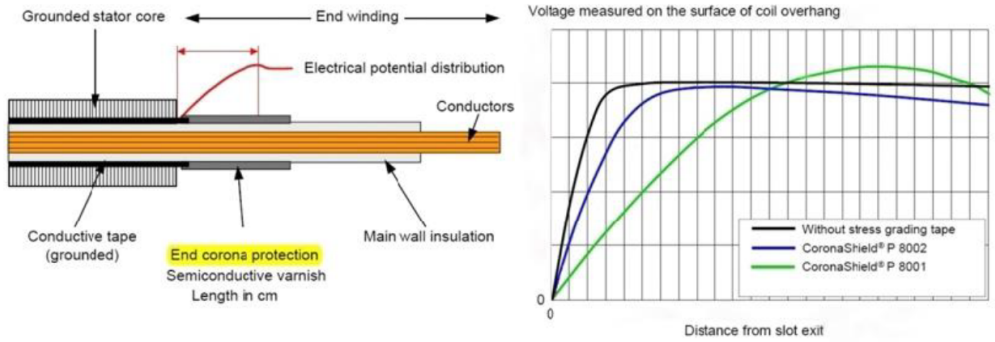

Application
In electricity, a corona discharge - also called partial discharge - is an electrical discharge caused by the ionization of a fluid surrounding a conductor. This occurs when the potential gradient exceeds a certain value but conditions are insufficient to cause complete electrical breakdown or arcing. Precautions must be taken to prevent the onset of corona, otherwise free radicals and ions generated in corona reactions will rapidly destroy organic materials such as binder resins and polymer films. These materials are necessary to provide a sufficient mechanical strength of the coil or bar and to give a tight fit in the slot. Erosion of organic materials in the insulation may be regarded as one of the initial steps leading to failure of the machine.
The use of corona protection materials is recommended for machines with a rated voltage ≥1 kV.

End Corona Protection (Stress Grading):
There is an increase of electric field strength at the slot exit of the stator which can cause flashovers on the surface of the coils or bars. This can be prevented by applying end corona protection materials. These materials have a nonlinear current-voltage characteristic and show a stress-grading effect on the main wall surface.

Von Roll Switzerland Ltd
CH-4226 Breitenbach
www.vonroll.com

8001
KA 3S311 23-12-2015 / 1

Properties	Unit	Value	Test norm
Density	g/cm³	ca. 1.28	ISO 2811-2
Flash point	°C	≥14	ISO 1523
Solid content	%	52 ± 3	IEC 60464-1/-2
Viscosity at 20°C	mPa.s	1000 ± 100	DIN 53019
Thermal class	°C	155	IEC 60085
Drying time at 23°C - Surface	minutes	30	DIN 46449
Drying time at 23°C – Complete dry	h	10	DIN 46449

Scope of Application:
By applying the product we add a semi conductive layer at the slot exit of high voltage coils. We thus reduce electrical stress outside the core, where the electrical field strength would otherwise lead to damages on the insulation.
The varnish is intended for use in both Resin Rich and VPI processed machines.

Basis for selection
The selection of suitable materials depends on the type of high-voltage machine that is to be deployed as well as the insulation system and techniques that are used (VPI or RR).
The main differences between CoronaShield® P 8001 and CoronaShield® P 8002 are the flexibility and the stress-grading characteristic.

	8001	8002
End corona protection	**strong**	**slight**
Adhesion on rigid insulation - e. g. Samicaflex	**good**	**good**
Adhesion on flexible insulation - e. g. Samicaflex	**medium**	**good**
Resistance to moisture, oil, solvents	**very good**	**good**
Thermal ageing	**good becomes hard**	**good remains flexible**

Processing

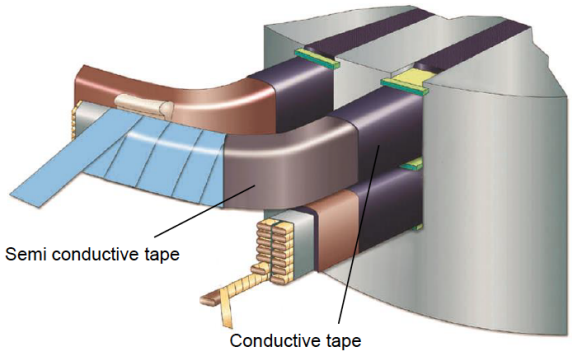

Von Roll Switzerland Ltd
CH-4226 Breitenbach
www.vonroll.com

8001
KA 3S311 23-12-2015 / 2

Processing instructions
Because of the high density of the pigment, it settles quickly at the bottom of the container, therefore the varnish must always be stirred thoroughly before use.
The varnish can be applied to all surfaces with a brush. The viscosity can be adjusted by using the appropriate thinner 9139.
We recommend to apply individual thin coatings, resulting in a final layer thickness of 0.2 - 0.5 mm. Between the different coatings at least 30 minutes must elapse, to enable drying of the previous layer.
The varnish should overlap the conductive layer by 20 mm. You can calculate the recommended axial length of the stress grading varnish with following formula:

- Length in cm from slot exit = Maximum test voltage of coil in kV / 2
- e.g. for 11 kV coil we have a test voltage = 2 x 11 kV + 1 = 23 kV
- L = 23 / 2 = 11.5 cm

For Resin Rich applications, either Epoflex® 215.01 or Epoflex® 219.61-10 should be applied over the semi conductive tape as a protective covering layer.
For VPI applications, we recommend a covering of the tape with a shrinkable woven polyester tape 106.01 or Epoflex® 324.03.

Please do not hesitate to contact us for detailed processing recommendations regarding your application.

Related products
Other End Corona Products:
• 8002 Semi conductive varnish (mainly for maintenance)
• 217.01 / 217.21 Semi conductive tape (B-stage "slight" stress-grading characteristic)
• 217.02 / 217.22 Semi conductive tape (B-stage “strong” stress-grading characteristic)
• 217.24 Semi conductive tape (B-stage “medium” stress-grading characteristic)
• 217.31 Semi conductive tape (C-stage “medium” stress-grading characteristic)

Complementary products:
• 215.51 / 215.51-03 / 215.55 Conductive polyester fleece tape (Internal/External Corona Protection)
• 215.71 Conductive glass fabric tape (Internal/External Corona Protection)
• 215.73 Conductive polyester/glass fabric mixed tape (Internal/External Corona Protection)
• 8003 Conductive varnish (External Corona Protection)
• 8004 / 8019 Conductive mastic (Internal Corona Protection)
• 432.10-01 / 432.11 Conductive Vetronite® sheet (slot packing material)
• 92200 Conductive Side Ripple Springs-Vetronite® (for side walls of slot wedges in generators)

Storage conditions
CoronaShield® P 8001 varnish should be stored in sealed original containers. Pigmented varnishes tend to settle and must be stirred before use.

Shelf life
12 months at 20 – 25°C

Form of delivery
CoronaShield® P 8001 varnish is supplied ready for use in cans of 1, 2, 5, 10, 20, or 25 kg.

Health and safety
CoronaShield® P 8001 varnish is non toxic. We recommend however, that good hygiene practices be adopted, including hand washing and the use of barrier and cleansing creams.

Von Roll Switzerland Ltd
CH-4226 Breitenbach
www.vonroll.com

Olav Henry Sagøy

Dielectric Characterization of Semi Conducting Field Grading Varnish for Hydro Generators

NTNU
Norwegian University of
Science and Technology